2005-08-24

A Biochemical Dissection of the RNA Interference Pathway in *Drosophila melanogaster*: A Dissertation

Benjamin Haley
University of Massachusetts

A BIOCHEMICAL DISSECTION OF THE RNA INTERFERENCE PATHWAY IN *Drosophila melanogaster*

A DISSERTATION PRESENTED

BY

Benjamin Haley

Submitted to the Faculty of the

University of Massachusetts Graduate School of Biomedical Sciences, Worcester

in partial fulfillment of the requirements for the degree of

DOCTOR OF PHILOSOPHY

August 24, 2005

BIOCHEMISTRY AND MOLECULAR PHARMACOLOGY

COPYRIGHT INFORMATION

A Biochemical Dissection of the RNA Interference Pathway
in *Drosophila melanogaster*

A Dissertation Presented

By

Benjamin J. Haley

Approved as to style and content by:

_____
Anthony Carruthers, Ph.D., Chair of Committee

_____
Reid Gilmore, Ph. D., Member of Committee

_____
Craig Peterson, Ph. D., Member of Committee

_____
Nicholas Rhind, Ph. D., Member of Committee

_____
Victor Ambros, Ph. D., Member of Committee

_____
Phillip D. Zamore, Ph. D., Thesis Advisor

_____
Anthony Carruthers, Ph. D.,
Dean of the Graduate School of Biomedical Sciences

Department of Biochemistry and Molecular Pharmacology

August 24th, 2005

Acknowledgements

I would like to begin by thanking my thesis advisor, Dr. Phil Zamore, for giving me the opportunity, and space, to both fail and succeed, and therefore mature, not just as a scientist, but also a person, here at UMass. In addition, I owe a debt of gratitude to all members of the Zamore lab, and alumni, who have provided me with a wealth of knowledge regarding world culture and science in general, but also camaraderie during both the good and difficult times. I would like to give particular thanks to Jochen Deckert and Antti Nykanen, two great guys whose friendship and support during the first few years of graduate school very likely kept me from reconsidering my long-standing goal of pursuing a scientific career. Antti (and Phil) had designed, performed, or optimized the experiments shown in Chapter II, Figures 1, 4, 5 and 6, and because of those, he provided clarity to much confusion over the details in this newly uncovered dsRNA response pathway. Furthermore, I will never forget Dianne Schwarz and Gyorgy Hutvagner, my cherished benchmates. Their unselfish sharing of both reagents and time was invaluable to my research, and the unpredictable and often inappropriate nature of our conversations definitely gave me something to look forward to each workday. Moreover, I will be forever fortunate to have worked with Yuki, Chris, Alla, Tingting, Guiliang, Klaus, and Herve. Also, I would be remiss if I did not give thanks for the thoughtful contributions of my thesis committee members, Drs. Anthony Carruthers, Craig Peterson, Reid Gilmore, Nick Rhind, and Victor Ambros.

Beyond the bench, I've had the pleasure of meeting all sorts of great and bizarre folk, all of whom have influenced my worldview in any number of ways. Therefore, my life would be far less interesting had I never meet people like Kiran and Sean (vive la palace), Brad, Melissas (Duck and Calmann), K-train, and countless others. Perhaps the most influential of this bunch is Heather, whose insightful critiques of my research and insistence on my getting a checking account (instead of living my life one money order at a time) had made my time here at UMass far more worthwhile and fruitful. Each moment of our time together will always be treasured.

Lastly, I cannot forget to thank the friends and family who have been with me every step of the way, from childhood to however old I am now. Thank you mom, grandparents, brothers, aunts and uncles and every family member in between, your sincere interest in what I have been doing with my life has given it value during the days I thought I could never make a difference. And to everyone else, remember...

"The brighter you are, the more you have to learn"

—Don Herold

TABLE OF CONTENTS

LIST OF FIGURES

LIST OF TABLES

ABSTRACT

In diverse eukaryotic organisms, double-stranded RNA (dsRNA) induces robust silencing of cellular RNA cognate to either strand of the input dsRNA; a phenomenon now known as RNA interference (RNAi). Within the RNAi pathway, small, 21 nucleotide (nt) duplexed RNA, dubbed small interfering RNAs (siRNAs), derived from the longer input dsRNA, guide the RNA induced silencing complex (RISC) to destroy its target RNA. Due to its ability to silence virtually any gene, whether endogenous or exogenous, in a variety of model organisms and systems, RNAi has become a valuable laboratory tool, and is even being heralded as a potential therapy for an array of human diseases. In order to understand this complex and unique pathway, we have undertaken the biochemical characterization of RNAi in the model insect, *Drosophila melanogaster*.

To begin, we investigated the role of ATP in the RNAi pathway. Our data reveal several ATP-dependent steps and suggest that the RNAi reaction comprises as least five sequential stages: ATP-dependent processing of double-stranded RNA into siRNAs, ATP-independent incorporation of siRNAs into an inactive ~360 kDa protein/RNA complex, ATP-dependent unwinding of the siRNA duplex to generate an active complex, ATP-dependent activation of RISC following siRNA unwinding, and ATP-independent recognition and cleavage of the RNA target. In addition, ATP is used to maintain 5′ phosphates on siRNAs, and only siRNAs with these characteristic 5′ phosphates gain entry into the RNAi pathway.

Next, we determined that RISC programmed exogenously with an siRNA, like that programmed endogenously with microRNAs (miRNAs), is an enzyme. However,

while RISC behaves like a classical Michaelis-Menten enzyme in the presence of ATP, without ATP, multiple rounds of catalysis are limited by release of RISC-produced cleavage products. Kinetic analysis of RISC suggests that different regions of the siRNA play distinct roles in the cycle of target recognition, cleavage and product release. Bases near the siRNA 5′ end disproportionately contribute to target RNA-binding energy, whereas base pairs formed by the central and 3′ region of the siRNA provide helical geometry required for catalysis. Lastly, the position of the scissile phosphate is determined during RISC assembly, before the siRNA encounters its RNA target.

In the course of performing the kinetic assessment of RISC, we observed that when siRNAs are designed with regard to 'functional asymmetry' (by unpairing the 5′ terminal nucleotide of the siRNA's guide strand, i.e. the strand anti-sense to the target RNA), not all of the RISC formed was active for target cleavage. We observed, somewhat paradoxically, that increased siRNA unwinding and subsequent accumulation of single-stranded RNA into RISC led to reduced levels of active RISC formation. This inactive RISC did not act as a competitor for the active fraction. In order to characterize this non-cleaving complex, we performed a series of protein-siRNA photo-crosslinking assays. From these assays we found that thermodynamic stability and termini structure play a role in determining which proteins an siRNA will associate with, and how association occurs. Furthermore, we have found, by means of the photo-crosslinking assays, that siRNAs commingle with components of the miRNA pathway, particularly Ago1, suggesting overlapping functions or crosstalk for factors thought to be involved in separate, distinct pathways.

CHAPTER I: INTRODUCTION

Since it was initially characterized in 1998, RNA interference (RNAi) has been accepted with near unanimity as one of the most influential tools accelerating the rapid pace of biological discovery[1]. This technique, built upon observations by Guo and Kemphues but first explained by Fire and Mello, allows the use of double-stranded RNA (dsRNA) to trigger a cellular response resulting in specific and considerable destruction of cellular RNA cognate to either strand of the input dsRNA, providing a fast and reliable alternative to oft difficult or cumbersome genetic manipulation[1,2]. While this was a boon for researchers working with organisms that lack general dsRNA response pathways, such an approach was thought to be of little use in mammalian systems, which react to dsRNA larger than 30 base-pairs in length by global (non-specific) inactivation of transcription (Figure 1). Fortunately for the mammalian biology community, in 2001, Tom Tuschl's group, with insight from years of previous work, was able to deduce a way to work around this problem[3]. At the time, it had been known that the long dsRNA molecule was not the true specificity determinant of this phenomenon. Rather, the trigger dsRNA was minced into smaller, ~21 nucleotide (nt) duplexes, bearing characteristic 5′ phosphate and 3′ hydroxyl moieties, by at least one member of the Dicer family, a group of RNAse-III-like dsRNA-specific enzymes[4-9]. After their production, these small duplexes were divided into single strands, which could now guide the RNA induced silencing complex (RISC) to a target RNA[9,10]. Bundled with each RISC is an Argonaute (Ago) family member, the effector proteins in each RNAi-like pathway. Tucked inside

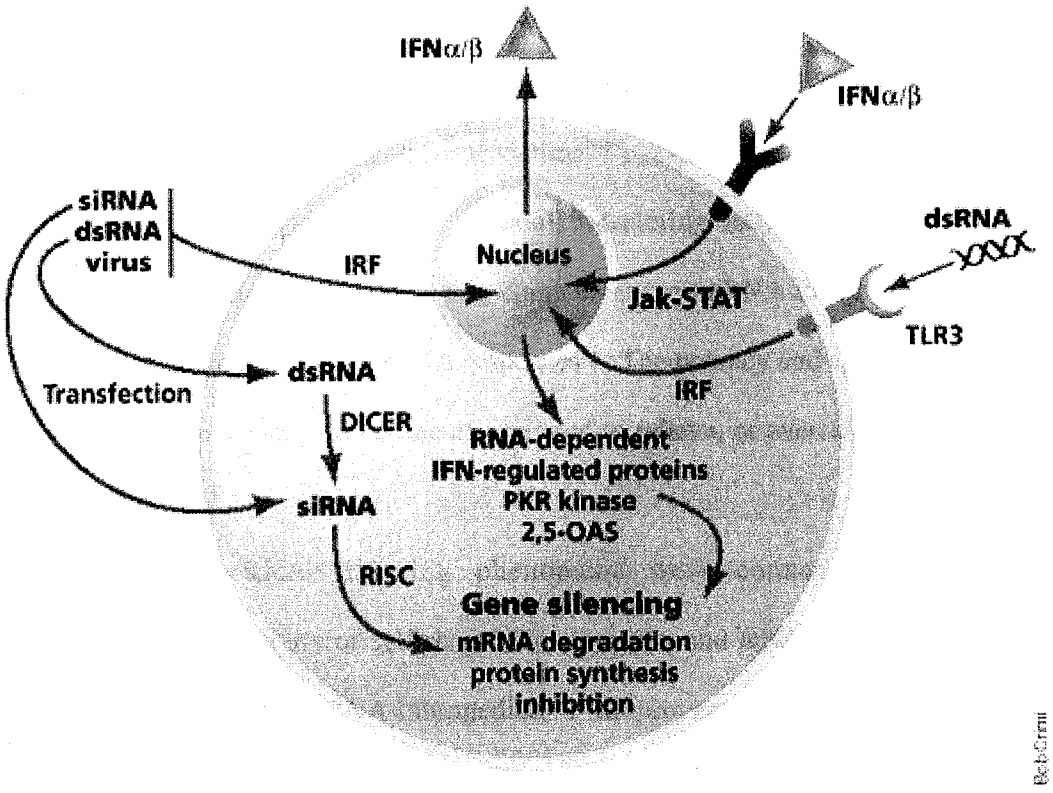

Figure 1. Mechanisms by which dsRNA functions as a molecular trigger to mediate changes in gene expression patterns.

These include sequence-specific gene silencing by RNAi via siRNAs that target cognate mRNA degradation, mediated through activation of RISC. The α/β family of IFNs are inducible by viruses and dsRNA, and IFNs in turn regulate the expression of dsRNA-dependent enzymes such as the PKR kinase that inhibits protein synthesis and 2',5'-oligoadenylate synthetase (2,5-OAS) synthetases that mediate RNA degradation through activation of RNase L. Finally, TLR3 recognizes dsRNA and induces a signal cascade that includes production of IFNs. Reproduced from Samuel, **Nature Biotechnology**, 2004[11].

Ago, the single-stranded RNA (ssRNA) guides RISC to its substrate by Watson-Crick base-pairing, whereupon RISC cleaves only the target RNA, and with its small RNA guide in hand, releases to find additional victims[12-18]. Tuschl and colleagues discovered that the ~21-nt RNA intermediates, or small interfering RNAs (siRNAs), could be delivered into mammalian cells, reducing complementary mRNA to nearly undetectable levels, while bypassing general dsRNA responses[3]. The potency and specificity of RNAi has lead to the belief that it could one day be used to relieve, or even eliminate, a variety of human ailments[19].

Originally, RNA silencing phenomena were connected to transgene overexpression, the activity of selfish genetic elements, and RNA viruses, all of which were thought to utilize a dsRNA intermediate[20]. Moreover, an organism could use this dsRNA, and more precisely, small RNAs derived from it, as both a beacon and a sequence-specific guide to home in on the intrusive genetic elements, and accordingly, RNA silencing was hypothesized to be an ancient genome defense mechanism[14,21]. However, the research world may have sold RNAi's reach a bit short, because in 2001 simultaneous reports hit the press describing hundreds unique 21-25-nt RNAs, identical in structure to siRNAs, that showed evolutionarily conserved sequence, and developmental or tissue specific regulation (*Saccharomyces cerevisiae* being a notable exception, as it has lost most known RNAi-associated genes from its genome[22-26]). Since their discovery, microRNAs (miRNAs, as they have come to be known) have been shown to regulate cellular phenomenon such as stem cell maintenance and differentiation, brain development, lymphocyte development, left/right asymmetry, and tumorigenesis,

amongst many others[24,27-36]. The crux of small RNA influence over such processes is their command over the two driving forces in the central dogma of molecular biology, transcription and translation.

Transcriptional silencing: mechanisms and phylogeny

While large, multi-kilobase, antisense RNA molecules are known to be associated with transcriptional silencing in mammals, X-chromosome inactivation being the most notable example, several groups have recently produced evidence of small RNA influence on the transcriptome across eukarya[37,38]. Rajewsky and colleagues have employed conditional gene targeting to remove the lone Dicer from murine cells, abrogating production of all examined small RNAs[39]. Adding credence to RNAi's role in silencing aberrant RNA species, this group observed up-regulation of centromeric-repeat-sequence-derived transcripts in the absence of Dicer, which correlated with reduced Histone H3 lysine 9 (H3-K9) methylation, a highly conserved mechanism for halting transcription[40]. In addition, like Bernstein et al. before them, they found that Dicer was essential for stem cell differentiation and ultimately development of the murine embryo[41]. Perhaps the most intriguing discovery from the Dicer conditional knockout mouse was that mouse embryonic fibroblasts (MEFs) devoid of Dicer retained the ability to perform siRNA induced post-transcriptional gene silencing (PTGS, discussed below), confirming the observations of Martinez et. al in human cell extracts[13]. These results were contrary to those gathered by separate groups, which found Dicer to be essential for siRNA mediated silencing in human and mouse cells[42,43]. However, as more becomes understood

of the players and mechanisms involved in transcriptional gene silencing (TGS) in mammals, researchers may be able to manipulate this system to use TGS as a future knock-out/knock-down technique. Highlighting this notion, exogenously added small RNAs specific to DNA sequence within the promotor of E-cadherin were shown to induce methylation of CpG islands within this region, silencing transcription of this gene in a human breast cancer cell line, and similar results were obtained by Looney and colleagues using lentiviral delivered small RNAs[44,45]. Recently, siRNA-directed transcriptional silencing in mammalian cells has been observed in the absence of DNA methylation, though the mechanism is unclear[46]. Nonetheless, the mammalian world of TGS has only recently been revealed, and a more complete understanding of the genes and mechanisms involved has come from work in non-mammalian systems[38].

In the plant model *Arabidopsis thaliana*, as in animals, dsRNA-directed methylation of DNA at specific cytosine bases, most often in the promotor region, results in ablation of that gene's expression[47,48]. Such regulation has shown to be of import in suppressing "intragenomic parasites", such as transposons[49,50]. Of interest here is that mutations in RNA silencing genes impair or completely disrupt methylation dependent silencing, as in human cells, phenocopying disruption of the core methylating enzymes themselves, *drm 1* and/or *drm 2* (or DNMT1 and DNMT2 in humans)[44,48,51,52]. Likely not limited to the plant kingdom, the length of a small RNA appears to play some role in establishing its destined function[53]. Particularly, of the four known Dicer family members in *A. Thaliana*, Dicer-like 3 (DCL3) with the RNA-dependent-RNA-polymerase (RdRP), RDR2, produces 24-nt RNAs, known to specifically direct

methylation through Ago4 and HEN1, a methyltransferase (miRNAs themselves are methylated during their biogenesis by HEN1[54-56]). However, it looks as though there may be compensation from RNA silencing relatives in this model system, as 21-mers derived from other Dicer-like members can direct similar, but distinct methylation events[48]. In addition, recent work has provided a glimpse at the specificity of the process. Here, miRNAs targeting PHABULOSA or PHAVULOTA mRNA display significant methylation of DNA that would be downstream, not upstream, in terms of exons, of the miRNA target site within the respective mRNAs[57], and Bao et al surmised that chromatin modification could be occurring co-transcriptionally once the miRNA target site is revealed on the nascent transcript.

One of the obvious features linking plant TGS with that of the evolutionarily distant yeast model, *Saccaromyces pombe*, is the requirement of an RNA-dependent RNA polymerase (RdRP) for the process, and lending credence to Bao et. al's speculation, separate groups have reported RdRP-dependent chromatin modification coupled to active transcription in fission yeast[58-60]. In *S. pombe*, TGS is regulated by the RNA-induced Initiation of Transcriptional Silencing (RITS) complex, which contains Ago1, Chp1 (a heterochromatin associated chromodomain protein), Tas3 (novel protein) and indirect association/activity of Rdp1, an RNA-dependent RNA polymerase[61]. Moreover, Moazed and colleagues have discovered the RDRC (for RNA-directed RNA polymerase complex), which directly associates with RITS through Dicer and the Clr4 histone methyltransferase. In addition to Dicer, this complex contains Hrr1 (an RNA helicase), Cid12 (a polymerase β nucleotidyltransferase superfamily member), and

Rdp1[62]. Notably, A Cid12 homolog, rde-3, was recently discovered in a screen for RNAi mutants in worms[63]. Moreover, the poly(A) polymerase (PAP) activity of a Cid12 ortholog is essential for elimination of defective RNA species in *S. cerevisiae*, analogous to PAP dependent destruction of RNA in bacteria[64-66]. How or why these proteins function within the context of RNA silencing remains to be seen. Moazed and colleagues suggest that RITS acts as a priming complex, which recruits the RDRC to its template through an siRNA/centromeric RNA association. The RITS-associated target is then amplified into dsRNA by the RDRC and subsequently diced into 21-nt RNAs, which could guide further priming and amplification, effectively silencing the target gene[62].

A convergence of the plant, yeast and animal world has recently come to light, as RNAi-driven TGS (hence known as RNAi-TGS) was uncovered in *C. elegans*[67]. Like plants and yeast, this pathway required, amongst other factors, a Dicer and Argonaute family member, as well as an RdRP. The screen for genes affecting RNAi-TGS in worms also identified a homolog of Tas3, further strengthening transcriptional silencing connections between evolutionarily distant organisms[61,67]. While an RdRP may indicate an evolutionary bridge between plants, yeast and worms, there have been no canonical RdRPs predicted within insect or mammalian genomes, although, RdRP-like activity has been observed *in vitro* for at least fruit flies and rabbits[68,69]. The additional requirement of Polycomb group (PcG) proteins in *C. elegans*' RNAi-TGS should be noted, because in *D. melanogaster*, a well-characterized mode of TGS goes through the PcG proteins[38,70,71]. Most often, these proteins are recruited to PcG response elements (PREs) lying within chromatin, whereupon their assembly into a multi-protein complex results in a variety of

covalent modifications, including H3-K9 methylation. Perhaps not by coincidence, H3-K9 methylation in *Drosophila* is reduced when RNAi-related family members are disrupted, notably *piwi* and *aubergine*, two Ago family members, and *spindle-E*, a DEAD-box helicase[70,72]. It is unclear whether mammalian PcG proteins play a role in the RNAi-TGS process, although they are required for X-chromosome inactivation[73].

Small RNAs and translational repression

At the time of this publication, the miRNA registry held 1650 different miRNAs, from 17 separate metazoans and 4 virus families[74]. Their presence has been connected to stress response in plants, brain development in zebrafish, developmental timing in plants, and hematopoeisis in mice[24]. The first function ascribed to miRNAs, as we know them today, was translational repression of a target mRNA[75]. From their seminal observations, Ambros, Ruvkun and colleagues introduced the world to two comparatively tiny RNAs, a 61 nt hairpin and a 22 nt RNA excised from that hairpin, derived from a single transcript within the lin-4 locus of *C. elegans*[75,76]. This locus, how its expression correlated with decreased lin-14 protein levels and embryonic development of the worm, were all curiously tied together, and an historical account of this discovery can be read in Lee et al[77]. Interestingly, the 22-nt species bore near complementarity to multiple sites along the lin-14 3′-UTR (Figure 2). It should be noted that there were virtually no base-pairs formed between the center of the small RNA and its target regions, suggesting that

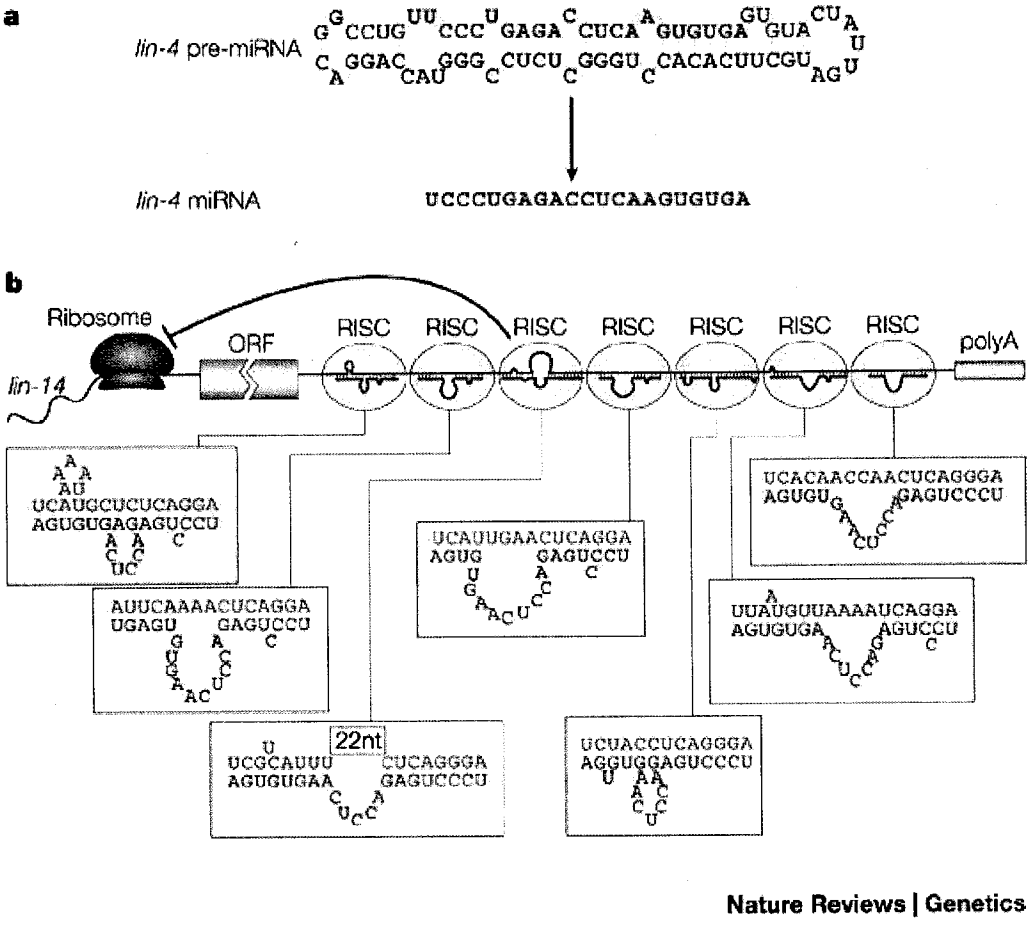

Figure 2. The molecular hallmarks of *lin-4*, the founding member of the microRNA family.

a. The precursor structure and mature microRNA (miRNA) sequence of *lin-4*. **b.** Sequence complementarity between *lin-4* (red) and the 3'-untranslated region (UTR) of *lin-14* mRNA (blue). *lin-4* is partially complementary to 7 sites in the *lin-14* 3' UTR; its binding to these sites of complementarity brings about repression of LIN-14 protein synthesis. RISC, RNA-induced silencing complex. Reproduced from He and Hannon, **Nature Reviews Genetics**, 2004[27].

specificity was determined by either the 5′ or 3′ region of the small RNA. Finally, clones of the lin-4 locus from 3 other *Caenorhabiditis* species rescued the lin-4 null allele. Therefore, the 1993 Ambros and Ruvkun papers defined the modern miRNA pathway by showing (1) a small ~22-nt RNA derived from a precursor molecule (Dicer excises this small molecule from its stem-loop parent[78,79]) (2) a potential antisense RNA-RNA interaction between this small RNA and the UTR of a co-expressed mRNA and (3) reduced gene-expression at the protein, not RNA, level[75,76]. Six years later, the rudimentary mechanism of this phenomenon began to be uncovered, as Olsen and Ambros observed that the mRNA being repressed by lin-4 contained a relatively normal polysome profile, indicative of repression following translational initiation. This process is perhaps analogous to the polysome stalling and translational arrest observed by Inada and Aiba[80]. Also, remarkable evolutionary conservation of the small RNA sequence is a hallmark of miRNA families, and many members are conserved, to the nucleotide, from worms to humans[24]. The recent prediction of at least 53 primate-specific miRNAs suggests that these small RNAs may even play a role in speciation[81].

Because of the apparent leniency towards its targets, the miRNA pathway was thought to be functionally distinct from another PTGS process, mRNA cleavage by small RNAs[24,27,82]. However, the distinction between these two pathways blurred when Zamore and colleagues discovered that human miRNAs will cleave a target mRNA if it is presented with perfect complementarity (as opposed to a central bulge, typical of most mammalian miRNAs and their targets[17]). Shortly thereafter, plant miRNAs were predicted and later confirmed to naturally form extensive base-pairing to their

endogenous targets, resulting in cleavage of the substrate mRNAs *in vivo* and *in vitro*, and further miRNA cloning and refined target algorithms have uncovered that miRNA directed cleavage is natural and conserved in mammals[83-87]. Induced and guided by smallRNAs, mRNA cleavage triggers the complete destruction of that mRNA, likely through RNA decay foci known as P-bodies, GW bodies or cytoplasmic bodies in insects and mammals, and a second decay complex known as the exosome[88-90]. In *A. thaliana*, lack of the exosomal ribonuclease, XRN4 leads to increased concentrations of aberrant RNA, presumably triggering RdRP dependent gene silencing[91,92]. This hints, that at least in plants, the RNAi pathway could be employed as a scavenger of mis-regulated or poorly processed transcripts.

Consequently, the recent observations of miRNA/target interaction inside of mammalian P-bodies, suggests a potential role for these structures in miRNA-mediated translational repression, such as sequestration of translationally dormant mRNA from ribosomes or exonuclease driven decay of miRNA-bound mRNA[93]. Indeed, keeping a target RNA away from ribosomes may enhance RNAi, as RNA destruction becomes more efficient when uncoupled from translation in human cells[94]. However, this may not always be the case, as core RISC proteins co-purify with ribosomal components, maternal mRNA in *D. melanogaster* oocytes must be translated before it can be targeted and destroyed by RISC, and in the early diverging protozoan, *Trypanosome brucei*, Ago association with polyribosomes is essential for RNAi. Such examples imply a functional or structural link, in at least some circumstances, between RISC activity and the

translational apparatus[95-98]. It is unknown whether mRNA cleavage by RISC occurs before, during or after Ago association with P-bodies or the exosome.

Self-regulation of small RNA-mediated pathways

Surprisingly, some of the experimentally confirmed miRNA targets are RNA silencing genes themselves. The Carrington group has observed that mutations of DCL1 (a plant Dicer member), Hen1 or the presence of the viral RNAi suppressor HC-Pro, led to accumulation of DCL1 transcript[99,100]. *In silico* analysis found a sequence in the center of the DCL1 coding region bearing near-perfect complementarity to miR162, upon which association of this miRNA, *in vivo*, results in cleavage of DCL1 mRNA. Soon thereafter, Bartel and collegues discovered that down-regulation of Ago1 mRNA levels by miR168 was essential for proper plant development[101]. Developmental defects caused by increased Ago1 levels indicates that too much of a good thing, RNAi proteins in this case, can be a bad thing, and perhaps the miRNA pathway uses itself to provide an internal feedback loop. Also, miRNA target prediction algorithms in humans detect potential hits in all known RNA silencing genes, indicating that miRNA self-regulation could extend beyond the plant kingdom[102,103].

In addition, Carrington and colleagues have encountered miRNA regulation not just at the RNAi protein level but also during small RNA precursor formation. Here, two miRNAs were found not to be negative regulators of their target RNAs, but rather they acted in a positive fashion, promoting proper trans-activating siRNA (ta-siRNA) formation[104]. ta-siRNAs are endogenous 21-nt RNAs associated with PTGS, but their

expression is governed by RdRP-dependent activity upon pol-II transcripts, as opposed to pol-II transcription alone, like miRNAs[105-107]. Bioinformatic analysis led this group to the discovery that miR173 and miR390 direct the proper phasing, or 21-nt interval, of ta-siRNA formation by clipping either the 5′ or 3′ terminis of pre-ta-siRNA transcripts[104]. This phenomenon is dependent on the fact that Dicer and Dicer-like proteins are known to processively chop their substrates beginning from the ends, not the center of a dsRNA[108]. Additionally, it should be noted that miRNA target algorithms detect a disproportionate number of miRNA-target sites within transcription factor (TF) mRNA[109,110]. To date, the promoters for RNA silencing genes have not been extensively described, though presumably these promoters could be the targets of potential miRNA regulated TFs. Therefore it is conceivable that miRNAs could adjust their own expression by regulating the levels of their transcription and/or the transcription of genes involved in their biogenesis. miRNA regulation of TFs could also be essential to their dominion over the transcriptome, as miRNA-mediated silencing of a single TF gene could alter the expression of multiple, distinct transcripts.

Small RNA biogenesis

Although they are structurally indistinguishable in mature form, the origins of siRNAs and miRNAs are quite distinct (Figure 3)[111]. In a nutshell, miRNAs originate from highly structured, multi-kilobase pol-II transcripts (pri-miRNA) from which the miRNA precursor hairpins (pre-miRNAs) are excised[105,112]. This process occurs exclusively within the nucleus by a complex known as the "microprocessor", which

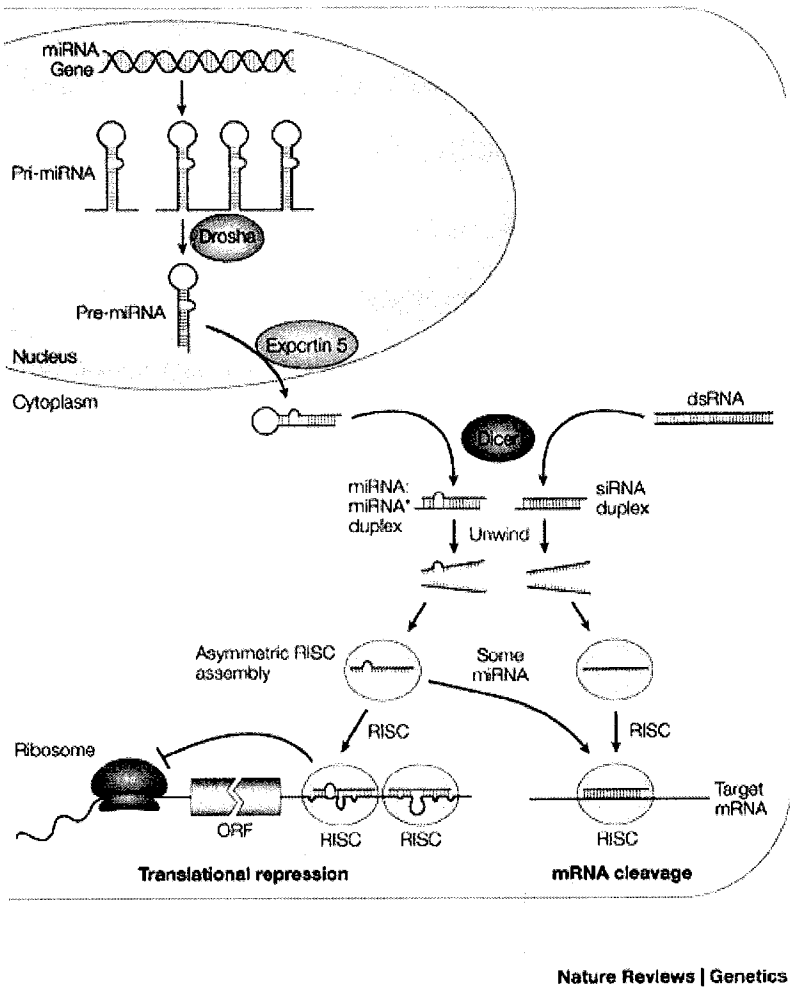

Figure 3. The current model for the biogenesis and post-transcriptional suppression by microRNAs and small interfering RNAs.

The nascent pri-microRNA (pri-miRNA) transcripts are first processed into 70-nucleotide pre-miRNAs by Drosha inside the nucleus. Pre-miRNAs are transported to the cytoplasm by Exportin 5 and are processed into miRNA:miRNA* duplexes by Dicer. Dicer also processes long dsRNA molecules into small interfering RNA (siRNA) duplexes. Only one strand of the miRNA:miRNA* duplex or the siRNA duplex is preferentially assembled into the RNA-induced silencing complex (RISC), which subsequently acts on its target by translational repression or mRNA cleavage, depending, at least in part, on the level of complementarity between the small RNA and its target. ORF, open reading frame. Reproduced from He and Hannon, **Nature Reviews Genetics**, 2004[27].

contains the Drosha (RNAse-III-like enzyme)/Pasha (DGCR8 in humans, dsRBD partner) heterodimer[113-116]. The pre-miRNAs are subsequently shuttled out of the nucleus by a member of the importin-β family of nuclear import/export factors, and once in the cytoplasm, a Dicer family member removes the miRNA from its stem-loop, whereupon it is shuttled into the RISC[78,79,117,118]. This is in contrast to siRNAs who emerge from long, contiguously base-paired (>100 bp) cytoplasmic dsRNA, but go through a similar maturation cascade of dsRNA to Dicer to ~21-nt dsRNA to the RISC[119].

In the natural setting, organisms seem to make an honest effort at distinguishing miRNAs from siRNAs. This is logical considering that miRNAs regulate a variety of cellular processes, some of which may require fine-tuning, rather than complete annihilation, of their expression for optimal performance[120]. siRNAs, on the other hand, are likely generated due to an intrusive or unexpected event, such as viral infection, that must be quelled quickly and efficiently. Furthermore, infiltration of small RNAs from one pathway into the other could potentially reduce the potency of their functions. As such, it has been suggested that viruses themselves encode small RNAs, hijacking the miRNA machinery to regulate their own expression, and perhaps even diluting anti-viral miRNAs transcribed by the host genome[121,122]. Because of its well-characterized *in vivo* and *in vitro* RNA silencing systems, perhaps the most simplified model organism for studying how and why this inherent distinction takes place between miRNAs and siRNAs is the fruit fly[123,124].

In *Drosophila*, the miRNA and siRNA pathways are neatly separated during the central phase of small RNA maturation, "Dicing", and the fruit fly genome encodes two

Dicer proteins, Dcr1 and Dcr2[125,126]. While Dcr1 was originally thought to be the main small RNA generator in fruit flies, it was later shown that Dcr2, heterodimerized with its double-stranded RNA binding domain (dsRBD) partner, R2D2 (named for its 2 dsRBD domains, R2, and association with Dcr2, D2), produced the majority of siRNAs[7,127]. Conversely, genetic data found that Dcr1 exclusively begot miRNAs, not siRNAs, thus providing clues into a likely checkpoint mechanism for small RNA categorization[125]. How does each Dicer know which pathway to place its small RNA product into? Can they recognize the difference between a miRNA precursor and that of an siRNA? The answer to the latter question is yes, but they need help. Wang and colleagues observed that Dcr2 was able to cleave long dsRNA into 21-mers without R2D2, but that R2D2 was required to bridge siRNA production to siRNA maturation, culminating with siRNA placement into the RISC[127]. R2D2's role in maturation was found to be in sensing which strand of the siRNA duplex should enter the RISC[128]. Defined as 'functional asymmetry', the process of strand selection by the RISC is determined, almost exclusively, by base-pairing strength in the 5′ region on either end of the siRNA duplex[129,130]. Simply, the strand with lower thermodynamic stability at its 5′ terminus will most often be associated with the RISC, while the other strand is degraded. R2D2 associates with the termini of higher base-pairing strength, possibly positioning a helicase to initiate unwinding from the less stable end, eventually sending that strand into an Ago[128]. Recently, a binding partner of Dcr1, called Loquacious (Loqs, a homolog of Tar Binding Protein, TRBP, in humans), has been uncovered[28,30,42,131]. Loqs is almost identical in domain composition to R2D2, except that it contains 3, rather than 2 dsRBDs. It should be noted that an

uncharacterized splice variant of Loqs contains only 2 dsRBDs, and this gene product does not associate with Dcr1. This suggests the C-terminal dsRBD is likely necessary for Dcr1/Loqs heterodimerization, consistent with previous reports detailing TRBP heterodimerization with a separate dsRNA-binding protein, PKR[132]. Dcr1 can produce siRNAs from a long dsRNA template in the absence of Loqs, similar to Dcr2, but when bound to Loqs, Dcr1 will leave these dsRNAs untouched. Instead, the Dcr1/Loqs heterodimer will only process pre-miRNA-like stem loops into what eventually become miRNAs[131]. It is unclear whether Loqs plays an analogous role to R2D2 in terms of miRNA strand selection after excision from the pre-miRNA, and Dcr 2/R2D2 mediated processing of pre-miRNA has not been described. Together, these data suggest the dsRBD partners of Dicer proteins direct the flow of small RNA traffic into the respective effector complexes.

RNAi effector proteins

At the heart of all RNA silencing phenomenon lies an effector complex called the RISC (or RITS in *S. Pombe*)[9,61]. This complex, consisting of numerous cofactors, and coming in a variety of sizes, contains two central components, an Ago family member and a small RNA guide[20]. While the RISC is associated with all known RNA silencing functions, from DNA methylation to translational repression, perhaps the burning question in RNAi up to this year was; what factor cleaves target RNAs, e.g. who or what was the elusive "Slicer"? It had been known that within RISC, small RNAs were tightly associated with the Ago proteins, and cleavage activity co-purified along with them[12,13,17].

However, there were no nucleolytic domains predicted within the Agos. A breakthrough in the field came when the structure of an Archaeal Ago (*Pyrococcus furiosus* Ago, PfAgo) was determined by Joshua-Tor and colleagues (Figure 4)[133]. Likely a shock to many, this Ago family member contained a cryptic, RNAse-H-like domain, similar to what one would expect based on biochemical characterization of the RNAi cleavage process[134-136]. A separate nuclease, Tudor-SN, co-purifies with RISC, and is a hyper-edited dsRNA-specific nuclease with an as-yet undefined biological function[137,138]. To date, crystal structures of two Archaeal Agos have been determined (PfAgo and *Archaeoglobus fulgidus* piwi, AfPiwi), with and without associated RNA guides[133,139-141]. Though neither of these Archaeal proteins have been described as a ribonuclease, at least one human and mouse Ago (eiF2c2, now known as Ago2) and both RISC-associated fruit fly Agos (Ago1 and 2) contain a catalytically active configuration of amino acids within their RNAse-H-like domain[142-145]. Curiously, regarding the human Ago family (Ago1-6), ectopic expression of these proteins suggests that each can bind endogenous or exogenous mature, single-stranded small RNAs with grossly similar affinity[144]. However, as described, only Ago2 can direct target RNA cleavage. In mice, Ago2 (Ago2) is essential for development, while other Ago members are dispensable, suggesting that RNA cleavage (or an unknown function of Ago2) plays an integral biological role for which other Ago members are unable to compensate[144]. Furthermore, the true functions of non-cleaving Agos have yet to be elucidated in mammalian systems and it is unknown whether or not each Ago associates with particular small RNAs (miRNAs, siRNAs or even tRNA) in an endogenous, not ectopic, context[146].

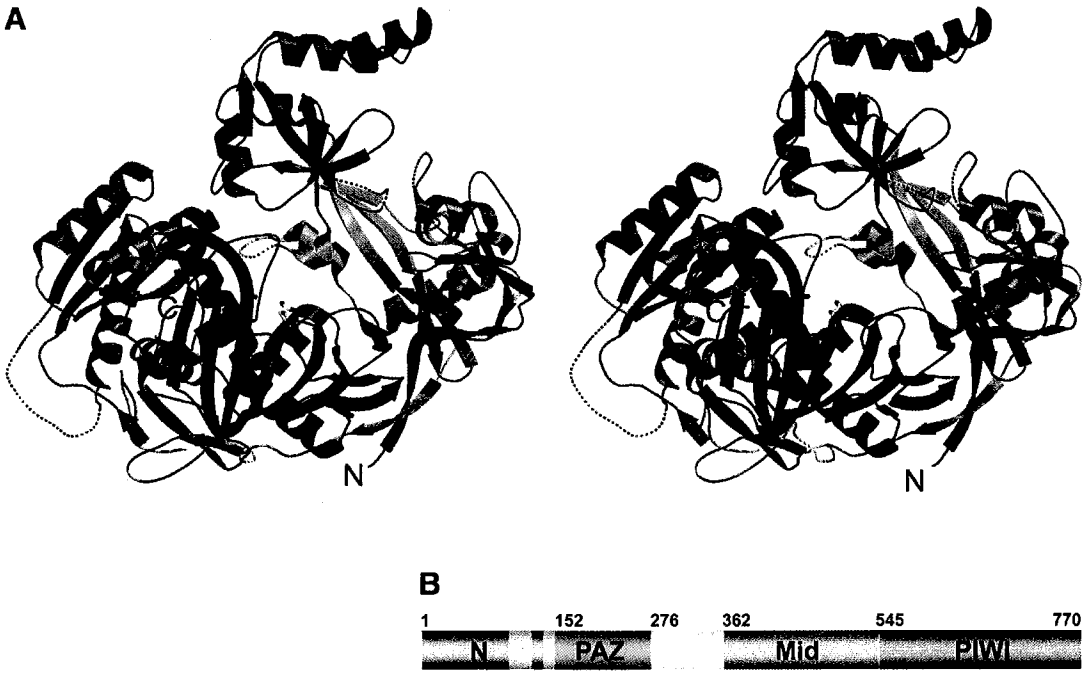

Figure 4. Crystal structure of *P. furiosus* Argonaute.

A. Stereoview ribbon representation of Argonaute showing the N-terminal domain (blue), the "stalk" (light blue), the PAZ domain (red), the middle domain (green), the PIWI domain (purple), and the interdomain connector (yellow). Active site residues are drawn in stick representation. Disordered loops are drawn as dotted lines. **B.** Schematic diagram of the domain borders. Reproduced from Song et al., **Science**, 2004[133].

Additionally, for at least one of the Archaeal proteins, small RNAs may not be the preferred substrate. Rather, it holds a higher affinity for ssDNA and dsDNA[141]. Together, these observations raise a few questions. First and foremost, what is the function of Ago proteins in Archea? Are they involved in transcriptional or translational control? As the Archaeal Agos cannot cleave RNA, did the ability of Ago to direct mRNA cleavage come later on the evolutionary timeline? Do Archaeal Agos use small DNAs as a guide, rather than small RNAs or do they bind directly to genomic DNA in their normal capacity? If these Archaeal Agos do incorporate DNA as a guide, do the Agos and RNAse-H share common ancestry or did they evolve independent of one another?

While little is known about the biological niche of Archaeal Agos, much has been learned about these proteins in their distant metazoan cousins[15]. For starters, there is considerable breadth in the number of Ago members across species. Genomic sequencing predicts at least 10 members in *A. thalina*, 5 members in *D. melanogaster*, 24 members in *C. elegans*, 6 in mice, 8 in humans, and only a single member in *S. pombe*. The Ago family is defined by the presence of a PIWI (site of the RNase-H-like fold) and/or PAZ domain (for Piwi/Argonatue/Zwille, this is absent in Archaeal Agos)[15,147]. Recent crystallographic studies have shown the PAZ domain to be involved in small RNA binding (notably to 3′ dangling ends of a small RNA duplex[148,149].) Ago proteins are also known to directly interact with Dicer family members, and this association likely takes place between an RNAse-III domain of Dicer and the PIWI domain of Ago[12,43,131,150]. It should also be noted that bioinformatic analysis predicts that many Dicer

family members across eukarya also contain a PAZ domain (*S. Pombe* Dicer is a notable exception). Therefore, it is conceivable that during siRNA production, Dicer passes a small RNA directly from its RNAse-III domain into the waiting PIWI domain of an empty Ago. After this passage, the Dicer/dsRBD-partner/Ago complex could orient the siRNA in such a way that it promotes proper strand entry into Ago by assisting the 3′ terminus of the eventual guide strand into the Ago PAZ domain and the 3′ terminus of the strand to be degraded into the Dicer PAZ domain. In *Drosophila*, a function of R2D2 binding to the more thermodynamically stable end of an siRNA duplex could be in preventing Dicer binding to the guide strand's 3′ region, orienting the proper transfer from Dcr to Ago[128].

In *D. Melanogaster*, similar to Dcr1 defects, only the miRNA pathway is disrupted by Ago1 mutation, while long dsRNA or siRNA mediated gene silencing is unaffected[125,143]. Conversely, as in Dcr 2 mutants, Ago2 mutation ablates gene silencing via exogenous dsRNA triggers, and the miRNA pathway remains functional[125,143]. Fruit fly, Dcr1, Dcr 2, Ago1 and Ago2 co-sediment as part of a single, large ribonucleoprotein complex *in vitro*, suggesting that spatial separation of siRNA and miRNA pathway components is unlikely to be involved in distinguishing which pathway a small RNA will eventually enter[151]. As described earlier, this decision is made by Loqs and R2D2, which link their respective Dicer partners to a particular Ago[28,30,42,127,128,131]. R2D2, in addition to being an siRNA symmetry sensor, bridges Ago2 specifically to Dcr 2, and to date no miRNAs have co-purified with Ago2. Similarly, Loqs provides the connection between Ago1 and Dcr1[30,131]. However, loading of Ago1 via Dcr1 may be more leaky than that of

Dcr 2/Ago2, as RNAi driven by long dsRNA was shown to be dependent on Ago1 in embryos (this conflicts with recent reports suggesting no association between long dsRNA induced RNAi and Ago1), and siRNAs derived from long dsRNA co-IP with both Ago2 and Ago1[152,153].

RNA-silencing pathway functions

Recently, Schedl and colleagues identified a function of *Drosophila* Ago2 in the absence of an exogenous dsRNA silencing trigger when they observed its requirement for a variety of events in early embryogenesis (heterochromatin assembly, nuclear division and migration and germ-cell formation[154]). The Ago2 mutants also displayed defects in cytoskeleton assembly, consistent with observed Ago association with microtubules in *Parcentrotus lividus* (Sea Urchin)[155]. Moreover, a previously unknown mode of ribonucleoprotein (RNP)-dependent stabilization of the mitotic spindle has been uncovered[156]. Here, a large RNP-complex maintains the spindle assembly through RNA dependent binding of microtubules. Interestingly, this complex contains Rae-1, a protein that interacts directly with importin-ß, the cousin of a miRNA export component. Maintenance of heterochromatin by Ago2 could be similar in mechanism to that of piwi or aubergine, which assist or establish localization of the heterochromatin proteins HP1 and HP2[38,72]. Though members of the Ago family (both have PIWI domains), neither piwi nor aubergine contain a PAZ domain and neither is known to directly interact with small RNAs. Furthermore, proper localization of Ago2 and Dcr1 in *D. melanogaster* ovarioles depends, indirectly, upon aubergine[157]. While aubergine is required for siRNA-

directed and repeated associated RNA (ra-siRNA) silencing, it is possibly dispensable for miRNA directed silencing[158,159]. Similar to mutations upstream in the RNAi pathway, loss of piwi results in defective germ-line stem cell division[28-30,160]. Moreover, connections between the core RNAi pathway components and cell-fate or differentiation are not limited to fruit flies[15,39,161].

RNAi and disease

As data continues to accumulate connecting RNAi with essential and diverse cellular and developmental phenomenon, it begs the question, what role does RNA silencing play in human disease? Recently, direct links between abnormalities in the steady-state levels of miRNAs and cancer have come to light[162]. It had been established that the genomic locus 13q31, a region that contains the miRNA polycistron miR17-19, was amplified in human B cell lymphomas[163]. Furthermore, miRNAs are known to be involved in directing B cell lineage choice in mice, implying a role for miRNAs in proper development of immune cells[32]. He et al have found that when the miR17-19-containing locus is over-expressed in a murine B cell lymphoma model, tumor onset in these mice is dramatically faster, implying that over-expression of miRNAs can be intimately involved in promoting at least one cancer type[36]. Curiously, over-expression of individual miRNAs from within the locus did not affect disease onset, although another group has described a correlation between over-expression of a separate miRNA, miR155, and B cell lymphomas[164]. Conversely, over-expression of small RNAs does not always correlate with cancer incidence or progression. Rather, global miRNA analysis by

separate groups has shown that many cancer cell types display an overall reduced miRNA expression profile when compared to non-cancerous cells, and specifically, loss of the 13q14 locus, which encodes miR15 and 16, is a potential indicator for B cell lymphomas[165,166]. Sorting through these tantalizing, but preliminary results will undoubtedly reveal the intricate balancing act of miRNAs on proper regulation of gene expression, and may even shed light on the cellular functions of the genes upon which they act.

Though the correlation between endogenous RNA silencing and human disease is just now coming to light, much like anti-sense technology in the 1980's and 90's, the idea that exogenously triggered RNAi could be used to treat a variety of conditions had been floated since its discovery[167-171]. This vision took a step closer to reality when Tuschl and colleagues presented evidence that synthetic siRNAs could induce specific and potent RNAi in human cell lines[3]. Since that time, small RNA chemistry and delivery vehicles have been enhanced to the point where RNAi can be induced in living, breathing animals[172-177]. In one of many such cases, Davidson and colleagues induced RNAi in mouse brains by intracerebellar injection of a recombinant adenovirus expressing short hairpin RNAs[177]. The resultant siRNAs targeted a mutant ataxin-1 allele, which causes polyglutamine-induced neurodegenration through a disease known as spinocerebellar ataxia type 1 (SCA1). Astoundingly, RNAi treatment of these mice led to the rapid alleviation of most symptoms involved with SCA1. However, while this technique has been proposed, or is entering clinical trials for cures of Huntington's disease, diabetes, a

variety of viruses, and age-related macular degenearation (AMD), amongst others, the specificity, or off-target effects, of RNAi has been called into question[168,178,179].

Concerns regarding RNAi-based therapy

In order to understand and utilize both the potency and specificity of RNAi, one must first grasp the mechanisms by which small RNAs and the RISC find, associate with and subsequently cleave their targets. Regarding miRNAs, multiple lines of evidence, both from the laptop and benchtop, have discerned that a region now referred to as the 'seed sequence', or nucleotides 2-8 of a small RNA, is remarkably conserved between both the miRNA and the reciprocal region in the target, throughout evolution[24,102,103]. This conservation implies that it must be important for the interaction between the small RNA and its substrate, and as it turns out, the 'seed sequence' is perhaps the major site of nucleation between a miRNA or siRNA and its target. Though, as Cohen and colleagues have recently discovered, a mismatch within the seed can be counterbalanced with multiple, compensatory base-pairs at the opposite end of the small RNA-target pair[180]. However, while pairing within this region may ensure small RNA association with a substrate RNA, it is not sufficient for cleavage, and both *in vitro* and *in vivo* evidence suggests that a single, contiguous turn of an A-form helix (10 base-pairs) overlapping the 5′ and central regions of a small RNA-target pair is required for minimal target destruction[16,135,181-183]. Lastly, pairing at the 3′ region of the siRNA-target duplex appears to be involved in stabilizing the overall helical geometry around the cleavage site, or is perhaps associated with RISC protein conformational changes after or during target

binding, and it contributes surprisingly little to the overall strength of the RISC-target interaction[16,119]. Therefore, the different regions of an siRNA contribute to the separate facilities of RISC association and activity, with the 5′ region being important for binding, the central region is the active site, and it has been speculated that the 3′ region assists in maintenance of geometry within the duplex and/or between the protein-RNA interactions. The fact that only 10 out of 21 nucleotides need to be paired to evoke the basal level of target RNA destruction implies that RNAi could be dramatically (~19-fold) less specific than first thought[16,135,182]. In addition, sequence-specific effects are triggered not only by the small RNA-target interaction; particular sequences within a small RNA itself can induce a systemic immune response in mice, likely through an interaction with Toll-like receptor 7 (TLR7), and mediated by interferon-α (IFN-α)[184]. However, as allele-specific RNAi has proven, careful selection of siRNAs, with attention to the biological details of RISC association with its targets and cellular responses to RNA silencing triggers, will ensure that this phenomenon propels the research of, and perhaps can even be used itself to treat both congenital (Huntington's, ALS, diabetes, etc.) and environmental (HIV, adenovirus, parasitic) disease[169,185-189].

CHAPTER II: ATP REQUIREMENTS AND SMALL INTERFERING RNA STRUCTURE IN THE RNA INTERFERENCE PATHWAY

SUMMARY

We examined the role of ATP in the RNA interference (RNAi) pathway. Our data reveal multiple new ATP-dependent steps and suggest that the RNAi reaction comprises at least four sequential steps: ATP-dependent processing of double-stranded RNA into small interfering RNAs (siRNAs), incorporation of siRNAs into an inactive ~360 kDa protein/RNA complex, ATP-dependent unwinding of the siRNA duplex to generate an active complex, and ATP-independent recognition and cleavage of the RNA target. Furthermore, ATP is used to maintain 5′ phosphates on siRNAs. A 5′ phosphate on the target-complementary strand of the siRNA duplex is required for siRNA function, suggesting that cells check the authenticity of siRNAs and license only bona fide siRNAs to direct target RNA destruction.

INTRODUCTION

In animals, double-stranded RNA (dsRNA) specifically silences expression of a corresponding gene, a phenomenon termed RNA interference (RNAi[1,190]). One function of the RNAi machinery is to maintain the integrity of the genome by suppressing the mobilization of transposons and the accumulation of repetitive DNA[191-194]. The RNAi machinery may also defend cells against viral infection (reviewed in [195-199]) and regulate expression of cellular genes[200,201].

RNAi bears striking similarity to post-transcriptional cosuppression in plants (posttranscriptional gene silencing, PTGS[202-204]) and *Neurospora crassa* (quelling[205,206]). Genetic screens in worms, fungi, plants, and green algae have identified genes required for RNAi or PTGS[14,207-213], and the RNAi and cosuppression pathways in *Caenorhabditis elegans*, *Neurospora*, and *Arabidopsis thaliana* require some of the same genes[193,210,214-216]. Mutations in a subset of these genes permit the mobilization of transposons[14,192,217], whereas a second class of mutants, including the *rde-1* and *rde-4* loci, are defective for RNAi but show no other phenotypic abnormalities[14]. Rde-1 is a member of the PPD family of proteins (PAZ and PIWI Domain), which are characterized by an N-terminal 'Piwi/Argonaute/Zwille' (PAZ) domain and a C-terminal 'PIWI' domain[147]. PPD proteins are required not only for RNAi in worms (RDE-1[14]) and flies (Ago2[12]), but also for PTGS in plants (AGO-1[210]) and quelling in fungi (Qde1[214]).

In vitro, dsRNA targets mRNA for cleavage in lysates of early *Drosophila* embryos or extracts of cultured *Drosophila* S2 cells[6,9,124]. RNAi in vitro requires ATP[6]. The molecular basis for the ATP requirement is due, in part, to a requirement for ATP in

the initial processing of long dsRNA into the 21-25 nt small interfering RNAs (siRNAs) which guide target cleavage[4,6-8]. siRNAs have been detected in vivo in plants[8,218], flies[219], worms[220], and trypanosomes[221]. Recent studies with synthetic RNA duplexes demonstrate that each siRNA duplex cleaves the target RNA at a single site[4]. Two- or three-nt overhanging 3′ ends within the siRNA duplex are required for efficient target cleavage[4]. Such 3′ overhangs are characteristic of the products of an RNase III cleavage reaction, and, in cultured *Drosophila* S2 cells, cleavage of the dsRNA into siRNAs requires the multi-domain RNase III enzyme, Dicer[7]. Intriguingly, Dicer interacts directly or indirectly with Ago-2, a PPD protein required for RNAi in cultured *Drosophila* S2 cells[12]. Dicer orthologs are found in the genomes of plants[222], worms, fission yeast, and humans[7,223]. In worms, the Dicer ortholog, Dcr-1, is required both for RNAi[224] and for the maturation of small temporal RNAs (stRNAs), single-stranded 21-22 nt RNAs that control the timing of development[79]. Dicer in flies and humans is likewise responsible for generating the *let-7* stRNA[78].

Here, we dissect the role of ATP in the RNAi pathway. Our data suggest that the RNAi reaction comprises at least four sequential steps: ATP-dependent dsRNA processing, ATP-independent incorporation of siRNAs into an inactive ~360 kDa complex, ATP-dependent unwinding of the siRNA duplex, and ATP-independent recognition and cleavage of the target RNA. Remarkably, a 5′ phosphate is required for entry of an siRNA into the RNAi pathway. In vitro, this phosphate is maintained by a kinase, which can recognize authentic siRNAs. Furthermore, the phosphorylation status of the 5′ ends of an siRNA duplex is monitored by the RNAi machinery, suggesting that

cells check the authenticity of siRNAs, ensuring that only bona fide siRNAs direct target RNA destruction.

RESULTS AND DISCUSSION

ATP and dsRNA processing

In vitro and in vivo studies suggest that RNAi is a multi-step process that begins with the ATP-dependent processing of long dsRNA into 21-23 nt siRNAs by Dicer protein, perhaps in conjunction with other proteins. In *Drosophila* embryo lysates, siRNAs are produced to six-fold higher levels in high ATP concentrations than in low[6], and dsRNA cleavage by immunoprecipitated Dicer protein requires ATP[7]. As a starting point for defining the role of ATP in the RNAi pathway, we re-examined the ATP-dependence of siRNA production during the initial phase of the cleavage reaction, when the rate of dsRNA cleavage is linear (Figure 1). A prior study assessed siRNA production at steady-state. The experiments presented here employed a revised ATP-depletion strategy that reduced ATP-levels by at least 5,000-fold, to < 100 nM. During the first 16 min of incubation of a uniformly ^{32}P-radiolabeled dsRNA derived from the *Renilla reniformis* luciferase (*Rr*-luc) gene, the rate of siRNA production was ~47-fold faster in the presence of ATP and an ATP-regenerating system (filled squares) than in their absence (open squares). In the presence of ATP, siRNA production increased dramatically after about 4 min incubation. This initial lag might reflect the ATP-dependent rearrangement of the dsRNA and/or the proteins required to produce siRNAs, such as Dicer. Consistent with this idea, we did not detect such an initial lag phase for

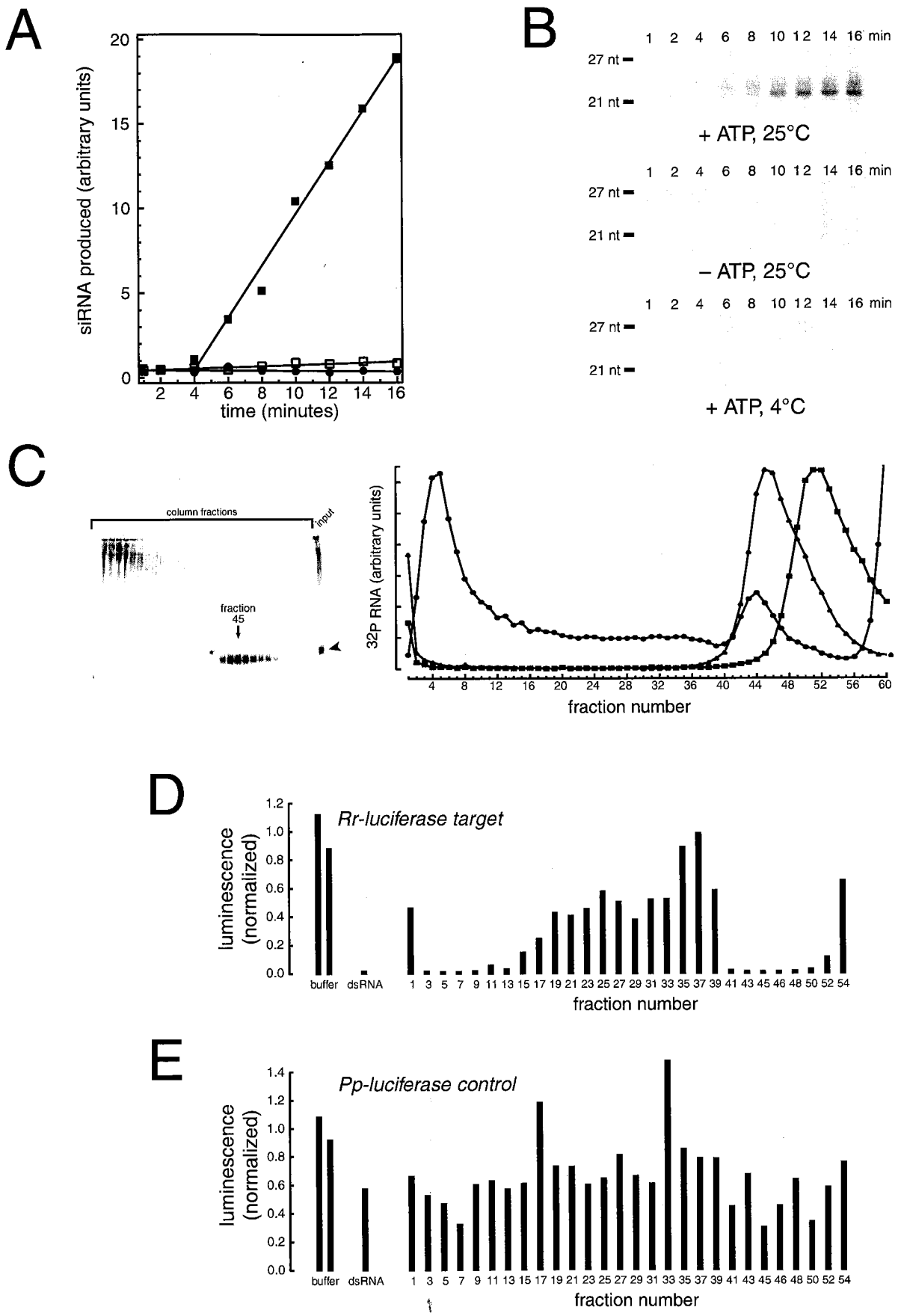
A
siRNA produced (arbitrary units)
time (minutes)
B
1 2 4 6 8 10 12 14 16 min
27 nt
21 nt
+ ATP, 25°C
– ATP, 25°C
+ ATP, 4°C
C
column fractions
input
fraction 45
32P RNA (arbitrary units)
fraction number
D
Rr-luciferase target
luminescence (normalized)
buffer
dsRNA
fraction number
E
Pp-luciferase control
luminescence (normalized)
buffer
dsRNA
fraction number

Figure 1. Production of the siRNAs that mediate sequence-specific interference requires ATP. (A) Measurement of the initial rate of siRNA production from uniformly ^{32}P-radiolabeled 501 bp *Rr*-luc dsRNA in the presence of 1mM ATP at 25°C (filled squares) or 4°C (filled circles) or at 25°C in the absence of ATP (open squares). (B) The data presented graphically in (A). (C) Isolation of native siRNAs by gel filtration. Uniformly ^{32}P-radiolabeled 501 bp *Rr*-luc dsRNA was processed in a standard RNAi reaction, deproteinized, and fractionated on a Superdex-200 gel filtration column. Fractions were analyzed by electrophoresis on a 15% acrylamide sequencing gel (left panel) and by scintillation counting (right panel, black circles). Double-stranded (red triangles) and single-stranded synthetic siRNAs (blue squares) were chromatographed as standards. The native siRNA peak and the synthetic siRNA duplex marker do not precisely co-migrate, likely because the native siRNAs are a mixture of 21- and 22-nt species and the synthetic siRNAs are 21 nt. (D, E) Analysis of each column fraction for RNAi activity in an in vitro reaction containing both *Rr*-luc and *Pp*-luc mRNAs. Luminescence was normalized to the average of the two buffer controls.

siRNA production in the absence of ATP. siRNA production in the presence of ATP required incubation at 25°C; no siRNAs were produced in the presence of ATP at 4°C (filled circles). These data quantitatively confirm previous observations that cleavage of the dsRNA into siRNAs requires ATP.

siRNA duplexes are bona fide intermediates in the RNAi pathway

RNAi can be initiated with synthetic siRNAs in vitro and in vivo suggesting that siRNAs are intermediates in the RNAi reaction. However, when purified from a denaturing gel, siRNAs generated by cleavage of dsRNA reduced target mRNA expression by only ~2-fold (unpublished data). To assess directly if the products of dsRNA cleavage—native siRNAs—are true intermediates in the RNAi reaction, we developed an isolation procedure designed to preserve their proposed double-stranded character. Uniformly ^{32}P-radiolabeled *Rr*-luc dsRNA was incubated in a standard RNAi reaction in the absence of target mRNA, deproteinized, and fractionated by gel filtration. Two peaks of radioactivity eluted from the column (Figure 1C, black circles). The first corresponded to unprocessed dsRNA; the second peak contained native siRNAs. The elution position of the native siRNAs from the gel-filtration column coincided with that of a synthetic siRNA duplex (red triangles), but not a single-stranded 21 nt RNA (blue squares). Thus, the siRNAs produced by Dicer-mediated cleavage of long dsRNA are double-stranded.

The gel filtration procedure was repeated with unlabeled *Rr*-luc dsRNA processed in vitro into native siRNAs, and the column fractions assessed for their ability to mediate

sequence-specific interference when added to lysate in the presence of ATP. Two peaks of interfering activity were detected (Figure 1D). The first peak, fractions 3-13, corresponded to unprocessed dsRNA and served as an internal control for the experiment. The second peak, fractions 41-50, corresponded to the native siRNAs. None of the column fractions exhibited any significant degradation of an unrelated *Photinus pyralis* luciferase (*Pp*-luc) mRNA (Figure 1E). Pre-heating the purified native siRNAs to 95°C for 5 min abolished their ability to initiate interference, suggesting that only double-stranded siRNAs can enter the pathway (data not shown). These results, together with those of Tuschl and coworkers, demonstrate that siRNAs are true intermediates in RNAi, not the products of an off-pathway side reaction[4]. Furthermore, they support the original proposal of Hamilton and Baulcombe that siRNAs are the specificity determinate for both PTGS and RNAi[8].

A second ATP-dependent step in RNAi

In performing the experiments in Figure 1D and 1E, we observed that none of the column fractions mediated sequence-specific interference when incubated with lysate in the absence of ATP. This observation was expected for the first peak (fractions 3-13), since dsRNA cleavage into siRNAs requires ATP, but unexpected for the second peak, which corresponds to fully processed, native siRNAs. Therefore, we asked if interference mediated by siRNAs, rather than dsRNA, also required ATP. Native siRNAs isolated by gel-filtration were added to a standard RNAi reaction in the presence or absence of ATP (Figure 2), incubated at room temperature for 30 min, and then a *Rr*-

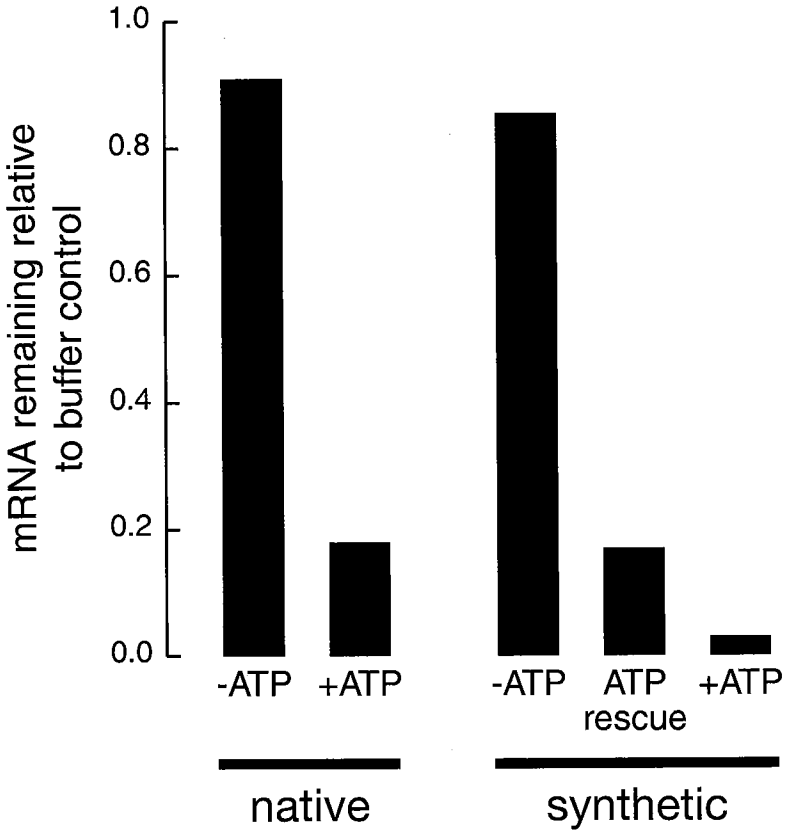
mRNA remaining relative to buffer control
1.0
0.8
0.6
0.4
0.2
0.0
-ATP
+ATP
-ATP
ATP rescue
+ATP
native
synthetic

Figure 2. RNAi mediated by siRNAs requires ATP. Native siRNAs targeting *Rr*-luc were assayed for RNAi against an *Rr*-luc RNA target. A synthetic siRNA duplex targeting *Pp*-luc was tested for RNAi against a *Pp*-luc mRNA.

luc target mRNA was added. In the presence of both native siRNAs and ATP, the target RNA was rapidly degraded (native, +ATP). In contrast, only non-specific degradation of the target RNA occurred in the absence of ATP (native, -ATP). These results point to the existence of a second ATP-dependent step, downstream in the RNAi reaction from dsRNA processing. However, an alternative explanation is that undetected dsRNA contaminated the native siRNA preparation. Since dsRNA processing requires ATP, this could, in principle, explain the apparent ATP-requirement for native siRNA-directed interference. To exclude this possibility, we assessed the ATP-dependence of interference directed by a chemically synthesized siRNA duplex targeting the *Pp*-luc mRNA (Figure 2). In the absence of ATP, no sequence-specific interference occurred (synthetic, -ATP). Addition of ATP and an energy regenerating system only partially restored normal ATP levels, because of the high concentrations of glucose used to deplete ATP. Under these conditions, partial interference was observed (synthetic, ATP rescue). In contrast, in a standard RNAi reaction containing 1 mM ATP, synthetic siRNAs mediated potent interference (synthetic, +ATP). Therefore, interference by both native and synthetic siRNAs requires ATP, revealing one or more novel ATP-dependent step(s) distinct from the ATP-dependent cleavage of long dsRNA into siRNAs.

Target recognition and cleavage are ATP-independent

One possible source for the ATP requirement might be that target cleavage, like the cleavage of dsRNA into siRNAs by Dicer, requires ATP. To test if either target recognition or cleavage requires ATP, we incubated a 501 bp *Rr*-luc or a 505 bp *Pp*-luc

dsRNA in a standard RNAi reaction to permit its processing into native siRNAs, then removed ATP from the reaction and evaluated its ability to cleave a corresponding target RNA (Figure 3). Two different strategies were employed to remove ATP from the reaction after the initial dsRNA processing step. In both strategies, the interfering RNA—dsRNA or siRNA—was pre-incubated with lysate in the presence of ATP, then ATP was removed from the reaction, and finally the target RNA was added in the presence or absence of ATP. In the first strategy (Figure 3A), the ATP regenerating enzyme, creatine kinase, was inactivated with *N*-ethylmaleimide (NEM), unreacted NEM quenched, and ATP depleted with hexokinase and glucose (Figure 3B, filled symbols). Then, a *Pp*-luc target mRNA was added to the reaction. Lysate treated with NEM, then DTT, prior to the addition of the creatine kinase supported RNAi (data not shown). In a separate series of controls, DTT was added prior to the NEM, and no hexokinase was added (open symbols). High ATP levels were maintained during the dsRNA processing portion of the experiment and throughout the experiment when DTT was added prior to NEM. However, when the reactions were sequentially treated with NEM, DTT, then hexokinase plus glucose, ATP levels were reduced ~5,000-fold to ≤100 nM. In all conditions in which the 505 bp *Pp*-luc dsRNA was included (triangles), the *Pp*-luc target mRNA was cleaved regardless of the ATP concentration at the time of target RNA addition. Under all conditions, interference remained sequence-specific : a 501 bp *Rr*-luc dsRNA did not affect the stability of the *Pp*-luc mRNA target in the presence (open circles) or absence of ATP (filled circles). Furthermore, when a synthetic siRNA duplex targeting the *Pp*-luc mRNA was first pre-incubated with lysate and ATP, the *Pp*-luc

A

dsRNA processing reaction
(1 mM ATP)
↓
10 mM NEM, 10 min, 4°C
↓
10 mM DTT
↓
hexokinase + glucose, 15 min, 25°C
↓
cleavage reaction, 25°C

B

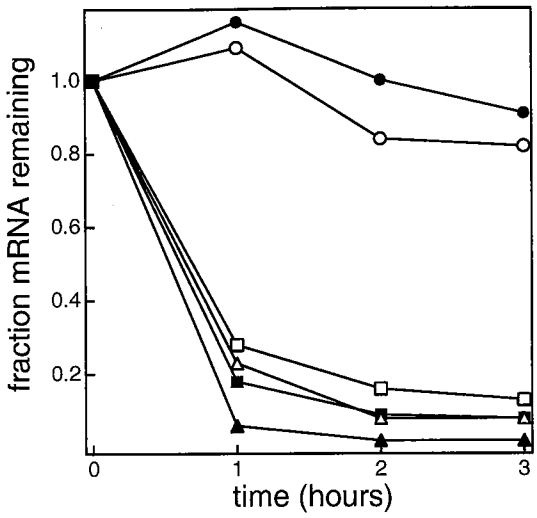

C

dsRNA processing reaction
(1 mM ATP)
↓
10 - 45% $(NH_4)_2SO_4$ cut
↓
dialysis, 16 h, 4°C
↓
hexokinase + glucose, 10 min, 25°C
↓
cleavage reaction, 25°C

D

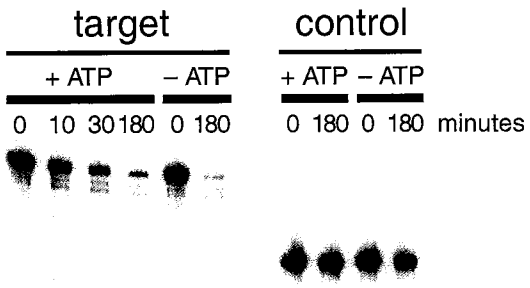

Figure 3. Target recognition and cleavage is ATP-independent. (A) Scheme for depleting ATP from the RNAi reaction after an initial pre-incubation in the presence of ATP. (B) After 30 min pre-incubation with ATP of a 505 bp *Pp*-luc dsRNA (triangles) or a 501 bp *Rr*-luc dsRNA (circles), ATP was depleted by the sequential addition of NEM, DTT, and hexokinase plus glucose (filled symbols), then a *Pp*-luc target mRNA added. In the controls, DTT was added before NEM, and hexokinase was omitted (open symbols). A synthetic siRNA duplex targeting the *Pp*-luc mRNA was also tested (squares). In all cases, the target RNA was a *Pp*-luc mRNA. (C) Alternative scheme for depleting ATP from the RNAi reaction. (D) After pre-incubation of a *Rr*-luc dsRNA with lysate and ATP, recognition and cleavage of a *Rr*-luc target RNA or a control 441 nt control RNA was measured in the presence or the absence of ATP.

target mRNA was subsequently cleaved both in the presence (open squares) and absence (filled squares) of ATP. These results strongly argue that neither target recognition nor target cleavage require ATP as a cofactor, and they suggest that ATP participates in a step prior to the encounter of the siRNA with its RNA target.

Nonetheless, the experiments in Figure 3B cannot exclude a requirement for some other small molecule cofactor (e.g., GTP) in target recognition and cleavage. To examine this possibility, we employed a second strategy to remove ATP and other small molecule cofactors (Figure 3C). A 501 bp *Rr*-luc dsRNA was incubated with lysate and ATP in a standard RNAi reaction, then the siRNA/protein complex was precipitated with ammonium sulfate. The resolubilized ammonium sulfate precipitate was extensively dialyzed to remove small molecule cofactors, then treated with hexokinase and glucose to further deplete ATP. The procedure reduced the initial 1 mM ATP concentration to ≤ 50 nM (data not shown). Furthermore, the dialysis step is expected to have significantly reduced endogenous pools of other nucleotide tri-, di-, and mono-phosphate cofactors. Finally, the ATP-depleted siRNA/protein complex was tested for cleavage of a 501 nt *Rr*-luc target RNA or an unrelated 441 nt control RNA in the presence or absence of ATP (Figure 3D). The *Rr*-luc dsRNA directed efficient target recognition and cleavage in the absence of exogenous ATP. In both the presence and absence of ATP, target cleavage was specific for the *Rr*-luc target mRNA; the control RNA was not cleaved. For ATP or some other small molecule cofactor to be involved in these steps in the RNAi reaction, it would have had to remain associated with the RNAi machinery through 16 h of dialysis

against multiple changes of a 5,000-fold excess of buffer. The simplest explanation is that both target recognition and target cleavage are ATP-independent steps.

The ATP-dependent step identified by the experiments in Figure 2 therefore lies downstream of dsRNA processing but upstream of target recognition. We can envision several types of ATP-dependent steps that might explain our findings. Formation of an siRNA/protein complex might require ATP. Alternatively, association of proteins with the siRNAs might be ATP-independent, but a conformational change in the siRNA itself might require ATP. For example, an ATP-dependent RNA helicase might unwind the two strands of the siRNA prior to its encounter with the target RNA. In support of this idea, proteins with the signature motifs of ATP-dependent RNA helicases have been implicated in RNAi in flies and worms[7,224], PTGS in *Chlamydomonas reinhardtii* and plants[211,225], and in *Stellate* silencing in flies[201].

siRNA-protein complex formation

To detect the formation of a protein complex on siRNAs, uniformly ^{32}P-radiolabeled 501 nt *Rr*-luc dsRNA was incubated in a standard RNAi reaction in the absence of target to permit its cleavage into siRNAs and to permit the resulting siRNAs to assemble into a protein/siRNA complex (siRNP). After 2 h incubation, the reaction was chromatographed on a Superdex-200 gel filtration column. siRNAs were predominantly associated with a ~360 kDa siRNP (Figure 4A). Formation of the siRNP complex required protein, since it was not observed when the complex was treated with proteinase K prior to gel filtration (Figure 1C). A second peak of ^{32}P-radiolabled siRNAs

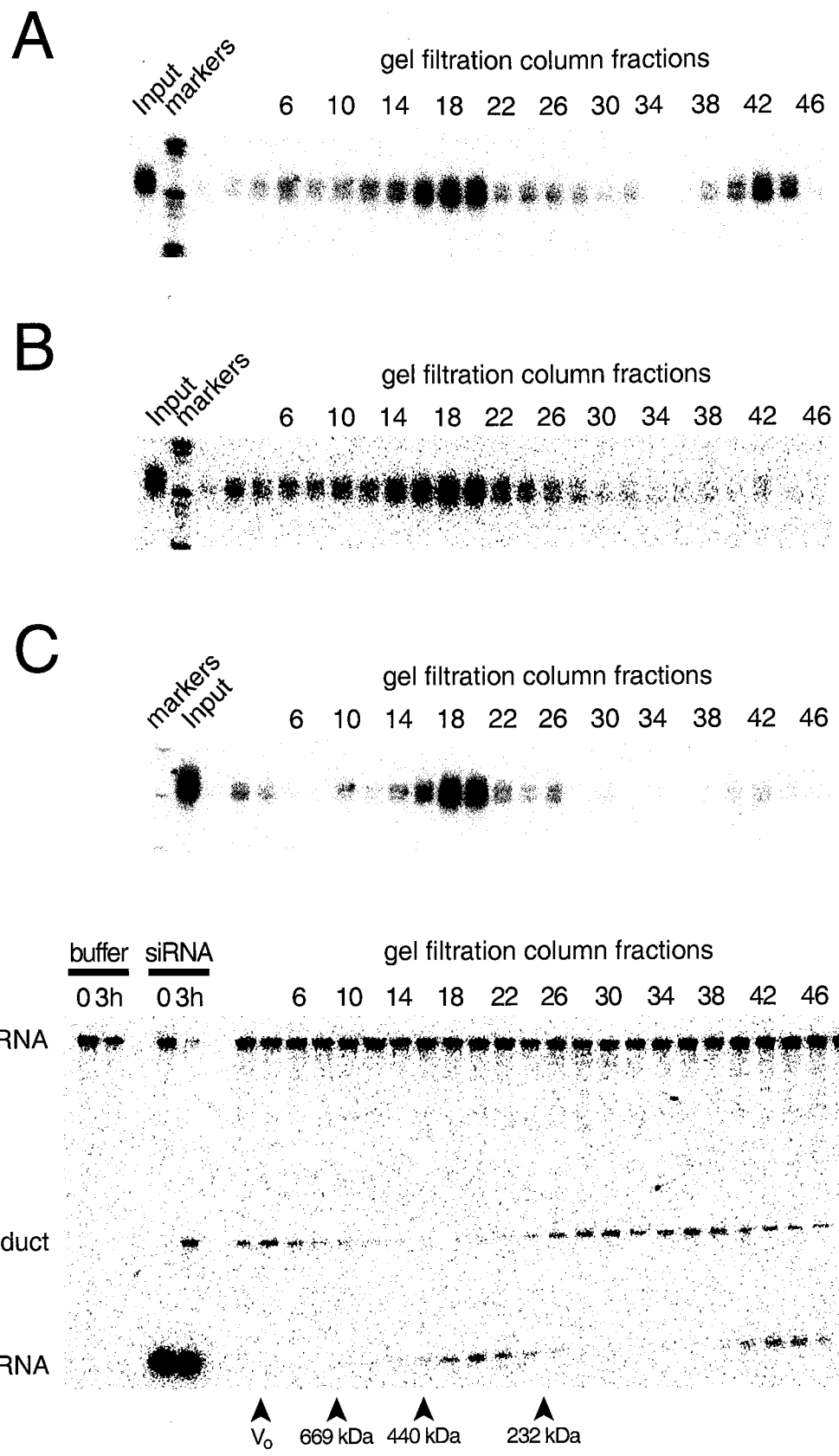
A
Input
markers
gel filtration column fractions
6 10 14 18 22 26 30 34 38 42 46
B
Input
markers
gel filtration column fractions
6 10 14 18 22 26 30 34 38 42 46
C
markers
Input
gel filtration column fractions
6 10 14 18 22 26 30 34 38 42 46
D
buffer
siRNA
0 3h 0 3h
gel filtration column fractions
6 10 14 18 22 26 30 34 38 42 46
target RNA
5´ cleavage product
siRNA
Vo
669 kDa
440 kDa
232 kDa

Figure 4. siRNP complex formation and activity. (A) Analysis of siRNP formation during the processing of a 501 *Rr*-luc dsRNA into native siRNAs in the presence of ATP. (B) Analysis of siRNP formation in the presence of ATP for purified, native siRNA duplexes. (C) As in (B), except in the absence of ATP. (D) RNAi activity of gel filtration fractions prepared as in (B), but using a synthetic siRNA duplex targeting the *Pp*-luc mRNA. The siRNA was incubated in an RNAi reaction for 1 h, then fractionated by gel filtration. A sample of the input to the column was used in a control reaction (siRNA); every other column fraction was analyzed for RNAi activity. The elution position of molecular weight markers for all four panels is shown in (D). V_o, void volume; 669 kDa, Thyroglobulin; 440 kDa, Ferritin; 232 kDa, Catalase.

coincides with siRNAs unbound by protein (compare Figures 1C and 4A), indicating that a significant fraction of the siRNAs generated by dsRNA processing in vitro do not stably associate with protein. Next, purified, ^{32}P-native siRNAs were incubated with lysate either in the presence (Figure 4B) or the absence (Figure 4C) of ATP. The same two siRNA-containing peaks were observed: a ~360 kDa siRNP (peaking in fractions 18-20) and native siRNAs not associated with protein (peaking in fractions 42-46). Thus, assembly of the siRNP does not require ATP.

Recently, Hannon and coworkers reported isolation of an siRNA-containing, ~500 kDa complex from cultured *Drosophila* S2 cells[12]. This ~500 kDa complex contained the target-cleaving nuclease. To assess the capacity of the ~360 kDa siRNP to direct target cleavage, we incubated a single synthetic siRNA duplex in the *Drosophila* embryo lysate in the presence of ATP, then fractionated the reaction by gel filtration on Superdex-200. The siRNA duplex was chosen because it directs cleavage of the 510 nt *Pp*-luc target RNA at a single site, 72 nt from the 5′ cap, yielding a 72 nt RNA product diagnostic of RNAi activity[4]. In these experiments, the synthetic siRNA duplex was 3′ radiolabeled on the sense siRNA strand. Control experiments showed that such a 3′ modified siRNA duplex does not impair the ability of the siRNA to mediate RNAi (data not shown). Thus, the 510 nt target RNA, the 72 nt RNAi cleavage product, and the siRNA itself can be detected simultaneously on a denaturing acrylamide gel. The ability of each gel filtration column fraction to support sequence-specific target cleavage was assessed (Figure 4D). A major peak of radiolabeled siRNA was detected in fractions 18-22, indicating formation of the siRNP complex. Although this siRNP complex contains

virtually all of the siRNAs associated with protein, it was not competent to cleave a target RNA. Instead, two peaks of RNAi activity were observed: one in the void volume of the column (fractions 2-6) and a broad peak of RNAi activity of apparent molecular weight < 232 kDa (fractions 26-40). Surprisingly, these peaks contained barely detectable levels of siRNA, but were nonetheless nearly as active as the unfractionated reaction, despite having suffered dilution from the gel filtration chromatography (compare the amount of ^{32}P-siRNA in the input to the column [lane labeled, "siRNA"] to that in the active column fractions). Control experiments (not shown) demonstrated that little if any degradation of siRNA duplexes occurs in the lysate, indicating that the distribution of ^{32}P-siRNAs accurately reflects the distribution of siRNA in the column fractions. Thus, the majority of siRNAs associated with protein are present in a ~360 kDa siRNP complex that is not competent to cleave a target RNA, whereas a minority of the siRNAs are in a smaller, highly active complex. Mixing experiments (not shown) demonstrated that the fraction containing the ~360 kDa siRNP does not contain an inhibitor of RNAi. We defer to below the question of whether the ~360 kDa complex is a productive intermediate in the RNAi pathway or a non-productive, off-pathway intermediate.

siRNA unwinding during the RNAi reaction

To test if ATP is used during the RNAi reaction to separate the two strands of the siRNA duplex, we developed a method to differentiate siRNA duplexes from single-stranded siRNAs (Figure 5A). In this assay, RNAi was initiated in vitro with a synthetic siRNA duplex in which the sense strand was 3′ radiolabeled. The RNAi reaction was

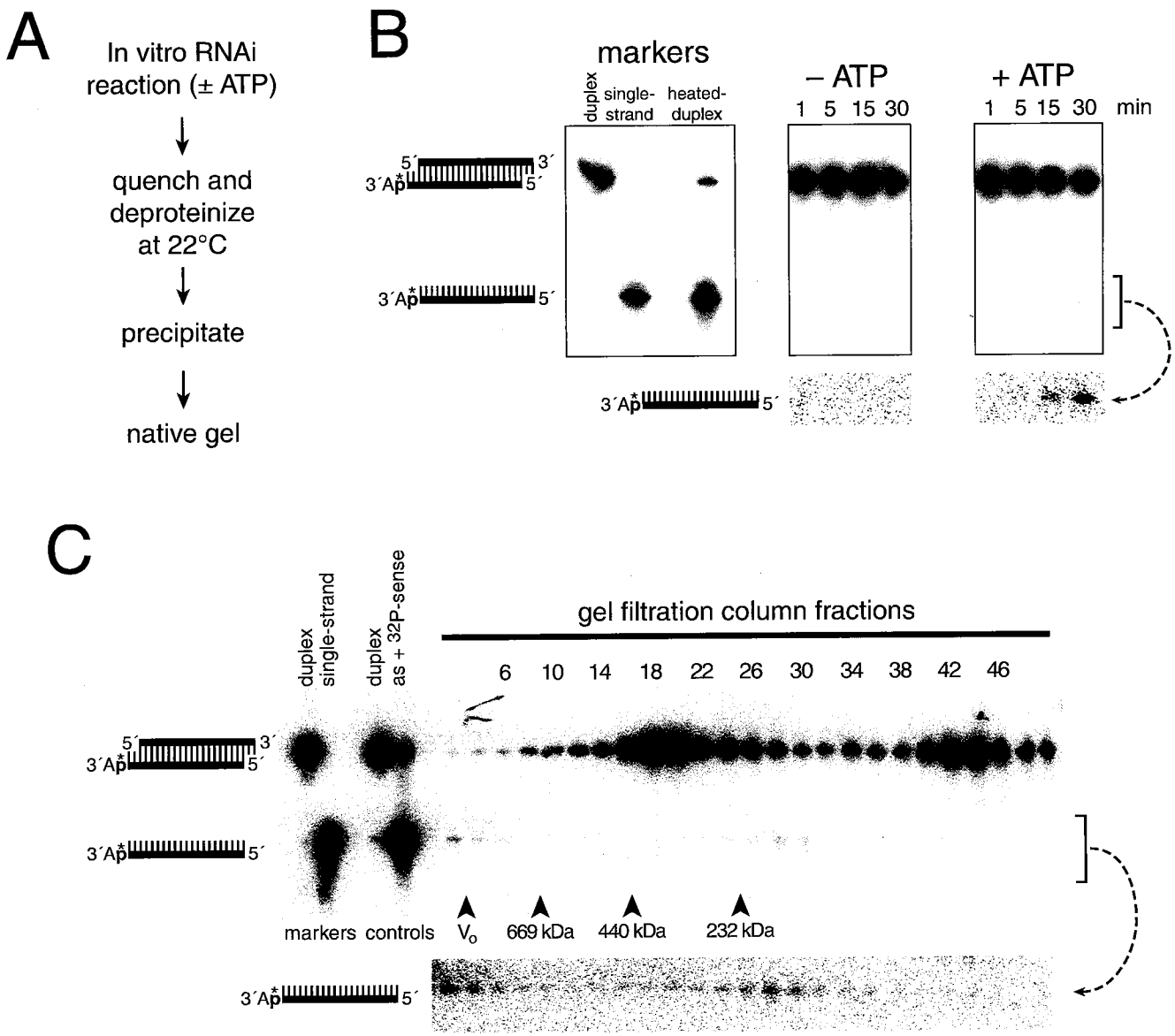
A
In vitro RNAi reaction (± ATP)
quench and deproteinize at 22°C
precipitate
native gel
B
markers
duplex
single-strand
heated-duplex
– ATP
+ ATP
1 5 15 30
1 5 15 30 min
5´
3´
3´Ap*
5´
C
duplex single-strand
duplex as + 32P-sense
gel filtration column fractions
6 10 14 18 22 26 30 34 38 42 46
markers controls
Vo
669 kDa
440 kDa
232 kDa

Figure 5. ATP-dependent siRNA unwinding correlates with RNAi activity. (A) Outline of the assay used in (B) and (C). (B) Native acrylamide gel analysis of siRNA unwinding in the absence and presence of ATP. An over-exposure of the region of the gel corresponding to single-stranded siRNA is shown in the lower panel. (C) Analysis of siRNA unwinding for the gel filtration fractions from Figure 4D. An over-exposure of the region of the gel corresponding to single-stranded siRNA is shown in the lower panel. Molecular weight standards are as in Figure 4D.

quenched by the simultaneous addition of an SDS-containing stop buffer, proteinase K, and a 25-fold molar excess of an unlabeled competitor RNA containing the sequence of the 19 paired nucleotides from the sense strand of the siRNA duplex. The samples were analyzed by non-denaturing acrylamide gel electrophoresis.

We used the assay to assess if the siRNA duplex is a target for ATP-dependent helicase proteins in the *Drosophila* embryo lysate. Unwinding of the siRNA duplex was monitored in an RNAi reaction in the presence and absence of ATP. No siRNA unwinding was detected in the absence of ATP, whereas a small percent (≤ 5%) of unwound siRNA was detected with ATP (Figure 5B). Furthermore, the siRNA was almost entirely double-stranded in the inactive ~360 kDa siRNP complex (Figure 5C). In contrast, single-stranded siRNA resided in the same two peaks that showed RNAi activity in the target cleavage assay: the void volume of the column and a peak of apparent molecular weight <232 kDa. These data suggest (1) that RNAi activity is associated with a population of siRNAs that are unwound and (2) that a protein-siRNA complex of <232 kDa contains all of the factors required for efficient, sequence-specific target cleavage. We propose that this complex, represents the minimal, active RNA-induced silencing complex (RISC[9]). We term this complex the RISC*. These results are at odds with previous findings that the active RISC is a ~500 kDa complex. A possible explanation is that our chromatographic procedure resolved the smaller active complex from a larger precursor complex, but that these two species remain associated in a single, ~500 kDa complex under other conditions. Alternatively, a dissociable cofactor, such as an ATP-dependent RNA helicase might be present in fractions 26-40. This factor might support

RNAi by acting on a small amount of the inactive ~360 kDa complex present in these fractions, converting it to the RISC* by unwinding the siRNA duplex.

5′ phosphorylation status and siRNA activity

Synthetic siRNAs bearing 5′ hydroxyl termini have been used successfully to initiate interference in *Drosophila* embryo lysates[4] and in cultured mammalian cells[3]. Nonetheless, native siRNAs, generated by cleavage of dsRNA, contain 5′ phosphate ends. Therefore, we asked if a 5′ phosphate is merely a consequence of the enzymatic mechanism of dsRNA cleavage by the RNase III enzyme Dicer or if it is an essential feature of an active siRNA. We first examined the 5′ phosphorylation status of the anti-sense strand of a synthetic siRNA duplex that contained 5′ hydroxyl groups on both strands. Figure 6A shows that upon incubation in the lysate with ATP, the siRNA was rapidly phosphorylated, so that after 15 minutes nearly all of the synthetic siRNA had a 5′ phosphate group (lysate, HO-rU). This finding was surprising, because *Drosophila* embryo lysates contain a potent phosphatase activity that rapidly dephosphorylated exogenous 5′ ^{32}P-radiolabeled siRNA duplexes (data not shown). The 5′ phosphate of the siRNA must be in rapid exchange, but the sum of the rates of phosphatase and kinase activities produces an siRNA bearing a 5′ phosphate at steady-state. Therefore, both synthetic (5′ hydroxyl) and native (5′ phosphate) siRNAs are expected to exist predominantly as 5′ phosphorylated species in the in vitro RNAi reaction and perhaps in vivo as well.

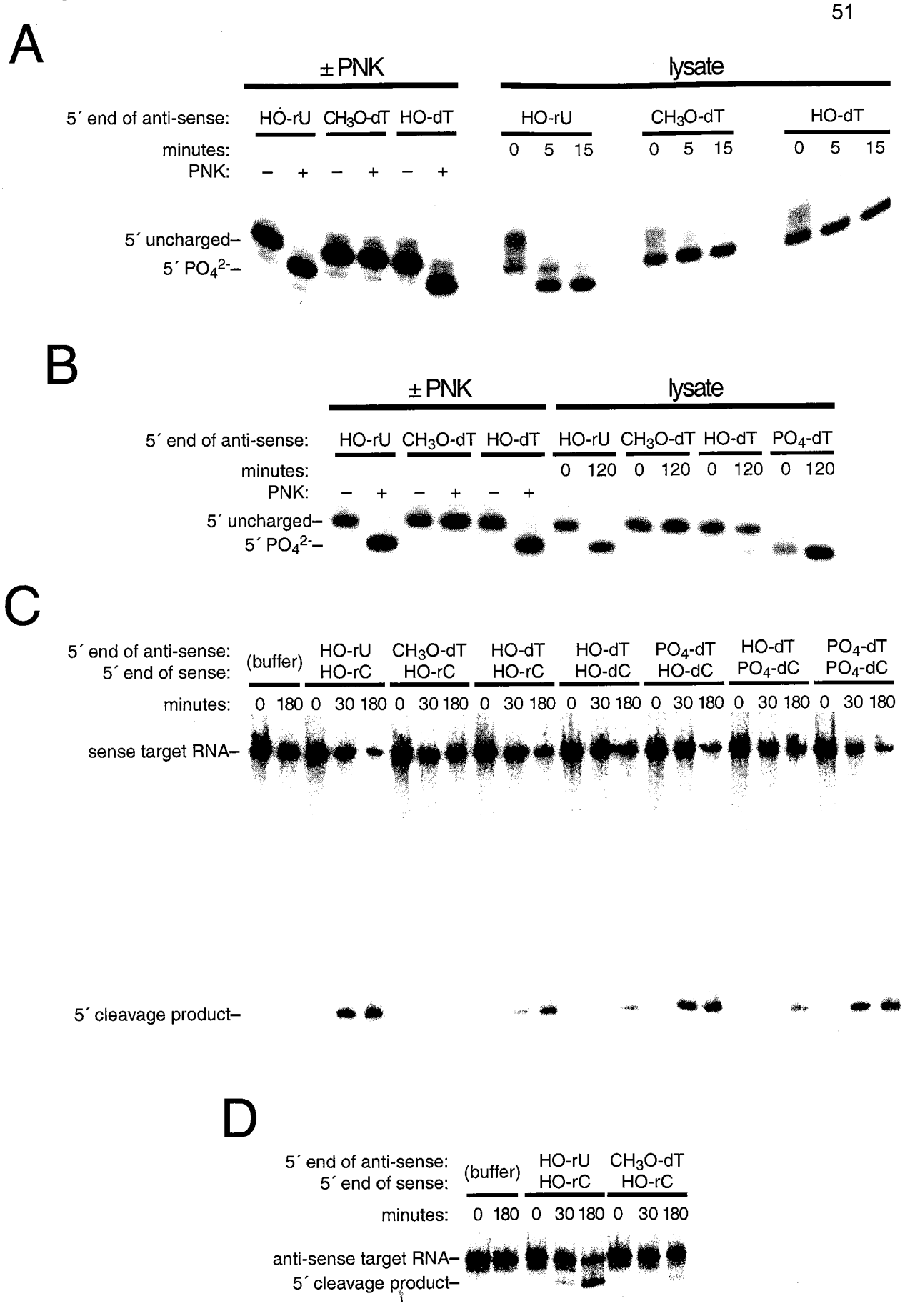
A
±PNK
lysate
5′ end of anti-sense:
HO-rU
CH3O-dT
HO-dT
HO-rU
CH3O-dT
HO-dT
minutes:
0 5 15
0 5 15
0 5 15
PNK:
– + – + – +
5′ uncharged–
5′ PO4 2–
B
±PNK
lysate
5′ end of anti-sense:
HO-rU
CH3O-dT
HO-dT
HO-rU
CH3O-dT
HO-dT
PO4-dT
minutes:
0 120 0 120 0 120 0 120
PNK:
– + – + – +
5′ uncharged–
5′ PO4 2–
C
5′ end of anti-sense:
5′ end of sense:
(buffer)
HO-rU
HO-rC
CH3O-dT
HO-rC
HO-dT
HO-rC
HO-dT
HO-dC
PO4-dT
HO-dC
HO-dT
PO4-dC
PO4-dT
PO4-dC
minutes:
0 180 0 30 180 0 30 180 0 30 180 0 30 180 0 30 180 0 30 180 0 30 180
sense target RNA–
5′ cleavage product–
D
5′ end of anti-sense:
5′ end of sense:
(buffer)
HO-rU
HO-rC
CH3O-dT
HO-rC
minutes:
0 180 0 30 180 0 30 180
anti-sense target RNA–
5′ cleavage product–

Figure 6. 5′ phosphates are critical determinants of siRNA activity. (A) and (B) Phosphorylation status of the anti-sense strand of synthetic siRNA duplexes upon incubation with polynucleotide kinase (PNK) or *Drosophila* embryo lysate. (C) RNAi activity of synthetic siRNA duplexes measured for a sense *Pp*-luc RNA target. (D) RNAi activity of synthetic siRNA duplexes measured for an anti-sense *Pp*-luc RNA target.

To assess if a 5′ phosphate is required for RNAi, we designed an siRNA duplex in which the 5′ end of the anti-sense strand was blocked by replacing the 5′ hydroxyl with a 5′ methoxy group (CH_3O). In order to facilitate chemical synthesis of the 5′ block, the first nucleotide of the anti-sense siRNA strand, uracil, was replaced with 2′ deoxythymidine (dT). An siRNA duplex in which the 5′ terminus was a hydroxyl group, but the first nucleotide was dT was prepared in parallel. The 5′ blocked (CH_3O-dT) and 5′ dT (HO-dT) anti-sense siRNA strands were each annealed to a standard, 5′ hydroxyl sense strand (HO-rC). The 5′ blocked siRNA was not phosphorylated after incubation with either polynucleotide kinase (PNK) or lysate (CH_3O-dT; Figure 6A and 6B). Surprisingly, the siRNA bearing a 5′ dT on the anti-sense strand (HO-dT) was a poor substrate for phosphorylation in the lysate, despite being a good substrate for PNK (Figure 6A): it was not detectably phosphorylated after 15 min in the lysate, although a small fraction was phosphorylated after 2 h (HO-dT; Figure 6A and B). These data show that *Drosophila* embryos contain a nucleic acid kinase that discriminates against 5′ deoxy siRNAs.

Next, we examined the capacity of these siRNA duplexes to trigger RNAi. This siRNA sequence directs cleavage of the 510 nt sense *Pp*-luc target RNA to yield a diagnostic 72-nt 5′ product ([4]and Figure 5D). As expected, the standard siRNA (anti-sense, HO-rU; sense, HO-rC) directed efficient cleavage of the target RNA (Figure 6C), as evidenced by the disappearance of the 510 nt RNA and the appearance of the 72 nt RNA. In contrast, no target cleavage was detected for the 5′ blocked anti-sense siRNA (CH_3O-dT), paired with a standard sense siRNA strand (HO-rC). These data suggest that

a 5′ phosphate is required on the siRNA strand that guides target cleavage. This hypothesis predicts that anti-sense siRNAs that are poorly phosphorylated in the lysate will be poor effectors of sense target cleavage. Consistent with the prediction, an siRNA in which the anti-sense strand is 5′ hydroxyl, 5′ dT (HO-dT), which is inefficiently phosphorylated in the lysate (Figures 6A and 6B), is less efficient in directing sense target cleavage than a standard siRNA (Figure 6C). To test if the defect was a direct consequence of the inefficiency with which the 5′ dT anti-sense RNA was phosphorylated, a 5′ dT anti-sense RNA bearing a 5′ phosphate was annealed to a 5′ hydroxyl, 5′ dC sense siRNA. Like the 5′ dT modification on the anti-sense strand, 5′ dC on the sense strand inhibits phosphorylation by the kinase in the lysate (data not shown). Use of a 5′ dC sense strand, therefore, allowed us to examine the effect of a 5′ phosphate on the 5′ dT, anti-sense strand in an siRNA duplex in which the sense strand was predominantly 5′ hydroxyl. This siRNA duplex (anti-sense, PO_4-dT; sense, HO-dC) was as efficient in cleaving the sense target RNA as a standard, siRNA duplex (anti-sense, HO-rU; sense, HO-rC; Figure 6C). Thus, the sole defect caused by a 5′ dT anti-sense strand is that it is a poor kinase substrate in the lysate. An siRNA in which both strands were 5′ phosphorylated and 5′ deoxy (anti-sense, PO_4-dT; sense, PO_4-dC) was no more efficient than the siRNA comprising a 5′ phosphate, 5′ dT anti-sense strand and a 5′ hydroxyl, 5′ dC sense strand (anti-sense, PO_4-dT; sense, HO-dC; Figure 6C). As expected, an siRNA in which both strands were 5′ deoxy and 5′ hydroxyl (anti-sense, HO-dT; sense, HO-dC) was defective in sense target cleavage. This defect was not remedied by adding a phosphate to the sense strand (anti-sense, HO-dT; sense, PO_4-dC),

lending further support to the idea that a 5′ phosphate on the anti-sense strand is required to guide sense target cleavage (Figure 6C). We conclude that a 5′ phosphate on the guide strand of an siRNA is required for RNAi. We note that RNAi directed by an siRNA in which both strands are 5′ phosphate but also 5′ deoxy, (PO_4-dT; Figure 6B), nonetheless required ATP (data not shown). This ATP-requirement likely reflects the role of ATP in siRNA unwinding (see above) rather than in 5′ phosphorylation.

In the course of these experiments, we observed that an siRNA in which both strands were 5′ hydroxyl and 5′ deoxy was slightly worse at guiding sense target cleavage than the 5′ hydroxyl siRNA in which only the anti-sense strand was 5′ deoxy. Therefore, we asked directly if the 5′ phosphate of the non-guiding strand is also important for siRNA function. We examined cleavage of an anti-sense target RNA for the siRNA with a 5′ methoxy anti-sense strand and a standard sense strand (anti-sense, CH_3O-dT; sense, HO-rC). With respect to an anti-sense target RNA, this siRNA duplex is blocked for 5′ phosphorylation only on the non-guiding strand. As expected, a standard siRNA (anti-sense, HO-rU; sense, HO-rC) cleaved a 510 nt, anti-sense *Pp*-luc target RNA to yield a diagnostic 436 nt cleavage product (Figure 6D). Significantly less target cleavage was observed for the siRNA containing a 5′ blocked anti-sense strand (anti-sense CH_3O-dT; sense, HO-rC). Since it is the sense strand that guides anti-sense target cleavage, these data imply that recognition of the 5′ phosphates of both siRNA strands occurs during the RNAi pathway. In support of this idea, an siRNA in which the 5′ residue of the anti-sense strand is dT was also less efficient in anti-sense target cleavage than a siRNA duplex with a rU at this position (data not shown). For the siRNA

sequence examined here, the 5′ phosphate of the non-guiding strand contributes to cleavage efficiency, whereas the 5′ phosphate of the target-complementary, guide strand is required for cleavage. The difference in effect of a 5′ phosphate on the guide versus the non-guiding strand suggest that two distinct 5′ phosphate-recognition steps occur in the RNAi reaction.

To test the idea that one of these 5′ phosphate recognition steps precedes assembly of a protein complex on the siRNA duplex, we repeated the experiments in Figure 4 using synthetic siRNA duplexes containing either 5′ hydroxyl or 5′ phosphate groups. siRNAs, radiolabeled on the 3′ end of the anti-sense strand, were incubated in a standard in vitro RNAi reaction in the presence or absence of ATP, then fractionated by gel filtration. siRNAs were detected by scintillation counting of the gel filtration fractions (Figure 7). As shown previously (Figure 4D), synthetic siRNA bearing 5′ hydroxyl groups are incorporated into a ~360 kDa complex upon incubation with *Drosophila* embryo lysate in the presence of ATP (Figure 7, filled circles). However, in the absence of ATP, no such complex is observed, and virtually all the siRNA remains unbound by protein (Figure 7, open circles). These results contrast with those of Figure 4C, in which purified, native siRNAs, generated by cleavage of long, dsRNA into siRNAs, readily assembled with proteins in the absence of ATP to yield a ~360 kDa complex. Unlike the synthetic siRNA duplexes used in Figure 7, native siRNAs contain 5′ phosphate groups. Thus, one explanation for our results is that 5′ phosphates are required for incorporation of siRNA duplexes into the ~360 kDa complex. In support of this idea, 5′-phosphorylated, synthetic siRNA duplexes form the ~360 kDa complex upon

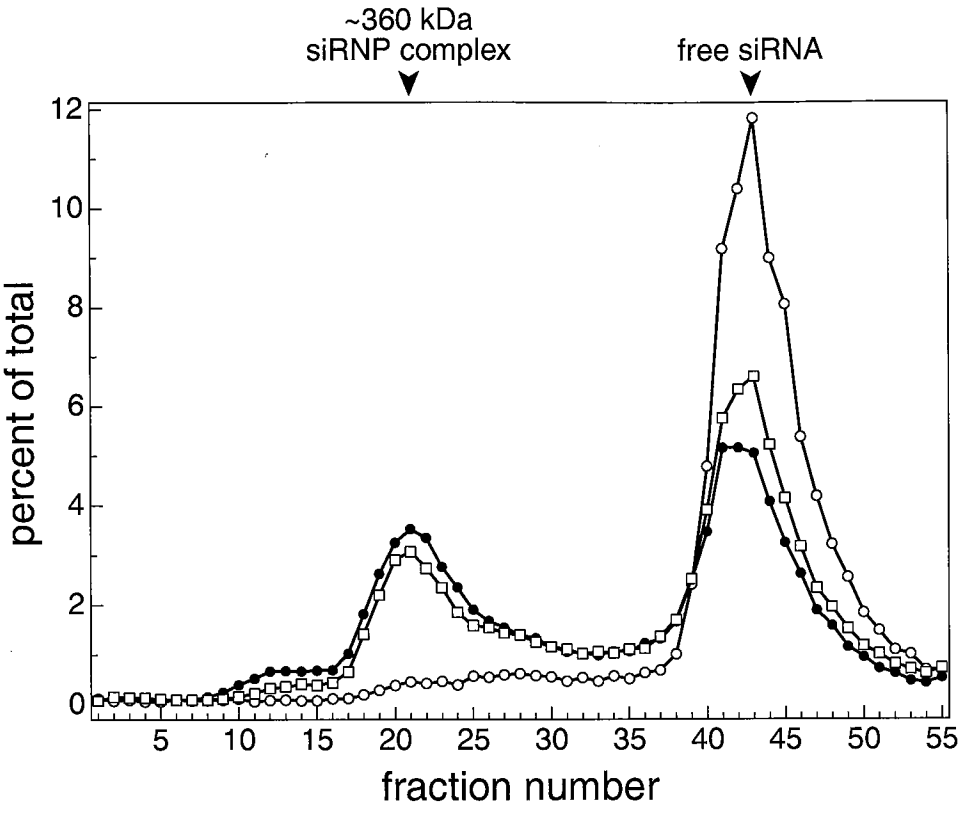
~360 kDa
siRNP complex
free siRNA
percent of total
fraction number
0
2
4
6
8
10
12
5
10
15
20
25
30
35
40
45
50
55

Figure 7. 5′ phosphates are required for siRNP formation. Complex formation was monitored by gel filtration on Superdex-200. Filled circles, siRNA duplex bearing 5′ hydroxyl groups incubated with *Drosophila* embryo lysate and ATP. Open circles, siRNA duplex bearing 5′ hydroxyl groups incubated in the absence of ATP. Open squares, siRNA duplex bearing 5′ phosphate groups incubated in the absence of ATP.

incubation in lysate in the absence of ATP (Figure 7, open squares). These results suggest that the ~360 kDa siRNA-protein complex, although inactive for target cleavage, is a bona fide intermediate in the assembly of the RISC*, the active siRNA complex. Furthermore, they argue that 5′ phosphate recognition occurs early in the RNAi pathway, since we detected no stable siRNA-protein complexes for siRNAs lacking a 5′ phosphate. Interestingly, normal levels of ~360 kDa complex were formed with an siRNA containing a 5′ blocked (CH_3O, dT) anti-sense strand paired with a 5′ hydroxyl sense strand (HO, rC), suggesting that a 5′ phosphate on one of the two siRNA strands is sufficient for siRNP formation (data not shown) and consistent with our finding that a 5′ PO_4, dT anti-sense siRNA strand paired with a 5′ HO, dC sense strand mediates efficient sense target cleavage (see above).

An ATP-dependent step downstream of siRNA unwinding

Additionally, separate groups have now shown that single-stranded 21 nt RNAs (ss-siRNAs) are able to induce RNAi *in vitro* and *in vivo*[13,18]. Therefore, we hypothesized that RNAi triggered by ss-siRNAs would be able to bypass all observed energy requiring steps in the pathway, since ATP-dependent siRNA duplex unwinding was predicted to be the final ATP-dependent step in the RNAi pathway. To test if loading of ss-siRNA into RISC requires ATP, we added 5′-phosphorylated, ss-siRNA to embryo lysates depleted of ATP. After incubation for 2 hr, no cleavage product was detected, suggesting that there is at least one ATP-dependent step downstream of siRNA unwinding (Figure 8A). The stability of ss-siRNA was not reduced by ATP depletion. In fact, ss-siRNA was

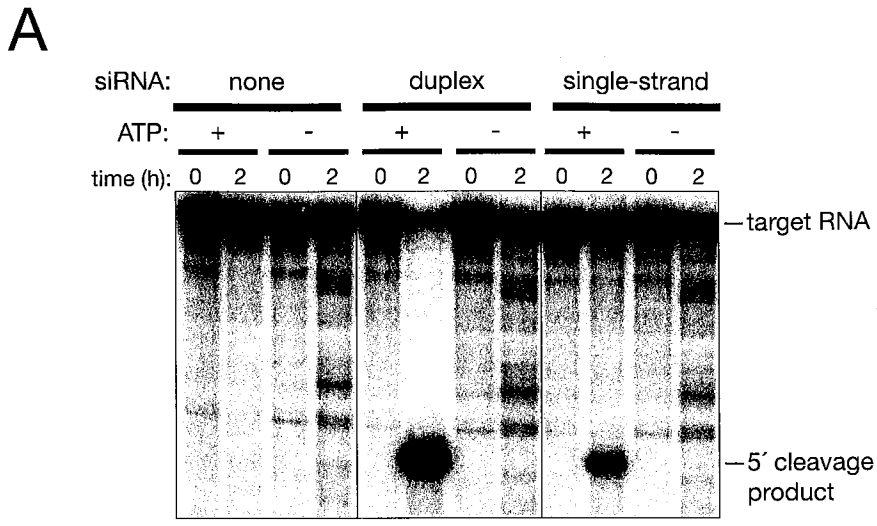
A
siRNA:
none
duplex
single-strand
ATP:
+
-
+
-
+
-
time (h):
0 2 0 2 0 2 0 2 0 2 0 2
target RNA
5′ cleavage product

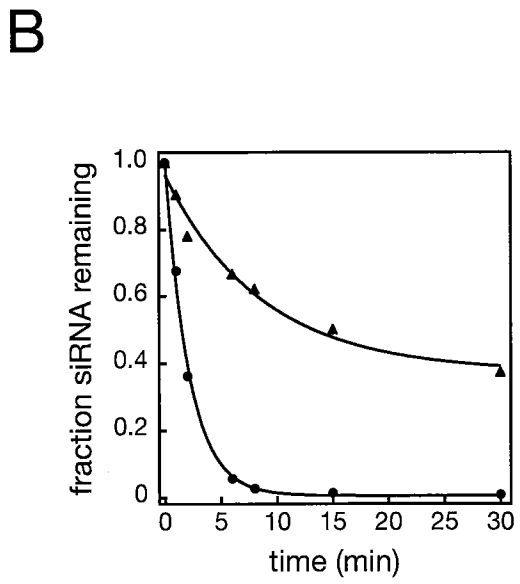
B
fraction siRNA remaining
1.0
0.8
0.6
0.4
0.2
0
0 5 10 15 20 25 30
time (min)

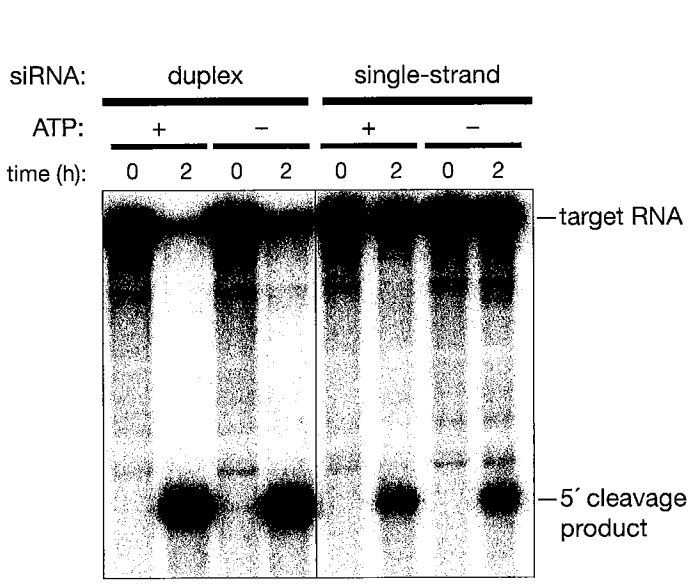
C
siRNA:
duplex
single-strand
ATP:
+
–
+
–
time (h):
0 2 0 2 0 2 0 2
target RNA
5′ cleavage product

Figure 8. ATP-dependent incorporation of single-stranded siRNA into RISC. (A) RNAi in embryo lysate using double- or single-stranded siRNA in the presence or the absence of ATP. (B) The fraction of single-stranded siRNA remaining after incubation in embryo lysate in the presence (circles) or the absence (triangles) of ATP. (C) Target recognition and cleavage directed by single-stranded siRNA does not require ATP. After 30 min preincubation of siRNA in the presence of ATP to permit RISC assembly, ATP was removed (–) or retained (+), and target RNA added to test for RISC-directed target cleavage.

slightly more stable in the absence of ATP (Figure 8B). Thus differential stability cannot account for the requirement of ATP in RNAi triggered by ss-siRNA. As described the RNAi pathway is comprised of at least three steps after siRNA unwinding: RISC assembly, target recognition, and target cleavage. To assess if either target recognition or cleavage was ATP dependent for siRNA or ss-siRNA activated RNAi, we incubated duplex or ss-siRNA in a standard RNAi reaction with ATP to assemble RISC. Next, NEM was added to inactivate the ATP-regenerating enzyme, creatine kinase, and to block further RISC assembly. NEM was quenched with dithiothreitol (DTT), and hexokinase and glucose added to deplete ATP. Finally, mRNA target was added and the reaction incubated for 2 hr. Using this protocol, high ATP levels were maintained during RISC assembly, but less than 100 nM ATP was present during the encounter of RISC with the target RNA. Target recognition and cleavage did not require ATP when RISC was programmed with either duplex or ss-siRNA, provided that ATP was supplied during RISC assembly (Figure 8C).

A model for the RNAi pathway

Our data suggest that ATP plays at least four distinct roles in the RNAi pathway, three of which have not previously been reported. In Figure 9, we propose a model for RNAi that incorporates these four ATP-dependent steps. First, as previously reported, ATP is essential for the cleavage of long dsRNA into native siRNAs. These siRNAs are fully competent to direct RNAi, since when purified they re-enter the RNAi pathway so long as their double-stranded character is maintained. siRNAs are then proposed to bind

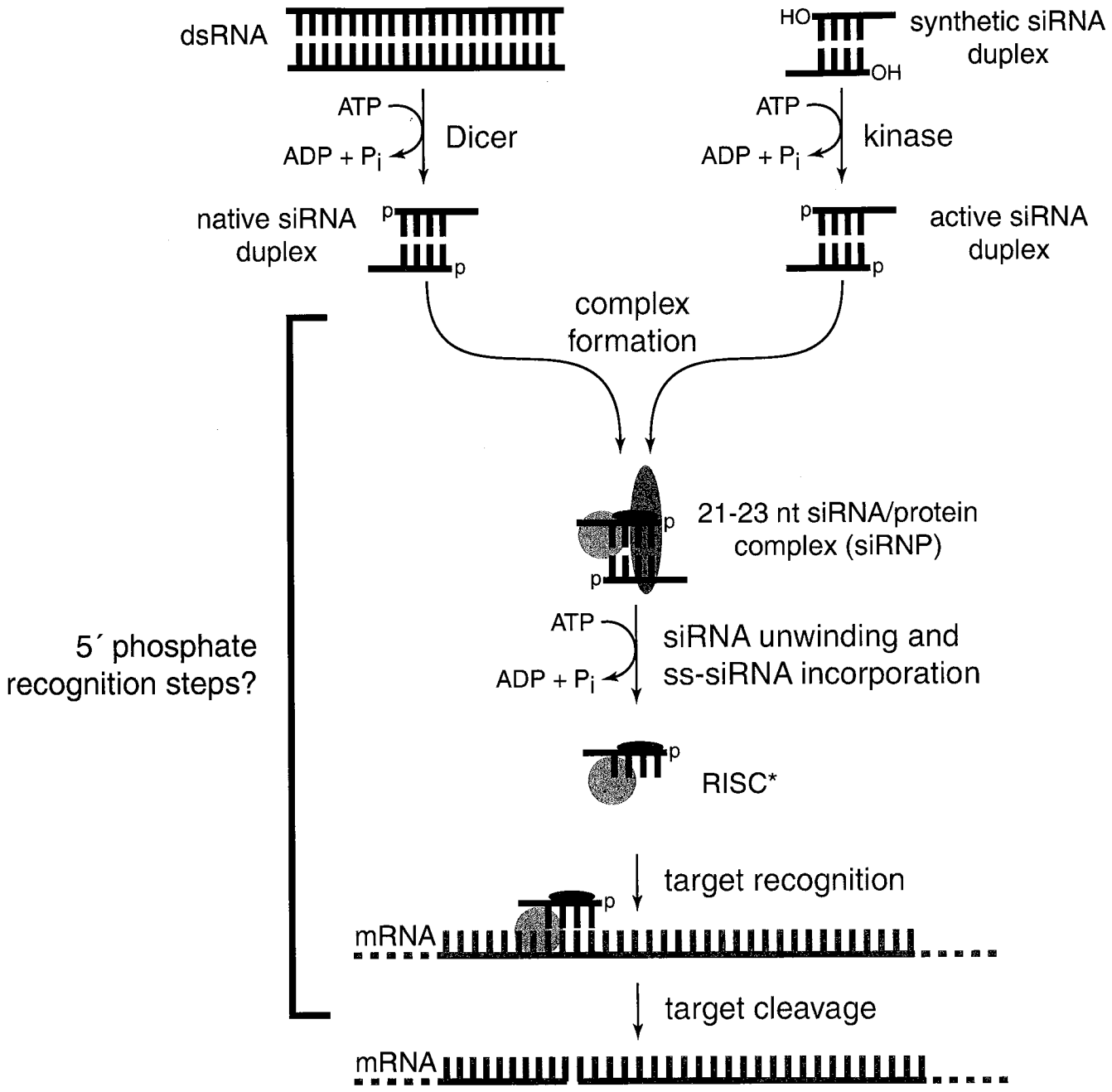
dsRNA
ATP
ADP + Pi
Dicer
native siRNA duplex
HO
OH
synthetic siRNA duplex
ATP
ADP + Pi
kinase
active siRNA duplex
complex formation
21-23 nt siRNA/protein complex (siRNP)
ATP
ADP + Pi
siRNA unwinding and ss-siRNA incorporation
RISC*
target recognition
mRNA
target cleavage
mRNA
5´ phosphate recognition steps?

Figure 9. A model for the RNAi pathway.

specific proteins that commit them to the RNAi pathway. In *Drosophila* embryo lysate, the majority of siRNAs are incorporated into a ~360 kDa complex. Although this complex is not competent to direct target cleavage, it seems likely that it is an intermediate in the RNAi pathway, since it is not formed with siRNAs that do not mediate RNAi because they lack 5′ phosphates. Conversion of the inactive ~360 kDa complex into an active complex, RISC*, is proposed to occur in a second ATP-dependent step: the unwinding of the siRNA duplex by an RNA helicase. We do not yet know if the two unwound, single-strands are retained in the same complex or if a single RISC* contains only one of the two strands of the original siRNA duplex. siRNA unwinding is likely to be a stable rather than a transient change in siRNA conformation, because siRNA duplexes pre-incubated with lysate and ATP are competent to recognize and cleave a corresponding target RNA after extensive dialysis to remove ATP and other cofactors. Furthermore, in the course of experimenting with suitable conditions for single-stranded siRNA-mediated target cleavage, we observed that induction of this response also required ATP, thus adding an additional energy dependent step immediately downstream of small RNA unwinding. The nature of the energy requirement for single-strand incorporation into, or activation of, RISC is the focus of current study.

5′ phosphorylation of siRNAs corresponds to a third ATP-dependent step in the pathway. Our experiments with synthetic siRNAs reveal the requirement for a 5′ phosphate on the siRNA strand complementary to the target RNA, and a partial requirement for 5′ phosphorylation of the siRNA strand sharing sequence with the target

RNA. Tuschl and coworkers have proposed that the site of cleavage of the target RNA is measured from the 5′ end of the complementary siRNA strand[5]. They find that additional nucleotides at the 3′ end of the siRNA do not alter the site of cleavage of the target RNA, but additional nucleotides at the 5′ end move the target cleavage site correspondingly[5]. The 5′ phosphate of the siRNA may therefore serve as a molecular reference point from which the cleavage site is measured. 5′ phosphorylation of synthetic siRNA duplexes in the *Drosophila* embryo lysate is catalyzed by a kinase that can discriminate between 5′ ribo and 5′ deoxy siRNAs. Might the kinase that phosphorylates synthetic 5′ hydroxyl-containing siRNAs also act on the native siRNAs generated by processing of long dsRNA? While we have not yet devised methods to follow a single phosphate from long dsRNA into an individual siRNA sequence, we note that in the lysate, the half-life of a 5′ ^{32}P on a synthetic siRNA is short, yet virtually all of these siRNAs are 5′ phosphorylated throughout the reaction. The 5′ phosphate of siRNAs generated by the cleavage of long dsRNA may also be exchanging rapidly, with an siRNA-specific kinase serving to regenerate functional siRNA duplexes. We propose that this kinase acts in vivo to maintain the 5′ phosphates of siRNAs, thereby allowing them to participate in multiple rounds of target cleavage.

Why should the RNAi machinery examine the phosphorylation status of an siRNA? Three features—a 21-23 nt length, a double-stranded structure with 2 nt 3′ overhangs, and 5′ phosphates—distinguish siRNAs in flies from other small RNAs, and therefore allow the cell to discriminate between authentic siRNAs and imposters. In this view, the 5′ phosphate is one feature that licenses an siRNA for RNAi. An siRNA-

specific kinase would maintain 5′ phosphates on bona fide siRNAs that have entered the RNAi pathway but have subsequently lost their 5′ phosphate, but would not add 5′ phosphates to other small RNAs, ensuring that only authentic siRNAs target mRNAs for cleavage.

Note: The siRNA unwinding experiments performed in Figure 5 were designed prior to the discovery of 'functional asymmetry' and therefore, rational siRNA design. As such, we have learned, after the fact, that the very small amount of ss-siRNA accumulation reflects our 5′ labeling and subsequent visualization of the passenger strand for the particular siRNA duplex tested, not the guide. A dramatically greater amount of ss-siRNA accumulation for the guide strand, compared to the passenger strand, of this particular siRNA duplex, can be observed in Figure 1 of Schwarz et al[130].

MATERIALS AND METHODS

General methods

Drosophila embryo lysate preparation, in vitro RNAi reactions, dsRNA processing reactions, 501 bp *Rr*-luc and 505 bp *Pp*-luc dsRNAs, full-length *Rr*-luc and *Pp*-luc target mRNAs, and cap-radiolabeling of target RNAs with guanylyl transferase were as described[6,124,226]. In Figure 4D, the control RNA was a 441 nt fragment of the *Drosophila pumilio* cDNA transcribed with T7 RNA polymerase from a PCR template prepared with the following primers: 5′ primer, GCG TAA TAC GAC TCA CTA TAG GCG CCC ACA ATT GCC ATA TC; 3′ primer, AAG GTT GAG CCT ACG GCT C. The 510 bp *Rr*-luc target RNA was transcribed with T7 RNA polymerase from a PCR template prepared with the following primers: 5′ primer, GCG TAA TAC GAC TCA CTA TAG GAA AAA CAT GCA GAA AAT GC; 3′ primer, GAA GAA TGG TTC AAG ATA TGC TG. The 510 bp *Pp*-luc sense target RNA was transcribed from a PCR template prepared with the following primers: 5′ primers, GCG TAA TAC GAC TCA CTA TAG GAG ATA CGC CCT GGT TCC TG; 3′ primer, GAA GAG AGG AGT TCA TGA TCA GTG. For transcription templates for the 510 nt *Pp*-luc anti-sense target RNA, the PCR primers were GCG TAA TAC GAC TCA CTA TAG GAG AGG AGT TCA TGA TCA GTG (5′ primer) and GAA GAG ATA CGC CCT GGT TCC TG (3′ primer). Gels were dried and exposed to image plates (Fuji or Kodak), which were scanned using a Bio-Rad Personal FX imager and analyzed with QuantityOne 4.0 (Bio-Rad). Images for figures were prepared with QuantityOne 4.0 and PhotoShop 5.5

(Adobe). Graphs were prepared and rates determined using Microsoft Excel and IgorPro 3.1 (Wavemetrics).

Synthetic siRNAs

The siRNA duplexes in Figures 4B, 5D, 6, and 7 were prepared from synthetic 21 nt RNAs (Dharmacon Research). Sense siRNA sequences were 5′-HO-CGU ACG CGG AAU ACU UCG AUU-3′ (HO-rC) and 5′-HO-dCGU ACG CGG AAU ACU UCG AUU-3′ (HO-dC). Anti-sense siRNAs used were 5′-HO-UCG AAG UAU UCC GCG UAC GUG-3′ (HO-rU); 5′-CH_3O-dTCG AAG UAU UCC GCG UAC GUG-3′ (5′ blocked; CH_3O-dT); and 5′-HO-dTCG AAG UAU UCC GCG UAC GUG-3′ (HO-dT). siRNAs were deprotected according to the manufacturer's instructions, dried in vacuo, resuspended in 400 µl water, dried in vacuo again, resuspended in water, and annealed to form duplex siRNAs as described[4]. siRNA duplexes were used at 50 nM final concentration. siRNA strands were phosphorylated with PNK (New England Biolabs) and 1 mM ATP according to the manufacturer's directions. siRNAs were 3′ end-labeled with a-^{32}P-cordycepin 5′ triphosphate (5000 Ci/mmol; New England Nuclear) and Poly(A) polymerase (Life Technologies) according to the manufacturer's instructions. Radiolabeled siRNA strands were purified from 15% denaturing acrylamide gels. 5′ phosphorylation status was monitored by electrophoresis of siRNAs on a 15% sequencing gel. The SOD1 mutant siRNA and target sequences used in Figure 8 can be found in[227].

Gel filtration of native siRNAs and siRNP complexes.

Preparative scale dsRNA processing reactions (1 ml) were deproteinized at room temperature by the addition of 1 ml 2x PK buffer (200 mM Tris-HCl, pH 7.5, 25 mM EDTA, 300 mM NaCl, 2% w/v sodium dodecyl sulfate) and Proteinase K (E.M. Merck; 20 mg/ml dissolved in water) to a final concentration of 1 mg/ml. After incubation at room temperature for 1 h, the reaction was extracted with an equal volume of phenol/chloroform/isoamyl alcohol (25:24:1) and the RNA recovered by precipitation with 3 volumes absolute ethanol. The precipitate was redissolved in 250 µl lysis buffer (30 mM Hepes-KOH, pH 7.5, 100 mM potassium acetate, 2 mM magnesium acetate) and chromatographed at room temperature on a Superdex-200 HR 10/30 column (Pharmacia) at 0.75 ml/min in lysis buffer using a BioCad Sprint (PerSeptive Biosystems). After 7.5 ml had passed through the column, sixty, 200-µl fractions were collected using a cooled stage to maintain the fractions at 4°C. To compensate for dilution of the original reaction on the gel filtration column, each fraction was concentrated by precipitation with ethanol and redissolved in 30 µl lysis buffer.

For siRNP analysis, a 200 µl RNAi reaction was assembled using the purified, native siRNAs (fractions 44 and 45) or synthetic siRNA duplexes, incubated for 1 h at 25°C, and fractionated on Superdex-200 HR 10/30 at 0.75 ml/min in lysis buffer containing 1 mM DTT, 0.1 mM EDTA, 10% (v/v) glycerol. Fractions were collected as described above. To analyze RNAi activity, 6 µl of each fraction was analyzed in a 10 µl standard RNAi reaction.

ATP depletion

ATP depletion by hexokinase-treatment was as described except that 20 mM glucose was used. In Figure 4B, NEM was freshly prepared from powder as a 1M stock in absolute ethanol, added to an RNAi reaction at 4°C to a final concentration of 5 mM, incubated 10 min, and quenched with 5 mM DTT added from a 1M stock dissolved in water. In Figure 4D, an RNAi reaction was adjusted to 10% saturation by addition of a 100% saturated solution of ammonium sulfate dissolved in lysis buffer containing 0.1 mM EDTA. After 30 min at 4°C, the reaction was centrifuged at 16,060 x g for 20 min at 4°C, and the supernatant adjusted to 45% saturation. After an additional 30 min at 4°C, the 10-45% ammonium sulfate precipitate was collected by centrifugation. The precipitate was redissolved in lysis buffer containing 2 mM DTT and dialyzed in a micro-dialysis chamber (Pierce; 10,000 MW cut-off) for 16 h against two changes of a >5,000-fold excess of lysis buffer containing 2 mM DTT and 20% w/v glycerol. ATP concentration was measured with a Bioluminescent ATP Assay Kit (Sigma) according to the manufacturer's directions. Luminescence was measured in a Mediators PhL luminometer.

siRNA unwinding assay

RNAi reactions (10 μl) were quenched with 90 ml of stop mix containing 1.11X PK buffer, 1.11ug/ul Proteinase K, 20 mg glycogen (Roche), and a 25-fold molar excess (12.5 pmoles) of either unlabeled 21 nt RNA identical to the radiolabeled siRNA strand

or a 510 nt *Pp*-luc RNA which contains the sequence of the first 19 nt of the radiolabeled siRNA strand, incubated at 25°C for 15 min, and immediately precipitated with 3 volumes absolute ethanol, chilled for at least 1 h at -20°C, collected by centrifugation, redissolved in 10 µl 3% w/v Ficoll-400, 0.04% w/v Bromophenol Blue, 2 mM Tris-HCl, pH 7.4, and immediately analyzed by electrophoresis at 10 W at 4°C through a 15% native polyacrylamide gel (19:1, acrylamide:bis-acrylamide) cast in 1X and run in 0.5X Tris-Borate-EDTA buffer.

ACKNOWLEDGEMENTS

The authors acknowledge Tom Tuschl for sharing data prior to publication and for numerous helpful conversations; Dave Bartel, Phil Sharp, Reid Gilmore, and Kendall Knight for continuing advice and encouragement; Stephen Scaringe for advice on siRNA design and synthesis; and members of the Zamore laboratory for comments on the manuscript and many helpful discussions. Guanylyl transferase was the kind gift of Jeff Wilusz. PDZ is a Pew Scholar in the Biomedical Sciences. This work was supported by a Cutler Award from the Worcester Foundation for Biomedical Research and by a grant from the National Institutes of Health (GM62862-01) to PDZ.

CHAPTER III: KINETIC ANALYSIS OF THE RNAi ENZYME COMPLEX

SUMMARY

The siRNA-directed ribonucleoprotein complex, RISC, catalyzes target RNA cleavage in the RNA interference pathway. Here, we show that siRNA-programmed RISC is a classical Michaelis-Menten enzyme in the presence of ATP. In the absence of ATP, the rate of multiple rounds of catalysis is limited by release of the cleaved products from the enzyme. Kinetic analysis suggests that different regions of the siRNA play distinct roles in the cycle of target recognition, cleavage, and product release. Bases near the siRNA 5′ end disproportionately contribute target RNA-binding energy, whereas base pairs formed by the central and 3′ regions of the siRNA provide a helical geometry required for catalysis. Finally, the position of the scissile phosphate on the target RNA appears to be determined during RISC assembly, before the siRNA encounters its RNA target.

INTRODUCTION

In the RNA interference (RNAi) pathway[1,4], 21-nucleotide (nt), double-stranded small interfering RNAs (siRNAs) guide the RISC[9,10,13] (RNA-induced silencing complex) to destroy its RNA target[20]. siRNA-directed RNAi has become an essential laboratory tool for reducing the expression of specific genes in mammalian cells[3], but the limits of siRNA specificity remain to be determined[5,84,228,229]. Some siRNAs can discriminate between mRNAs that differ by only a single nucleotide[4,5,227,230], but genome-wide assessments of siRNA specificity suggest that mRNAs with only partial complementarity to an siRNA can also be targeted for destruction[182]. Why some mismatches are tolerated, whereas others are not, remains poorly understood. One hypothesis is that the 5′ region of siRNAs and the related microRNAs (miRNAs) plays a special role in target recognition, nucleating binding of RISC to the RNA target[24,231,232]. Alternatively, mismatched siRNA might recruit RISC to targets lacking complementarity to the 5′ region of the siRNA, but the geometry of such siRNA:target pairing is incompatible with target silencing.

To understand how the 5′, central and 3′ sequences of the siRNA guide strand function to direct cleavage, we undertook a detailed *in vitro* kinetic analysis of a single siRNA sequence. Here, we show that RISC can cleave RNA targets with up to five contiguous mismatches at the siRNA 5′ end and eight mismatches at the siRNA 3′ end. Our data show that 5′ bases contribute disproportionately to target RNA binding, but do not play a role in determining the catalytic rate, k_{cat}. This finding is strikingly similar to observations by Doench and Sharp that 5′ complementarity is essential for translational

repression by siRNAs designed to act like animal miRNAs, which typically repress translation[233]. For siRNA directing target cleavage, we find that the 3′ bases of the siRNA contribute much less than 5′ bases to the overall strength of binding, but instead help to establish the helical geometry required for RISC-mediated target cleavage, consistent with the view that catalysis by RISC requires a central A-form helix[234]. Finally, we show that when an siRNA fails to pair with the first three-to-five nucleotides of the target RNA, the phosphodiester bond severed in the target RNA is unchanged; for perfectly matched siRNA, RISC measures the site of cleavage from the siRNA 5′ end[4,5]. We conclude that the identity of the scissile phosphate is determined prior to the encounter of the RISC with its target RNA, perhaps because the RISC endonuclease is positioned with respect to the siRNA 5′ end during RISC assembly.

RESULTS

The siRNA-programmed RISC is an enzyme

RISC programmed with small RNA *in vivo* catalyzes the destruction of target RNA *in vitro* without consuming its small RNA guide[17,84]. To begin a kinetic analysis of RISC, we first confirmed that RISC programmed *in vitro* with siRNA is likewise a multiple-turnover enzyme. To engineer an RNAi reaction that contained a high substrate concentration relative to RISC, we used an siRNA in which the guide strand is identical to the *let-7* miRNA, but unlike the miRNA, the *let-7* siRNA is paired to an RNA strand anti-sense to *let-7*[17]. The *let-7* strand of this siRNA has a high intrinsic cleaving activity, but a reduced efficiency of incorporation into RISC (**Supplementary Fig. 1**).

After incubating the *let-7* siRNA with *Drosophila* embryo lysate in the presence of ATP, RISC assembly was inactivated by treatment with *N*-ethyl maleimide (NEM), and the amount of RISC generated was measured using the previously described tethered 2′-*O*-methyl oligonucleotide assay[130,235] (**Supplementary Fig. 1**). The amount of *let-7* programmed RISC increased with increasing siRNA concentration, until the assembly reaction began to saturate at ~50 nM, reaching an asymptote between 3 and 4 nM RISC. Using 0.6 nM RISC, we observed >50 cycles of target recognition and cleavage per enzyme complex (data not shown), confirming that siRNA-programmed RISC is a multiple-turnover enzyme.

Multiple-turnover by RISC is limited by product release

Next, we evaluated the kinetics of siRNA-directed target cleavage in the presence or absence of ATP (-ATP; **Fig. 1**). RISC was assembled in the presence of ATP, then the energy regenerating enzyme, creatine kinase was inactivated with NEM, and ATP depleted by adding hexokinase and glucose. For +ATP measurements, we added back creatine kinase to the reaction after NEM-treatment, and omitted the hexokinase treatment. We observed a faster rate of cleavage in the presence than in the absence of ATP. This difference was only apparent late in the reaction time course, suggesting that the ATP-dependent rate of cleavage was faster than the ATP-independent rate only at steady state (**Fig. 1a**). We therefore repeated the analysis in more detail (**Fig. 1b**). In the absence of ATP, we observed a burst of cleaved product early in the reaction, followed by a ~4-fold slower rate of target cleavage. No burst was observed in the presence of

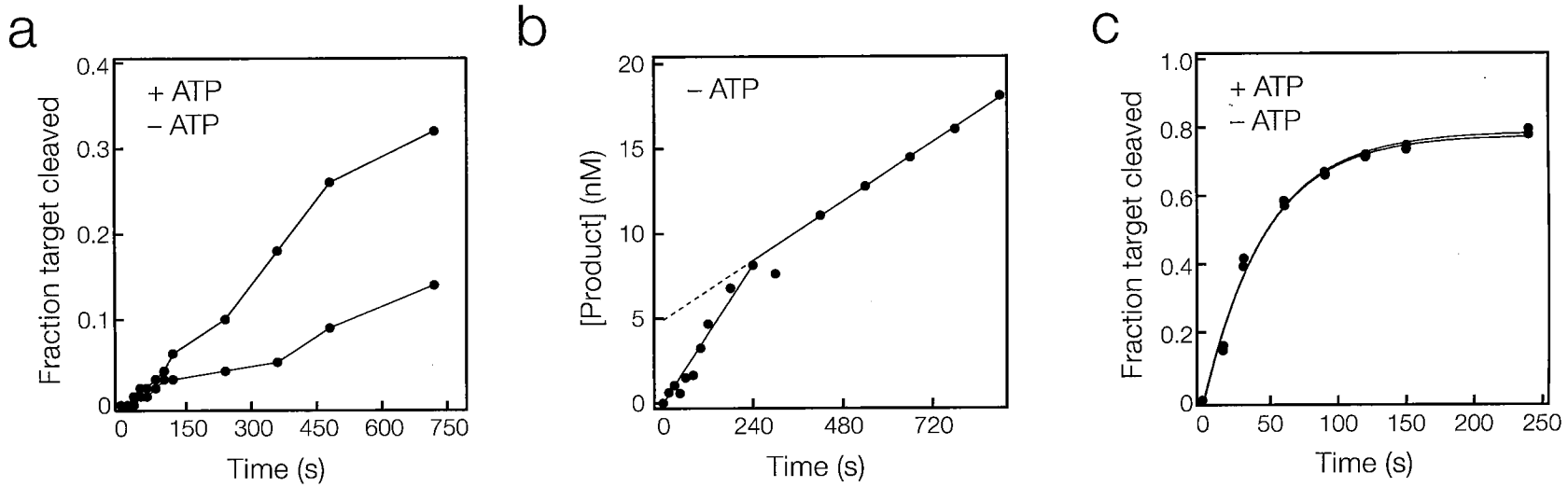
a
Fraction target cleaved
+ ATP
– ATP
0
0.1
0.2
0.3
0.4
0
150
300
450
600
750
Time (s)
b
[Product] (nM)
– ATP
0
5
10
15
20
0
240
480
720
Time (s)
c
Fraction target cleaved
+ ATP
– ATP
0
0.2
0.4
0.6
0.8
1.0
0
50
100
150
200
250
Time (s)

Figure 1 Product release limits the rate of catalysis by RISC. (**a**) ATP stimulates multiple rounds of RISC cleavage of the RNA target. siRNA was incubated with ATP in *Drosophila* embryo lysate, then NEM was added to quench RISC assembly and to disable the ATP-regenerating system. The energy regenerating system was either restored by adding additional creatine kinase (black) or the reaction was ATP-depleted by adding hexokinase and glucose (red). The target RNA concentration was 49 nM and the concentration of RISC was ~4 nM. The siRNA sequence is given in **Supplementary Figure 3**. (**b**) In the absence of ATP, cleavage by RISC produces a pre-steady state burst equal, within error, to the concentration of active RISC. The target concentration was 110 nM and the RISC concentration was ~4 nM. (**c**) Catalysis by RISC is not enhanced by ATP under single-turnover conditions. RISC was present in about eight-fold excess over target. Each data point represents the average of two trials.

ATP (**Fig. 1a**). If the burst corresponds to a single-turnover of enzyme, then extrapolation of the slower steady state rate back to the y-axis should give the amount of active enzyme in the reaction. The y-intercept at the start of the reaction for the steady-state rate was 4.9 nM, in good agreement with the amount of RISC estimated using the tethered 2′-*O*-methyl oligonucleotide assay (~4 nM; **Fig. 1b**).

In principle, ATP could enhance target recognition by RISC, promote a rearrangement of the RISC:target complex to an active form, facilitate cleavage itself, promote the release of the cleavage products from the siRNA guide strand, or help restore RISC to a catalytically competent state after product release. All of these steps, except product release and restoration to catalytic competence, should affect the rate of both multiple and single-turnover reactions. Therefore, we next analyzed the rate of reaction in the presence and in the absence of ATP under conditions in which RISC was in excess over the RNA target. At early times under these conditions, the reaction rate should reflect only single-turnover cleavage events, in which events after cleavage do not determine the rate of reaction. Using single-turnover reaction conditions, we observed identical rates of RISC-mediated cleavage in the presence and absence of ATP (**Fig. 1c**). Thus, ATP must enhance a step that occurs only when each RISC catalyzes multiple cycles of target cleavage.

If product release is rate-determining for multiple-turnover catalysis by RISC in the absence, but not the presence, of ATP, then modifications that weaken the strength of pairing to the target RNA might enhance product release, but would not be expected to accelerate the return of the RISC to a catalytically competent state. We incorporated

mismatches between the siRNA and its RNA target at the 3′ end of the siRNA guide strand and designed the siRNAs to be functionally asymmetric, ensuring efficient and predictable incorporation of the *let-7* strand into RISC (**Fig. 2a**)[130]. We compared the reaction velocity under conditions of substrate excess in the presence and in the absence of ATP for siRNAs with zero to four mismatches between the guide strand 3′ end and the RNA target. The cleavage was measured from 100 and 540 s, when > 90% of the target remained uncleaved, ensuring that the multiple-turnover reaction was at steady state. Even a single 3′ mismatch between the siRNA and its target increased the rate of reaction without ATP, relative to the rate with ATP, and siRNAs with two or more mismatches showed no significant difference in rate between the presence and absence of ATP (**Fig. 2b**). We conclude that in the absence of ATP, product release is the rate-determining step for siRNAs fully matched to their RNA targets.

siRNA-target complementarity and RISC function

Mismatches between the siRNA and its target facilitate product release, but not without cost: the rate of reaction, irrespective of ATP concentration, decreases with each additional 3′ mismatch. When the concentration of RISC was ~16-80-fold greater than the target RNA concentration, each additional mismatch between the 3′ end of the siRNA guide strand and the RNA target further slowed the reaction (**Figs. 2c,d**). Under conditions of substrate excess, the effect of mismatches between the 3′ end of the siRNA guide strand and its RNA target was more marked (**Fig. 3a**): the rate of cleavage slowed ~20% for each additional mismatch. To test the limits of the tolerance of RISC for 3′


arget + perfect match siRNA
3′-...CCAACUCCAUCAUCCAACAUAUCACUU...-5′
5′-UGAGGUAGUAGGUUGUAUAGU-3′
3′-UUACUCCAUCAUCCAACAUAU-5′
1 nt 3′ mismatched siRNA
3′-...CCAACUCCAUCAUCCAACAUAUCACUU...-5′
5′-UGAGGUAGUAGGUUGUAUAGG-3′,
UUACUCCAUCAUCCAACAUAU
2 nt 3′ mismatched siRNA
3′-...CCAACUCCAUCAUCCAACAUAUCACUU...-5′
5′-UGAGGUAGUAGGUUGUAUAAG-3′
UUCCUCCAUCAUCCAACAUAU
3 nt 3′ mismatched siRNA
3′-...CCAACUCCAUCAUCCAACAUAUCACUU...-5′
5′-UGAGGUAGUAGGUUGUAUCAG-3′
UUCCUCCAUCAUCCAACAUAG
4 nt 3′ mismatched siRNA
3′-...CCAACUCCAUCAUCCAACAUAUCACUU...-5′
5′-UGAGGUAGUAGGUUGUAGCAG-3′
UUCCUCCAUCAUCCAACAUCG

b

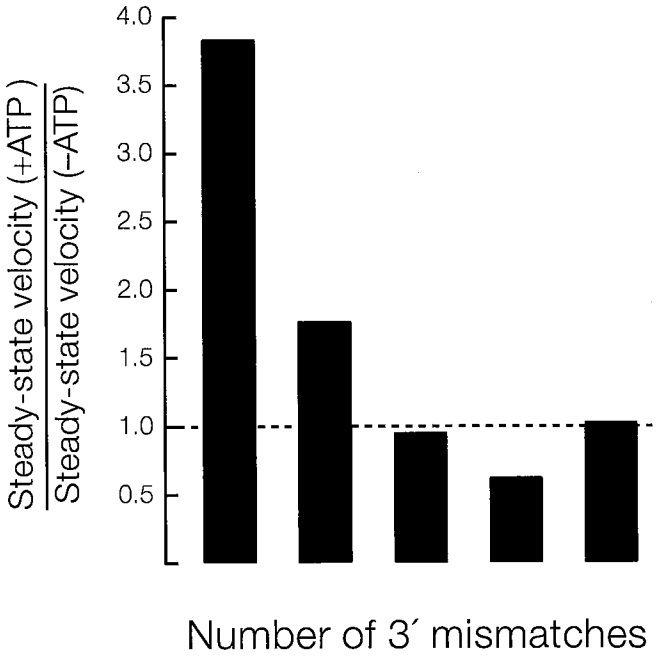
Steady-state velocity (+ATP) / Steady-state velocity (−ATP)
4.0
3.5
3.0
2.5
2.0
1.5
1.0
0.5
Number of 3′ mismatches

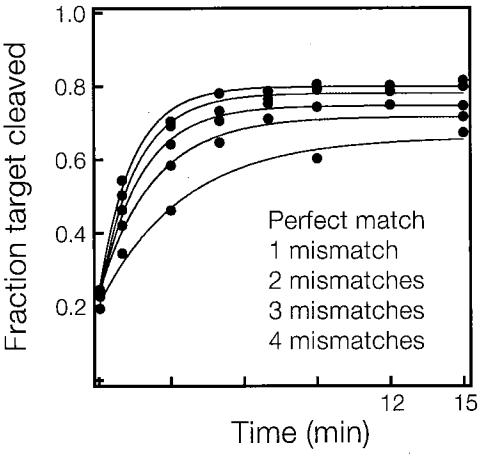
Fraction target cleaved
1.0
0.8
0.6
0.4
0.2
Perfect match
1 mismatch
2 mismatches
3 mismatches
4 mismatches
12
15
Time (min)

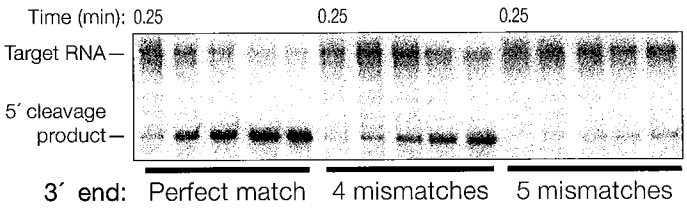
Time (min): 0.25
0.25
0.25
Target RNA—
5′ cleavage product—
3′ end: Perfect match
4 mismatches
5 mismatches

Figure 2 In the absence of ATP, mismatches between the 3′ end of the siRNA guide strand and the target RNA facilitate product release, but reduce the rate of target cleavage. (**a**) Representative siRNA sequences aligned with the target sequence. The siRNA guide strand is colored (5′ to 3′) and the mismatch with the target site is colored yellow. A complete list of siRNA sequences appears in **Supplementary Figure 3**. (**b**) The steady-state rate of cleavage in the presence and absence of ATP was determined for siRNAs with zero to four 3′ mismatches with the target site. The target RNA concentration was 49 nM and the concentration of RISC was either ~4 nM (no mismatches) or ~6 nM (1 to 4 mismatches). The steady-state velocity with ATP, relative to the velocity without ATP, is shown for each siRNA. (**c**) Time course of cleavage for perfectly matched (~16-fold excess of RISC relative to target) and mismatched (~80-fold excess of RISC) siRNA. Black, perfectly matched siRNA; red, one 3′ mismatch; purple, two 3′ mismatches; blue, three 3′ mismatches; green, four 3′ mismatches. (**d**) Data representative of those used in the analysis in (**c**) for target cleavage for siRNAs with zero, four, and five 3′ mismatches.

a

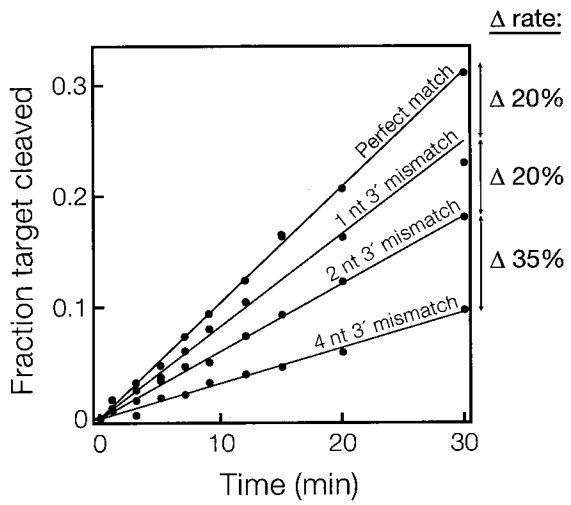
Δ rate:
Δ 20%
Δ 20%
Δ 35%
Perfect match
1 nt 3′ mismatch
2 nt 3′ mismatch
4 nt 3′ mismatch
Fraction target cleaved
0
0.1
0.2
0.3
0
10
20
30
Time (min)

c

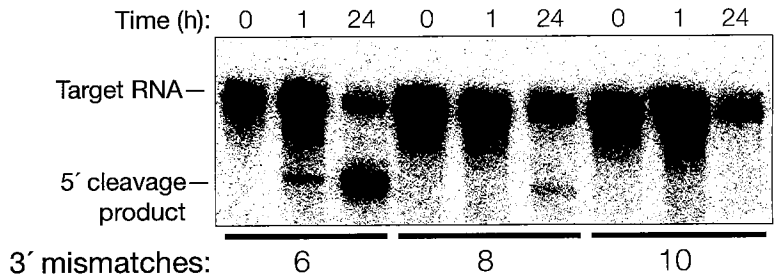
Time (h): 0 1 24 0 1 24 0 1 24
Target RNA—
5′ cleavage—
product
3′ mismatches: 6 8 10

b

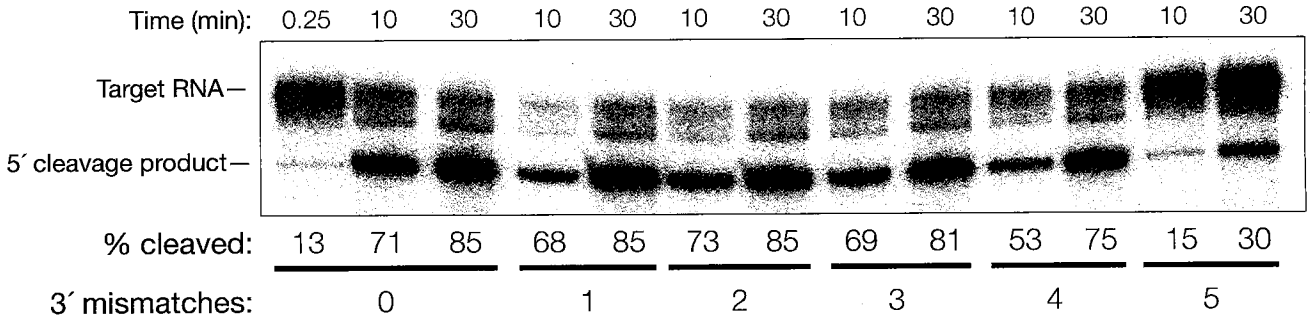
Time (min): 0.25 10 30 10 30 10 30 10 30 10 30 10 30
Target RNA—
5′ cleavage product—
% cleaved: 13 71 85 68 85 73 85 69 81 53 75 15 30
3′ mismatches: 0 1 2 3 4 5

Figure 3 Tolerance of RISC for 3′ mismatches. (**a**) Each additional 3′ mismatch further reduced the rate of cleavage by RISC. The steady-state rates of cleavage were determined for siRNA with zero, one, two, and four mismatches under multiple-turnover conditions (~49 nM target mRNA and ~4-6 nM RISC). (**b**) Analysis of siRNAs bearing zero to five 3′ mismatches with the target RNA under conditions of slight enzyme excess (about two-fold more RISC than target). siRNA sequences used in (a) and (b) are shown in **Figure 2a** and **Supplementary Figure 3**. (**c**) Extended endpoint analysis of RISC cleavage under conditions of ~80-fold enzyme excess reveals that cleavage can occur for siRNAs with as many as eight mismatches to the target RNA. Note the different time scales in (**c**) versus (**b**). All reactions were under standard *in vitro* RNAi (+ATP) conditions.

mismatches, we analyzed cleavage under modest (8-fold, **Fig. 3b**) and vast (~80-fold, **Figs. 3c** and **4**) enzyme excess over target RNA. Notably, cleavage was detected for siRNAs with as many as nine 3′ mismatches to the RNA target (**Figs. 3c** and **4c**), but only after 24 h incubation. No cleavage was detected for an siRNA with ten 3′ mismatches to the RNA target (**Fig. 3c**).

Linsley and colleagues have proposed siRNA-directed down-regulation of an mRNA with as few as eleven contiguous bases complementary to the siRNA guide strand[182]. In that study, the mRNA target paired with both nts 2-5 and nts 7-17 of the siRNA guide strand, but mismatched at nts 1 and 6 of the siRNA. We find that up to five mismatched bases are tolerated between the 5′ end of the siRNA and its RNA target (**Fig. 4a**,**b**). No cleavage was detected for siRNAs with six, seven, or eight 5′ mismatches to the target, even after 24 h incubation. The siRNA bearing eight mismatches between its 5′ end and the *let-7* complementary target was fully active when eight compensatory mutations were introduced into the *let-7* binding site (**Figs. 3c** and **4b**), demonstrating that mutation of the siRNA was not the cause for its inactivity against the mismatched target. Similarly, when eight mismatches with the 3′ or 5′ end of the siRNA were created by changing the sequence of the RNA target, we detected target RNA cleavage when the target contained eight mismatches with the siRNA 3′ end, but not with the 5′ end (**Fig. 4b,c**).

To begin to estimate the minimal number of base pairs between the siRNA and its target that permit detectable cleavage by RISC at 24 h incubation, we combined seven, eight, or nine 3′ mismatches with increasing numbers of 5′ mismatches (**Fig. 4c**).

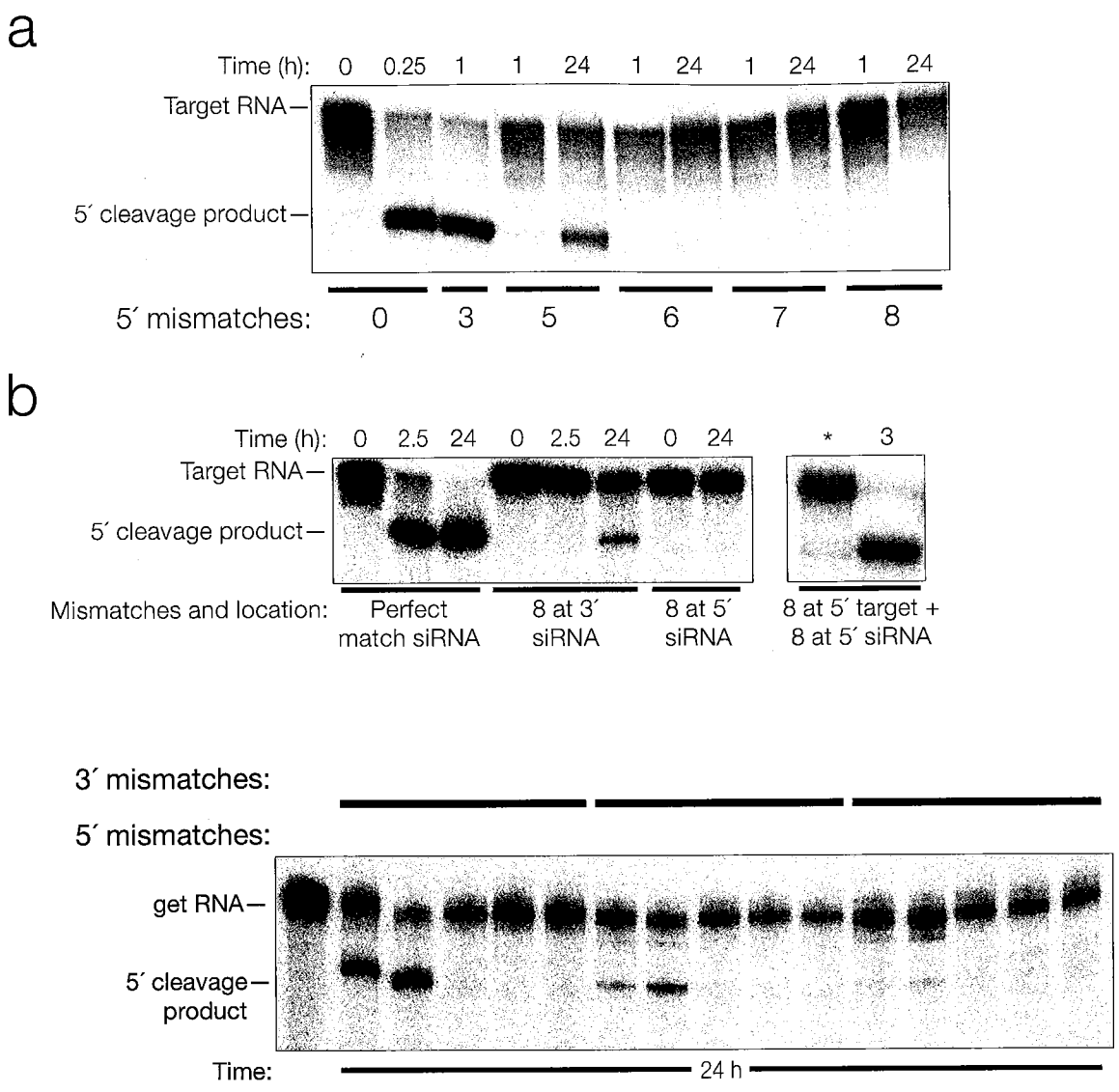
a
Time (h): 0 0.25 1 1 24 1 24 1 24 1 24
Target RNA—
5′ cleavage product—
5′ mismatches: 0 3 5 6 7 8
b
Time (h): 0 2.5 24 0 2.5 24 0 24 * 3
Target RNA—
5′ cleavage product—
Mismatches and location: Perfect match siRNA
8 at 3′ siRNA
8 at 5′ siRNA
8 at 5′ target + 8 at 5′ siRNA
3′ mismatches:
5′ mismatches:
get RNA—
5′ cleavage— product
Time: 24 h
d
5′ mismatches:
OH⁻ 0 2 20 30 45 60 min
—5′ cleavage product

Figure 4 Limited tolerance of RISC for 5′ mismatches. (**a**) RISC cleavage was analyzed as in **Figure 3c** using 5′ mismatched siRNAs, whose sequences are given in **Supplementary Figure 3**. The target RNA was the same for all siRNAs. (**b**) RISC cleavage was analyzed using a single siRNA sequence. Mismatches were created by altering the sequence of the target RNA. For the target containing compensatory mutations, the target concentration was 0.25 nM and the siRNA concentration was ~20 nM; RISC concentration was not determined. Asterisk, 15-s time point. (**c**) RISC cleavage was analyzed by incubating 50 nM siRNA with 0.5 nM target RNA. 3′ mismatches were created by modifying the target sequence, and 5′ mismatches by changing the siRNA. Target and siRNA sequences are given in **Supplementary Figure 3**. (**d**) Perfectly base-paired and 5′ mismatched siRNAs direct cleavage at the same phosphodiester bond. Cleavage reactions were performed with ~20 nM RISC generated from 50 nM siRNA and 0.5 nM target RNA and analyzed on an 8% (w/v) denaturing PAGE. The lengths of the target mRNA and 5′ cleavage product were 172-nt and 100-nt, respectively. After RISC was assembled, the extract was treated with NEM to inactivate nucleases[134]. After NEM treatment, the ATP regenerating system was restored by adding additional creatine kinase, then target RNA was added and the incubation continued for the indicated time. OH^- denotes a base hydrolysis ladder.

Cleavage was detected for as many as nine 3′ mismatches. But no detectable cleavage occurred when seven, eight, or nine 3′ mismatches were combined with two or more 5′ mismatches. In contrast, a single 5′ mismatch (p1) enhanced target cleavage directed by all three 3′mismatched siRNAs. Whereas, only 6% of the target RNA was cleaved after 24 h when the siRNA contained nine contiguous 3′ mismatches with the target RNA, 10% was cleaved when the siRNA contained both nine 3′ mismatches and a single (p1) 5′ mismatch (10% cleaved). Cleavage was similarly enhanced by the addition of a p1 mismatch to seven 3′ mismatches (49% cleavage versus 75% cleavage at 24 h) or to eight 3′ mismatches (21% versus 42% cleavage at 24 h). The finding that unpairing of the first base of the siRNA guide strand potentiated cleavage under single-turnover conditions suggests that a conformational change occurs in RISC during which the paired p1 base becomes unpaired prior to cleavage. Intriguingly, p1 is often predicted to be unpaired for miRNAs bound to their targets[102,236,237].

For siRNAs that pair fully with their RNA targets, the scissile phosphate always lies between the target nucleotides that pair with siRNA bases 10 and 11. Analysis at single nucleotide resolution of the 5′ cleavage products generated by siRNAs with three, four, or five 5′ mismatches (**Fig. 4d**) or six 3′ terminal mismatches (data not shown) revealed that the scissile phosphate on the target RNA remained the same, even when five 5′ nts of the siRNA guide strand were mismatched with the target RNA (**Fig. 4d**). As discussed below, this result suggests that the identity of the scissile phosphate is a consequence of the structure of RISC, rather than being measured from the 5′ end of the helix formed between the siRNA and its RNA target.

Kinetic analysis of RISC catalysis

What role do nucleotides in the terminal regions of the siRNA guide strand play in directing RISC activity? Reduced pairing between an siRNA and its target might disrupt the binding of RISC to its target. Alternatively, mismatches might disrupt the structure, but not the affinity, of the siRNA:target interaction. Fully matched siRNAs are thought to form a 21 base-pair, A-form helix with the target RNA[183,234], but do all parts of this helix contribute equally to target binding or do some regions provide only a catalytically permissive geometry? To distinguish between these possibilities, we analyzed the Michaelis-Menten kinetics of siRNA-directed target-RNA cleavage for a perfectly matched siRNA and for three siRNAs mismatched at their termini. siRNAs were assembled at high concentration into RISC, then diluted with reaction buffer to the desired concentration and mixed with target RNA. For each siRNA, the initial velocity of reaction was determined at multiple substrate concentrations (**Supplementary Fig. 3**), and K_M and k_{cat} determined from a non-linear least squares fit of substrate concentration versus initial velocity (**Fig. 5a**). By this assay, we estimate that the K_M of the *let-7* siRNA with complete complementarity to its target was ~8.4 nM (**Table 1**). We could not detect a significant difference in K_M, within error, between the fully paired siRNA and siRNA variants bearing three to five mismatches at their 3′ end or three mismatches at their 5′ end (**Fig. 5a** and **Table 1**). We note that for the mismatched siRNAs we used a higher than optimal enzyme concentration in order to detect cleavage. Therefore, our K_M measurements for the mismatched siRNAs represent an upper bound for the actual K_M values.

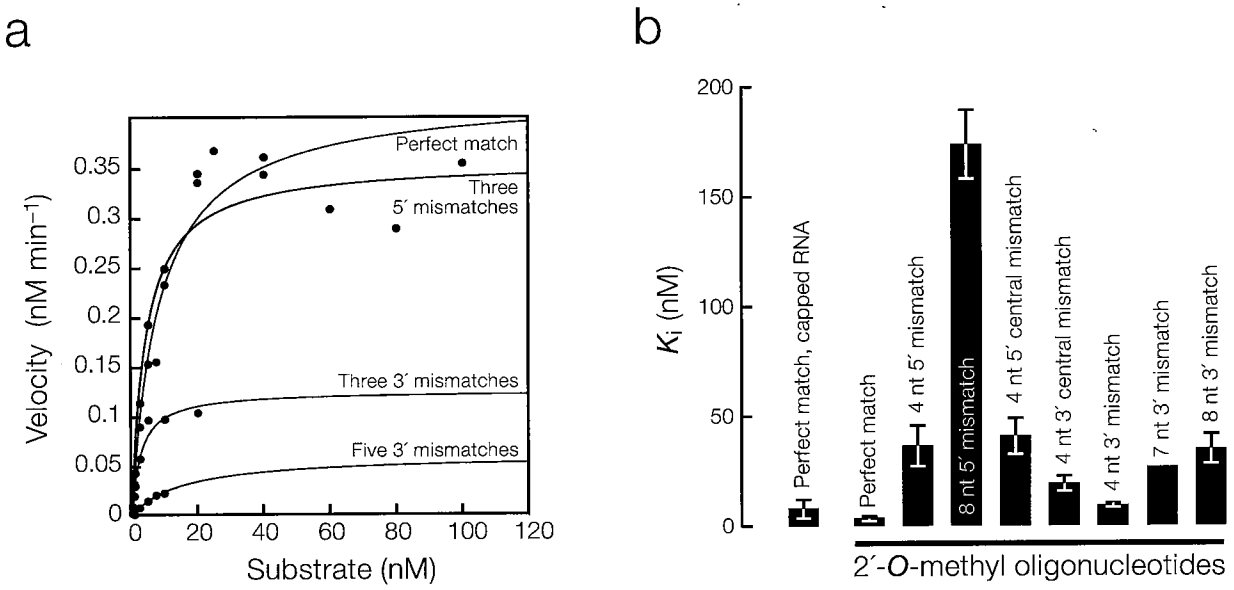
a
Velocity (nM min⁻¹)
0.35
0.3
0.25
0.2
0.15
0.1
0.05
0
0
20
40
60
80
100
120
Substrate (nM)
Perfect match
Three 5′ mismatches
Three 3′ mismatches
Five 3′ mismatches
b
K_i (nM)
200
150
100
50
0
Perfect match, capped RNA
Perfect match
4 nt 5′ mismatch
8 nt 5′ mismatch
4 nt 5′ central mismatch
4 nt 3′ central mismatch
4 nt 3′ mismatch
7 nt 3′ mismatch
8 nt 3′ mismatch
2′-O-methyl oligonucleotides

Figure 5 Michaelis-Menten and K_i analysis for matched and mismatched siRNAs reveal distinct contributions to binding and catalysis for the 5′, central, and 3′ regions of the siRNA. (a) siRNA was assembled into RISC under standard *in vitro* RNAi conditions, then diluted to achieve the desired RISC concentration. The initial rates of cleavage were determined for increasing concentrations of 5′ ^{32}P-cap-radiolabled target mRNA. Plot of initial velocity versus substrate concentration. K_M and V_{max} were determined by fitting the data to the Michaelis-Menten equation. See **Table 1** for analysis. Representative initial rate determinations appear in **Supplementary Figure 2**. (b) Ki values were determined in competition assays using 2′-*O*-methyl oligonucleotides bearing 5′, central and 3′ mismatches to the siRNA guide strand. Representative data are presented in **Supplementary Figure 2**, and a complete list of the 2′-*O*-methyl oligonucleotides used appears in **Supplementary Figure 3**.

Although the K_M was unaltered for the *let-7* siRNA containing several terminal mismatches, the turnover number, k_{cat}, was decreased by terminal mismatches (**Table 1**). Three mismatches at the 5′ end of the siRNA halved the k_{cat}, whereas three 3′ mismatches decreased k_{cat} more than six-fold. The introduction of five 3′ mismatches did not increase the K_M, yet decreased $k_{cat} > 25$-fold.

K_M largely reflects the binding strength of RISC

To estimate the contribution of binding to K_M, we used a competition assay that measures the ability of 2′-*O*-methyl oligonucleotides to inhibit target cleavage by RISC (**Fig. 5b**). Such a strategy was used previously to analyze the mechanism of target destruction by antisense oligonucleotides that recruit RNase H[238]. We anticipated that 2′-*O*-methyl oligonucleotides would act as competitive inhibitors of RISC, because they bind to RISC containing complementary siRNA but not to RISC containing unrelated siRNA. We designed 31-nt, 2′-*O*-methyl oligonucleotides as described[235], taking care to exclude sequences predicted to form stable internal structures. We chose 2′-*O*-methyl oligonucleotides because of their marked stability in *Drosophila* lysate and because they can be added to the reaction at high micromolecular concentration.

Competition by 2′-*O*-methyl oligonucleotides and authentic RNA targets was quantitatively similar. We analyzed the reaction velocities of siRNA-directed cleavage of a ^{32}P-radiolabled target in the presence of increasing concentrations of unlabeled capped RNA target or a 31-nt 2′-*O*-methyl oligonucleotide corresponding to the region of the target containing the siRNA binding site (**Fig. 5b**). Lineweaver-Burk analysis of the data

confirm that 2′-*O*-methyl oligonucleotides act as competitive inhibitors of RISC (data not shown). These data were used to calculate K_i values for the perfectly matched RNA and 2′-*O*-methyl competitors. For the capped RNA competitor, the K_i was ~7.7 ± 4 nM (**Fig. 5b**), nearly identical to the K_M, 8.4 nM, for this siRNA (**Table 1**). The K_i for the perfectly matched 2′-*O*-methyl competitor oligonucleotide was 3.2 ± 1 nM (**Fig. 5b**), essentially the same, within error, as that of the all-RNA competitor. We conclude that 2′-*O*-methyl oligonucleotides are good models for 5′-capped RNA targets and that the K_M for target cleavage by RISC is largely determined by the affinity (K_d) of RISC for its target RNA.

Although targets with more than five contiguous mismatches to either end of the siRNA are poor substrates for cleavage, they might nonetheless bind RISC and compete with the ^{32}P-radiolabeled target RNA. We used the 2′-*O*-methyl oligonucleotide competition assay to determine the K_i values for oligonucleotides containing as many as eight mismatches to the siRNA guide strand (**Fig. 5b**). 2′-*O*-methyl oligonucleotides with 3′ terminal mismatches to the siRNA were good competitors: a four nucleotide mismatch with the 3′ end of the siRNA reduced the K_i by only ~3-fold (9.0 ± 0.9 nM) and an eight nucleotide mismatch with the 3′ end of the siRNA reduced the K_i by ~10-fold (34.8 ± 7 nM). In contrast, mismatches with the 5′ end of the siRNA had a dramatic effect on binding. A four nucleotide mismatch to the 5′ end of the siRNA reduced the K_i ~12-fold (36.4 ± 9.2 nM) and an eight nucleotide mismatch to the 5′ end of the siRNA reduced the K_i 53-fold (173 ± 16 nM). The differential effect on binding between 5′ and 3′ mismatches was maintained even at the center of the siRNA: a 2′-*O*-methyl oligonucleotide bearing four mismatches with siRNA nucleotides 11, 12, 13, and 14 (4-nt

3′ central mismatch, **Fig. 5b**) bound more tightly to RISC (i.e., had a lower K_i) than an oligonucleotide with four mismatches to siRNA positions 7, 8, 9, and 10 (4-nt 5′ central mismatch, **Fig. 5b**).

DISCUSSION

RISC programmed with exogenous siRNA is an enzyme, capable of multiple rounds of target cleavage. Our previous work showed that cleavage of a target RNA by RISC does not require ATP[10,239]. The more detailed kinetic analysis presented here suggests that there are no ATP-assisted steps in either target recognition or cleavage by *Drosophila* RISC: we can detect no difference in rate in the presence or absence of ATP for RNAi reactions analyzed under conditions of substrate excess at early time points (pre-steady state) or under conditions of enzyme excess where the reaction was essentially single-turnover. In contrast, the steady-state rate of cleavage under multiple turnover conditions is enhanced four-fold by ATP. Our data suggest that release of the products of the RISC endonuclease is rate-determining under these conditions in the absence of ATP, but not in the presence of ATP. The most straightforward explanation for this finding is that an ATP-dependent RNA helicase facilitates the dissociation of the products of target cleavage from the RISC-bound siRNA. The involvement of such an ATP-dependent helicase in RNAi *in vivo* may explain why siRNAs can be active within a broad range of GC content[240].

In the presence of ATP, siRNA-programmed *Drosophila* RISC is a classical Michaelis-Menten enzyme. The guide strand of the siRNA studied here has the sequence

of *let-7*, an endogenous miRNA. *In vivo*, *let-7* is not thought to direct mRNA cleavage, but rather is believed to repress productive translation of its mRNA targets. Nonetheless, the *let-7* siRNA is among the most potent of the siRNAs we have studied *in vitro* and provides a good model for effective siRNA in general. With a k_{cat} of ~7 x 10^{-3} s^{-1}, the *let-7* siRNA-programmed RISC was slow compared to enzymes with small molecule substrates (**Table 1**). The K_M for this RISC was ~8 nM. Enzymes typically have K_M values between 1- and 100-fold greater than the physiological concentrations of their substrates. Our data suggest that RISC is no exception: individual abundant mRNA species are present in eukaryotic cells at high pM or low nM concentration. The K_M of RISC is likely determined primarily by the strength of its interaction with the target RNA, because the K_M is nearly identical to the K_i of a non-cleavable 2′-*O*-methyl oligonucleotide inhibitor.

Recently, Tuschl and colleagues have measured the kinetic parameters of target RNA cleavage by human RISC[135]. In that study, the minimal active RISC was highly purified; in this study, D. melanogaster RISC activity was measured for the unpurified, intact holo-RISC, believed to be an 80S multiprotein complex. Different siRNAs were used in the two studies. Nonetheless, the K_M and k_{cat} values reported here and for the minimal RISC are markedly similar: The K_M was 2.7-8.4 nM and the kcat was 7.1 x $10^{-3}s^{-1}$ for the *let-7* siRNA-programmed *D. melanogaster* holo-RISC versus a K_M of 1.1-2.3 nM and a k_{cat} of 1.7 x $10^{-2}s^{-1}$ for a differenct siRNA in minimal human RISC. As in this study, Tuschl and colleagues observed a pre-steady-state burst in the absence of ATP, consistent with the idea that product release is ATP-assissted *in vivo*.

Mismatches, position	K_M (nM)	V_{max} (nM s^{-1})	[RISC] (nM)	k_{cat} (s^{-1})	$k_{cat}\,K_M^{-1}$ ($nM^{-1}\,s^{-1}$)	fold change, $k_{cat}\,K_M^{-1}$
none	8.4 ± 1.6	0.0071	1	7.1×10^{-3}	8.4×10^{-4}	1.00
three nt 3′	2.7 ± 0.6	0.0022	2	1.1×10^{-3}	3.8×10^{-4}	0.46
five nt 3′	6.0 ± 1.8	0.0054	2	2.7×10^{-4}	4.5×10^{-5}	0.05
three nt 5′	4.7 ± 1.3	0.0063	2	3.2×10^{-3}	6.7×10^{-4}	0.80

Reference enzymes	K_M (nM)	k_{cat} (s^{-1})	$k_{cat}\,K_M^{-1}$ ($nM^{-1}\,s^{-1}$)	$k_{cat}\,K_M^{-1}$ relative to RISC
Urease	2.5×10^{7}	1×10^{4}	4.0×10^{-4}	0.47
Fumarase	5.0×10^{3}	8×10^{2}	1.6×10^{-1}	190
Catalase	2.5×10^{7}	1×10^{7}	4.0×10^{-1}	8940
RNase H1	3.8×10^{1}	5×10^{2}	1.3×10^{-3}	0.03

Table 1. Kinetic analysis of RISC

The ratio of k_{cat} to K_M is a classical measure of enzyme efficiency and corresponds to the second order rate constant for the reaction when the concentration of substrate is much less than the K_M. For the *let-7* programmed RISC, k_{cat}/K_M equals ~8.4 x 10^5 M^{-1} s^{-1} (~8.4 x 10^{-4} nM^{-1} s^{-1}), a value far slower than the expected rate of collision of RISC with mRNA, which is expected to be ≥10^7 M^{-1} s^{-1}. What then limits the rate of catalysis by RISC? Perhaps cleavage by RISC is constrained by the rate of conformational changes required for formation of the enzyme-substrate complex or by subsequent conformational rearrangements required for catalysis. Future studies will be needed to determine if siRNAs can be designed that significantly improve either the k_{cat} or K_M of RISC without compromising specificity.

Although siRNAs are typically envisioned to bind their target RNAs through 19 to 21 complementary base pairs, we find that the 5′, central, and 3′ regions of the siRNA make distinct contributions to binding and catalysis (**Fig. 6**). Measurements of K_M and K_i suggest that the 5′ nucleotides of the siRNA contribute more to target binding than do the 3′ nucleotides. At least for the siRNA examined here, the first three and the last five nucleotides of a 21 nt siRNA contribute little to binding. If the K_d of RISC bound to its target RNA is essentially its K_M, ~8 nM, then the free energy ($\Delta G° = -RT \ln K_d$) of the *let-7*-programmed RISC:target interaction is approximately -11 kcal/mole, considerably less than the -35 kcal/mole (K_d ~10^{-29}) predicted (http://ozone2.chem.wayne.edu/Hyther/hytherm1main.html) for the *let-7* RNA bound to a fully complementary RNA in 100 mM K^+ and 1.2 mM Mg^{2+} at 25°C. Why does RISC seem to discard so much potential binding energy? Perhaps by binding less tightly to its

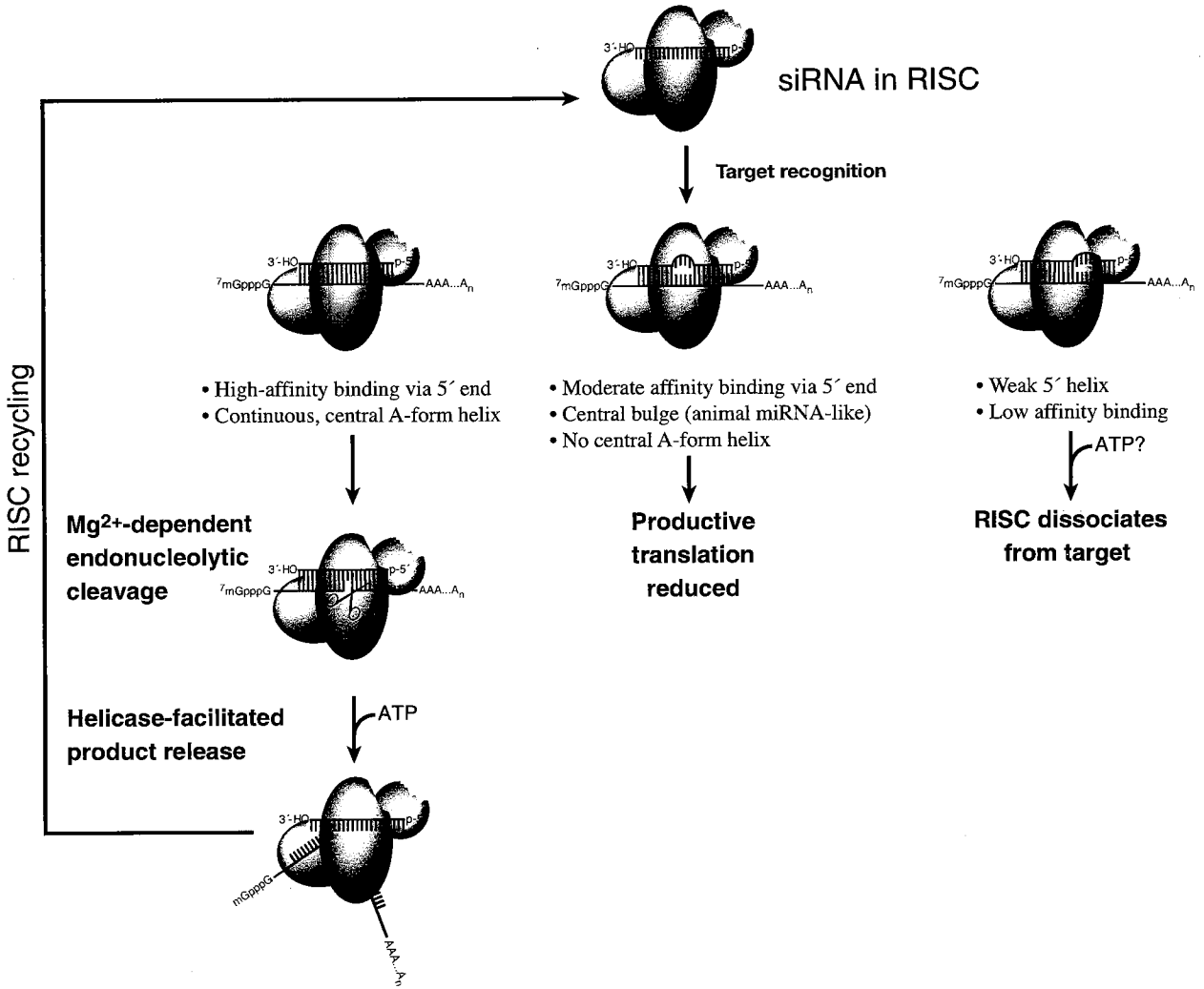
siRNA in RISC
Target recognition
• High-affinity binding via 5′ end
• Continuous, central A-form helix
• Moderate affinity binding via 5′ end
• Central bulge (animal miRNA-like)
• No central A-form helix
• Weak 5′ helix
• Low affinity binding
ATP?
Mg2+-dependent endonucleolytic cleavage
Productive translation reduced
RISC dissociates from target
Helicase-facilitated product release
ATP
RISC recycling

Figure 6. A model for the cycle of RISC assembly, target recognition, catalysis and recycling.

target, an siRNA in RISC gains the ability to discriminate between well matched and poorly match targets, but only for bases in the 5′ region of the siRNA guide strand.

Mismatches between the central and 3′ regions of an siRNA and its target RNA reduce k_{cat} far more than mismatches at the 5′ end of the siRNA. These results fit well with recent findings by Doench and Sharp that translational repression by siRNA, designed to act like animal miRNA, is dramatically disrupted by mismatches with the 5′ end of the siRNA, but not with similar mismatches at the 3′ end[233]. These authors propose that miRNA binding is mediated primarily by nucleotides at the 5′ end of the small RNA. Our finding that central and 3′ siRNA sequences must pair with the target sequence for effective target cleavage but not for target binding reinforces this view; both central and 3′ miRNA sequences are usually mismatched with their binding sites in their natural targets. In fact, complementarity between the 5′ end of miRNAs and their targets has been required by all computational approaches for predicting animal miRNA targets[102,110,231,236]. Our finding that central and 3′ miRNA sequences must pair with the target sequence for effective target cleavage but not for target binding reinforces this view; both central and 3′ miRNA sequences are usually mismatched with their binding sites in their natural targets[76,241-245].

Formation of a contiguous A-form helix surrounding the scissile phosphate of the target mRNA has been proposed to be a quality control step for RISC-mediated target cleavage[234]. We find that RISC can direct cleavage when the siRNA is paired with the target RNA only at nts 2-12 of the guide strand, corresponding to one complete turn of an RNA-RNA helix. This region of the siRNA includes nts 2-8, which seem to be critical

for miRNA recognition of mRNAs targeted for translational repression, plus two nucleotides flanking either side of the scissile phosphate. Our finding that unpairing the first nucleotide of the guide strand enhances the activity of siRNAs with seven, eight or nine 3′ mismatches to the RNA target is notable, as many miRNAs do not pair with their targets at this position. Furthermore, such pairing resembles that reported by Linsley and colleagues for siRNA-directed off-target effects in cultured mammalian cells[182].

The requirement for a full turn of a helix may reflect a mechanism of 'quality control' by RISC. Since RISC can apparently assemble on any siRNA sequence, it must use the structure of the siRNA paired to its target to determine whether or not to cleave. Despite the apparent surveillance of the structure of the siRNA-target pair, the identity of the scissile phosphate is unaltered by extensive mismatch between the 5′ end of the siRNA and its target. Yet the scissile phosphate is determined by its distance from the 5′ end of the siRNA guide strand[4,5]. The simplest explanation for our findings is that the scissile phosphate is identified by a protein loaded onto the siRNA during RISC assembly, i.e., before the encounter of the RISC with its target RNA.

The remarkable tolerance of RISC for mismatches between the siRNA and its targets—up to nine contiguous 3′ nucleotides—implies that a large number off-target genes should be expected for many siRNA sequences when RISC is present in excess over its RNA targets. However, RISC with extensive mismatches between the siRNA and target are quite slow to cleave, so off-target effects may be minimized by keeping the amount of RISC as low as possible. As our understanding of the molecular basis of

siRNA-directed gene silencing grows, we anticipate that siRNA will be able to be designed to balance the competing demands of siRNA efficacy and specificity.

MATERIALS AND METHODS

General methods. *Drosophila* embryo lysate, siRNA labeling with polynucleotide kinase (New England Biolabs), target RNA preparation and labeling with guanylyl transferase were carried out as described, and the forward primer sequence for 379 nt target mRNA was 5′-CGC TAA TAC GAC TCA CTA TAG CAG TTG GCG CCG CGA ACG A-3′, and 5′-GCG TAA TAC GAC TCA CTA TAG TCA CAT CTC ATC TAC CTC C-3 for the 172 nt target. Reverse primers used to generate fully matched and mismatched target RNAs were: 5′-CCC ATT TAG GTG ACA CTA TAG ATT TAC ATC GCG TTG AGT GTA GAA CGG TTG TAT AAA AGG TTG AGG TAG TAG GTT GTA TAG TGA AGA GAG GAG TTC ATG ATC AGT G-3′ (perfect match to let-7); 5′-CCC ATT TAG GTG ACA CTA TAG ATT TAC ATC GCG TTG AGT GTA GAA CGG TTG TAT AAA AGG TTG AGG TAG TAG GTT CAT GCA GGA AGA GAG GAG TTC ATG ATC AGT G-3′(7 nt 3′ mismatch); 5′-CCC ATT TAG GTG ACA CTA TAG ATT TAC ATC GCG TTG AGT GTA GAA CGG TTG TAT AAA AGG TTG AGG TAG TAG GTA CAU GCA GGA AGA GAG GAG TTC ATG ATC AGT G-3′ (8 nt 3′ mismatch); 5′-CCC ATT TAG GTG ACA CTA TAG ATT TAC ATC GCG TTG AGT GTA GAA CGG TTG TAT AAA AGG TTG AGG TAG TAG GAA CAT GCA GGA AGA GAG GAG TTC ATG ATC AGT G-3′ (9 nt 3′ mismatch); 5′-CCC ATT TAG GTG ACA CTA TAG ATT TAC ATC GCG TTG AGT GTA GAA CGG TTG TAT AAA AGG TAC TCC ATC TAG GTT GTA TAG TGA AGA GAG GAG TTC ATG ATC AGT G-3′(8 nt 5′mismatch); 5′-CCC ATT TAG GTG ACA CTA TAG ATT TAC ATC GCG TTG AGT GTA GAA CGG TTG TAT AAA AGG TAC TCG

TAG TAG GTT GTA TAG TGA AGA GAG GAG TTC ATG ATC AGT G-3′ (4 nt 5′mismatch). In **Figs. 1-3**, and **5a**, and **Supplementary Figures 1** and **2**, the target sequence was 613 nt long; 379 nt in **Figures 4a-c** and **5b**, and **Supplementary Figure 2**; and 172 nt in **Fig. 4d**. All siRNAs were deprotected according to the manufacturer's protocol (Dharmacon), 5′-radiolabeled where appropriate, then gel purified on a 15% denaturing polyacrylamide gel. 2′-*O*-methyl oligonucleotides were from Dharmacon. siRNA strands were annealed at high concentrations and serially diluted into lysis buffer (30 nM HEPES pH 7.4, 100 mM KOAc, and 2 mM $MgCl_2$). Gels were dried and imaged as described. Images were analyzed using Image Gauge 4.1 (Fuji). Initial rates were determined by linear regression using Excel X (Microsoft) or IgorPro 5.01 (Wavemetrics). Kaleidagraph 3.6.2 (Synergy Software) was used to determine K_M and K_i by global fitting to the equations: $V=(V_{max} \times S)/(K_M + S)$ and $V=(V_{max} \times K_{i(app)})/(K_{i(app)} + I)$, where V is velocity, S is target RNA concentration, and I is the concentration of 2′-*O*-methyl oligonucleotide competitor. K_i was calculated by correcting $K_{i(app)}$ by the K_M and substrate concentration, $K_i=K_{i(app)}/(1+S/K_M)$.

ATP-depletion and *N*-ethyl maleimide (NEM) inhibition.

RNAi reactions using *Drosophila* embryo lysate were as described[226]. To compare 'minus' and 'plus' ATP conditions, samples were treated with 10 mM NEM (Pierce) for 10 min at 4°C, then the NEM was quenched with 11 mM dithiothreitol (DTT). For ATP depletion (–ATP), 1 unit of hexokinase and 20 mM (final concentration) glucose were added and the incubation continued for 30 min at 25°C. For

'plus' ATP reactions, 0.05 mg/ml (final concentration) creatine kinase and one-tenth volume H_2O substituted for hexokinase and glucose. The addition of fresh creatine kinase after NEM treatment did not rescue the defect in RISC assembly, but did restore ATP to high levels[10]. ATP levels were measured using an ATP assay kit (Sigma) and a PhL luminometer (Mediators Diagnostika).

ACKNOWLEDGEMENTS

We thank Juanita McLachlan for maintaining our fly colony, members of the Zamore lab, Steve Blacklow, Tony Carruthers, and Doug Turner for encouragement, helpful discussions, and comments on the manuscript. P.D.Z. is a Pew Scholar in the Biomedical Sciences and a W.M. Keck Foundation Young Scholar in Medical Research. Supported in part by grants from the National Institutes of Health to P.D.Z. (GM62862-01 and GM65236-01).

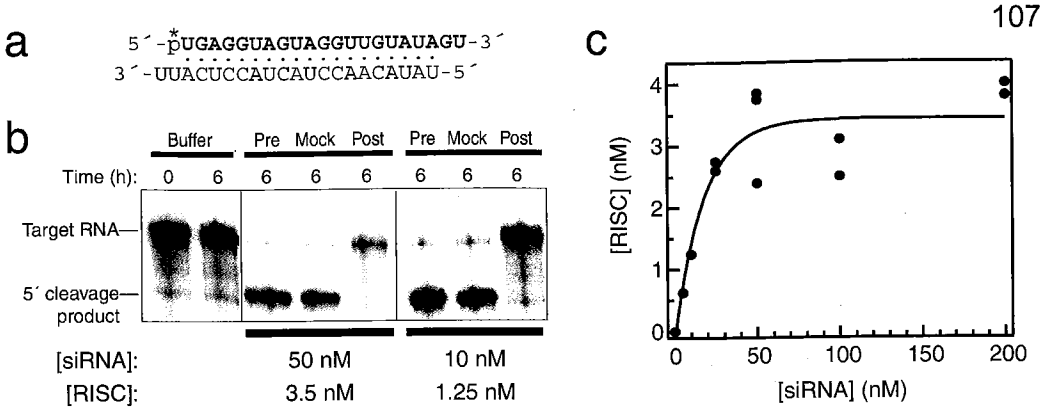

Supplementary Figure 1 Exogenously programmed RISC is a bona fide enzyme siRNA was assembled into RISC for 1 h in a standard *in vitro* RNAi reaction, then assembly was quenched with *N*-ethyl maleimide (NEM)[21,29]. The amount of RISC formed was determined by measuring ^{32}P-radiolabeled siRNA retained on a tethered 5′-biotinylated, 31-nt, 2′-*O*-methyl oligonucleotide complementary to the guide strand of the siRNA. RISC binds essentially irreversibly to tethered 2′-*O*-methyl oligonucleotides, but cannot cleave these RNA-analogs[21,22]. In all experiments, target-cleaving activity was not detected in the supernatant, demonstrating that all the active RISC was retained on the beads. (**a**) Sequence of the siRNA used (guide strand in red, ^{32}P-radiolabel marked with an asterisk). *D. melanogaster let-7* is not expressed in 0–2 h embryos[44], so the only source of *let-7* in the *in vitro* reactions was the exogenous *let-7* siRNA. The 5′ end of the guide strand of the *let-7* siRNA is predicted to be thermodynamically more stable than the 5′ end of the passenger strand, explaining why only a low concentrations of *let-7*-programmed RISC is formed[22,45]. The maximum amount of RISC assembled varies widely with siRNA sequence. The siRNAs used in **Figures 3–8** were designed to load ≥5-fold more guide strand-containing RISC[21,22]. (**b**) Representative gel confirming that the RISC was removed by the tethered 2′-*O*-methyl oligonucleotide. A reaction prior to incubation with the tethered 2′-*O*-methyl oligonucleotide (pre) was compared to the supernatant of a reaction incubated with beads alone (mock), and the supernatant of a reaction incubated with the complementary tethered 2′-*O*-methyl oligonucleotide (post). The buffer reaction contained no siRNA. (**c**) Analysis of the amount of RISC assembled at various siRNA concentrations. 5′ ^{32}P-radiolabeled siRNA was incubated with lysate for 1 h, then reactions were quenched by treatment with NEM, and RISC concentration was measured using the tethered 2′-*O*-methyl oligonucleotide method.

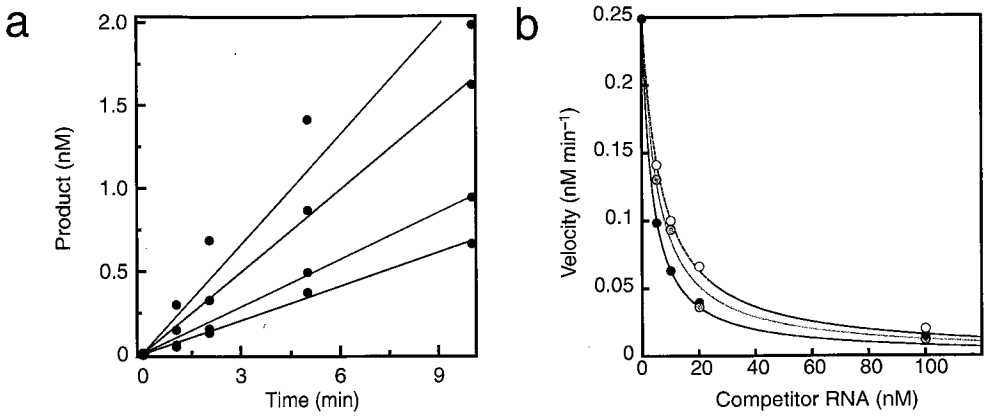

Supplementary Figure 2 Michaelis-Menten and competitor analysis of RISC (**a**) Representative data for the determination of initial velocities for the perfectly matched siRNA. Black, 1 nM target; red, 5 nM; blue, 20 nM; and green, 60 nM. (**b**) Three independent experiments for inhibition by a fully complementary 2′-*O*-methyl oligonucleotide competitor. ~1 nM RISC and 5 nM ^{32}P-cap-radiolabeled target mRNA were incubated with increasing concentration of competitor, and the initial velocities were calculated and plotted versus competitor concentration.

Target and siRNA	Figure #
target : fully matched siRNA 3´-...CCAACUCCAUCAUCCAACAUAUCACUU...-5´ 5´-UGAGGUAGUAGGUUGUAUAGU-3´ 3´-UUACUCCAUCAUCCAACAUAU-5´ target : 1 nt 3´ mismatched siRNA 3´-...CCAACUCCAUCAUCCAACAUAUCACUU...-5´ 5´-UGAGGUAGUAGGUUGUAUAGG-3´ UUACUCCAUCAUCCAACAUAU target : 2 nt 3´ mismatched siRNA 3´-...CCAACUCCAUCAUCCAACAUAUCACUU...-5´ 5´-UGAGGUAGUAGGUUGUAUAAG-3´ UUCCUCCAUCAUCCAACAUAU target : 3 nt 3´ mismatched siRNA 3´-...CCAACUCCAUCAUCCAACAUAUCACUU...-5´ 5´-UGAGGUAGUAGGUUGUAUCAG-3´ UUCCUCCAUCAUCCAACAUAG target : 4 nt 3´ mismatched siRNA 3´-...CCAACUCCAUCAUCCAACAUAUCACUU...-5´ 5´-UGAGGUAGUAGGUUGUAGCAG-3´ UUCCUCCAUCAUCCAACAUCG target : 5 nt 3´ mismatched siRNA 3´-...CCAACUCCAUCAUCCAACAUAUCACUU...-5´ 5´-UGAGGUAGUAGGUUGUUGCAG-3´ UUCCUCCAUCAUCCAACAACG	**Figures 2b-d, 3a,b** and **5a**
target : 6 nt 3´ mismatched siRNA 3´-...CCAACUCCAUCAUCCAACAUAUCACUU...-5´ 5´-UGAGGUAGUAGGUUGAUGCAG-3´ UUCCUCCAUCAUCCAACUACG target : 8 nt 3´ mismatched siRNA 3´-...CCAACUCCAUCAUCCAACAUAUCACUU...-5´ 5´-UGAGGUAGUAGGUACAUGCAG-3´ UUCCUCCAUCAUCCAAGUACG target : 10 nt 3´ mismatched siRNA 3´-...CCAACUCCAUCAUCCAACAUAUCACUU...-5´ 5´-UGAGGUAGUAGCAACAUGCAG-3´ UUCCUCCAUCAUCCUUGUACG	**Figure 3c**

target : 1 nt 5′ mismatched siRNA

```
3′-...CCAACUCCAUCAUCCAACAUAUCACUU...-5′
     5′-AGAGGUAGUAGGUUGUAUAGU-3′
       UUCCUCCAUCAUCCAACAUAU
```

target : 3 nt 5′ mismatched siRNA

```
3′-...CCAACUCCAUCAUCCAACAUAUCACUU...-5′
     5′-ACUGGUAGUAGGUUGUAUAGU-3′
       UUCGACCAUCAUCCAACAUAU
```

target : 5 nt 5′ mismatched siRNA

```
3′-...CCAACUCCAUCAUCCAACAUAUCACUU...-5′
     5′-ACUCCUAGUAGGUUGUAUAGU-3′
       UUCGAGGAUCAUCCAACAUAU
```

target : 6 nt 5′ mismatched siRNA

```
3′-...CCAACUCCAUCAUCCAACAUAUCACUU...-5′
     5′-ACUCCAAGUAGGUUGUAUAGU-3′
       UUCGAGGUUCAUCCAACAUAU
```

target : 7 nt 5′ mismatched siRNA

```
3′-...CCAACUCCAUCAUCCAACAUAUCACUU...-5′
     5′-ACUCCAUGUAGGUUGUAUAGU-3′
       UUCGAGGUACAUCCAACAUAU
```

target : 8 nt 5′ mismatched siRNA

```
3′-...CCAACUCCAUCAUCCAACAUAUCACUU...-5′
     5′-ACUCCAUCUAGGUUGUAUAGU-3′
       UUCGAGGUAGAUCCAACAUAU
```

Figures 4a, d and **5a**

8 nt 3′ mismatched target : siRNA

```
3′-...CCAACUCCAUCAUCCAUGUACGUCCUU...-5′
     5′-UGAGGUAGUAGGUUGUAUAGU-3′
       UUCCUCCAUCAUCCAACAUAU
```

8 nt 5′ mismatched target : siRNA

```
3′-...CCAUGAGGUAGAUCCAACAUAUCACUU...-5′
     5′-UGAGGUAGUAGGUUGUAUAGU-3′
       UUCCUCCAUCAUCCAACAUAU
```

Figure 4b

8 nt 5′ mismatched target : 8 nt 5′ mismatch siRNA

```
3′-...CCAUGAGGUAGAUCCAACAUAUCACUU...-5′
     5′-ACUCCAUCUAGGUUGUAUAGU-3′
       UUCGAGGUAGAUCCAACAUAU
```

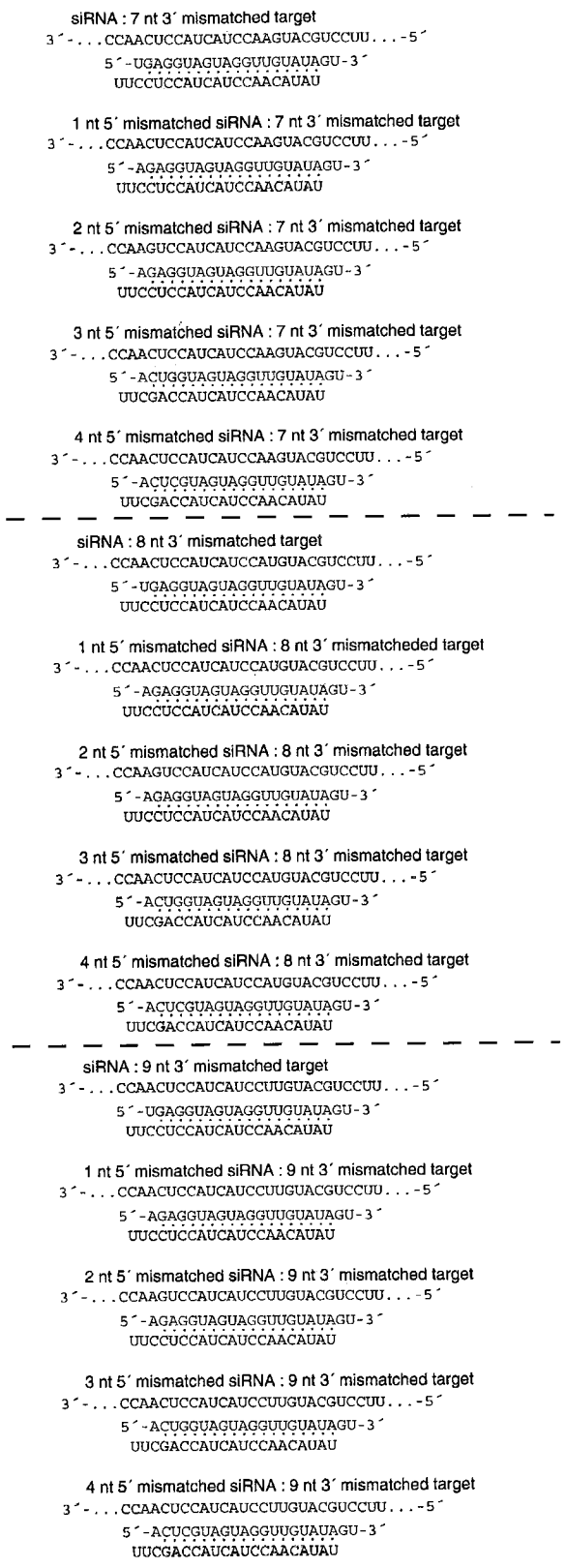
siRNA : 7 nt 3′ mismatched target
3′-...CCAACUCCAUCAUCCAAGUACGUCCUU...-5′
5′-UGAGGUAGUAGGUUGUAUAGU-3′
UUCCUCCAUCAUCCAACAUAU
1 nt 5′ mismatched siRNA : 7 nt 3′ mismatched target
3′-...CCAACUCCAUCAUCCAAGUACGUCCUU...-5′
5′-AGAGGUAGUAGGUUGUAUAGU-3′
UUCCUCCAUCAUCCAACAUAU
2 nt 5′ mismatched siRNA : 7 nt 3′ mismatched target
3′-...CCAAGUCCAUCAUCCAAGUACGUCCUU...-5′
5′-AGAGGUAGUAGGUUGUAUAGU-3′
UUCCUCCAUCAUCCAACAUAU
3 nt 5′ mismatched siRNA : 7 nt 3′ mismatched target
3′-...CCAACUCCAUCAUCCAAGUACGUCCUU...-5′
5′-ACUGGUAGUAGGUUGUAUAGU-3′
UUCGACCAUCAUCCAACAUAU
4 nt 5′ mismatched siRNA : 7 nt 3′ mismatched target
3′-...CCAACUCCAUCAUCCAAGUACGUCCUU...-5′
5′-ACUCGUAGUAGGUUGUAUAGU-3′
UUCGACCAUCAUCCAACAUAU
siRNA : 8 nt 3′ mismatched target
3′-...CCAACUCCAUCAUCCAUGUACGUCCUU...-5′
5′-UGAGGUAGUAGGUUGUAUAGU-3′
UUCCUCCAUCAUCCAACAUAU
1 nt 5′ mismatched siRNA : 8 nt 3′ mismatcheded target
3′-...CCAACUCCAUCAUCCAUGUACGUCCUU...-5′
5′-AGAGGUAGUAGGUUGUAUAGU-3′
UUCCUCCAUCAUCCAACAUAU
2 nt 5′ mismatched siRNA : 8 nt 3′ mismatched target
3′-...CCAAGUCCAUCAUCCAUGUACGUCCUU...-5′
5′-AGAGGUAGUAGGUUGUAUAGU-3′
UUCCUCCAUCAUCCAACAUAU
3 nt 5′ mismatched siRNA : 8 nt 3′ mismatched target
3′-...CCAACUCCAUCAUCCAUGUACGUCCUU...-5′
5′-ACUGGUAGUAGGUUGUAUAGU-3′
UUCGACCAUCAUCCAACAUAU
4 nt 5′ mismatched siRNA : 8 nt 3′ mismatched target
3′-...CCAACUCCAUCAUCCAUGUACGUCCUU...-5′
5′-ACUCGUAGUAGGUUGUAUAGU-3′
UUCGACCAUCAUCCAACAUAU
siRNA : 9 nt 3′ mismatched target
3′-...CCAACUCCAUCAUCCUUGUACGUCCUU...-5′
5′-UGAGGUAGUAGGUUGUAUAGU-3′
UUCCUCCAUCAUCCAACAUAU
1 nt 5′ mismatched siRNA : 9 nt 3′ mismatched target
3′-...CCAACUCCAUCAUCCUUGUACGUCCUU...-5′
5′-AGAGGUAGUAGGUUGUAUAGU-3′
UUCCUCCAUCAUCCAACAUAU
2 nt 5′ mismatched siRNA : 9 nt 3′ mismatched target
3′-...CCAAGUCCAUCAUCCUUGUACGUCCUU...-5′
5′-AGAGGUAGUAGGUUGUAUAGU-3′
UUCCUCCAUCAUCCAACAUAU
3 nt 5′ mismatched siRNA : 9 nt 3′ mismatched target
3′-...CCAACUCCAUCAUCCUUGUACGUCCUU...-5′
5′-ACUGGUAGUAGGUUGUAUAGU-3′
UUCGACCAUCAUCCAACAUAU
4 nt 5′ mismatched siRNA : 9 nt 3′ mismatched target
3′-...CCAACUCCAUCAUCCUUGUACGUCCUU...-5′
5′-ACUCGUAGUAGGUUGUAUAGU-3′
UUCGACCAUCAUCCAACAUAU

Figure 4c

perfect matched 2′-*O*-methyl target : siRNA
3′-UUCCAACUCCAUCAUCCAACAUAUCACUUCU-bi-5′
5′-UGAGGUAGUAGGUUGUAUAGU-3′
UUACUCCAUGAUCCAACAUAU

4 nt 5′ mismatched 2′-*O*-methyl target : siRNA
3′-UUCCAACUCCAUCAUCCAACAUAUCACUUCU-bi–5′
5′-ACUCGUAGUAGGUUGUAUAGU-3′
UUCGAGGUAGAUCCAACAUAU

8 nt 5′ mismatched 2′-*O*-methyl target : siRNA
3′-UUCCAACUCCAUCAUCCAACAUAUCACUUCU-bi-5′
5′-ACUCCAUCUAGGUUGUAUAGU-3′
UUCGAGGUAGAUCCAACAUAU

4 nt 5′ central mismatched 2′-*O*-methyl target : siRNA
3′-UUCCAACUCCAAGAACCAACAUAUCACUUAA-5′
5′-UGAGGUAGUAGGUUGUAUAGU-3′
UUACUCCAUCAUCCAACAUAU

4 nt 3′ central mismatched 2′-*O*-methyl target : siRNA
3′-UUCCAACUCCAUCAAGGUACAUAUCACUUCU-5′
5′-UGAGGUAGUAGGUUGUAUAGU-3′
UUACUCCAUCAUCCAACAUAU

4 nt 3′ mismatched 2′-*O*-methyl target : siRNA
3′-UUCCAACUCCAUCAUCCAACAUCAACCUUCU-5′
5′-UGAGGUAGUAGGUUGUAUAGU-3′
UUACUCCAUCAUCCAACAUAU

7 nt 3′ mismatched 2′-*O*-methyl target : siRNA
3′-UUCCAACUCCAUCAUCCAGAACCAACCUUCU-5′
5′-UGAGGUAGUAGGUUGUAUAGU-3′
UUACUCCAUCAUCCAACAUAU

8 nt 3′ mismatched 2′-*O*-methyl target : siRNA
3′-UUCCAACUCCAUCAUCCAACAUAUCACUUCU-bi–5′
5′-UGAGGUAGUAGGUACAUGCAG-3′
UUCCUCCAUCAUCCAAGUACG

Figure 5c

Supplementary Figure 3. siRNAs, target sites, and 2′-*O*-methyl oligonucleotides used in this study.

CHAPTER IV: OBSERVATIONS ON THE SUBJECT OF RISC ASSEMBLY DYNAMICS

INTRODUCTION

Following Dicer-mediated excision from their respective precursor molecules, small interfering RNAs (siRNAs) and microRNAs (miRNAs) enter a cascade of events that will eventually decide their functional destinies[111,119]. At least two groups of proteins are thought to direct these small RNAs to their fates: the double-stranded RNA (dsRNA) binding partners of the Dicers and the Argonautes.

The RISC assembly cascade has been best characterized in *Drosophila melanogaster* due to the robust combination of *in vitro* and *in vivo* RNA silencing systems[123,124]. In *D. melanogaster*, each of the two distinct Dicer proteins (Dcr1 and Dcr2) has a unique binding partner. The first characterized interaction of this kind was between Dcr2 and the tandem dsRNA binding domain (dsRBD) protein, R2D2[127]. It was shown that this binding partner "bridges" the ability of Dcr2 to produce siRNAs from a long (>100 base-pair, bp) dsRNA molecule to its incorporation into a cleavage-competent RISC complex. Liu et al. observed that Dcr2 was able to make siRNAs in the absence of R2D2, but these small RNAs remained in a non-functional state. However, when both Dcr2 and R2D2 were heterodimerized, the siRNAs were assembled into RISC, but more precisely into Ago2 (notably, Dcr2 alone did not bind siRNA, but the Dcr2/R2D2 heterodimer could)[128]. In addition, Liu et al. found that only a Dcr2 knockdown, not Dcr1, substantially reduced siRNA production, suggesting that Dcr1 plays an auxiliary or

secondary role regarding dsRNA response (similar results were obtained in a second insect model, *Anopheles gambiae*, at approximately the same time[126].) This observation was expanded through a genetic screen of Dcr1 and Dcr2 mutations. Carthew and colleagues established that Dcr2 is indeed the siRNA generator within fruit flies, while Dcr1 is the exclusive producer of miRNAs, and therefore, dicing appears to be a checkpoint for small RNA entry into either the miRNA or siRNA pathways[125]. For reasons still unknown, Dcr1 mutation adversely affects dsRNA-mediated RNAi downstream of siRNA production, implying that Dcr1 plays a facilitative role in siRNA- as well as miRNA-induced RISC assembly.

While Dcr2/R2D2 was known to assist siRNAs into the RISC, it was unclear how Dcr1 and Dcr2 could differentiate miRNA-bound dsRNA triggers (typically small hairpin RNAs) from those siRNA-bound. The answer came this year when several groups reported on the discovery that Loquacious (Loqs, or TRBP in humans) was the dsRBD partner of Dcr1[28,30,42,131]. Like Dcr2 alone, Dcr1 by itself can produce siRNAs[30,131]. However, with Loqs bound to it, Dcr1 was unable to recognize long dsRNA as a substrate, and it preferentially cleaved dsRNA with pre-miRNA structure, i.e. hairpins. Ergo, while dicing provides an initial filter point for miRNA or siRNA distinction, and the dsRBD partners of the Dicers appear to administer the specificity for this process.

Yet another point of divergence between the RISC assembly pathways comes after dicing—placement into pathway-specific Ago proteins. While early work on the Agos had established their necessity for all aspects RNA silencing, it was unclear whether any of the RISC-associated Agos (Ago1, 2 and perhaps 3) was unique to

miRNAs or siRNAs[15]. Initially, Ago2 was shown to exclusively co-purify with long dsRNA-derived siRNAs, and to be an interactor of Dcr1[12]. Soon thereafter, Williams and Rubin found that Ago1 was essential for RNAi in fruit fly embryos, and Hannon and colleagues discovered that Ago1 co-immunoprecipitated with both siRNAs and miRNAs[152,153]. Although there appeared to be little, if any, pathway-specific preference for the Agos observed in these initial studies, Siomi and colleagues have provided what could be conclusive proof that indeed, like the Dicers, miRNAs and siRNAs can be distinguished by which Ago they associate with[143].

In their study, Siomi and colleagues provide both genetic and biochemical evidence that Ago1 is directly connected to the miRNA pathway, while Ago2 is exclusive to siRNAs. Here, Ago1 mutant flies were fully able to destroy target RNA via long dsRNA or siRNA-directed silencing triggers, but these flies displayed marked miRNA specific defects (reduced miRNA levels and severe phenotypic defects similar to Dcr1 mutant flies[125]). Conversely, like Dcr2 flies, Ago2 mutants were "outwardly normal," though these flies were unresponsive to dsRNA or siRNA silencing triggers, and retained a superficially normal miRNA profile[125]. In addition, Ago1 was found to selectively associate with Dcr1 and Loqs, while direct association between Ago2 and Dcr2 has not been described[28,30,131]. Curiously, all known RNA silencing components (miRNA or siRNA biogenesis and effector machinery) associate in a single larger complex termed the 'holo-RISC'[125]. Though structurally indistinguishable in their mature forms, both the origins (long dsRNA or hairpin RNA, and Dicer) and the destinations (Ago) of small RNAs define whether they will enter the miRNA or siRNA pathways[111,119].

Beyond Dicing and Ago association, RISC assembly within either the siRNA or miRNA pathway requires a process by which a particular strand of the small RNA is preferentially incorporated into the silencing complex. It had been established during the massive miRNA cloning efforts that usually just one, and always the same strand of the conceptually diced miRNA duplex would be represented in any given tissue and stage of development (though rare, sometimes both strands were cloned[24]). How does the assembly machinery determine which strand should be incorporated at the expense of the other? The answer, as it turns out, lies in the ability of this machinery to assess the thermodynamic stabilities of the small RNA duplex termini. In a high-throughput screen for functional siRNAs, Khvorova and colleagues discovered that the majority of active sequences within a given duplex exhibited lower internal stability at their 5′ termini[129]. Furthermore, a similar statistical analysis was performed on 'conceptually diced' miRNA duplexes, revealing that indeed, the miRNA sequences most often represented by cloning also exhibited reduced base-pairing strength at their 5′ end[130]. Zamore and colleagues also presented similar data showing that a non-functional siRNA sequence could be 'revived' into cleavage competence by reducing the stability of that strand's 5′ termini[130]. One particular trick used in this study was 'fraying' or unpairing the 5′ most base for one strand of the duplex, which results in plenary association of the frayed strand into RISC, while the other is wholly excluded (Figure 1A-C). The principle of siRNA design based on this thermodynamic rule has been termed 'functional asymmetry.'

But how does the RISC loading machinery distinguish between the thermodynamically asymmetric terminal sequences? The answer, at least for siRNAs, is

A

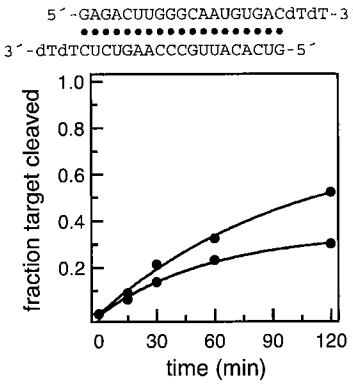

B

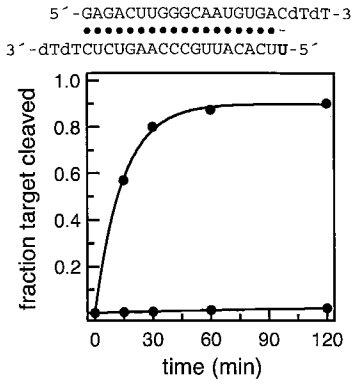

C

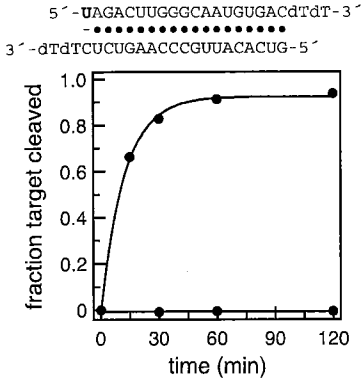

(from Schwarz et al., **Cell**, 2003)

D

non-frayed *let-7*

5´-UGAGGUAGUAGGUUGUAUAGU-3´
3´-UUACUCCAUCAUCCAACAUAU-5´
ΔG = -10.4 = -6.8

E

frayed *let-7*

5´-UGAGGUAGUAGGUUGUAUAGU-3´
3´-UUCCUCCAUCAUCCAACAUAU-5´
ΔG = ? = -6.8

F

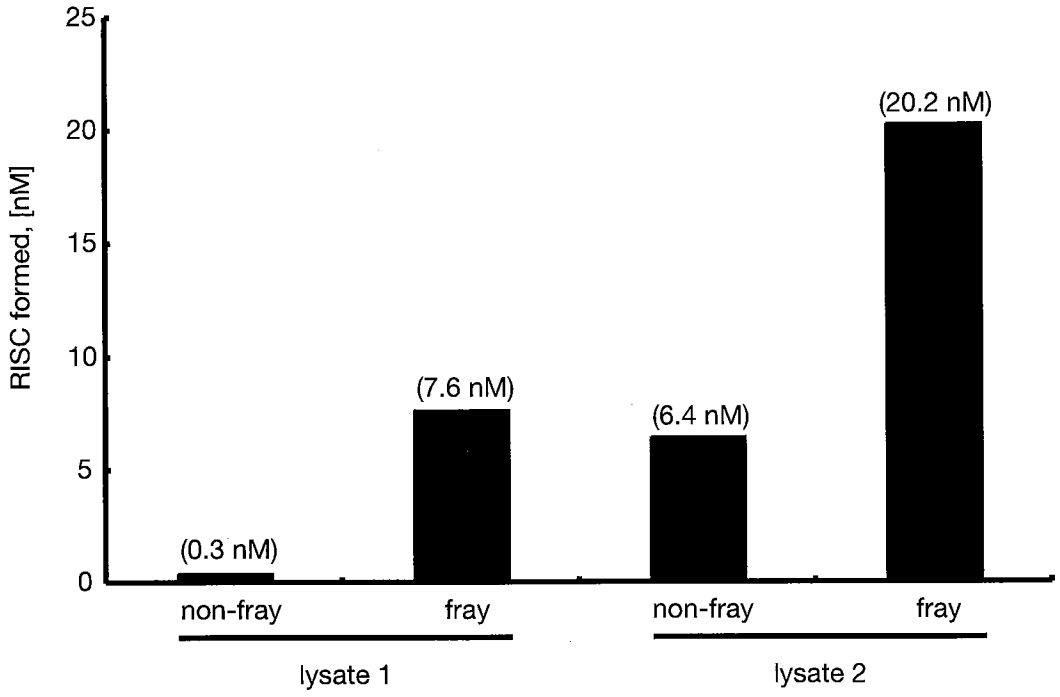

Figure 1. Design of a functionally asymmetric *let-7* siRNA. A-C. From Schwarz et al.[130] (A) Representative plot of sense (red) and anti-sense (black) strand-mediated target cleavage. This particular siRNA, by nature of its 5′ end internal stabilities, is functionally *symmetric* (both strands cleave their targets with equal fervor.) (B) A G:U mutation of the sense strand creates a C:U mismatch (fray) at the sense strand's 5′ terminus. This induces formation of RISC upon only the sense strand (red). (C) A U:C mismatch results from a G:U mutation of the anti-sense 5′ terminus. This induces rapid and exclusive formation of RISC upon the anti-sense strand. (D) Fully base-paired, 'non-frayed' *let-7* duplex RNA. *let-7* guide (anti-sense) sequence is in red. Internal stability conferred by the highlighted region governs the probability of either strand assembling into RISC. Because the sense (black) 5′ terminus displays lower internal stability, it is the strand predicted to enter RISC. (E) Functionally asymmetric *let-7* duplex created by an A:C mutation of the 18th nucleotide in the sense (black) or passenger strand and subsequent 5′ terminal mismatch of the *let-7* guide sequence. (F) Comparison of RISC assembly upon 50 nM, 5′[^{32}P] radiolabeled (guide only) non-frayed or frayed *let-7* duplex RNAs in two unique batches of *D. melanogaster* 0-2 hour embryo extract. Amount of RISC formed as measured by 2′-*O*-methyl pullout is shown for each circumstance. Pullout was performed as described in[16,130,235].

R2D2. Tomari et al. have recently elucidated R2D2's particular talent for sniffing out and subsequently associating with the more double-stranded terminus within a given siRNA duplex, orienting the otherwise symmetric dsRNA within the RISC loading machinery, and facilitating proper strand entry into Ago. It is unknown whether Loqs plays a similar role for miRNA strand selection.

However, while functional asymmetry is defined by the probability of one strand in a duplex entering RISC at the expense of the other, it does not describe the functional state of the RISC assembled upon this strand. Furthermore, it was implicit from our previous studies of RISC *in vitro* that every protected single strand (within RISC, and presumably Ago2) from a given duplex was active for cleavage in *D. melanogaster* embryo extracts[16,130]. Though, in the course of producing functionally symmetric siRNAs for kinetic analysis, it was discovered that single-strand protection does not correlate with activity, and in fact, rapid and exclusive RISC association of a particular strand may be detrimental in terms of RISC-mediated cleavage.

RESULTS

Design and characterization of a 'functionally asymmetric' *let-7* siRNA

A *let-7* siRNA was used in our prior attempts to define the kinetic parameters of *D. melanogaster* RISC *in vitro*, and all of the studies herein were performed in the well-characterized, cell-free *D. melanogaster* embryo extract (Figure 1D)[16,17,226]. One curious aspect of this siRNA was that, to date, it was perhaps one of the most active (in regard to target RNA cleavage) siRNAs examined, although based upon the thermodynamic

stability of its 5′ terminus, the guide strand was not predicted to form a substantial amount of RISC. In order to make this siRNA more functionally asymmetric and therefore enhance cleavage directed by this strand, we unpaired its 5′ most base by creating an U:C mutation at the 18th nucleotide of the passenger strand, akin to siRNA fraying in the Schwarz et al. study (Figure 1E)[130]. The result of this was a substantial (up to 23 fold) increase in the *let-7* strand association with RISC, as measured by a 2′-*O*-methyl pullout assay[16,130,235]. *let-7* strand association differed, but was always greater when comparing the frayed siRNA to the uniformly base-paired duplex (non-frayed), across unique batches of embryo lysate (Figure 1F). At present, we are unable to quantify a 5′ dangling end's influence on terminal stability, so it is unclear whether the upsurge in let-7 strand association is due to overall terminal pairing strength, *per se*, or rather the defined structure of a 5′ mismatch. Recent crystal structures have deduced that Ago, when bound to a target RNA, prefers a conformation where the first nucleotide of the small RNA is unpaired to its target[139,141]. Therefore, 5′ unpairing (specifically at the first base within an siRNA) before or during assembly may facilitate a particular strand's entrance into Ago/RISC because of a structural, not general thermodynamic stability, preference by Ago.

However, while more RISC was created using the frayed versus the non-frayed *let-7* siRNA, this higher amount of RISC was less active, under multiple turnover conditions than the non-frayed duplex (Figure 2A-C). Furthermore, the 5′ terminal phosphate status of the siRNA prior to its entry into reaction mixture did not affect this pattern (as described previously, pre-phosphorylating the duplex resulted in enhanced

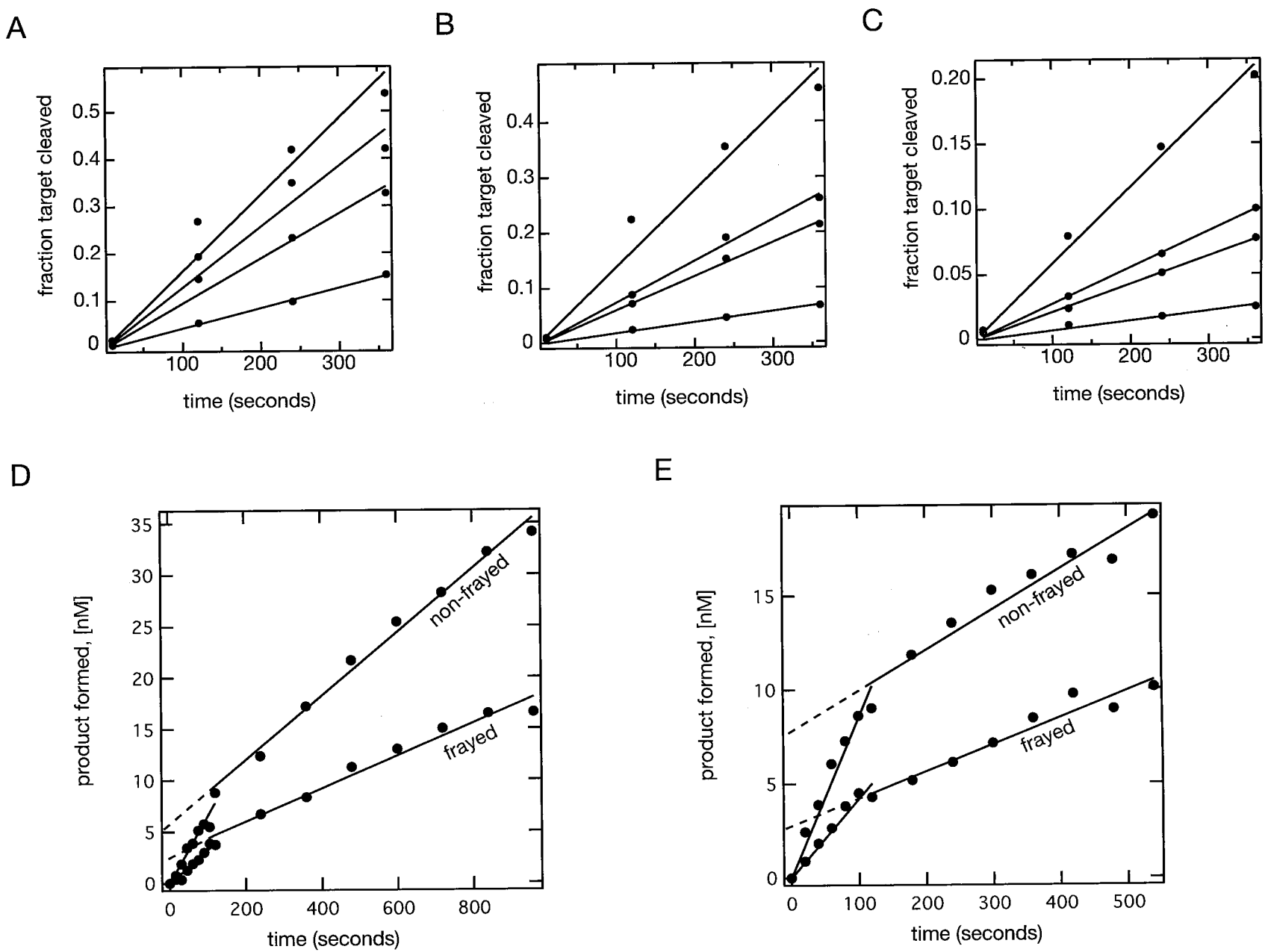
A
fraction target cleaved
0
0.1
0.2
0.3
0.4
0.5
100
200
300
time (seconds)
B
fraction target cleaved
0
0.1
0.2
0.3
0.4
100
200
300
time (seconds)
C
fraction target cleaved
0
0.05
0.10
0.15
0.20
100
200
300
time (seconds)
D
product formed, [nM]
0
5
10
15
20
25
30
35
0
200
400
600
800
time (seconds)
non-frayed
frayed
E
product formed, [nM]
0
5
10
15
0
100
200
300
400
500
time (seconds)
non-frayed
frayed

Figure 2. Non-frayed *let-7* siRNA induces more RISC activity than frayed siRNA. (A) 5′ [^{32}P] radiolabeled target RNA cleavage induced by 25 nM frayed *let-7* siRNA, pre-phosphorylated (red) or not (green) was compared to 25 nM non-frayed *let-7* pre-phosphorylated (black) or not (blue) under multiple-turnover conditions (50 nM target RNA) in *Drosophila* embryo extract. (B) As in (A) but with 12.5 nM siRNA. (C) As in (A) but with 6.25 nM siRNA. (D) Burst analysis of frayed (red) versus non-frayed (black) *let-7* siRNAs under normal (2 mM Mg^{2+}) conditions, as measured by accumulation of 5′[^{32}P] radiolabeled 5′ cleavage product formed from 100 nM input target RNA and 50 nM siRNA. (E) As in (D) but with magnesium infused (4.5 mM final Mg^{2+}) conditions. Assembly conditions for (D) and (E) were performed as described in[16].

RISC activity.) Because RISC activity was uniformly decreased when using the frayed versus the non-frayed *let-7* siRNA under substrate-excess conditions, we reasoned that there was less *let-7* associated enzyme (active, target cleaving RISC) in the frayed compared to non-frayed programmed reactions. In order to test this directly, we assayed active RISC concentration by means of burst analysis, using the two *let-7* duplex forms[16]. Under normal or magnesium infused (shown to enhance RISC activity, C. Matranga, unpublished) and RISC saturating (50 nM siRNA) conditions, the non-frayed siRNA assembled more *active* RISC than frayed (Figure 2D and E). Two separate and unique siRNA-target pairings produced similarly disproportionate values of protected or target-bound siRNA to *active* RISC concentration (D.S. Schwarz, unpublished). Based upon the multiple-turnover assessment of RISC activity in Figure 2A-C, this pattern is also expected under non-RISC saturating siRNA concentrations.

Non-cleaving RISC is not a competitive inhibitor of cleaving RISC

The fact that more RISC was leading to less activity led us to hypothesize that an accumulation of a target binding but cleavage incompetent siRNA associated ribonucleoprotein (RNP) complex was acting as a competitive inhibitor for the target site of *active* RISC. A direct way of assaying this is by Michaelis-Menten kinetic analysis. If the frayed siRNA was creating a population of competitive inhibitors we expect the apparent K_M to increase, and because *active* RISC will overcome this inhibition at high [S] (target RNA), V_{max} should remain unchanged. However, if this *inactive* RISC is unable to act as a competitive inhibitor and is instead performing in a non-competitive or

mixed fashion, we would expect the K_M to remain unchanged, but V_{max} would be markedly decreased, suggesting that there was simply less enzyme formed per nM of input duplex. Shown in Figure 3A is a representative plot of frayed versus non-frayed Michealis-Menten analysis. An average of two separate assays shows that frayed, *inactive* RISC does not act as a competitive inhibitor since K_M remains steady, while there is a noticeable decrease in V_{max} (~1.6 fold), suggesting non-competitive inhibition or more likely less active siRNA-associated enzyme. We can also infer that k_{cat} (rate of target cleavage) is unchanged if there is simply less active RISC for the frayed compared to non-frayed, which would be consistent with the similar steady-state rates of product formation following the burst phase (Figure 2D and E).

In order to confirm that this apparent inhibition is not competitive, we performed two separate mixing experiments. In the first, RISC was formed in separate reactions using saturating conditions of either frayed or non-frayed siRNA, and burst analysis was performed for both. Separately, the reactions were mixed in a 1:1 ratio to assay whether the relatively high concentration of non-cleaving RISC in the frayed condition could inhibit the non-frayed siRNA programmed reaction. Here we would expect there to be an average of the two *active* RISC concentrations if there is no inhibition, greater than the average concentration if one reaction is enhancing the other, and conversely, less than the average if one condition is inhibiting the other. The mixed reaction produced a slightly higher than average concentration of the frayed and non-frayed conditions, suggesting that the frayed siRNA-programmed RISC does not competitively inhibit the non-frayed counterpart (Figure 4A). In the second mixing experiment, RISC was formed in separate

A

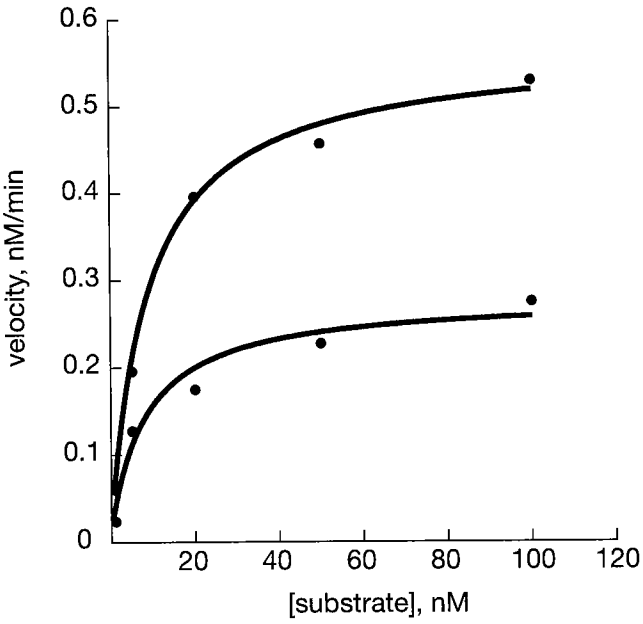

B

	non-frayed	frayed
K_m	9.4 nM	8.4 nM
V_{max}	0.45 nM/min	0.28 nM/min

Figure 3. Michaelis-Menten analysis of frayed (red) versus non-frayed (black) *let-7* siRNAs in *Drosophila* embryo extract. RISC was assembled under normal conditions using 15 nM siRNA. After one hour the reaction was diluted 1:3 into lysis buffer supplemented with an energy (ATP) regenerating system. Initial rates were calculated in two separate analyses for at least 4 increasing substrate (5′[^{32}P] radiolabeled target RNA) concentrations. (B) Average and summary of two separate Michaelis-Menten analyses. K_M and V_{max} were determined by fitting the data to the Michaelis-Menten equation as described in[16].

A

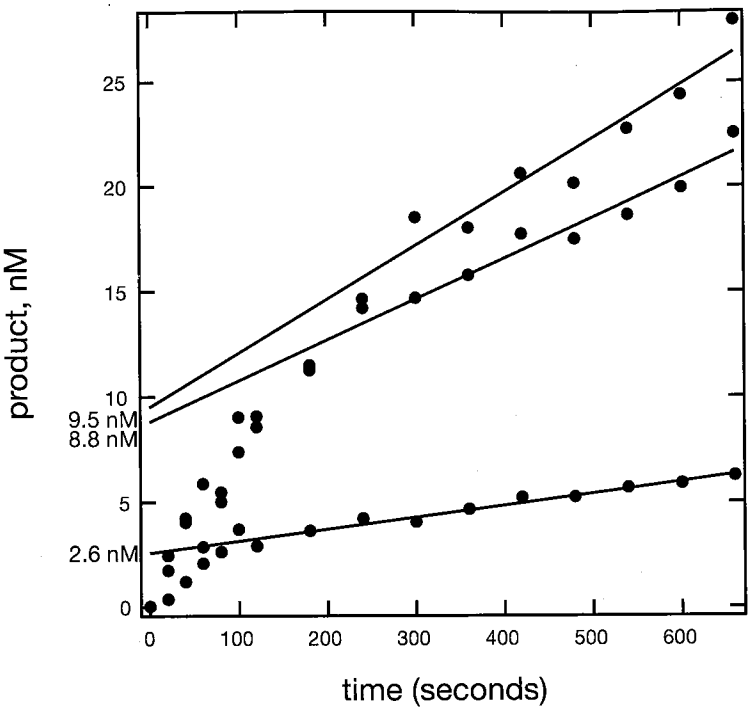
product, nM
time (seconds)
25
20
15
10
9.5 nM
8.8 nM
5
2.6 nM
0
0
100
200
300
400
500
600

B

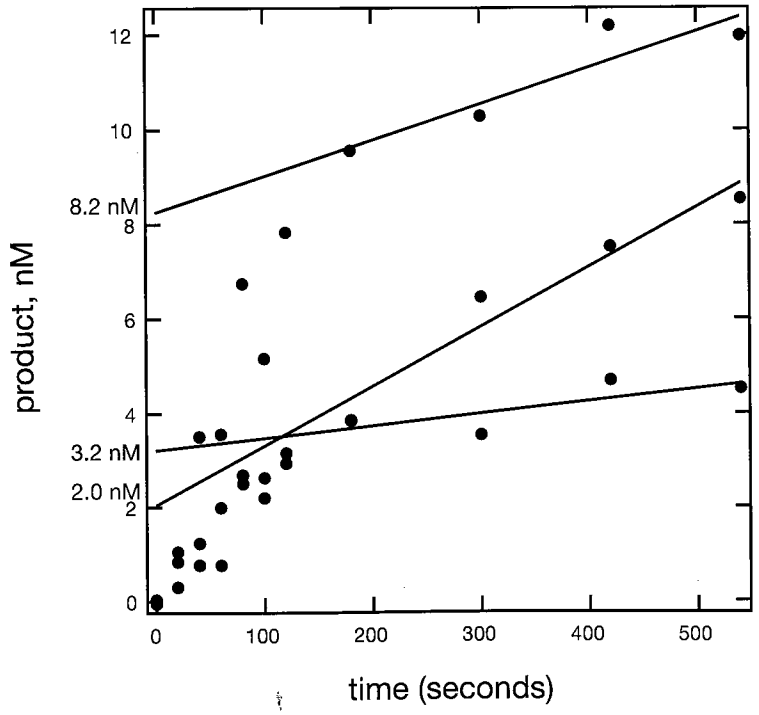
product, nM
time (seconds)
12
10
8.2 nM
8
6
4
3.2 nM
2.0 nM
2
0
0
100
200
300
400
500

Figure 4. Non-cleaving RISC is not a competitive inhibitor of cleaving RISC. (A) Burst analysis for 50 nM non-frayed (Fig. 1D, red), frayed (Fig. 1E, black) or 1:1 mixture of both siRNAs (blue). All reaction were pre-incubated with an ATP regenerating system for one hour, NEM treated, and then ATP was removed by hexokinase and glucose treatment. 1:1 mixture represents mixing the final, processed reactions (lysates with siRNA) together into one reaction prior to 5′ cap-radiolabeled target addition. Active enzyme concentration, Y-intercept, is indicated at left. (B) Burst analysis for 50 nM non-frayed (red), frayed (black) or 1:1 mixture of both siRNAs (blue). Unlike above experiment, non-frayed or frayed siRNA reactions (processed and ATP depleted as above) were diluted 1:1 in lysis buffer prior to target addition. 1:1 mixture included both non-diluted siRNA reactions into a single final reaction. 100 nM target RNA was used for both (A) and (B) experiments.

reactions with a saturating concentration of frayed or non-frayed siRNA, treated with NEM (to halt RISC assembly and inactivate the ATP-regenerating system) and ATP was depleted. Next, these reactions were diluted 1:1 with unprogrammed NEM-treated lysate, and burst analysis was performed to determine each reaction's *active* RISC concentration. In addition, the original, undiluted reactions were mixed, as described above in a 1:1 ratio and *active* RISC concentration was assessed. Mixing the two reactions should give an additive amount of *active* RISC, i.e. the sum of the two 1/2 diluted samples should be greater than either sample alone if there is no inhibitor, greater if there is an enhancer, or less, if there is an inhibitor. We observed a modestly higher amount of RISC expected if there was no inhibitor via this assay, suggesting no competitive inhibition by the frayed siRNA-programmed RISC (Figure 4B).

Photo-crosslinking analysis of siRNA-protein associations

Not all Ago family members contain a catalytic amino acid configuration within their PIWI domain (site of endonucleolytic activity) in mammals[15,142,144,145]. Assembly of an siRNA or miRNA into such Agos results in a RISC unable to direct target RNA cleavage. However, both RISC associated Agos (Ago1 and 2) in fruit flies are able to invoke cleavage when programmed with a small RNA, though, as described Ago1 is dedicated to the miRNA pathway while siRNA-directed RISC is associated with Ago2[143]. Coincidentally, Dcr2 is only involved with siRNA assembly into RISC, while Dcr1 is involved in both siRNA and miRNA induced RISC formation[125]. Furthermore, conceptually diced *let-7*, as well as other miRNAs, contain an assortment of mismatched

bases, particularly at their 5′ end, and we postulated that siRNA fraying was confusing the RISC assembly machinery into distributing this siRNA to both the miRNA and siRNA pathway, perhaps creating non-functional RISC due to improper assembly. A hallmark of such distribution would be an accumulation of the frayed, but not contiguously paired siRNA into Ago1. In order to assess this scenario we created zero-length photo-crosslinkable *let-7* siRNAs. Such siRNAs have been used previously to survey direct siRNA interactor proteins[128,239]. From these early studies it was concluded that a 5-iodo-uridine (U[5I]) substitution at the first base in a given siRNA could crosslink efficiently to Ago1, while the identical substitution at the 20th nucleotide could crosslink to Ago2 most efficiently. By combining photo-crosslinking, with 2′-*O*-methyl-based affinity purification it is possible to determine the configuration of siRNA bound proteins that also interact with the target RNA[128]. To deduce siRNA-protein photo-crosslinks, we can radiolabel the siRNA and separate the covalently bound siRNA-protein interactions via denaturing SDS-PAGE. By such an approach, we were able to observe Ago1 association with both forms (frayed or non-frayed) of siRNA when the substitution was placed at the first base (Figure 5A). There was not a dramatic difference in Ago1 association with either the frayed or non-frayed. Interestingly, Ago1 was found to interact with the target RNA in both cases under moderately harsh wash conditions (1X RIPA). A sizable portion of Ago1 was not removed upon 2′-*O*-methyl target addition, suggesting that Ago1 was perhaps bound to ds-siRNA (as in the case of Dcr2 and R2D2), or that Ago1 and the siRNA were components of a separate complex that is unable to bind a target RNA. However, we cannot exclude the possibility that the target

A

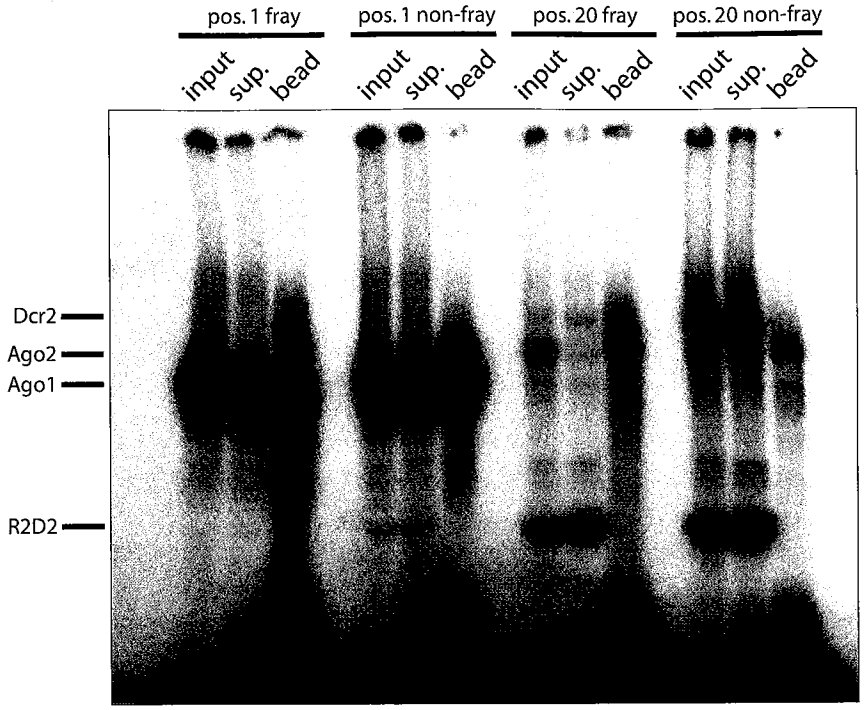
pos. 1 fray
pos. 1 non-fray
pos. 20 fray
pos. 20 non-fray
input
sup.
bead
Dcr2
Ago2
Ago1
R2D2

B

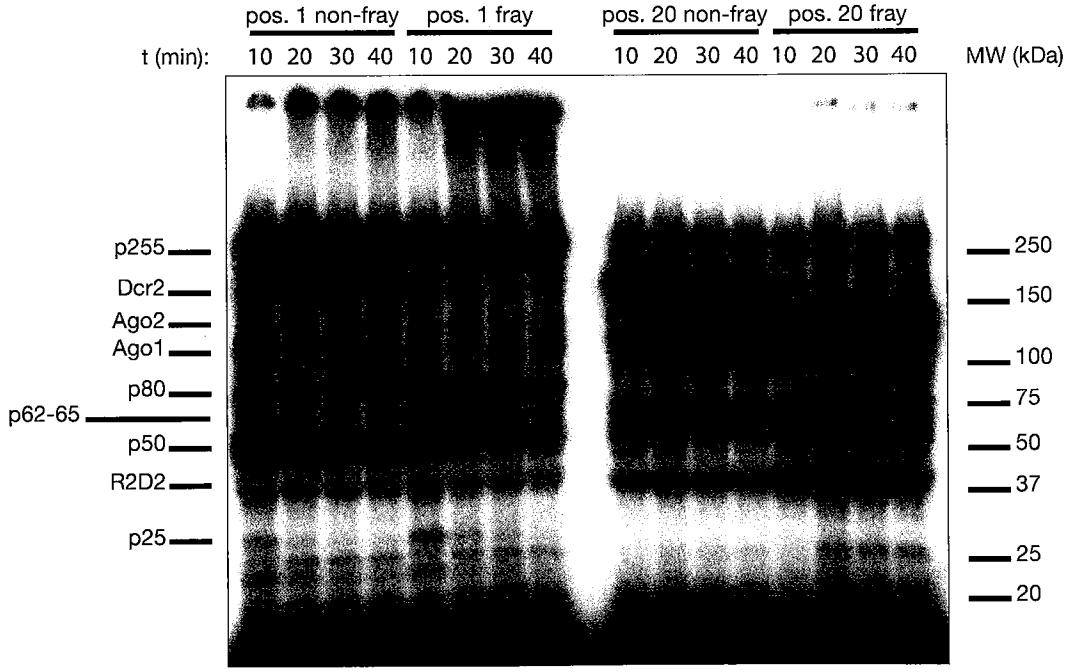
pos. 1 non-fray
pos. 1 fray
pos. 20 non-fray
pos. 20 fray
t (min):
10 20 30 40 10 20 30 40 10 20 30 40 10 20 30 40
MW (kDa)
p255
Dcr2
Ago2
Ago1
p80
p62-65
p50
R2D2
p25
250
150
100
75
50
37
25
20

Figure 5. *Drosophila* Ago1 can associate with siRNA and can use that siRNA to bind a target sequence *in vitro*. (A) U[5I] was substituted at nucleotide 1 (pos. 1) or nucleotide 20 (pos. 20) of the *let-7* guide strand. After a 60 minute incubation under normal *in vitro* RNAi conditions with a 5′[^{32}P] guide-strand radiolabeled siRNA, siRNA-protein photo-crosslinking was induced by 5 minute exposure to UV light at room temperature. Each reaction was introduced to *let-7* complementary 2′-*O*-methyl targets conjugated to streptavidin-coated beads for one hour as described in[128]. Reactions were washed multiple times in 1X RIPA buffer (150 mM NaCl, 1% NP-40, 0.5% NaDOC, 0.1% SDS and 25 mM Tris pH 7.6) and eluted from beads by boiling in SDS loading buffer. Input samples were compared to crosslinked proteins remaining after exposure to the 2′-*O*-methyl conjugated beads (sup.) and those proteins that bound to the tethered oligo (bead). All samples were loaded with equal stoichiometry. Resultant siRNA protein crosslinks were analyzed by 4-20% gradient denaturing PAGE. Confirmed identities of the crosslinked protein bands are shown (for confirmation data, see[128].) (B) 5′[^{32}P] radiolabeled (on guide) *let-7* frayed or non-frayed *let-7* siRNA with nucleotide 1 (pos. 1) or 20 (pos. 20) 4-S-U substitutions were incubated in embryo lysate under normal reaction conditions. siRNA-protein association was assessed following photo-crosslinking and subsequent separation by 4-20% gradient denaturing PAGE. Incubation times listed above include 7-minute exposure to UV light at room temperature.

bound Ago1 is interacting through a separate, un-crosslinked protein factor. Moreover, we did not see substantially different association of the siRNA with Ago2 when the U[5I] photo-crosslinkable moiety was placed at the 20th position, and as shown previously, only Ago2, not Dcr2 or R2D2, was removed from the reaction upon affinity purification, thus providing an internal control for target binding-specific interactions[128].

A U[5I] substitution is only able to crosslink to Tyrosine, Histidine, Methionine and Phenylalanine amino acids, and in order to assess protein-siRNA associations that may have been missed or undetectable by using this substitution we incorporated the more ubiquitously cross-linkable 4-thio-uridine (4-S-U) moiety at positions one and twenty of the *let-7* siRNA. A short time course of RISC assembly was performed as described in Tomari et al., and siRNA-protein photo-crosslinks were determined as above (Figure 5B)[128]. Distinct frayed or non-frayed patterns of siRNA-protein interactions were observed, included both confirmed and unconfirmed siRNA-interacting proteins. At position one, Dcr2 and Ago1 associated with more prominence to the non-frayed siRNA (similar results are observed with U[5I] substitution, data not shown), whereas Ago2 is completely absent. In regard to unconfirmed interactions, a highly visible protein of ~255 kDa (similar to the predicted size of Dcr1) is present on both the frayed and non-frayed siRNAs, a protein of ~80-85 kDa is more prominent upon the frayed siRNA, and an ~50 kDa protein is present on both siRNAs. The assembly dynamics appear grossly similar, except for the ~80 kDa upon the frayed siRNA, when assessed by cross-linking via the first nucleotide of the *let-7* siRNA. Conversely, there were considerable differences when siRNA-protein associations were determined by 4-S-U photo-

crosslinking at the 20th nucleotide. Dcr2 association is substantially higher for the non-frayed siRNA, and R2D2 is present upon both siRNAs. However, we observed dramatically greater association of both Ago1, but especially Ago2 in the frayed compared to non-frayed siRNA, perhaps due to the enhanced RISC association by the functionally asymmetric duplex. Regarding unconfirmed siRNA-protein interactions at this particular nucleotide, we again observe a protein at ~255 kDa, ~50 kDa, but also a pair of proteins of ~65 kDa (similar to the predict size of the Loqs variants) upon both siRNAs. Together with the affinity purification experiment performed above, we have provided the first evidence of *bona fide* siRNA association with Ago1, and perhaps the Dcr1 (~255 kDa)-Loqs (~60-65 kDa) heterodimer. We did not observe a dramatic increase in Ago1 association with the frayed compared to the non-frayed siRNA. Rather, the most striking difference between the two siRNA forms was the substantial incorporation of the frayed siRNA into Ago2. When we performed an identical analysis on an siRNA that was predicted to form substantial RISC with or without a fray, we observed approximately equal association with Ago2 (data not shown), suggesting that this could be a consequence of 'overloading' the RISC machinery with single-stranded RNA, not a consequence of unpairing the 5′ terminal nucleotide *per se*. To date we are unable to determine if each siRNA-programmed Ago2 protein within this population is active for cleavage, although the conspicuously lower 'crosslinkability' the non-frayed *let-7* siRNA has for this particular Ago, at this particular base, suggests that it may be a non-productive (regarding catalysis), or intermediate association with Ago2, in that it represent a non-cleaving siRNA-RISC conformation. As mentioned, several mammalian

Agos function without being able to cleave a target RNA, and therefore it is conceivable that Ago2 may assemble upon an siRNA in such a manner/conformation that would prevent it from 'slicing' a target RNA and allowing it to perform such 'non-slicing' duties.

At present, ten proteins are known to associate with the *D. melanogaster* RISC (Table 1). To determine what, if any of these proteins can be found as discrete complexes, we combined photo-crosslinking with size exclusion chromatography (Figure 6)[239]. When we assayed the non-frayed siRNA with a 4-S-U at position one by this method we observed several distinct complexes (Figure 6A). In the void, crosslinked Ago2 and Ago1 were the most obvious, while there were faint bands at ~255 kDa, ~200 kDa (Dcr2), and ~50 kDa. Notably, the ~250 kDa protein concentrated between fractions 7-11 (~450 kDa), along with an ~60 kDa band. The sizes of the crosslinked proteins, as well as their localization in this particular gel filtration column are reminiscent of Dcr1 and Loqs localization as determined by western blot in a similar experiment using a fly S2 cell extract[28]. We therefore believe that this is a direct interaction between an siRNA and the Dcr1/Loqs heterodimer. Curiously, the Ago1 crosslink is present across a broad range of column fractions. Though this protein is only ~110 kDa, its presence in fractions ranging from the void to ~100 kDa, suggests that it is likely a component of several distinct RNP complexes at any given time. Lastly, we observed, the Dcr2/R2D2 heterodimer bound to an siRNA migrating at ~260 kDa. In order to observe such interactions at the 3′ termini of these siRNAs, were performed a similar analysis using *let-7* siRNAs with 4-S-U at the 20th nucleotide. As observed in our time course assay

Protein	Function	Size
Dcr1[1]	miRNA biogenesis, RISC formation	~250 kDa
Dcr2[1]	siRNA biogenesis, RISC formation	~200 kDa
Ago1[1]	miRNA association, endonuclease	~130 kDa
Ago2[1,2]	siRNA association, endonuclease	~110 kDa
Tudor-SN (TSN)[3]	A:I edited-specific dsRNA nuclease	~103 kDa
fragile-X protein (dFMR1)[4,5]	RNA binding	~80 kDa
Vasa intronic gene (VIG)[4]	unknown	~60 kDa
Dmp68[5]	DEAD-box helicase	~55 kDa
L5[5]	ribosomal component (60S subunit)	~33 kDa
L11[5]	ribosomal component (60S subunit)	~21 kDa

References:

1. Pham et al., **Cell**, 2004
2. Hammond et al., **Science**, 2001
3. Caudy et al., **Nature**, 2003
4. Caudy et al., **Genes & Development**, 2002
5. Ishizuka et al., **Genes & Development**, 2002

Table 1. Confirmed RISC-associated proteins. References refer to first observed interaction with siRNA- or long dsRNA-programmed RISC.

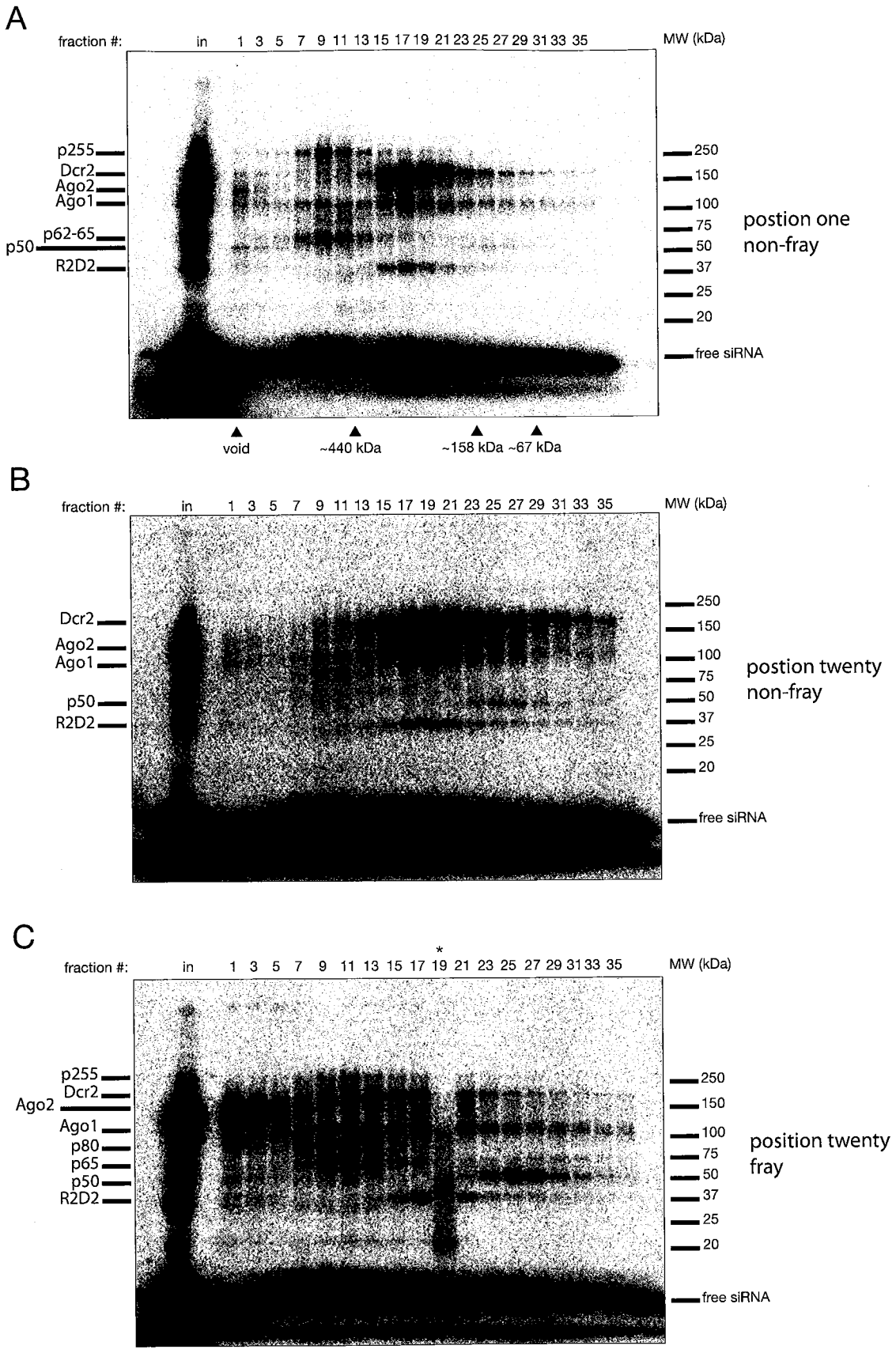
A
fraction #: in 1 3 5 7 9 11 13 15 17 19 21 23 25 27 29 31 33 35
MW (kDa)
p255
Dcr2
Ago2
Ago1
p62-65
p50
R2D2
250
150
100
75
50
37
25
20
free siRNA
postion one
non-fray
void
~440 kDa
~158 kDa
~67 kDa
B
fraction #: in 1 3 5 7 9 11 13 15 17 19 21 23 25 27 29 31 33 35
MW (kDa)
Dcr2
Ago2
Ago1
p50
R2D2
250
150
100
75
50
37
25
20
free siRNA
postion twenty
non-fray
C
*
fraction #: in 1 3 5 7 9 11 13 15 17 19 21 23 25 27 29 31 33 35
MW (kDa)
p255
Dcr2
Ago2
Ago1
p80
p65
p50
R2D2
250
150
100
75
50
37
25
20
free siRNA
position twenty
fray

Figure 6. Visualizing multiple siRNA associated ribonucleoprotein complexes by photo-crosslinking and size exclusion chromatography. (A) Following a 60 minute incubation of *Drosophila* embryo extract with 50 nM, 5´[^{32}P] radiolabeled (guide only) *let-7*, non-frayed siRNA with a 4-S-U substitution at position 1 (100 μL reaction), photo-crosslinking was induced by exposure to UV light for 7 minutes, at room temperature. The reaction was then diluted 1:1 in cold lysis buffer, supplemented with 2 mM DTT and the injected onto a Superdex 200 size exclusion column. siRNA-protein crosslinking was assessed for odd fractions by 4-20% denaturing PAGE. Proteins of interest are labeled to the left. Size determination was determined in[28]. (B) As in (A), but with a 4-S-U substitution at position 20 of a non-frayed *let-7* siRNA. (C) As in (A), but with a 4-S-U substitution at position 20 of a frayed *let-7* siRNA. Fraction 19 (marked with *) was a victim to indeterminate degradation.

(Figure 5B), there were striking differences regarding crosslinking patterns. For the non-frayed siRNA, we observed only a few prominent bands, particular the Dcr2 and R2D2, running as their heterodimer (~260 kDa), as well as faint bands representing Ago2 and Ago1 (Figure 6B). However, there was a smaller ~50 kDa siRNA-protein crosslink running as an ~120 kDa complex (Figure 6C). Conversely, the frayed siRNA displayed substantially more crosslinkable siRNA-protein interactions. Here, we observed a conspicuously greater amount of Ago2 crosslinking in the void (and slightly more Ago1), compared to the non-frayed siRNA. Furthermore, we readily found complexes containing Dcr2 and what appears to be Dcr1. It was perhaps not surprising to see a peak of Ago1 running in a similar sized complex as Dcr1[30,131].

After observing a vastly higher amount of Ago2 crosslinked to the frayed siRNA in the void compared to the non-frayed siRNA, we were curious if this was a functional (catalytic) interaction. To assess this, we observed cleavage product formation in an end-point assay across similarly prepared, but not crosslinked, column fractions (Figure 7A and B). As shown, there is little, if any difference in target cleaving activity between the non-frayed or frayed siRNAs, particularly in the void. In addition, a second, quantifiable peak of activity can be seen in fractions 23-27 (~160 kDa) of Figure 7A, consistent with the small, RISC* observed in our previous experiments[10]. The implications of this result are discussed below.

Finally, a similar position one, 4-S-U crosslinking and gel filtration experiment was performed using frayed or non-frayed siRNAs predicted to be functionally asymmetric regardless of a 5′ unpaired nucleotide (Figure 8). This siRNA set was

A

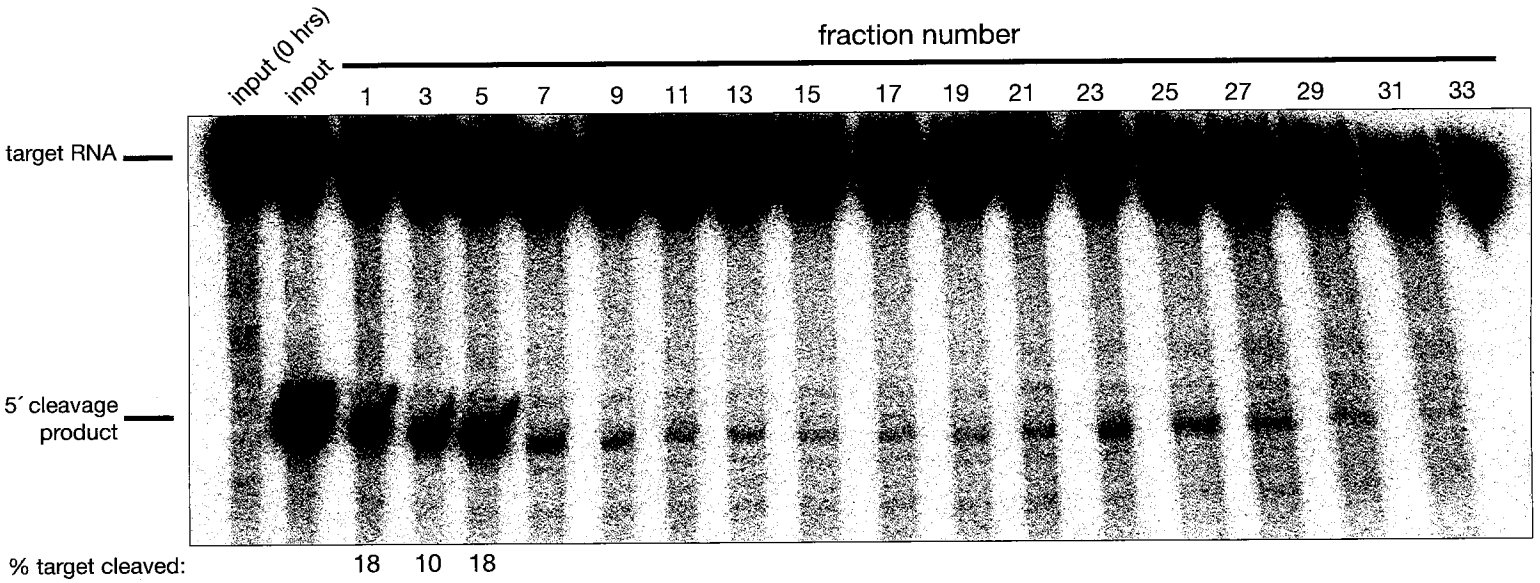
input (0 hrs)
input
fraction number
1 3 5 7 9 11 13 15 17 19 21 23 25 27 29 31 33
target RNA
5′ cleavage product
% target cleaved:
18 10 18

B

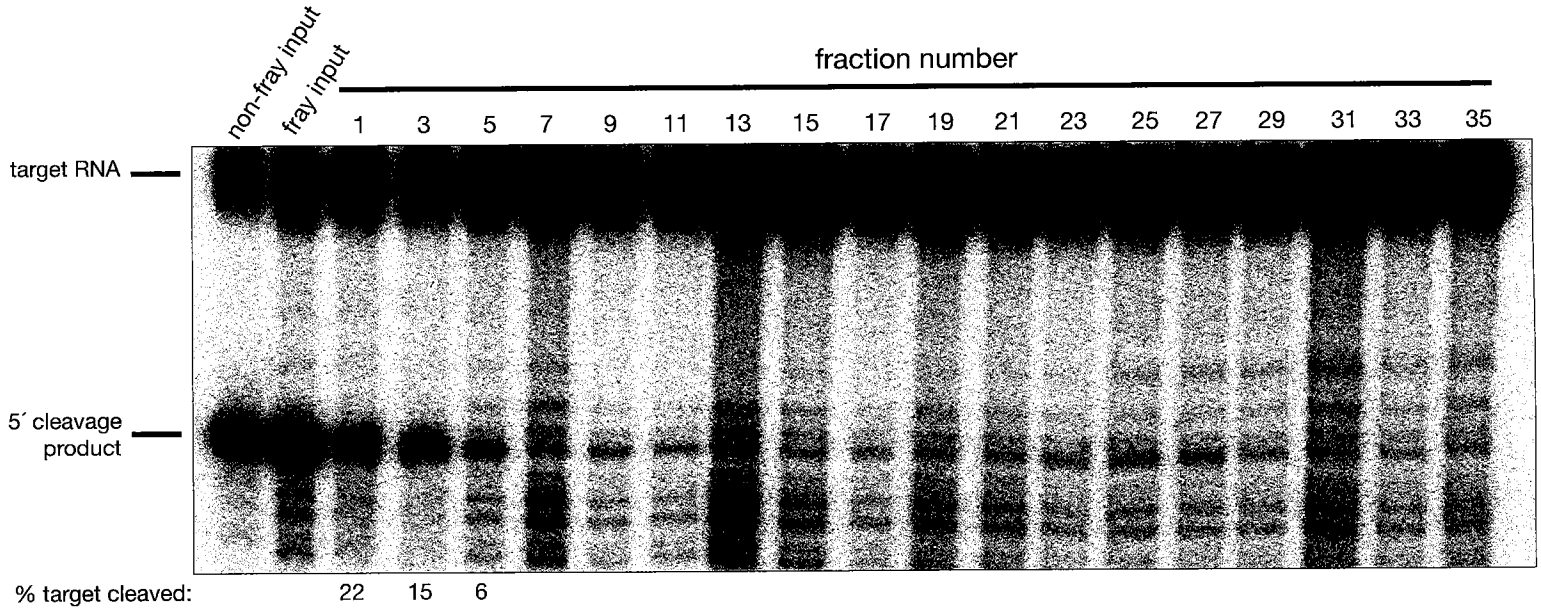
non-fray input
fray input
fraction number
1 3 5 7 9 11 13 15 17 19 21 23 25 27 29 31 33 35
target RNA
5′ cleavage product
% target cleaved:
22 15 6

Figure 7. Target cleavage activity profile for non-frayed versus frayed *let-7* siRNA programmed *Drosophila* embryo lysate following separation by size exclusion chromatography. (A) RISC was assembled for 60 minutes in a 200 μL reaction with 50 nM non-frayed siRNA. 180 μL of the reaction was injected directly onto a Superdex 200 size exclusion column. Odd fractions were supplemented with an energy regenerating system and assayed for target cleaving activity after a 2-hour incubation with 2 nM 5′[^{32}P] radiolabeled target RNA. Input and cleaved target RNAs were separated using 8% denaturing PAGE. (B) As in (A), but with a frayed *let-7* siRNA.

A

5´-**U**UCACAUUGCCCAAGUCUCUU-3´
3´-UUAAGUGUAACGGGUUCAGAG-5´

ΔG = -8.2 ΔG = -10.2

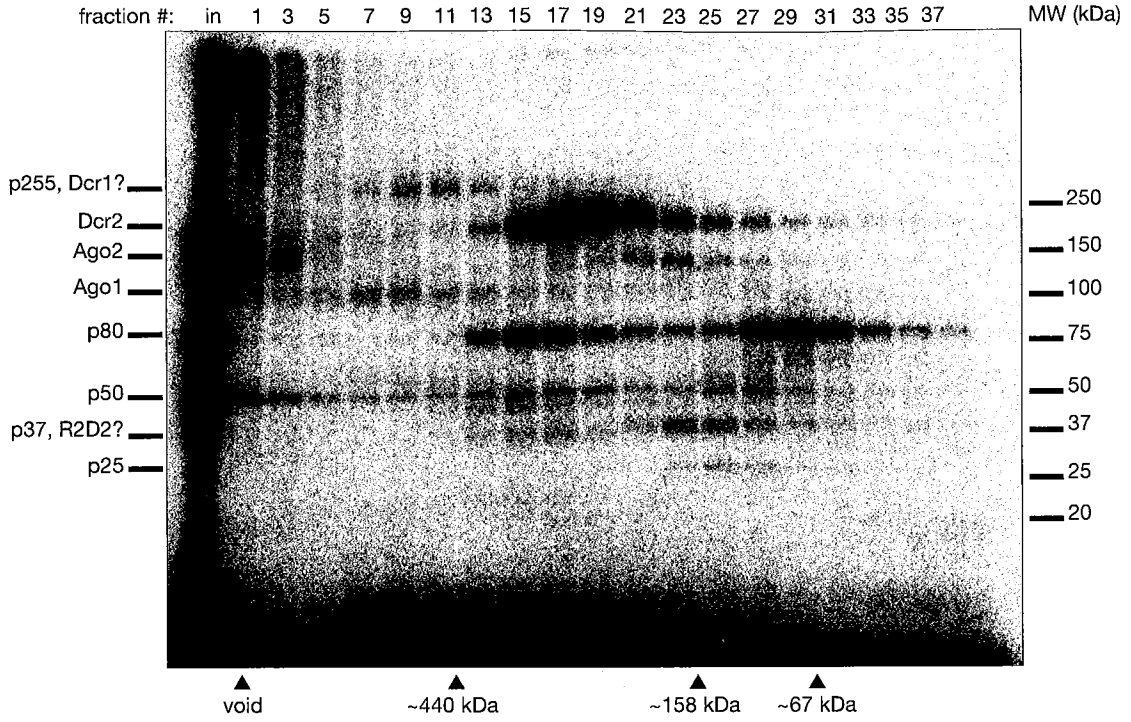

B

5´-**U**UCACAUUGCCCAAGUCUCUU-3´
3´-UUCAGUGUAACGGGUUCAGAG-5´

ΔG = ? ΔG = -10.2

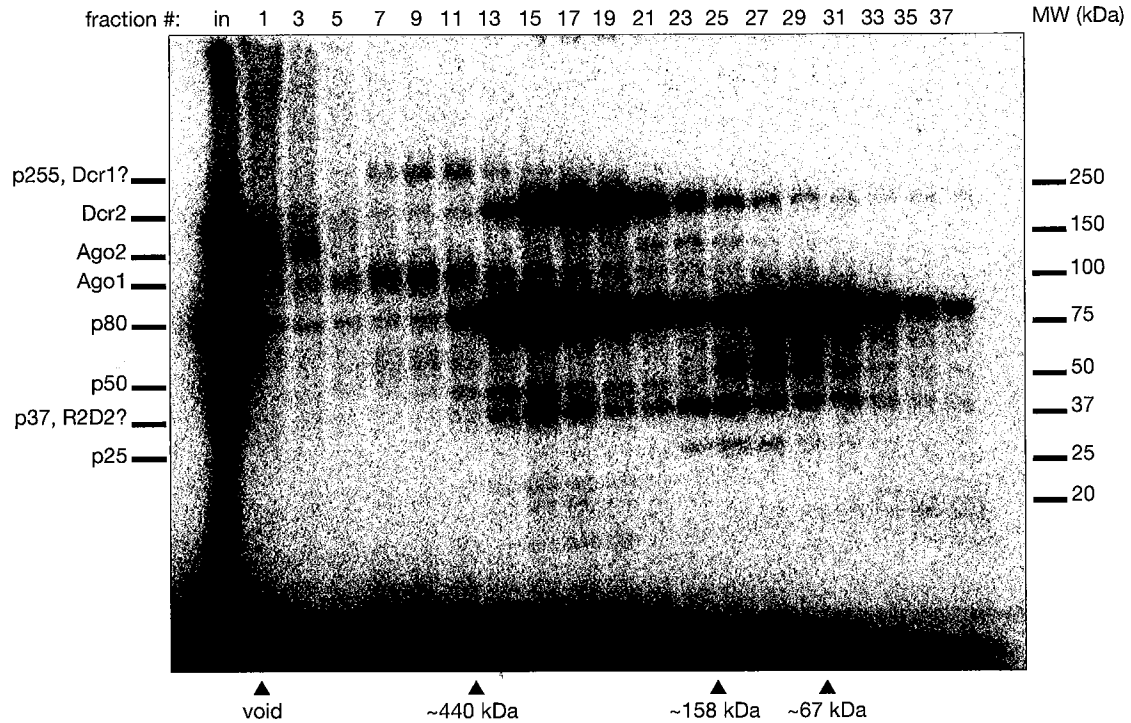

Figure 8. Visualization of siRNA associated ribonucleoprotein complexes, as measured by photo-crosslinking followed by size exclusion chromatography, for an siRNA that naturally displays 'functional asymmetry.' (A) Position 1, non-frayed 4-S-U substituted siRNA, the substituted base is highlighted red. Reaction conditions and crosslinking was performed as in Figure 5. However, the 100 L reaction was injected directly onto the gel filtration column without dilution. (B) As in (A), but with a frayed siRNA.

chosen because it displays a somewhat different pattern of crosslinkable proteins when compared to either the frayed or non-frayed *let-7* forms (data not shown). In particular, these siRNAs do not crosslink efficiently to R2D2, or the ~62-65 kDa band we predict to be Loqs, rather they crosslink with higher efficiency to an ~80 kDa band, compared to the *let-7* duplexes. When assayed as above, the frayed and non-frayed siRNAs display characteristically different crosslink patterns, not just from *let-7*, but also from one another. The ~80 kDa protein appears in two distinct complexes, at ~350-400 kDa and ~80 kDa with both siRNAs, though it crosslinks with higher efficiency to the frayed form. This ~80 kDa protein, in either complex, was unable to direct target RNA binding as measured by photo-crosslinking followed by 2´-*O*-Methyl pullout (data not shown), suggesting that it is either binding to ds-siRNA or is in a complex that does not present the siRNA for target binding. As before, we could detect substantial siRNA-Ago2 crosslinking associated with the void, however, there was a second peak detected at ~150 kDa (fractions 21-27), which was coincident with the smaller, secondary peak of activity observed for *let-7* siRNA-directed cleavage across a size exclusion column (compare Figures 7A and 8A). We cannot confirm whether or not the smaller Ago2 peak was the result of dissociation from a larger complex during gel filtration. In addition, we could detect a peak of siRNA-Ago1 crosslinking coincident with the apparent Dcr1 band. This would be expected, as Dcr1 and Ago1 are known to interact, as observed by co-immunoprecipitation, in at least a transient complex. Lastly, an ~50 kDa crosslinked protein was unique to non-frayed siRNAs. This protein associated with distinctly large

complexes (from ~150 kDa to the void), and was also an interactor of the *let-7* siRNAs. The functional relevance of this and other unconfirmed bands is the focus of future study.

DISCUSSION

The discovery of 'functional asymmetry' has undoubtedly answered many concerns regarding the manner in which siRNAs enter the RISC, particularly how the RISC machinery chooses one strand over the other in a given duplex. This concept is based solely upon the observation that for each duplex, the small RNA strand with comparatively lower internal stabilities at its 5′ termini is more likely to enter the RISC, while the opposing strand is degraded[129,130]. 'Functional asymmetry' does not define what happens after the loading machinery has chosen a small RNA strand for assembly. Are all siRNAs protected and assembled into RISC truly functional in regard to RNAi, i.e. will they all direct target RNA cleavage? We have found for at least three 'functionally asymmetric' siRNAs that the majority of RISC formed is non-functional, although it is able to associate, in a sequence-dependent manner, with its target RNA. Curiously, this non-cleaving RISC does not act as an inhibitor of the cleavage competent RISC, suggest that cleaving RISC, for reasons still to be determined, has priority access over a give target site. In addition, for at least one siRNA sequence we have observed that internal stability *per se* at the 5′ terminus may not be the sole determinant for entry into RISC (Figure 8). Rather, it appears that structure, this case in the form of a single base pair mismatch, will result in differential siRNA-protein association. Perhaps this difference plays a role in determining the fate of each siRNA strand.

It has now been shown numerous times that Ago2 is the siRNA-specific catalytic engine for *D. melanogaster* RNAi, while Ago1 is unique to the miRNA pathway[12,30,131,143,246]. For a *let-7* siRNA designed prior to the discovery of functional asymmetry, each siRNA that entered RISC, and presumably Ago2, was shown to be in a cleavage-competent state[16]. As expected, we were able to coax additional RISC formation by designing the *let-7* siRNA to be functionally asymmetric (via fraying of the 5′ terminal nucleotide). We also observed that as more RISC was made, more Ago2 became associated with that siRNA as measured by 4-S-U crosslinking at the 20th nucleotide (the 3′ termini), but paradoxically, less *active* RISC was made compared to the earlier designed siRNA predicted to form little if any RISC. As anticipated, the strand that was poorly incorporated into RISC associated dramatically less with Ago2 compared to the functionally asymmetric strand. We hypothesize that the lack of functionality for this RISC is a direct consequence of incomplete, improper, or perhaps a specific non-cleaving mode of Ago loading. In this scenario, Ago2 loading involves 3′ termini (of the siRNA) insertion into the Ago2 PAZ domain[148,149]. Subsequent removal of the siRNA's 3′ end, either by intra- or inter-molecular forces, from the PAZ domain then places Ago2 in a cleavage-competent conformation[119,247]. If the PAZ domain still contains the siRNA's 3′ end, it will be able to bind a target, albeit with slightly reduced affinity, but will not induce endonucleolytic activity. Such a scenario is consistent with our previously published kinetic assessment of the value for the 5′, central, and 3′ regions for a given siRNA in regard to both target cleavage and association for *D. melanogaster* RISC, as well as structural studies on Archaeal Agos[16,139,141]. We found that the 5′ and

central regions governed RISC binding to and cleavage of the target RNA. Conversely, the 3´ region contributed very little to target binding, but mismatches between the siRNA and target in this area substantially reduced catalysis. Therefore, incomplete RISC assembly would mimic mismatches within the 3´ region, as both would appear to bind the target as normal, but catalysis would be considerably reduced. This hypothesis would also suggest that in addition to proper amino acid configuration within the PIWI domain, intra-Ago conformational changes are essential for Ago2-mediated cleavage[142,144,145]. The mechanism for such intra-Ago conformational changes is the focus of future studies.

Moreover, our siRNA-protein crosslinking analysis has added yet another layer of complexity upon the RISC assembly pathway. As mentioned, Ago1 and Ago2 have been shown to be specific for the miRNA and siRNA-mediated RNA silencing pathways, respectively[143]. To the contrary, we found for at least one siRNA, that it was able to associate with and direct target binding through Ago1. We predict this to be a functional (in terms of RNA cleavage) interaction, because for the non-frayed *let-7* siRNA, all protected single-strand was able to direct cleavage, yet, it was doled out to some degree (as measured by crosslinking) to both Ago1 and Ago2, and both siRNA-Ago associations can bind target RNA[16]. Adding credence to the idea that some, and perhaps most siRNAs can enter the miRNA pathway, we observed an interaction between two separate siRNAs (both in frayed or non-frayed form) in association with what we predict to be the Dcr1/Loqs heterodimer, previously shown to be involved, specifically in Ago1 loading. siRNA-Dcr1 (not Dcr1/Loqs) photo-crosslinking has been observed in a separate study[151]. We cannot exclude a functionally redundant association between the Dcr1/Loqs

heterodimer (in a manner similar to Dcr2/R2D2) and the siRNA-RISC loading machinery. Future studies will attempt to elucidate the nature of Ago1 binding to what appears to be ds-siRNA, and efforts are underway to identify and characterize the numerous siRNA-protein crosslinks.

MATERIALS AND METHODS

General methods

D. melanogaster embryo lysate preparation, siRNA labeling with polynucleotide kinase (New England Biolabs), target RNA preparation, and labeling with guanylyl transferase were carried out as described[226]. ATP depletion and kinetic assessment was performed and analyzed as in[16]. The method for determining RISC concentration by 2′-*O*-methyl pullout can be found in[16,235]. All small RNAs, modified or otherwise and biotinylated, 2′-*O*-methyl oligonucleotides were purchased from Dharmacon. Gel filtration was performed as described in Nykänen et al. except that a 'Tricorn' Superdex 200 10/300 GL column (Amersham Biosciences) was used[10].

CHAPTER V: GENERAL DISCUSSION

This thesis examined the biochemical mechanisms of RNAi induction and function in *Drosophila melanogaster*. To do so, the experiments in Chapters II and III were designed to exploit the absolute requirement of energy/ATP for RNAi *in vitro*. From these studies we elucidated at least five ATP-dependent or facilitated steps along the RNAi pathway; siRNA production from a long double-stranded RNA trigger, maintenance of an siRNA's 5′ phosphate, separation of the resulting siRNA duplex into individual single-stranded 21-nucleotide RNAs, RISC activation or assembly upon these single-stranded RNA species, and lastly product RNA removal following RISC-mediated endonucleolytic cleavage. In addition, experiments performed in Chapter III clearly show that distinct regions of a small RNA contribute to the unique intra- and inter-molecular mechanisms of RISC. We observed, like Doench et al. for miRNA function, that siRNAs rely almost solely upon their 5′ region for target-RNA binding[233]. Notably, the most conserved segment of a given miRNA throughout evolution is its 5′ region, or nucleotides 2-8, now termed the 'seed sequence'[24]. The minimal region required for target RNA cleavage is between nucleotides 2 and 12, which equates to a single turn of an A-form RNA-RNA helix, and it had been previously reported that the A-form helical conformation is required for siRNA-mediated target cleavage[234]. Lastly, we found that the 3′ region of an siRNA contributes very little to siRNA stability upon its target RNA. Instead, this region plays an integral part in maintaining or establishing a proper, endonucleolytically active conformation for RISC. Interestingly, a comprehensive study

detailing miRNA-target binding modes has found that compensation by 3′ base-pairs for 5′ mismatches between the miRNA and target can rescue miRNA-mediated translational repression[180]. We observed a similar phenomenon in regard to target cleavage, where mismatches at the 5′ end of an siRNA were tolerated to a much higher degree if the 3′ region was contiguously paired, suggesting that there is considerable cooperation between the two termini of a small RNA when guiding RISC activity.

In Chapter IV we sought to explicate the functionality of RISC after its assembly with 'functionally asymmetric' siRNAs. Here, we discovered, quite unexpectedly, that not all RISC formed *in vitro* was active for target cleavage, as we had previously inferred. In addition, we performed a series of siRNA-protein crosslinking studies using separate, zero-length, photo-crosslinkable chemical substitutions at both ends (5′ or 3′) of distinct siRNAs. We observed a swath of siRNA-protein associations, and the identities of the siRNA-binding proteins and their functional relationship to the RNAi pathway will undoubtedly be the subject of much future research. Moreover, the apparent inverse correlation of increased siRNA-Ago2 association to reduced target cleaving activity was surprising to us, as Ago2 is the catalytic factor for siRNA-mediated RNA cleavage in *Drosophila*[12,143,246]. However, these observations are consistent with the two-state model for Ago activity proposed by Tomari and Zamore and expanded by Filipowicz[119,247] (Figure 1). Here, the 5′ phosphate of an siRNA is anchored within the PIWI domain of Ago, while the 3′ terminus is bound to the PAZ domain. Upon association with a target RNA, the siRNA's 3′ end is pulled out of the PAZ domain, creating two turns of an A-form helix between the siRNA and target, the optimal nucleic acid pairing configuration

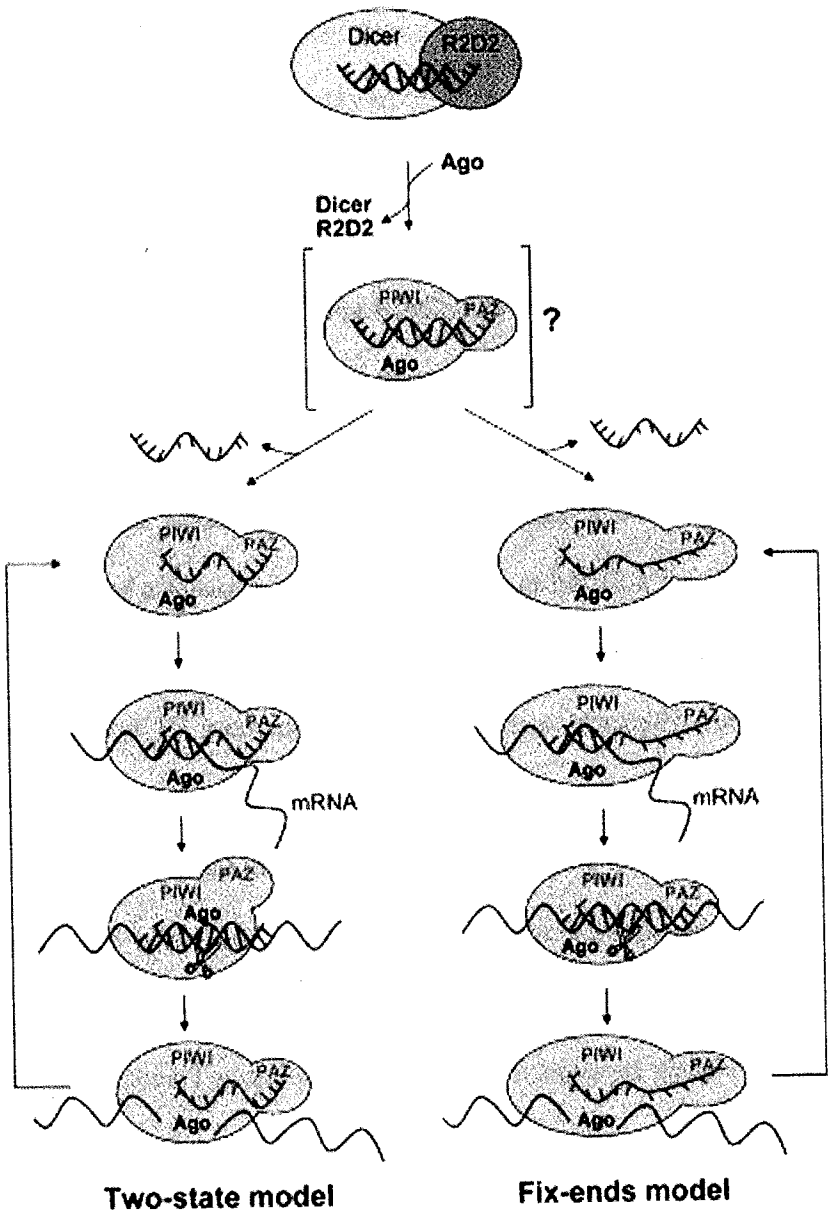

Figure 1. Models of the assembly and function of the minimal Ago-containing RISC.

Reproduced from Filipowicz, **Cell**, 2005[247].

for RISC-mediated cleavage. If the 3′ region of an siRNA is not removed from Ago, then an intra-Ago conformation unfavorable for endonucleolytic cleavage persists, though Ago, as a component of RISC, may still be able to associate with a target via the 'seed sequence' within the siRNA, inducing miRNA-like translational repression. It is currently unclear why these non-cleaving RISC complexes are ineffective competitors for the target site upon an RNA when in the presence of cleavage-competent RISC, and we do not yet known if any activity inducing, intra-Ago conformational changes occur before, during or after siRNA-target association. Such a non-cleaving conformation could be indicative of a separate, cleavage-independent function for *Drosophila* Ago2, as would be the case for the many non-catalytic mammalian Agos. Furthermore, the results presented in Chapter III were not consistent with a 'fix-ends' model proposed by Filipowicz, where the 3′ region of an siRNA is perdurably associated with the PAZ domain of Ago, and stretching of Ago once bound to a target RNA produces an endonucleolytically active configuration, as we observed reduced RISC activity with greater association between an siRNA's 3′ terminus and Ago.

Recently, Joshua-Tor and colleagues have discovered that recombinant, human Ago2 alone can reconstitute RISC activity *in vitro*[142]. While target RNA cleavage by the recombinant RISC is both endonucleolytic and magnesium dependent, like RISC in *Drosophila*, assembly of the small RNA guide into this ribonucleoprotein complex, as well as events downstream of target RNA cleavage, appear to be quite different compared to *Drosophila* RISC. In contrast to *Drosophila* RISC, recombinant human Ago2 cannot be programmed with a duplex siRNA, and it will only accept single stranded RNA during

the assembly process, suggesting that one strand of the input siRNA duplex must be removed, perhaps by an ATP-dependent RNA helicase, for RISC to become active. Furthermore, unlike *Drosophila* RISC, assembly of catalytically active, recombinant RISC did not require ATP[142,144]. Therefore, acceptance of a single stranded siRNA into *Drosophila* RISC in the absence of ATP could be blocked by the lack of an ATP-dependent conformational rearrangement within the complex, or perhaps by the ATP-dependent removal of an siRNA-associated protein factor within the lysate. However, we have yet to establish whether *Drosophila* RISC can bind a single stranded siRNA in the absence of ATP, as the recombinant, human Ago2 is able to do. Regarding 5´ phosphate necessity for RISC assembly, unlike *Drosophila* RISC, recombinant RISC was able to use a non-phosphorylated guide strand for target cleavage, albeit with a reduced efficiency, and the authors suggest that this is indicative of the 5´ phosphate being used for enzyme stability and fidelity, not assembly. Lastly, unlike the RISC formed in *Drosophila* embryo extracts, human, recombinant RISC activity is not stimulated by ATP, and human Ago2 alone displays burst kinetics in the presence or absence of this nucleotide cofactor. As the authors point out, this result suggests that, in agreement with our studies, removal of cleavage products formed during RISC-mediated target cleavage is facilitated by ATP, likely by means of an as-yet identified ATP-dependent RNA helicase (perhaps even the same helicase that unwinds the siRNA duplex itself during RISC assembly).

As each month passes, we discover that the influence and ubiquity of RNA silencing on modern biology reaches ever further. Together with the exceptional efforts

on the genetic side, the biochemical studies performed herein and elsewhere have brought light upon the various intricacies of these phenomena. Presently, one of the most exciting developments in RNAi has been the crystallographic studies on the Ago family of proteins, the catalytic engines (endonucleases) of the various RNA silencing pathways[133,139,141]. While the RNAse-H-like mechanism of the RISC was known, these structures have undeniably identified Ago as the elusive 'slicer'. Therefore, as the field matures and additional pathway components are found and characterized, without a doubt we will be treated to future surprises. Such future studies will likely involve, for example, the functional and structural nature of the Dicer proteins and their dsRBD partners. Why are they unstable without one another[42,127]? How do Loqs or R2D2 help their Dicers to distinguish between pre-miRNA or long dsRNA substrates[30,127,131]? Furthermore, as we learn more about the Agos, perhaps the biological functions of their non-cleaving brethren will be revealed[144,145].

Likely the most important role of RNAi in the broad scope of molecular biology is its usefulness as a key to unlocking the wide-range of recently sequenced genomes. Such sequencing, combined with robotically transfected dsRNA, has made it possible to perform high-throughput, systematic analyses for any gene, in organisms ranging from *Drosophila* to *C. elegans* to humans, with cell-based functions[248-254]. With genome-wide siRNA or short-hairpin RNA (shRNA) libraries now available, such whole-genome analyses by RNAi is fast becoming the favorite tool amongst pharmaceutical companies for drug discovery. Moreover, it has taken a remarkably short six years from the first dsRNA injection into worms to the first clinical trial for RNAi-based therapy in living,

breathing humans, and the potential for using small RNAs in general human therapy only grows as we further our understanding of RNAi[1,179].

REFERENCES

1. Fire, A. et al. Potent and specific genetic interference by double-stranded RNA in Caenorhabditis elegans. *Nature* **391**, 806-11 (1998).

2. Guo, S. & Kemphues, K.J. par-1, a gene required for establishing polarity in C. elegans embryos, encodes a putative Ser/Thr kinase that is asymmetrically distributed. *Cell* **81**, 611-20 (1995).

3. Elbashir, S.M. et al. Duplexes of 21-nucleotide RNAs mediate RNA interference in cultured mammalian cells. *Nature* **411**, 494-8 (2001).

4. Elbashir, S.M., Lendeckel, W. & Tuschl, T. RNA interference is mediated by 21- and 22-nucleotide RNAs. *Genes Dev* **15**, 188-200 (2001).

5. Elbashir, S.M., Martinez, J., Patkaniowska, A., Lendeckel, W. & Tuschl, T. Functional anatomy of siRNAs for mediating efficient RNAi in Drosophila melanogaster embryo lysate. *Embo J* **20**, 6877-88 (2001).

6. Zamore, P.D., Tuschl, T., Sharp, P.A. & Bartel, D.P. RNAi: double-stranded RNA directs the ATP-dependent cleavage of mRNA at 21 to 23 nucleotide intervals. *Cell* **101**, 25-33 (2000).

7. Bernstein, E., Caudy, A.A., Hammond, S.M. & Hannon, G.J. Role for a bidentate ribonuclease in the initiation step of RNA interference. *Nature* **409**, 363-6 (2001).

8. Hamilton, A.J. & Baulcombe, D.C. A species of small antisense RNA in posttranscriptional gene silencing in plants. *Science* **286**, 950-2 (1999).

9. Hammond, S.M., Bernstein, E., Beach, D. & Hannon, G.J. An RNA-directed nuclease mediates post-transcriptional gene silencing in Drosophila cells. *Nature* **404**, 293-6 (2000).

10. Nykanen, A., Haley, B. & Zamore, P.D. ATP requirements and small interfering RNA structure in the RNA interference pathway. *Cell* **107**, 309-21 (2001).

11. Samuel, C.E. Knockdown by RNAi-proceed with caution. *Nat Biotechnol* **22**, 280-2 (2004).

12. Hammond, S.M., Boettcher, S., Caudy, A.A., Kobayashi, R. & Hannon, G.J. Argonaute2, a link between genetic and biochemical analyses of RNAi. *Science* **293**, 1146-50 (2001).

13. Martinez, J., Patkaniowska, A., Urlaub, H., Luhrmann, R. & Tuschl, T. Single-stranded antisense siRNAs guide target RNA cleavage in RNAi. *Cell* **110**, 563-74 (2002).

14. Tabara, H. et al. The rde-1 gene, RNA interference, and transposon silencing in C. elegans. *Cell* **99**, 123-32 (1999).

15. Carmell, M.A., Xuan, Z., Zhang, M.Q. & Hannon, G.J. The Argonaute family: tentacles that reach into RNAi, developmental control, stem cell maintenance, and tumorigenesis. *Genes Dev* **16**, 2733-42 (2002).

16. Haley, B. & Zamore, P.D. Kinetic analysis of the RNAi enzyme complex. *Nat Struct Mol Biol* **11**, 599-606 (2004).

17. Hutvagner, G. & Zamore, P.D. A microRNA in a multiple-turnover RNAi enzyme complex. *Science* **297**, 2056-60 (2002).

18. Schwarz, D.S., Hutvagner, G., Haley, B. & Zamore, P.D. Evidence that siRNAs function as guides, not primers, in the Drosophila and human RNAi pathways. *Mol Cell* **10**, 537-48 (2002).

19. Hannon, G.J. & Rossi, J.J. Unlocking the potential of the human genome with RNA interference. *Nature* **431**, 371-8 (2004).

20. Hannon, G.J. RNA interference. *Nature* **418**, 244-51 (2002).

21. Lindbo, J.A., Silva-Rosales, L., Proebsting, W.M. & Dougherty, W.G. Induction of a Highly Specific Antiviral State in Transgenic Plants: Implications for Regulation of Gene Expression and Virus Resistance. *Plant Cell* **5**, 1749-1759 (1993).

22. Lau, N.C., Lim, L.P., Weinstein, E.G. & Bartel, D.P. An abundant class of tiny RNAs with probable regulatory roles in Caenorhabditis elegans. *Science* **294**, 858-62 (2001).

23. Lee, R.C. & Ambros, V. An extensive class of small RNAs in Caenorhabditis elegans. *Science* **294**, 862-4 (2001).

24. Bartel, D.P. MicroRNAs: genomics, biogenesis, mechanism, and function. *Cell* **116**, 281-97 (2004).

25. Lagos-Quintana, M., Rauhut, R., Lendeckel, W. & Tuschl, T. Identification of novel genes coding for small expressed RNAs. *Science* **294**, 853-8 (2001).

26. Aravind, L., Watanabe, H., Lipman, D.J. & Koonin, E.V. Lineage-specific loss and divergence of functionally linked genes in eukaryotes. *Proc Natl Acad Sci U S A* **97**, 11319-24 (2000).

27. He, L. & Hannon, G.J. MicroRNAs: small RNAs with a big role in gene regulation. *Nat Rev Genet* **5**, 522-31 (2004).

28. Forstemann, K. et al. Normal microRNA maturation and germ-line stem cell maintenance requires Loquacious, a double-stranded RNA-binding domain protein. *PLoS Biol* **3**, e236 (2005).

29. Hatfield, S.D. et al. Stem cell division is regulated by the microRNA pathway. *Nature* **435**, 974-8 (2005).

30. Jiang, F. et al. Dicer-1 and R3D1-L catalyze microRNA maturation in Drosophila. *Genes Dev* **19**, 1674-9 (2005).

31. Giraldez, A.J. et al. MicroRNAs regulate brain morphogenesis in zebrafish. *Science* **308**, 833-8 (2005).

32. Chen, C.Z., Li, L., Lodish, H.F. & Bartel, D.P. MicroRNAs modulate hematopoietic lineage differentiation. *Science* **303**, 83-6 (2004).

33. Chang, S., Johnston, R.J., Jr., Frokjaer-Jensen, C., Lockery, S. & Hobert, O. MicroRNAs act sequentially and asymmetrically to control chemosensory laterality in the nematode. *Nature* **430**, 785-9 (2004).

34. O'Donnell, K.A., Wentzel, E.A., Zeller, K.I., Dang, C.V. & Mendell, J.T. c-Myc-regulated microRNAs modulate E2F1 expression. *Nature* **435**, 839-43 (2005).

35. Johnston, R.J. & Hobert, O. A microRNA controlling left/right neuronal asymmetry in Caenorhabditis elegans. *Nature* **426**, 845-9 (2003).

36. He, L. et al. A microRNA polycistron as a potential human oncogene. *Nature* **435**, 828-33 (2005).

37. Andersen, A.A. & Panning, B. Epigenetic gene regulation by noncoding RNAs. *Curr Opin Cell Biol* **15**, 281-9 (2003).

38. Matzke, M.A. & Birchler, J.A. RNAi-mediated pathways in the nucleus. *Nat Rev Genet* **6**, 24-35 (2005).

39. Kanellopoulou, C. et al. Dicer-deficient mouse embryonic stem cells are defective in differentiation and centromeric silencing. *Genes Dev* **19**, 489-501 (2005).

40. Zamore, P.D. Ancient pathways programmed by small RNAs. *Science* **296**, 1265-9 (2002).

41. Bernstein, E. et al. Dicer is essential for mouse development. *Nat Genet* **35**, 215-7 (2003).

42. Chendrimada, T.P. et al. TRBP recruits the Dicer complex to Ago2 for microRNA processing and gene silencing. *Nature* (2005).

43. Doi, N. et al. Short-interfering-RNA-mediated gene silencing in mammalian cells requires Dicer and eIF2C translation initiation factors. *Curr Biol* **13**, 41-6 (2003).

44. Kawasaki, H., Taira, K. & Morris, K.V. siRNA induced transcriptional gene silencing in mammalian cells. *Cell Cycle* **4**, 442-8 (2005).

45. Morris, K.V., Chan, S.W., Jacobsen, S.E. & Looney, D.J. Small interfering RNA-induced transcriptional gene silencing in human cells. *Science* **305**, 1289-92 (2004).

46. Ting, A.H., Schuebel, K.E., Herman, J.G. & Baylin, S.B. Short double-stranded RNA induces transcriptional gene silencing in human cancer cells in the absence of DNA methylation. *Nat Genet* (2005).

47. Mette, M.F., Aufsatz, W., van der Winden, J., Matzke, M.A. & Matzke, A.J. Transcriptional silencing and promoter methylation triggered by double-stranded RNA. *Embo J* **19**, 5194-201 (2000).

48. Chan, S.W., Henderson, I.R. & Jacobsen, S.E. Gardening the genome: DNA methylation in Arabidopsis thaliana. *Nat Rev Genet* **6**, 351-60 (2005).

49. Miura, A. et al. Mobilization of transposons by a mutation abolishing full DNA methylation in Arabidopsis. *Nature* **411**, 212-4 (2001).

50. Yoder, J.A., Walsh, C.P. & Bestor, T.H. Cytosine methylation and the ecology of intragenomic parasites. *Trends Genet* **13**, 335-40 (1997).

51. Chan, S.W. et al. RNA silencing genes control de novo DNA methylation. *Science* **303**, 1336 (2004).

52. Cao, X. & Jacobsen, S.E. Role of the arabidopsis DRM methyltransferases in de novo DNA methylation and gene silencing. *Curr Biol* **12**, 1138-44 (2002).

53. Hamilton, A., Voinnet, O., Chappell, L. & Baulcombe, D. Two classes of short interfering RNA in RNA silencing. *Embo J* **21**, 4671-9 (2002).

54. Park, W., Li, J., Song, R., Messing, J. & Chen, X. CARPEL FACTORY, a Dicer homolog, and HEN1, a novel protein, act in microRNA metabolism in Arabidopsis thaliana. *Curr Biol* **12**, 1484-95 (2002).

55. Yu, B. et al. Methylation as a crucial step in plant microRNA biogenesis. *Science* **307**, 932-5 (2005).

56. Boutet, S. et al. Arabidopsis HEN1: a genetic link between endogenous miRNA controlling development and siRNA controlling transgene silencing and virus resistance. *Curr Biol* **13**, 843-8 (2003).

57. Bao, N., Lye, K.W. & Barton, M.K. MicroRNA binding sites in Arabidopsis class III HD-ZIP mRNAs are required for methylation of the template chromosome. *Dev Cell* **7**, 653-62 (2004).

58. Volpe, T.A. et al. Regulation of heterochromatic silencing and histone H3 lysine-9 methylation by RNAi. *Science* **297**, 1833-7 (2002).

59. Kato, H. et al. RNA polymerase II is required for RNAi-dependent heterochromatin assembly. *Science* **309**, 467-9 (2005).

60. Schramke, V. et al. RNA-interference-directed chromatin modification coupled to RNA polymerase II transcription. *Nature* **435**, 1275-9 (2005).

61. Verdel, A. et al. RNAi-mediated targeting of heterochromatin by the RITS complex. *Science* **303**, 672-6 (2004).

62. Motamedi, M.R. et al. Two RNAi complexes, RITS and RDRC, physically interact and localize to noncoding centromeric RNAs. *Cell* **119**, 789-802 (2004).

63. Chen, C.C. et al. A member of the polymerase beta nucleotidyltransferase superfamily is required for RNA interference in C. elegans. *Curr Biol* **15**, 378-83 (2005).

64. Vanacova, S. et al. A new yeast poly(A) polymerase complex involved in RNA quality control. *PLoS Biol* **3**, e189 (2005).

65. Wyers, F. et al. Cryptic pol II transcripts are degraded by a nuclear quality control pathway involving a new poly(A) polymerase. *Cell* **121**, 725-37 (2005).

66. LaCava, J. et al. RNA degradation by the exosome is promoted by a nuclear polyadenylation complex. *Cell* **121**, 713-24 (2005).

67. Grishok, A., Sinskey, J.L. & Sharp, P.A. Transcriptional silencing of a transgene by RNAi in the soma of C. elegans. *Genes Dev* **19**, 683-96 (2005).

68. Lipardi, C., Wei, Q. & Paterson, B.M. RNAi as random degradative PCR: siRNA primers convert mRNA into dsRNAs that are degraded to generate new siRNAs. *Cell* **107**, 297-307 (2001).

69. Downey, K.M., Byrnes, J.J., Jurmark, B.S. & So, A.G. Reticulocyte RNA-dependent RNA polymerase. *Proc Natl Acad Sci U S A* **70**, 3400-4 (1973).

70. Pal-Bhadra, M., Bhadra, U. & Birchler, J.A. RNAi related mechanisms affect both transcriptional and posttranscriptional transgene silencing in Drosophila. *Mol Cell* **9**, 315-27 (2002).

71. Lund, A.H. & van Lohuizen, M. Polycomb complexes and silencing mechanisms. *Curr Opin Cell Biol* **16**, 239-46 (2004).

72. Pal-Bhadra, M. et al. Heterochromatic silencing and HP1 localization in Drosophila are dependent on the RNAi machinery. *Science* **303**, 669-72 (2004).

73. Marx, J. Developmental biology. Combing over the Polycomb group proteins. *Science* **308**, 624-6 (2005).

74. Griffiths-Jones, S. The microRNA Registry. *Nucleic Acids Res* **32**, D109-11 (2004).

75. Wightman, B., Ha, I. & Ruvkun, G. Posttranscriptional regulation of the heterochronic gene lin-14 by lin-4 mediates temporal pattern formation in C. elegans. *Cell* **75**, 855-62 (1993).

76. Lee, R.C., Feinbaum, R.L. & Ambros, V. The C. elegans heterochronic gene lin-4 encodes small RNAs with antisense complementarity to lin-14. *Cell* **75**, 843-54 (1993).

77. Lee, R., Feinbaum, R. & Ambros, V. A short history of a short RNA. *Cell* **116**, S89-92, 1 p following S96 (2004).

78. Hutvagner, G. et al. A cellular function for the RNA-interference enzyme Dicer in the maturation of the let-7 small temporal RNA. *Science* **293**, 834-8 (2001).

79. Grishok, A. et al. Genes and mechanisms related to RNA interference regulate expression of the small temporal RNAs that control C. elegans developmental timing. *Cell* **106**, 23-34 (2001).

80. Inada, T. & Aiba, H. Translation of aberrant mRNAs lacking a termination codon or with a shortened 3'-UTR is repressed after initiation in yeast. *Embo J* **24**, 1584-95 (2005).

81. Bentwich, I. et al. Identification of hundreds of conserved and nonconserved human microRNAs. *Nat Genet* **37**, 766-70 (2005).

82. Meister, G. & Tuschl, T. Mechanisms of gene silencing by double-stranded RNA. *Nature* **431**, 343-9 (2004).

83. Jones-Rhoades, M.W. & Bartel, D.P. Computational identification of plant microRNAs and their targets, including a stress-induced miRNA. *Mol Cell* **14**, 787-99 (2004).

84. Tang, G., Reinhart, B.J., Bartel, D.P. & Zamore, P.D. A biochemical framework for RNA silencing in plants. *Genes Dev* **17**, 49-63 (2003).

85. Llave, C., Xie, Z., Kasschau, K.D. & Carrington, J.C. Cleavage of Scarecrow-like mRNA targets directed by a class of Arabidopsis miRNA. *Science* **297**, 2053-6 (2002).

86. Davis, E. et al. RNAi-mediated allelic trans-interaction at the imprinted Rtl1/Peg11 locus. *Curr Biol* **15**, 743-9 (2005).

87. Yekta, S., Shih, I.H. & Bartel, D.P. MicroRNA-directed cleavage of HOXB8 mRNA. *Science* **304**, 594-6 (2004).

88. Liu, J., Valencia-Sanchez, M.A., Hannon, G.J. & Parker, R. MicroRNA-dependent localization of targeted mRNAs to mammalian P-bodies. *Nat Cell Biol* **7**, 719-23 (2005).

89. Orban, T.I. & Izaurralde, E. Decay of mRNAs targeted by RISC requires XRN1, the Ski complex, and the exosome. *Rna* **11**, 459-69 (2005).

90. Sen, G.L. & Blau, H.M. Argonaute 2/RISC resides in sites of mammalian mRNA decay known as cytoplasmic bodies. *Nat Cell Biol* **7**, 633-6 (2005).

91. Souret, F.F., Kastenmayer, J.P. & Green, P.J. AtXRN4 degrades mRNA in Arabidopsis and its substrates include selected miRNA targets. *Mol Cell* **15**, 173-83 (2004).

92. Gazzani, S., Lawrenson, T., Woodward, C., Headon, D. & Sablowski, R. A link between mRNA turnover and RNA interference in Arabidopsis. *Science* **306**, 1046-8 (2004).

93. Wickens, M. & Goldstrohm, A. Molecular biology. A place to die, a place to sleep. *Science* **300**, 753-5 (2003).

94. Gu, S. & Rossi, J.J. Uncoupling of RNAi from active translation in mammalian cells. *Rna* **11**, 38-44 (2005).

95. Kennerdell, J.R., Yamaguchi, S. & Carthew, R.W. RNAi is activated during Drosophila oocyte maturation in a manner dependent on aubergine and spindle-E. *Genes Dev* **16**, 1884-9 (2002).

96. Shi, H., Ullu, E. & Tschudi, C. Function of the Trypanosome Argonaute 1 protein in RNA interference requires the N-terminal RGG domain and arginine 735 in the Piwi domain. *J Biol Chem* **279**, 49889-93 (2004).

97. Nelson, P.T., Hatzigeorgiou, A.G. & Mourelatos, Z. miRNP:mRNA association in polyribosomes in a human neuronal cell line. *Rna* **10**, 387-94 (2004).

98. Ishizuka, A., Siomi, M.C. & Siomi, H. A Drosophila fragile X protein interacts with components of RNAi and ribosomal proteins. *Genes Dev* **16**, 2497-508 (2002).

99. Xie, Z., Kasschau, K.D. & Carrington, J.C. Negative feedback regulation of Dicer-Like1 in Arabidopsis by microRNA-guided mRNA degradation. *Curr Biol* **13**, 784-9 (2003).

100. Anandalakshmi, R. et al. A viral suppressor of gene silencing in plants. *Proc Natl Acad Sci U S A* **95**, 13079-84 (1998).

101. Vaucheret, H., Vazquez, F., Crete, P. & Bartel, D.P. The action of ARGONAUTE1 in the miRNA pathway and its regulation by the miRNA pathway are crucial for plant development. *Genes Dev* **18**, 1187-97 (2004).

102. Lewis, B.P., Shih, I.H., Jones-Rhoades, M.W., Bartel, D.P. & Burge, C.B. Prediction of mammalian microRNA targets. *Cell* **115**, 787-98 (2003).

103. Lewis, B.P., Burge, C.B. & Bartel, D.P. Conserved seed pairing, often flanked by adenosines, indicates that thousands of human genes are microRNA targets. *Cell* **120**, 15-20 (2005).

104. Allen, E., Xie, Z., Gustafson, A.M. & Carrington, J.C. microRNA-directed phasing during trans-acting siRNA biogenesis in plants. *Cell* **121**, 207-21 (2005).

105. Lee, Y. et al. MicroRNA genes are transcribed by RNA polymerase II. *Embo J* **23**, 4051-60 (2004).

106. Vazquez, F. et al. Endogenous trans-acting siRNAs regulate the accumulation of Arabidopsis mRNAs. *Mol Cell* **16**, 69-79 (2004).

107. Peragine, A., Yoshikawa, M., Wu, G., Albrecht, H.L. & Poethig, R.S. SGS3 and SGS2/SDE1/RDR6 are required for juvenile development and the production of trans-acting siRNAs in Arabidopsis. *Genes Dev* **18**, 2368-79 (2004).

108. Zhang, H., Kolb, F.A., Brondani, V., Billy, E. & Filipowicz, W. Human Dicer preferentially cleaves dsRNAs at their termini without a requirement for ATP. *Embo J* **21**, 5875-85 (2002).

109. John, B. et al. Human MicroRNA targets. *PLoS Biol* **2**, e363 (2004).

110. Enright, A.J. et al. MicroRNA targets in Drosophila. *Genome Biol* **5**, R1 (2003).

111. Kim, V.N. MicroRNA biogenesis: coordinated cropping and dicing. *Nat Rev Mol Cell Biol* **6**, 376-85 (2005).

112. Lee, Y., Jeon, K., Lee, J.T., Kim, S. & Kim, V.N. MicroRNA maturation: stepwise processing and subcellular localization. *Embo J* **21**, 4663-70 (2002).

113. Lee, Y. et al. The nuclear RNase III Drosha initiates microRNA processing. *Nature* **425**, 415-9 (2003).

114. Gregory, R.I. et al. The Microprocessor complex mediates the genesis of microRNAs. *Nature* **432**, 235-40 (2004).

115. Denli, A.M., Tops, B.B., Plasterk, R.H., Ketting, R.F. & Hannon, G.J. Processing of primary microRNAs by the Microprocessor complex. *Nature* **432**, 231-5 (2004).

116. Landthaler, M., Yalcin, A. & Tuschl, T. The human DiGeorge syndrome critical region gene 8 and Its D. melanogaster homolog are required for miRNA biogenesis. *Curr Biol* **14**, 2162-7 (2004).

117. Yi, R., Qin, Y., Macara, I.G. & Cullen, B.R. Exportin-5 mediates the nuclear export of pre-microRNAs and short hairpin RNAs. *Genes Dev* **17**, 3011-6 (2003).

118. Lund, E., Guttinger, S., Calado, A., Dahlberg, J.E. & Kutay, U. Nuclear export of microRNA precursors. *Science* **303**, 95-8 (2004).

119. Tomari, Y. & Zamore, P.D. Perspective: machines for RNAi. *Genes Dev* **19**, 517-29 (2005).

120. Bartel, D.P. & Chen, C.Z. Micromanagers of gene expression: the potentially widespread influence of metazoan microRNAs. *Nat Rev Genet* **5**, 396-400 (2004).

121. Lecellier, C.H. et al. A cellular microRNA mediates antiviral defense in human cells. *Science* **308**, 557-60 (2005).

122. Pfeffer, S. et al. Identification of virus-encoded microRNAs. *Science* **304**, 734-6 (2004).

123. Kennerdell, J.R. & Carthew, R.W. Use of dsRNA-mediated genetic interference to demonstrate that frizzled and frizzled 2 act in the wingless pathway. *Cell* **95**, 1017-26 (1998).

124. Tuschl, T., Zamore, P.D., Lehmann, R., Bartel, D.P. & Sharp, P.A. Targeted mRNA degradation by double-stranded RNA in vitro. *Genes Dev* **13**, 3191-7 (1999).

125. Lee, Y.S. et al. Distinct roles for Drosophila Dicer-1 and Dicer-2 in the siRNA/miRNA silencing pathways. *Cell* **117**, 69-81 (2004).

126. Hoa, N.T., Keene, K.M., Olson, K.E. & Zheng, L. Characterization of RNA interference in an Anopheles gambiae cell line. *Insect Biochem Mol Biol* **33**, 949-57 (2003).

127. Liu, Q. et al. R2D2, a bridge between the initiation and effector steps of the Drosophila RNAi pathway. *Science* **301**, 1921-5 (2003).

128. Tomari, Y., Matranga, C., Haley, B., Martinez, N. & Zamore, P.D. A protein sensor for siRNA asymmetry. *Science* **306**, 1377-80 (2004).

129. Khvorova, A., Reynolds, A. & Jayasena, S.D. Functional siRNAs and miRNAs exhibit strand bias. *Cell* **115**, 209-16 (2003).

130. Schwarz, D.S. et al. Asymmetry in the assembly of the RNAi enzyme complex. *Cell* **115**, 199-208 (2003).

131. Saito, K., Ishizuka, A., Siomi, H. & Siomi, M.C. Processing of pre-microRNAs by the Dicer-1-Loquacious complex in Drosophila cells. *PLoS Biol* **3**, e235 (2005).

132. Gupta, V., Huang, X. & Patel, R.C. The carboxy-terminal, M3 motifs of PACT and TRBP have opposite effects on PKR activity. *Virology* **315**, 283-91 (2003).

133. Song, J.J., Smith, S.K., Hannon, G.J. & Joshua-Tor, L. Crystal structure of Argonaute and its implications for RISC slicer activity. *Science* **305**, 1434-7 (2004).

134. Schwarz, D.S., Tomari, Y. & Zamore, P.D. The RNA-induced silencing complex is a Mg2+-dependent endonuclease. *Curr Biol* **14**, 787-91 (2004).

135. Martinez, J. & Tuschl, T. RISC is a 5' phosphomonoester-producing RNA endonuclease. *Genes Dev* **18**, 975-80 (2004).

136. Nowotny, M., Gaidamakov, S.A., Crouch, R.J. & Yang, W. Crystal Structures of RNase H Bound to an RNA/DNA Hybrid: Substrate Specificity and Metal-Dependent Catalysis. *Cell* **121**, 1005-16 (2005).

137. Caudy, A.A. et al. A micrococcal nuclease homologue in RNAi effector complexes. *Nature* **425**, 411-4 (2003).

138. Scadden, A.D. The RISC subunit Tudor-SN binds to hyper-edited double-stranded RNA and promotes its cleavage. *Nat Struct Mol Biol* **12**, 489-96 (2005).

139. Parker, J.S., Roe, S.M. & Barford, D. Structural insights into mRNA recognition from a PIWI domain-siRNA guide complex. *Nature* **434**, 663-6 (2005).

140. Parker, J.S., Roe, S.M. & Barford, D. Crystal structure of a PIWI protein suggests mechanisms for siRNA recognition and slicer activity. *Embo J* **23**, 4727-37 (2004).

141. Ma, J.B. et al. Structural basis for 5'-end-specific recognition of guide RNA by the A. fulgidus Piwi protein. *Nature* **434**, 666-70 (2005).

142. Rivas, F.V. et al. Purified Argonaute2 and an siRNA form recombinant human RISC. *Nat Struct Mol Biol* **12**, 340-9 (2005).

143. Okamura, K., Ishizuka, A., Siomi, H. & Siomi, M.C. Distinct roles for Argonaute proteins in small RNA-directed RNA cleavage pathways. *Genes Dev* **18**, 1655-66 (2004).

144. Liu, J. et al. Argonaute2 is the catalytic engine of mammalian RNAi. *Science* **305**, 1437-41 (2004).

145. Meister, G. et al. Human Argonaute2 mediates RNA cleavage targeted by miRNAs and siRNAs. *Mol Cell* **15**, 185-97 (2004).

146. Maniataki, E. & Mourelatos, Z. Human mitochondrial tRNAMet is exported to the cytoplasm and associates with the Argonaute 2 protein. *Rna* **11**, 849-52 (2005).

147. Cerutti, L., Mian, N. & Bateman, A. Domains in gene silencing and cell differentiation proteins: the novel PAZ domain and redefinition of the Piwi domain. *Trends Biochem Sci* **25**, 481-2 (2000).

148. Lingel, A. & Sattler, M. Novel modes of protein-RNA recognition in the RNAi pathway. *Curr Opin Struct Biol* **15**, 107-15 (2005).

149. Song, J.J. et al. The crystal structure of the Argonaute2 PAZ domain reveals an RNA binding motif in RNAi effector complexes. *Nat Struct Biol* **10**, 1026-32 (2003).

150. Tahbaz, N. et al. Characterization of the interactions between mammalian PAZ PIWI domain proteins and Dicer. *EMBO Rep* **5**, 189-94 (2004).

151. Pham, J.W., Pellino, J.L., Lee, Y.S., Carthew, R.W. & Sontheimer, E.J. A Dicer-2-dependent 80s complex cleaves targeted mRNAs during RNAi in Drosophila. *Cell* **117**, 83-94 (2004).

152. Williams, R.W. & Rubin, G.M. ARGONAUTE1 is required for efficient RNA interference in Drosophila embryos. *Proc Natl Acad Sci U S A* **99**, 6889-94 (2002).

153. Caudy, A.A., Myers, M., Hannon, G.J. & Hammond, S.M. Fragile X-related protein and VIG associate with the RNA interference machinery. *Genes Dev* **16**, 2491-6 (2002).

154. Deshpande, G., Calhoun, G. & Schedl, P. Drosophila argonaute-2 is required early in embryogenesis for the assembly of centric/centromeric heterochromatin, nuclear division, nuclear migration, and germ-cell formation. *Genes Dev* **19**, 1680-5 (2005).

155. Rodriguez, A.J. et al. Seawi--a sea urchin piwi/argonaute family member is a component of MT-RNP complexes. *Rna* **11**, 646-56 (2005).

156. Blower, M.D., Nachury, M., Heald, R. & Weis, K. A Rae1-containing ribonucleoprotein complex is required for mitotic spindle assembly. *Cell* **121**, 223-34 (2005).

157. Findley, S.D., Tamanaha, M., Clegg, N.J. & Ruohola-Baker, H. Maelstrom, a Drosophila spindle-class gene, encodes a protein that colocalizes with Vasa and RDE1/AGO1 homolog, Aubergine, in nuage. *Development* **130**, 859-71 (2003).

158. Aravin, A.A. et al. The small RNA profile during Drosophila melanogaster development. *Dev Cell* **5**, 337-50 (2003).

159. Aravin, A.A. et al. Dissection of a natural RNA silencing process in the Drosophila melanogaster germ line. *Mol Cell Biol* **24**, 6742-50 (2004).

160. Cox, D.N., Chao, A. & Lin, H. piwi encodes a nucleoplasmic factor whose activity modulates the number and division rate of germline stem cells. *Development* **127**, 503-14 (2000).

161. Cheng, L.C., Tavazoie, M. & Doetsch, F. Stem cells: from epigenetics to microRNAs. *Neuron* **46**, 363-7 (2005).

162. Meltzer, P.S. Cancer genomics: small RNAs with big impacts. *Nature* **435**, 745-6 (2005).

163. Ota, A. et al. Identification and characterization of a novel gene, C13orf25, as a target for 13q31-q32 amplification in malignant lymphoma. *Cancer Res* **64**, 3087-95 (2004).

164. Eis, P.S. et al. Accumulation of miR-155 and BIC RNA in human B cell lymphomas. *Proc Natl Acad Sci U S A* **102**, 3627-32 (2005).

165. Calin, G.A. et al. Frequent deletions and down-regulation of micro- RNA genes miR15 and miR16 at 13q14 in chronic lymphocytic leukemia. *Proc Natl Acad Sci U S A* **99**, 15524-9 (2002).

166. Lu, J. et al. MicroRNA expression profiles classify human cancers. *Nature* **435**, 834-8 (2005).

167. Alisky, J.M. & Davidson, B.L. Towards therapy using RNA interference. *Am J Pharmacogenomics* **4**, 45-51 (2004).

168. Karagiannis, T.C. & El-Osta, A. RNA interference and potential therapeutic applications of short interfering RNAs. *Cancer Gene Ther* (2005).

169. Shankar, P., Manjunath, N. & Lieberman, J. The prospect of silencing disease using RNA interference. *Jama* **293**, 1367-73 (2005).

170. Gleave, M.E. & Monia, B.P. Antisense therapy for cancer. *Nat Rev Cancer* **5**, 468-79 (2005).

171. Zamecnik, P.C. & Stephenson, M.L. Inhibition of Rous sarcoma virus replication and cell transformation by a specific oligodeoxynucleotide. *Proc Natl Acad Sci U S A* **75**, 280-4 (1978).

172. Chang, H.S., Lin, C.H., Chen, Y.C. & Yu, W.C. Using siRNA technique to generate transgenic animals with spatiotemporal and conditional gene knockdown. *Am J Pathol* **165**, 1535-41 (2004).

173. McCaffrey, A.P. et al. Inhibition of hepatitis B virus in mice by RNA interference. *Nat Biotechnol* **21**, 639-44 (2003).

174. McCaffrey, A.P. et al. RNA interference in adult mice. *Nature* **418**, 38-9 (2002).

175. Soutschek, J. et al. Therapeutic silencing of an endogenous gene by systemic administration of modified siRNAs. *Nature* **432**, 173-8 (2004).

176. de Fougerolles, A., Manoharan, M., Meyers, R. & Vornlocher, H.P. RNA interference in vivo: toward synthetic small inhibitory RNA-based therapeutics. *Methods Enzymol* **392**, 278-96 (2005).

177. Xia, H. et al. RNAi suppresses polyglutamine-induced neurodegeneration in a model of spinocerebellar ataxia. *Nat Med* **10**, 816-20 (2004).

178. Jackson, A.L. & Linsley, P.S. Noise amidst the silence: off-target effects of siRNAs? *Trends Genet* **20**, 521-4 (2004).

179. Leung, R.K. & Whittaker, P.A. RNA interference: From gene silencing to gene-specific therapeutics. *Pharmacol Ther* **107**, 222-39 (2005).

180. Brennecke, J., Stark, A., Russell, R.B. & Cohen, S.M. Principles of microRNA-target recognition. *PLoS Biol* **3**, e85 (2005).

181. Doench, J.G., Petersen, C.P. & Sharp, P.A. siRNAs can function as miRNAs. *Genes Dev* **17**, 438-42 (2003).

182. Jackson, A.L. et al. Expression profiling reveals off-target gene regulation by RNAi. *Nat Biotechnol* **21**, 635-7 (2003).

183. Chiu, Y.L. & Rana, T.M. RNAi in human cells: basic structural and functional features of small interfering RNA. *Mol Cell* **10**, 549-61 (2002).

184. Hornung, V. et al. Sequence-specific potent induction of IFN-alpha by short interfering RNA in plasmacytoid dendritic cells through TLR7. *Nat Med* **11**, 263-70 (2005).

185. Stevenson, M. Therapeutic potential of RNA interference. *N Engl J Med* **351**, 1772-7 (2004).

186. Xu, Z. & Xia, X.G. RNAi therapy: Dominant disease gene gets silenced. *Gene Ther* (2005).

187. Ralph, G.S. et al. Silencing mutant SOD1 using RNAi protects against neurodegeneration and extends survival in an ALS model. *Nat Med* **11**, 429-33 (2005).

188. Randall, G. & Rice, C.M. Interfering with hepatitis C virus RNA replication. *Virus Res* **102**, 19-25 (2004).

189. Simons, J. Ten tech trends. Genetic medicine's next big step. *Fortune* **151**, 54-5 (2005).

190. Montgomery, M.K. & Fire, A. Double-stranded RNA as a mediator in sequence-specific genetic silencing and co-suppression. *Trends Genet* **14**, 255-8 (1998).

191. Jensen, S., Gassama, M.P. & Heidmann, T. Cosuppression of I transposon activity in Drosophila by I-containing sense and antisense transgenes. *Genetics* **153**, 1767-74 (1999).

192. Ketting, R.F., Haverkamp, T.H., van Luenen, H.G. & Plasterk, R.H. Mut-7 of C. elegans, required for transposon silencing and RNA interference, is a homolog of Werner syndrome helicase and RNaseD. *Cell* **99**, 133-41 (1999).

193. Ketting, R.F. & Plasterk, R.H. A genetic link between co-suppression and RNA interference in C. elegans. *Nature* **404**, 296-8 (2000).

194. Malinsky, S., Bucheton, A. & Busseau, I. New insights on homology-dependent silencing of I factor activity by transgenes containing ORF1 in Drosophila melanogaster. *Genetics* **156**, 1147-55 (2000).

195. Montgomery, M.K., Xu, S. & Fire, A. RNA as a target of double-stranded RNA-mediated genetic interference in Caenorhabditis elegans. *Proc Natl Acad Sci U S A* **95**, 15502-7 (1998).

196. Fire, A. RNA-triggered gene silencing. *Trends Genet* **15**, 358-63 (1999).

197. Hunter, C.P. Genetics: a touch of elegance with RNAi. *Curr Biol* **9**, R440-2 (1999).

198. Li, W.X. & Ding, S.W. Viral suppressors of RNA silencing. *Curr Opin Biotechnol* **12**, 150-4 (2001).

199. Sharp, P.A. RNA interference--2001. *Genes Dev* **15**, 485-90 (2001).

200. Smardon, A. et al. EGO-1 is related to RNA-directed RNA polymerase and functions in germ-line development and RNA interference in C. elegans. *Curr Biol* **10**, 169-78 (2000).

201. Aravin, A.A. et al. Double-stranded RNA-mediated silencing of genomic tandem repeats and transposable elements in the D. melanogaster germline. *Curr Biol* **11**, 1017-27 (2001).

202. Baulcombe, D.C. Gene silencing: RNA makes RNA makes no protein. *Curr Biol* **9**, R599-601 (1999).

203. Ratcliff, F.G., MacFarlane, S.A. & Baulcombe, D.C. Gene silencing without DNA. rna-mediated cross-protection between viruses. *Plant Cell* **11**, 1207-16 (1999).

204. Grant, S.R. Dissecting the mechanisms of posttranscriptional gene silencing: divide and conquer. *Cell* **96**, 303-6 (1999).

205. Cogoni, C. et al. Transgene silencing of the al-1 gene in vegetative cells of Neurospora is mediated by a cytoplasmic effector and does not depend on DNA-DNA interactions or DNA methylation. *Embo J* **15**, 3153-63 (1996).

206. Cogoni, C., Romano, N. & Macino, G. Suppression of gene expression by homologous transgenes. *Antonie Van Leeuwenhoek* **65**, 205-9 (1994).

207. Cogoni, C. & Macino, G. Isolation of quelling-defective (qde) mutants impaired in posttranscriptional transgene-induced gene silencing in Neurospora crassa. *Proc Natl Acad Sci U S A* **94**, 10233-8 (1997).

208. Cogoni, C. & Macino, G. Posttranscriptional gene silencing in Neurospora by a RecQ DNA helicase. *Science* **286**, 2342-4 (1999).

209. Elmayan, T. et al. Arabidopsis mutants impaired in cosuppression. *Plant Cell* **10**, 1747-58 (1998).

210. Fagard, M., Boutet, S., Morel, J.B., Bellini, C. & Vaucheret, H. AGO1, QDE-2, and RDE-1 are related proteins required for post-transcriptional gene silencing in plants, quelling in fungi, and RNA interference in animals. *Proc Natl Acad Sci U S A* **97**, 11650-4 (2000).

211. Wu-Scharf, D., Jeong, B., Zhang, C. & Cerutti, H. Transgene and transposon silencing in Chlamydomonas reinhardtii by a DEAH-box RNA helicase. *Science* **290**, 1159-62 (2000).

212. Dalmay, T., Hamilton, A., Rudd, S., Angell, S. & Baulcombe, D.C. An RNA-dependent RNA polymerase gene in Arabidopsis is required for posttranscriptional gene silencing mediated by a transgene but not by a virus. *Cell* **101**, 543-53 (2000).

213. Mourrain, P. et al. Arabidopsis SGS2 and SGS3 genes are required for posttranscriptional gene silencing and natural virus resistance. *Cell* **101**, 533-42 (2000).

214. Catalanotto, C., Azzalin, G., Macino, G. & Cogoni, C. Gene silencing in worms and fungi. *Nature* **404**, 245 (2000).

215. Dernburg, A.F., Zalevsky, J., Colaiacovo, M.P. & Villeneuve, A.M. Transgene-mediated cosuppression in the C. elegans germ line. *Genes Dev* **14**, 1578-83 (2000).

216. Hammond, S.M., Caudy, A.A. & Hannon, G.J. Post-transcriptional gene silencing by double-stranded RNA. *Nat Rev Genet* **2**, 110-9 (2001).

217. Grishok, A., Tabara, H. & Mello, C.C. Genetic requirements for inheritance of RNAi in C. elegans. *Science* **287**, 2494-7 (2000).

218. Hutvagner, G., Mlynarova, L. & Nap, J.P. Detailed characterization of the posttranscriptional gene-silencing-related small RNA in a GUS gene-silenced tobacco. *Rna* **6**, 1445-54 (2000).

219. Yang, D., Lu, H. & Erickson, J.W. Evidence that processed small dsRNAs may mediate sequence-specific mRNA degradation during RNAi in Drosophila embryos. *Curr Biol* **10**, 1191-200 (2000).

220. Parrish, S., Fleenor, J., Xu, S., Mello, C. & Fire, A. Functional anatomy of a dsRNA trigger: differential requirement for the two trigger strands in RNA interference. *Mol Cell* **6**, 1077-87 (2000).

221. Djikeng, A., Shi, H., Tschudi, C. & Ullu, E. RNA interference in Trypanosoma brucei: cloning of small interfering RNAs provides evidence for retroposon-derived 24-26-nucleotide RNAs. *Rna* **7**, 1522-30 (2001).

222. Jacobsen, S.E., Running, M.P. & Meyerowitz, E.M. Disruption of an RNA helicase/RNAse III gene in Arabidopsis causes unregulated cell division in floral meristems. *Development* **126**, 5231-43 (1999).

223. Matsuda, S. et al. Molecular cloning and characterization of a novel human gene (HERNA) which encodes a putative RNA-helicase. *Biochim Biophys Acta* **1490**, 163-9 (2000).

224. Knight, S.W. & Bass, B.L. A role for the RNase III enzyme DCR-1 in RNA interference and germ line development in Caenorhabditis elegans. *Science* **293**, 2269-71 (2001).

225. Dalmay, T., Horsefield, R., Braunstein, T.H. & Baulcombe, D.C. SDE3 encodes an RNA helicase required for post-transcriptional gene silencing in Arabidopsis. *Embo J* **20**, 2069-78 (2001).

226. Haley, B., Tang, G. & Zamore, P.D. In vitro analysis of RNA interference in Drosophila melanogaster. *Methods* **30**, 330-6 (2003).

227. Ding, H. et al. Selective silencing by RNAi of a dominant allele that causes amyotrophic lateral sclerosis. *Aging Cell* **2**, 209-17 (2003).

228. Holen, T., Amarzguioui, M., Babaie, E. & Prydz, H. Similar behaviour of single-strand and double-strand siRNAs suggests they act through a common RNAi pathway. *Nucleic Acids Res* **31**, 2401-7 (2003).

229. Amarzguioui, M., Holen, T., Babaie, E. & Prydz, H. Tolerance for mutations and chemical modifications in a siRNA. *Nucleic Acids Res* **31**, 589-95 (2003).

230. Phipps, K.M., Martinez, A., Lu, J., Heinz, B.A. & Zhao, G. Small interfering RNA molecules as potential anti-human rhinovirus agents: in vitro potency, specificity, and mechanism. *Antiviral Res* **61**, 49-55 (2004).

231. Rajewsky, N. & Socci, N.D. Computational identification of microRNA targets. *Dev Biol* **267**, 529-35 (2004).

232. Lai, E.C. Micro RNAs are complementary to 3' UTR sequence motifs that mediate negative post-transcriptional regulation. *Nat Genet* **30**, 363-4 (2002).

233. Doench, J.G. & Sharp, P.A. Specificity of microRNA target selection in

234. Chiu, Y.L. & Rana, T.M. siRNA function in RNAi: a chemical modification analysis. *Rna* **9**, 1034-48 (2003).

235. Hutvagner, G., Simard, M.J., Mello, C.C. & Zamore, P.D. Sequence-specific inhibition of small RNA function. *PLoS Biol* **2**, E98 (2004).

236. Stark, A., Brennecke, J., Russell, R.B. & Cohen, S.M. Identification of Drosophila MicroRNA targets. *PLoS Biol* **1**, E60 (2003).

237. Rhoades, M.W. et al. Prediction of plant microRNA targets. *Cell* **110**, 513-20 (2002).

238. Lima, W.F. & Crooke, S.T. Binding affinity and specificity of Escherichia coli RNase H1: impact on the kinetics of catalysis of antisense oligonucleotide-RNA hybrids. *Biochemistry* **36**, 390-8 (1997).

239. Tomari, Y. et al. RISC assembly defects in the Drosophila RNAi mutant armitage. *Cell* **116**, 831-41 (2004).

240. Reynolds, A. et al. Rational siRNA design for RNA interference. *Nat Biotechnol* **22**, 326-30 (2004).

241. Abrahante, J.E. et al. The Caenorhabditis elegans hunchback-like gene lin-57/hbl-1 controls developmental time and is regulated by microRNAs. *Dev Cell* **4**, 625-37 (2003).

242. Brennecke, J., Hipfner, D.R., Stark, A., Russell, R.B. & Cohen, S.M. bantam encodes a developmentally regulated microRNA that controls cell proliferation and regulates the proapoptotic gene hid in Drosophila. *Cell* **113**, 25-36 (2003).

243. Xu, P., Vernooy, S.Y., Guo, M. & Hay, B.A. The Drosophila microRNA Mir-14 suppresses cell death and is required for normal fat metabolism. *Curr Biol* **13**, 790-5 (2003).

244. Vella, M.C., Choi, E.Y., Lin, S.Y., Reinert, K. & Slack, F.J. The C. elegans microRNA let-7 binds to imperfect let-7 complementary sites from the lin-41 3'UTR. *Genes Dev* **18**, 132-7 (2004).

245. Reinhart, B.J. et al. The 21-nucleotide let-7 RNA regulates developmental timing in Caenorhabditis elegans. *Nature* **403**, 901-6 (2000).

246. Rand, T.A., Ginalski, K., Grishin, N.V. & Wang, X. Biochemical identification of Argonaute 2 as the sole protein required for RNA-induced silencing complex activity. *Proc Natl Acad Sci U S A* **101**, 14385-9 (2004).

247. Filipowicz, W. RNAi: The Nuts and Bolts of the RISC Machine. *Cell* **122**, 17-20 (2005).

248. Philips, J.A., Rubin, E.J. & Perrimon, N. Drosophila RNAi Screen Reveals CD36 Family Member Required for Mycobacterial Infection. *Science* (2005).

249. Pelkmans, L. et al. Genome-wide analysis of human kinases in clathrin- and caveolae/raft-mediated endocytosis. *Nature* **436**, 78-86 (2005).

250. Agaisse, H. et al. Genome-Wide RNAi Screen for Host Factors Required for Intracellular Bacterial Infection. *Science* (2005).

251. Westbrook, T.F. et al. A genetic screen for candidate tumor suppressors identifies REST. *Cell* **121**, 837-48 (2005).

252. Cherry, S. et al. Genome-wide RNAi screen reveals a specific sensitivity of IRES-containing RNA viruses to host translation inhibition. *Genes Dev* **19**, 445-52 (2005).

253. Paddison, P.J. et al. A resource for large-scale RNA-interference-based screens in mammals. *Nature* **428**, 427-31 (2004).

254. Friedman, A. & Perrimon, N. Genome-wide high-throughput screens in functional genomics. *Curr Opin Genet Dev* **14**, 470-6 (2004).

Cell, Vol. 107, 309–321, November 2, 2001, Copyright ©2001 by Cell Press

ATP Requirements and Small Interfering RNA Structure in the RNA Interference Pathway

Antti Nykänen, Benjamin Haley, and Phillip D. Zamore[1]
Department of Biochemistry
and Molecular Pharmacology
University of Massachusetts Medical School
55 Lake Avenue North
Worcester, Massachusetts 01655

Summary

We examined the role of ATP in the RNA interference (RNAi) pathway. Our data reveal two ATP-dependent steps and suggest that the RNAi reaction comprises at least four sequential steps: ATP-dependent processing of double-stranded RNA into small interfering RNAs (siRNAs), incorporation of siRNAs into an inactive ~360 kDa protein/RNA complex, ATP-dependent unwinding of the siRNA duplex to generate an active complex, and ATP-independent recognition and cleavage of the RNA target. Furthermore, ATP is used to maintain 5′ phosphates on siRNAs. A 5′ phosphate on the target-complementary strand of the siRNA duplex is required for siRNA function, suggesting that cells check the authenticity of siRNAs and license only bona fide siRNAs to direct target RNA destruction.

Introduction

In animals, double-stranded RNA (dsRNA) specifically silences expression of a corresponding gene, a phenomenon termed RNA interference (RNAi; Fire et al., 1998; Montgomery et al., 1998). One function of the RNAi machinery is to maintain the integrity of the genome by suppressing the mobilization of transposons and the accumulation of repetitive DNA (Jensen et al., 1999; Ketting et al., 1999; Ketting and Plasterk, 2000; Malinsky et al., 2000). The RNAi machinery may also defend cells against viral infection (reviewed in Montgomery and Fire, 1998; Fire, 1999; Hunter, 1999; Li and Ding, 2001; Sharp, 2001) and regulate expression of cellular genes (Smardon et al., 2000; Aravin et al., 2001).

RNAi bears a striking similarity to posttranscriptional cosuppression in plants (posttranscriptional gene silencing, PTGS; Baulcombe, 1999; Grant, 1999; Ratcliff et al., 1999) and *Neurospora crassa* (quelling; Cogoni et al., 1994, 1996). Genetic screens in worms, fungi, plants, and green algae have identified genes required for RNAi or PTGS (Cogoni and Macino, 1997, 1999; Elmayan et al., 1998; Tabara et al., 1999; Fagard et al., 2000; Wu-Scharf et al., 2000; Dalmay et al., 2000; Mourrain et al., 2000), and the RNAi and cosuppression pathways in *Caenorhabditis elegans*, *Neurospora*, and *Arabidopsis thaliana* require some of the same genes (Catalanotto et al., 2000; Dernburg et al., 2000; Fagard et al., 2000; Ketting and Plasterk, 2000; Hammond et al., 2001b). Mutations in a subset of these genes permit the mobilization of transposons (Ketting et al., 1999; Tabara et al., 1999; Grishok et al., 2000), whereas a second class of mutants, including the *rde-1* and *rde-4* loci, are defective for RNAi but show no other phenotypic abnormalities (Tabara et al., 1999). Rde-1 is a member of the PPD family of proteins (*P*AZ and *P*IWI *D*omain), which are characterized by an N-terminal "Piwi/Argonaute/Zwille" (PAZ) domain and a C-terminal 'PIWI' domain (Cerutti et al., 2000). PPD proteins are required not only for RNAi in worms (Rde-1; Tabara et al., 1999) and flies (Ago-2; Hammond et al., 2001a), but also for PTGS in plants (AGO-1; Fagard et al., 2000) and quelling in fungi (Qde-1; Catalanotto et al., 2000).

In vitro, dsRNA targets mRNA for cleavage in lysates of early *Drosophila* embryos or extracts of cultured *Drosophila* S2 cells (Tuschl et al., 1999; Hammond et al., 2000; Zamore et al., 2000). RNAi in vitro requires ATP (Zamore et al., 2000). The molecular basis for the ATP requirement is due, in part, to a requirement for ATP in the initial processing of long dsRNA into the 21–25 nt small interfering RNAs (siRNAs) which guide target cleavage (Hamilton and Baulcombe, 1999; Zamore et al., 2000; Elbashir et al., 2001a; Bernstein et al., 2001). siRNAs have been detected in vivo in plants (Hamilton and Baulcombe, 1999; Hutvágner et al., 2000), flies (Yang et al., 2000), worms (Parrish et al., 2000), and trypanosomes (Djikeng et al., 2001). Recent studies with synthetic RNA duplexes demonstrate that each siRNA duplex cleaves the target RNA at a single site (Elbashir et al., 2001a). 2- or 3-nt overhanging 3′ ends within the siRNA duplex are required for efficient target cleavage (Elbashir et al., 2001a). Such 3′ overhangs are characteristic of the products of an RNase III cleavage reaction, and, in cultured *Drosophila* S2 cells, cleavage of the dsRNA into siRNAs requires the multidomain RNase III enzyme, Dicer (Bernstein et al., 2001). Intriguingly, Dicer interacts directly or indirectly with Ago-2, a PPD protein required for RNAi in cultured *Drosophila* S2 cells (Hammond et al., 2001a). Dicer orthologs are found in the genomes of plants (Jacobsen et al., 1999), worms, fission yeast, and humans (Matsuda et al., 2000; Bernstein et al., 2001). In worms, the Dicer ortholog, Dcr-1, is required both for RNAi (Knight and Bass, 2001) and for the maturation of small temporal RNAs (stRNAs), single-stranded 21–22 nt RNAs that control the timing of development (Grishok et al., 2001). Dicer in flies and humans is likewise responsible for generating the *let-7* stRNA (Hutvágner et al., 2001).

Here, we dissect the role of ATP in the RNAi pathway. Our data suggest that the RNAi reaction comprises at least four sequential steps: ATP-dependent dsRNA processing, ATP-independent incorporation of siRNAs into an inactive ~360 kDa complex, ATP-dependent unwinding of the siRNA duplex, and ATP-independent recognition and cleavage of the target RNA. Remarkably, a 5′ phosphate is required for entry of an siRNA into the RNAi pathway. In vitro, this phosphate is maintained by a kinase which can recognize authentic siRNAs. Furthermore, the phosphorylation status of the 5′ ends of an siRNA duplex is monitored by the RNAi machinery, sug-

[1]Correspondence: phillip.zamore@umassmed.edu

gesting that cells check the authenticity of siRNAs, ensuring that only bona fide siRNAs direct target RNA destruction.

Results and Discussion

ATP and dsRNA Processing

In vitro and in vivo studies suggest that RNAi is a multistep process that begins with the ATP-dependent processing of long dsRNA into 21–23 nt siRNAs by Dicer protein, perhaps in conjunction with other proteins. In *Drosophila* embryo lysates, siRNAs are produced to 6-fold higher levels in high ATP concentrations than in low (Zamore et al., 2000), and dsRNA cleavage by immunoprecipitated Dicer protein requires ATP (Bernstein et al., 2001). As a starting point for defining the role of ATP in the RNAi pathway, we reexamined the ATP dependence of siRNA production during the initial phase of the cleavage reaction, when the rate of dsRNA cleavage is linear (Figure 1A). A prior study assessed siRNA production at steady state (Zamore et al., 2000). The experiments presented here employed a revised ATP depletion strategy that reduced ATP-levels by at least 5,000-fold, to <100 nM. During the first 16 min of incubation of a uniformly ^{32}P-radiolabeled dsRNA derived from the *Renilla reniformis* luciferase (*Rr*-luc) gene, the rate of siRNA production was ~47-fold faster in the presence of ATP and an ATP-regenerating system (filled squares) than in their absence (open squares). In the presence of ATP, siRNA production increased dramatically after about 4 min incubation. This initial lag might reflect the ATP-dependent rearrangement of the dsRNA and/or the proteins required to produce siRNAs, such as Dicer. Consistent with this idea, we did not detect such an initial lag phase for siRNA production in the absence of ATP. siRNA production in the presence of ATP required incubation at 25°C; no siRNAs were produced in the presence of ATP at 4°C (filled circles). These data quantitatively confirm previous observations that cleavage of the dsRNA into siRNAs requires ATP (Zamore et al., 2000; Bernstein et al., 2001).

siRNA Duplexes Are Bona Fide Intermediates in the RNAi Pathway

RNAi can be initiated with synthetic siRNAs in vitro and in vivo, suggesting that siRNAs are intermediates in the RNAi reaction (Elbashir et al., 2001a, 2001b; Caplen et al., 2001). However, when purified from a denaturing gel, siRNAs generated by cleavage of dsRNA reduced target mRNA expression by only ~2-fold (unpublished data). To assess directly if the products of dsRNA cleavage—native siRNAs—are true intermediates in the RNAi reaction, we developed an isolation procedure designed to preserve their proposed double-stranded character. Uniformly ^{32}P-radiolabeled *Rr*-luc dsRNA was incubated in a standard RNAi reaction in the absence of target mRNA, deproteinized, and fractionated by gel filtration. Two peaks of radioactivity eluted from the column (Figure 1C, black circles). The first corresponded to unprocessed dsRNA; the second peak contained native siRNAs. The elution position of the native siRNAs from the gel-filtration column coincided with that of a synthetic siRNA duplex (red triangles), but not a single-stranded 21 nt RNA (blue squares). Thus, the siRNAs produced by Dicer-mediated cleavage of long dsRNA are double-stranded.

The gel filtration procedure was repeated with unlabeled *Rr*-luc dsRNA processed in vitro into native siRNAs, and the column fractions assessed for their ability to mediate sequence-specific interference when added to lysate in the presence of ATP. Two peaks of interfering activity were detected (Figure 1D). The first peak, fractions 3–13, corresponded to unprocessed dsRNA and served as an internal control for the experiment. The second peak, fractions 41–50, corresponded to the native siRNAs. None of the column fractions exhibited any significant degradation of an unrelated *Photinus pyralis* luciferase (*Pp*-luc) mRNA (Figure 1E). Preheating the purified native siRNAs to 95°C for 5 min abolished their ability to initiate interference, suggesting that only double-stranded siRNAs can enter the pathway (data not shown). These results, together with those of Tuschl and coworkers (Elbashir et al., 2001a), demonstrate that siRNAs are true intermediates in RNAi, not the products of an off-pathway side reaction. Furthermore, they support the original proposal of Hamilton and Baulcombe that siRNAs are the specificity determinate for both PTGS and RNAi (Hamilton and Baulcombe, 1999).

A Second ATP-Dependent Step in RNAi

In performing the experiments shown in Figures 1D and 1E, we observed that none of the column fractions mediated sequence-specific interference when incubated with lysate in the absence of ATP. This observation was expected for the first peak (fractions 3–13), since dsRNA cleavage into siRNAs requires ATP, but unexpected for the second peak, which corresponds to fully processed, native siRNAs. Therefore, we asked if interference mediated by siRNAs, rather than dsRNA, also required ATP. Native siRNAs isolated by gel-filtration were added to a standard RNAi reaction in the presence or absence of ATP (Figure 2) and incubated at room temperature for 30 min, and then a *Rr*-luc target mRNA was added. In the presence of both native siRNAs and ATP, the target RNA was rapidly degraded (native, +ATP). In contrast, only nonspecific degradation of the target RNA occurred in the absence of ATP (native, −ATP). These results point to the existence of a second ATP-dependent step, downstream in the RNAi reaction from dsRNA processing. However, an alternative explanation is that undetected dsRNA contaminated the native siRNA preparation. Since dsRNA processing requires ATP, this could, in principle, explain the apparent ATP requirement for native siRNA-directed interference. To exclude this possibility, we assessed the ATP dependence of interference directed by a chemically synthesized siRNA duplex targeting the *Pp*-luc mRNA (Figure 2). In the absence of ATP, no sequence-specific interference occurred (synthetic, −ATP). Addition of ATP and an energy regenerating system only partially restored normal ATP levels, because of the high concentrations of glucose used to deplete ATP. Under these conditions, partial interference was observed (synthetic, ATP rescue). In contrast, in a standard RNAi reaction containing 1 mM ATP, synthetic siRNAs mediated potent interference (synthetic, +ATP). Therefore, interference by both native

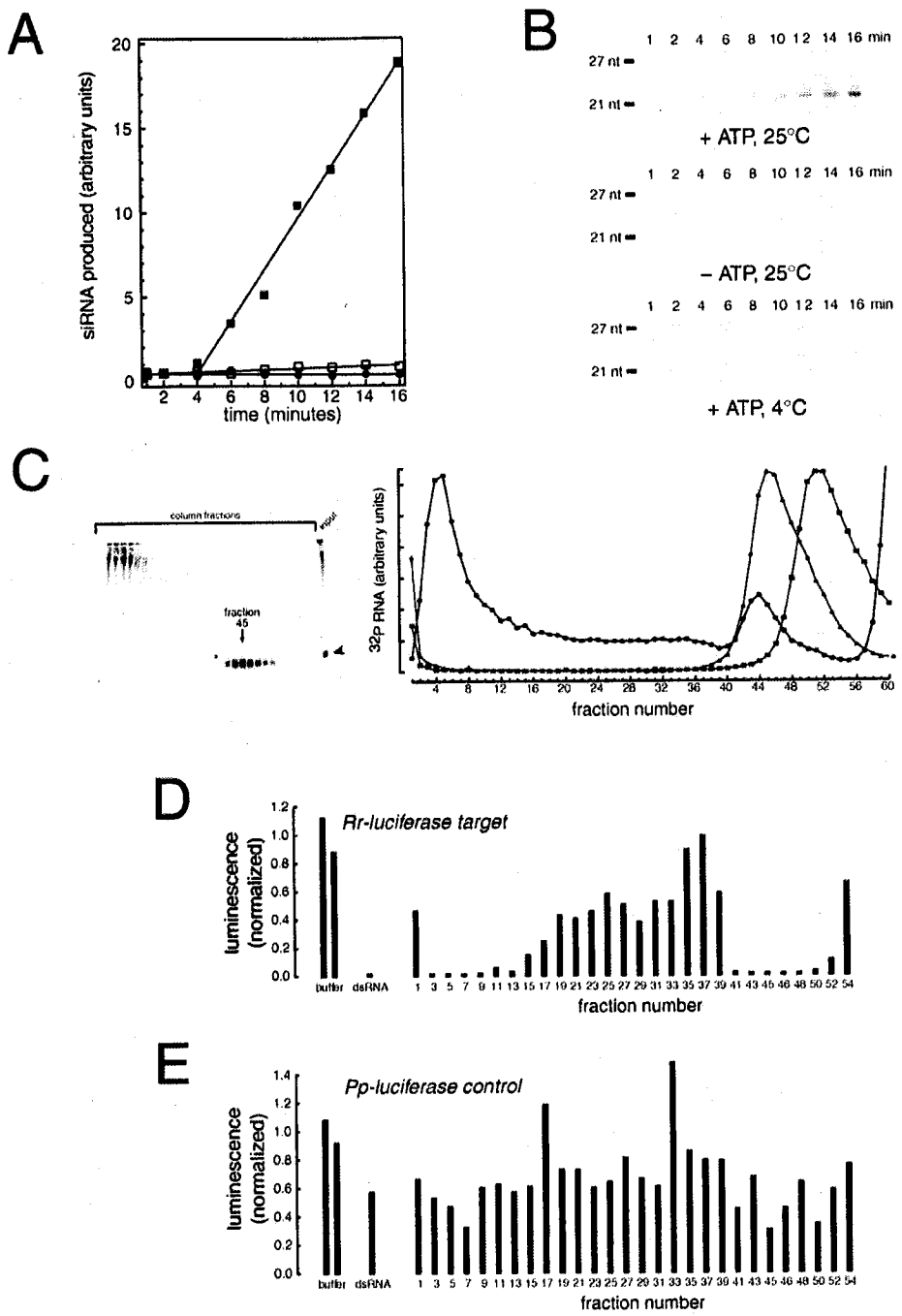

Figure 1. Production of the siRNAs that Mediate Sequence-Specific Interference Requires ATP

(A) Measurement of the initial rate of siRNA production from uniformly ^{32}P-radiolabeled 501 bp *Rr*-luc dsRNA in the presence of 1 mM ATP at 25°C (filled squares) or 4°C (filled circles), or at 25°C in the absence of ATP (open squares).

(B) The data presented graphically in (A).

(C) Isolation of native siRNAs by gel filtration. Uniformly ^{32}P-radiolabeled 501 bp *Rr*-luc dsRNA was processed in a standard RNAi reaction, deproteinized, and fractionated on a Superdex-200 gel filtration column. Fractions were analyzed by electrophoresis on a 15% acrylamide sequencing gel (left panel) and by scintillation counting (right panel, black circles). Double-stranded (red triangles) and single-stranded (blue squares) synthetic siRNAs were chromatographed as standards. The native siRNA peak and the synthetic siRNA duplex marker do not precisely comigrate, likely because the native siRNAs are a mixture of 21- and 22-nt species (Zamore et al., 2000; Elbashir et al., 2001a) and the synthetic siRNAs are 21 nt.

(D and E) Analysis of each column fraction for RNAi activity in an in vitro reaction containing both *Rr*-luc and *Pp*-luc mRNAs. Luminescence was normalized to the average of the two buffer controls.

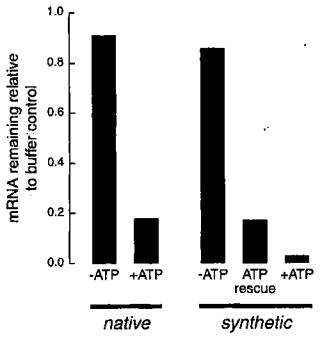

Figure 2. RNAi Mediated by siRNAs Requires ATP

Native siRNAs targeting *Rr*-luc were assayed for RNAi against an *Rr*-luc RNA target. A synthetic siRNA duplex targeting *Pp*-luc was tested for RNAi against a *Pp*-luc mRNA.

and synthetic siRNAs requires ATP, revealing one or more novel ATP-dependent step(s) distinct from the ATP-dependent cleavage of long dsRNA into siRNAs.

Target Recognition and Cleavage Are ATP-Independent

One possible source for the ATP requirement might be that target cleavage, like the cleavage of dsRNA into siRNAs by Dicer, requires ATP. To test if either target recognition or cleavage requires ATP, we incubated a 501 bp *Rr*-luc or a 505 bp *Pp*-luc dsRNA in a standard RNAi reaction to permit its processing into native siRNAs, then removed ATP from the reaction and evaluated its ability to cleave a corresponding target RNA (Figure 3). Two different strategies were employed to remove ATP from the reaction after the initial dsRNA processing step. In both strategies, the interfering RNA—dsRNA or siRNA—was preincubated with lysate in the presence of ATP, then ATP was removed from the reaction, and finally, the target RNA was added in the presence or absence of ATP. In the first strategy (Figure 3A), the ATP regenerating enzyme, creatine kinase, was inactivated with *N*-ethylmaleimide (NEM; Worthington, 1988), unreacted NEM quenched, and ATP depleted with hexokinase and glucose (Figure 3B, filled symbols). Then, a *Pp*-luc target mRNA was added to the reaction. Lysate treated with NEM, then DTT, prior to the addition of the creatine kinase supported RNAi (data not shown). In a separate series of controls, DTT was added prior to the NEM, and no hexokinase was added (open symbols). High ATP levels were maintained during the dsRNA processing portion of the experiment and throughout the experiment when DTT was added prior to NEM. However, when the reactions were sequentially treated with NEM, DTT, then hexokinase plus glucose, ATP levels were reduced ~5,000-fold to ≤100 nM. In all conditions in which the 505 bp *Pp*-luc dsRNA was included (triangles), the *Pp*-luc target mRNA was cleaved regardless of the ATP concentration at the time of target RNA addition. Under all conditions, interference remained sequence-specific: a 501 bp *Rr*-luc dsRNA did not affect the stability of the *Pp*-luc mRNA target in the presence (open circles) or absence of ATP (filled circles). Furthermore, when a synthetic siRNA duplex targeting the *Pp*-luc mRNA was first preincubated with lysate and ATP, the *Pp*-luc target mRNA was subsequently cleaved both in the presence (open squares) and absence (filled squares) of ATP. These results strongly argue that neither target recognition nor target cleavage requires ATP as a cofactor, and they suggest that ATP participates in a step prior to the encounter of the siRNA with its RNA target.

Nonetheless, the experiments shown in Figure 3B cannot exclude a requirement for some other small molecule cofactor (e.g., GTP) in target recognition and cleavage. To examine this possibility, we employed a second strategy to remove ATP and other small molecule cofactors (Figure 3C). A 501 bp *Rr*-luc dsRNA was incubated with lysate and ATP in a standard RNAi reaction, then the siRNA/protein complex was precipitated with ammonium sulfate. The resolubilized ammonium sulfate precipitate was extensively dialyzed to remove small molecule cofactors, then treated with hexokinase and glucose to further deplete ATP. The procedure reduced the initial 1 mM ATP concentration to ≤50 nM (data not shown). Furthermore, the dialysis step is expected to have significantly reduced endogenous pools of other nucleotide tri-, di-, and monophosphate cofactors. Finally, the ATP-depleted siRNA/protein complex was tested for cleavage of a 501 nt *Rr*-luc target RNA or an unrelated 441 nt control RNA in the presence or absence of ATP (Figure 3D). The *Rr*-luc dsRNA directed efficient target recognition and cleavage in the absence of exogenous ATP. In both the presence and absence of ATP, target cleavage was specific for the *Rr*-luc target mRNA; the control RNA was not cleaved. For ATP or some other small molecule cofactor to be involved in these steps in the RNAi reaction, it would have had to remain associated with the RNAi machinery through 16 hr of dialysis against multiple changes of a 5,000-fold excess of buffer. The simplest explanation is that both target recognition and target cleavage are ATP-independent steps.

The ATP-dependent step identified by the experiments in Figure 2 therefore lies downstream of dsRNA processing but upstream of target recognition. We can envision several types of ATP-dependent steps that might explain our findings. Formation of an siRNA/protein complex might require ATP. Alternatively, association of proteins with the siRNAs might be ATP-independent, but a conformational change in the siRNA itself might require ATP. For example, an ATP-dependent RNA helicase might unwind the two strands of the siRNA prior to its encounter with the target RNA. In support of this idea, proteins with the signature motifs of ATP-dependent RNA helicases have been implicated in RNAi in flies and worms (Bernstein et al., 2001; Knight and Bass, 2001), PTGS in *Chlamydomonas reinhardtii* and plants (Wu-Scharf et al., 2000; Dalmay et al., 2001), and *Stellate* silencing in flies (Aravin et al., 2001).

siRNA-Protein Complex Formation

To detect the formation of a protein complex on siRNAs, uniformly ^{32}P-radiolabeled 501 nt *Rr*-luc dsRNA was incubated in a standard RNAi reaction in the absence of target to permit its cleavage into siRNAs and to permit the resulting siRNAs to assemble into a protein/siRNA

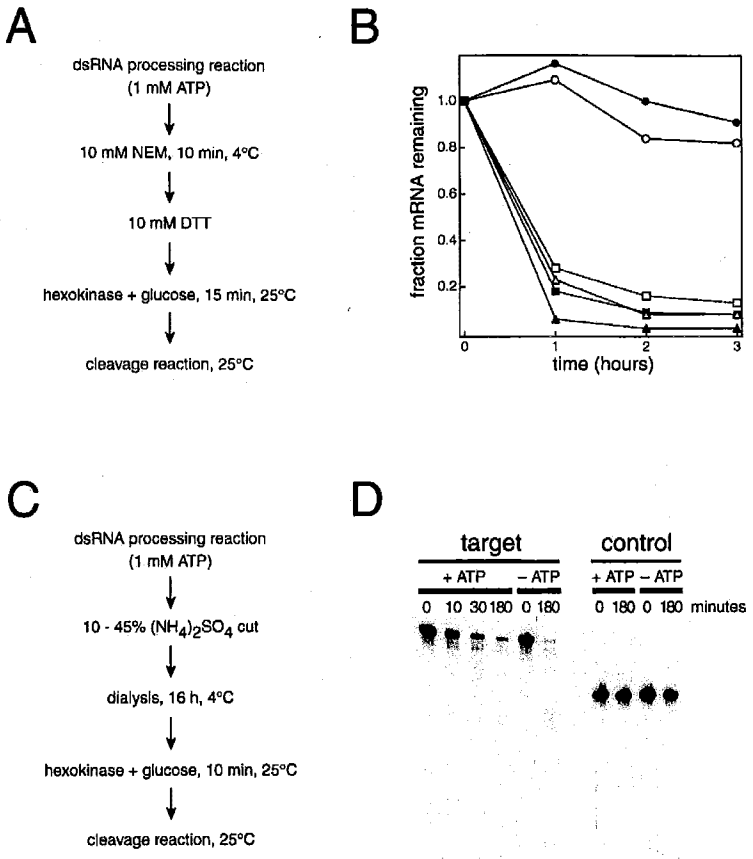

Figure 3. Target Recognition and Cleavage Is ATP-Independent

(A) Scheme for depleting ATP from the RNAi reaction after an initial preincubation in the presence of ATP.

(B) After 30 min preincubation with ATP of a 505 bp *Pp*-luc dsRNA (triangles) or a 501 bp *Rr*-luc dsRNA (circles), ATP was depleted by the sequential addition of NEM, DTT, and hexokinase plus glucose (filled symbols), then a *Pp*-luc target mRNA added. In the controls, DTT was added before NEM, and hexokinase was omitted (open symbols). A synthetic siRNA duplex targeting the *Pp*-luc mRNA was also tested (squares). In all cases, the target RNA was a *Pp*-luc mRNA.

(C) Alternative scheme for depleting ATP from the RNAi reaction.

(D) After preincubation of a *Rr*-luc dsRNA with lysate and ATP, recognition and cleavage of a *Rr*-luc target RNA or a 441 nt control RNA was measured in the presence or the absence of ATP.

complex (siRNP). After 2 hr incubation, the reaction was chromatographed on a Superdex-200 gel filtration column. siRNAs were predominantly associated with a ~360 kDa siRNP (Figure 4A). Formation of the siRNP complex required protein, since it was not observed when the complex was treated with proteinase K prior to gel filtration (Figure 1C). A second peak of ^{32}P-radiolabled siRNAs coincides with siRNAs unbound by protein (compare Figures 1C and 4A), indicating that a significant fraction of the siRNAs generated by dsRNA processing in vitro do not stably associate with protein. Next, purified, ^{32}P-native siRNAs were incubated with lysate either in the presence (Figure 4B) or the absence (Figure 4C) of ATP. The same two siRNA-containing peaks were observed: a ~360 kDa siRNP (peaking in fractions 18–20) and native siRNAs not associated with protein (peaking in fractions 42–46). Thus, assembly of the siRNP does not require ATP.

Recently, Hannon and coworkers reported isolation of an siRNA-containing, ~500 kDa complex from cultured *Drosophila* S2 cells (Hammond et al., 2001a). This ~500 kDa complex contained the target-cleaving nuclease (Hammond et al., 2001a). To assess the capacity of the ~360 kDa siRNP to direct target cleavage, we incubated a single synthetic siRNA duplex in the *Drosophila* embryo lysate in the presence of ATP, then fractionated the reaction by gel filtration on Superdex-200. The siRNA duplex was chosen because it directs cleavage of the 510 nt *Pp*-luc target RNA at a single site, 72 nt from the 5′ cap, yielding a 72 nt RNA product diagnostic of RNAi activity (Elbashir et al., 2001a). In these experiments, the synthetic siRNA duplex was 3′ radiolabeled on the sense siRNA strand. Control experiments showed that such a 3′ modified siRNA duplex does not impair the ability of the siRNA to mediate RNAi (data not shown). Thus, the 510 nt target RNA, the 72 nt RNAi cleavage product, and the siRNA itself can be detected simultaneously on a denaturing acrylamide gel. The ability of each gel filtration column fraction to support sequence-specific target cleavage was assessed (Figure 4D). A major peak of radiolabeled siRNA was detected in fractions 18–22, indicating formation of the siRNP complex. Although this siRNP complex contains virtually all of the siRNAs associated with protein, it was not competent to cleave a target RNA. Instead, two peaks of RNAi activity were observed: one in the void volume of the column (fractions 2–6), and a broad peak of RNAi activity of apparent molecular weight <232 kDa (fractions 26–40). Surprisingly, these peaks contained barely detectable levels of siRNA, but were nonetheless nearly as active as the unfractionated reaction, despite having suffered dilution from the gel filtration chromatography (Figure 4D, compare the amount of ^{32}P-siRNA in the input to the column [lane labeled "siRNA"] to that in the active column fractions). Control experiments (not shown) demonstrated that little if any degradation of siRNA duplexes occurs in the lysate, indicating that the distribution of ^{32}P-siRNAs accurately reflects the distri-

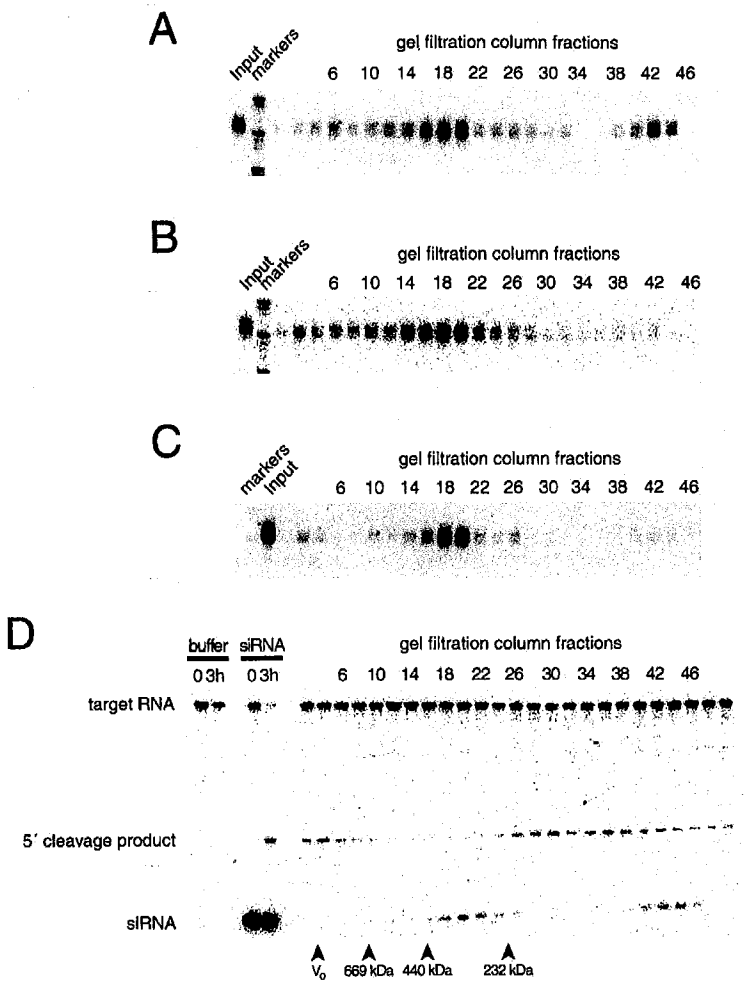

Figure 4. siRNP Complex Formation and Activity

(A) Analysis of siRNP formation during the processing of a 501 *Rr*-luc dsRNA into native siRNAs in the presence of ATP.

(B) Analysis of siRNP formation in the presence of ATP for purified, native siRNA duplexes.

(C) As in (B), except in the absence of ATP.

(D) RNAi activity of gel filtration fractions prepared as in (B), but using a synthetic siRNA duplex targeting the *Pp*-luc mRNA. The siRNA was incubated in an RNAi reaction for 1 hr, then fractionated by gel filtration. A sample of the input to the column was used in a control reaction (siRNA); every other column fraction was analyzed for RNAi activity. The elution position of molecular weight markers for all four panels is shown in (D). V_o, void volume; 669 kDa, Thyroglobulin; 440 kDa, Ferritin; 232 kDa, Catalase.

bution of siRNA in the column fractions. Thus, the majority of siRNAs associated with protein are present in a ~360 kDa siRNP complex that is not competent to cleave a target RNA, whereas a minority of the siRNAs are in a smaller, highly active complex. Mixing experiments (not shown) demonstrated that the fraction containing the ~360 kDa siRNP does not contain an inhibitor of RNAi. We defer to below the question of whether the ~360 kDa complex is a productive intermediate in the RNAi pathway or a nonproductive, off-pathway intermediate.

siRNA Unwinding during the RNAi Reaction

To test if ATP is used during the RNAi reaction to separate the two strands of the siRNA duplex, we developed a method to differentiate siRNA duplexes from single-stranded siRNAs (Figure 5A). In this assay, RNAi was initiated in vitro with a synthetic siRNA duplex in which the sense strand was 3′ radiolabeled. The RNAi reaction was quenched by the simultaneous addition of an SDS-containing stop buffer, proteinase K, and a 25-fold molar excess of an unlabeled competitor RNA containing the sequence of the 19 paired nucleotides from the sense strand of the siRNA duplex. The samples were analyzed by nondenaturing acrylamide gel electrophoresis.

We used the assay to assess if the siRNA duplex is a substrate for ATP-dependent helicase proteins in the *Drosophila* embryo lysate. Unwinding of the siRNA duplex was monitored in an RNAi reaction in the presence and absence of ATP. No siRNA unwinding was detected in the absence of ATP, whereas a small percent (≤5%) of unwound siRNA was detected with ATP (Figure 5B). Furthermore, the siRNA was almost entirely double-stranded in the inactive ~360 kDa siRNP complex (Figure 5C). In contrast, single-stranded siRNA resided in the same two peaks that showed RNAi activity in the target cleavage assay: the void volume of the column and a peak of apparent molecular weight <232 kDa. These data suggest (1) that RNAi activity is associated with a population of siRNAs that are unwound and (2) that a protein-siRNA complex of <232 kDa contains all of the factors required for efficient, sequence-specific target cleavage. We propose that this complex represents the minimal, active RNA-induced silencing complex (RISC; Hammond et al., 2000). We term this complex the RISC*. These results are at odds with previous findings that the active RISC is a ~500 kDa complex (Hammond et al., 2001a). A possible explanation is that our chromatographic procedure resolved the smaller active complex from a larger precursor complex, but that these

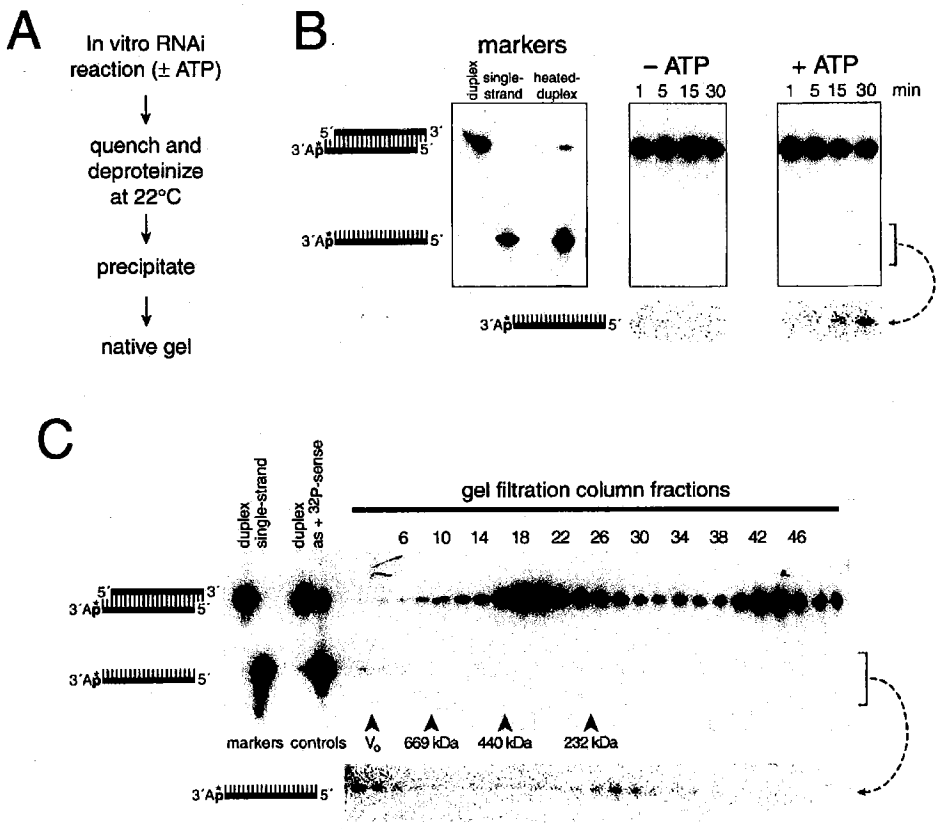

Figure 5. ATP-Dependent siRNA Unwinding Correlates with RNAi Activity

(A) Outline of the assay used in (B) and (C).

(B) Native acrylamide gel analysis of siRNA unwinding in the absence and presence of ATP. An overexposure of the region of the gel corresponding to single-stranded siRNA is shown in the lower panel.

(C) Analysis of siRNA unwinding for the gel filtration fractions from Figure 4D. An overexposure of the region of the gel corresponding to single-stranded siRNA is shown in the lower panel. Molecular weight standards are as in Figure 4D.

two species remain associated in a single, ~500 kDa complex under other conditions. Alternatively, a dissociable cofactor, such as an ATP-dependent RNA helicase, might be present in fractions 26–40. This factor might support RNAi by acting on a small amount of the inactive ~360 kDa complex present in these fractions, converting it to the RISC* by unwinding the siRNA duplex.

5′ Phosphorylation Status and siRNA Activity

Synthetic siRNAs bearing 5′ hydroxyl termini have been used successfully to initiate interference in *Drosophila* embryo lysates (Elbashir et al., 2001a) and in cultured mammalian cells (Elbashir et al., 2001b). Nonetheless, native siRNAs, generated by cleavage of dsRNA, contain 5′ phosphate ends (Elbashir et al., 2001a). Therefore, we asked if a 5′ phosphate is merely a consequence of the enzymatic mechanism of dsRNA cleavage by the RNase III enzyme Dicer, or if it is an essential feature of an active siRNA. We first examined the 5′ phosphorylation status of the anti-sense strand of a synthetic siRNA duplex that contained 5′ hydroxyl groups on both strands. Figure 6A shows that upon incubation in the lysate with ATP, the siRNA was rapidly phosphorylated, so that after 15 min nearly all of the synthetic siRNA had a 5′ phosphate group (lysate, HO-rU). This finding was surprising, because *Drosophila* embryo lysates contain a potent phosphatase activity that rapidly dephosphorylated exogenous 5′ ^{32}P-radiolabeled siRNA duplexes (data not shown). The 5′ phosphate of the siRNA must be in rapid exchange, but the sum of the rates of phosphatase and kinase activities produces an siRNA bearing a 5′ phosphate at steady-state. Therefore, both synthetic (5′ hydroxyl) and native (5′ phosphate) siRNAs are expected to exist predominantly as 5′ phosphorylated species in the in vitro RNAi reaction, and perhaps in vivo as well.

To assess if a 5′ phosphate is required for RNAi, we designed an siRNA duplex in which the 5′ end of the anti-sense strand was blocked by replacing the 5′ hydroxyl with a 5′ methoxy group (CH_3O). In order to facilitate chemical synthesis of the 5′ block, the first nucleotide of the anti-sense siRNA strand, uracil, was replaced with 2′ deoxythymidine (dT). An siRNA duplex in which the 5′ terminus was a hydroxyl group, but the first nucleotide was dT, was prepared in parallel. The 5′ blocked (CH_3O-dT) and 5′ dT (HO-dT) anti-sense siRNA strands were each annealed to a standard, 5′ hydroxyl sense

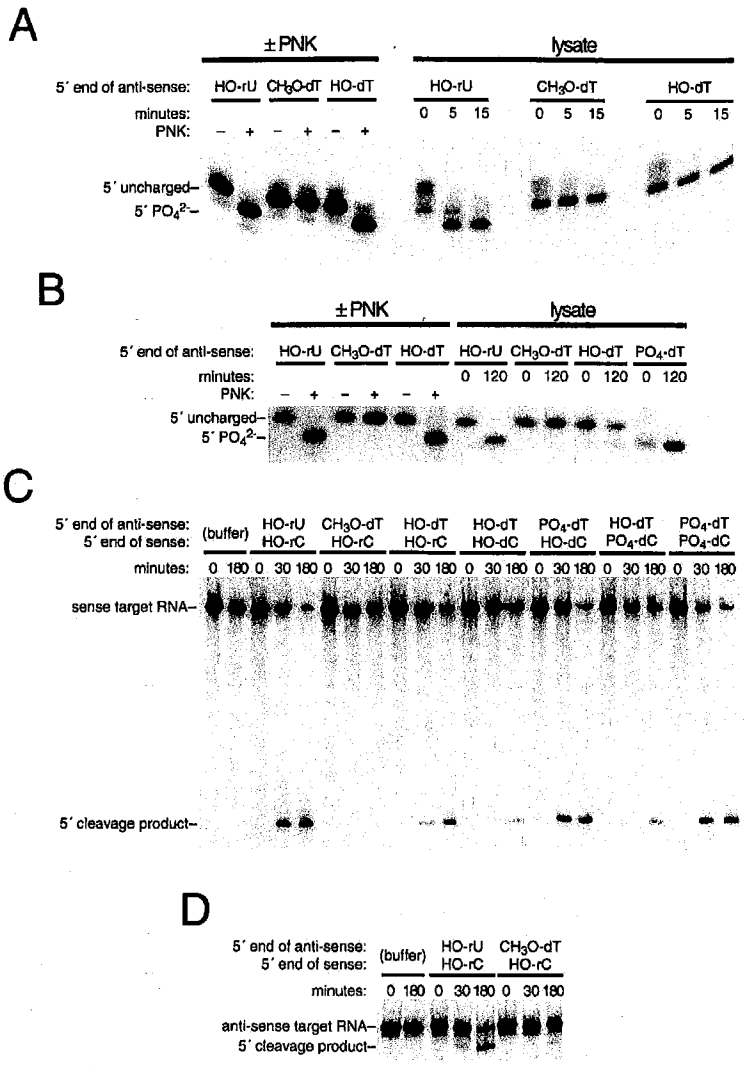

Figure 6. 5′ Phosphates Are Critical Determinants of siRNA Activity

(A and B) Phosphorylation status of the anti-sense strand of synthetic siRNA duplexes upon incubation with polynucleotide kinase (PNK) or *Drosophila* embryo lysate.

(C) RNAi activity of synthetic siRNA duplexes measured for a sense *Pp*-luc RNA target.

(D) RNAi activity of synthetic siRNA duplexes measured for an anti-sense *Pp*-luc RNA target.

strand (HO-rC). The 5′ blocked siRNA was not phosphorylated after incubation with either polynucleotide kinase (PNK) or lysate (CH_3O-dT; Figures 6A and 6B). Surprisingly, the siRNA bearing a 5′ dT on the anti-sense strand (HO-dT) was a poor substrate for phosphorylation in the lysate, despite being a good substrate for PNK (Figure 6A): it was not detectably phosphorylated after 15 min in the lysate, although a small fraction was phosphorylated after 2 hr (HO-dT; Figures 6A and 6B). These data show that *Drosophila* embryos contain a nucleic acid kinase that discriminates against 5′ deoxy siRNAs.

Next, we examined the capacity of these siRNA duplexes to trigger RNAi. This siRNA sequence directs cleavage of the 510 nt sense *Pp*-luc target RNA to yield a diagnostic 72-nt 5′ product (Elbashir et al., 2001a and Figure 5D). As expected, the standard siRNA (anti-sense, HO-rU; sense, HO-rC) directed efficient cleavage of the target RNA (Figure 6C), as evidenced by the disappearance of the 510 nt RNA and the appearance of the 72 nt RNA. In contrast, no target cleavage was detected for the 5′ blocked anti-sense siRNA (CH_3O-dT) paired with a standard sense siRNA strand (HO-rC). These data suggest that a 5′ phosphate is required on the siRNA strand that guides target cleavage. This hypothesis predicts that anti-sense siRNAs that are poorly phosphorylated in the lysate will be poor effectors of sense target cleavage. Consistent with the prediction, an siRNA in which the anti-sense strand is 5′ hydroxyl, 5′ dT (HO-dT), which is inefficiently phosphorylated in the lysate (Figures 6A and 6B), is less efficient in directing sense target cleavage than a standard siRNA (Figure 6C). To test if the defect was a direct consequence of the inefficiency with which the 5′ dT anti-sense RNA was phosphorylated, a 5′ dT anti-sense RNA bearing a 5′ phosphate was annealed to a 5′ hydroxyl, 5′ dC sense siRNA. Like the 5′ dT modification on the anti-sense strand, 5′ dC on the sense strand inhibits phosphorylation by the kinase in the lysate (data not shown). Use of a 5′ dC sense strand, therefore, allowed us to examine the effect of a 5′ phosphate on the 5′ dT, anti-sense strand in an siRNA duplex in which the sense strand was predominantly 5′ hydroxyl. This siRNA duplex (anti-sense, PO_4-dT; sense, HO-dC) was as efficient in cleaving the sense target RNA as a standard, siRNA duplex (anti-sense,

HO-rU; sense, HO-rC; Figure 6C). Thus, the sole defect caused by a 5′ dT anti-sense strand is that it is a poor kinase substrate in the lysate. An siRNA in which both strands were 5′ phosphorylated and 5′ deoxy (anti-sense, PO_4-dT; sense, PO_4-dC) was no more efficient than the siRNA comprising a 5′ phosphate, 5′ dT anti-sense strand and a 5′ hydroxyl, 5′ dC sense strand (anti-sense, PO_4-dT; sense, HO-dC; Figure 6C). As expected, an siRNA in which both strands were 5′ deoxy and 5′ hydroxyl (anti-sense, HO-dT; sense, HO-dC) was defective in sense target cleavage. This defect was not remedied by adding a phosphate to the sense strand (anti-sense, HO-dT; sense, PO_4-dC), lending further support to the idea that a 5′ phosphate on the anti-sense strand is required to guide sense target cleavage (Figure 6C). We conclude that a 5′ phosphate on the guide strand of an siRNA is required for RNAi. We note that RNAi directed by an siRNA in which both strands are 5′ phosphate but also 5′ deoxy), nonetheless required ATP (data not shown). This ATP-requirement likely reflects the role of ATP in siRNA unwinding (see above) rather than in 5′ phosphorylation.

In the course of these experiments, we observed that an siRNA in which both strands were 5′ hydroxyl and 5′ deoxy was slightly worse at guiding sense target cleavage than the 5′ hydroxyl siRNA in which only the anti-sense strand was 5′ deoxy. Therefore, we asked directly if the 5′ phosphate of the nonguiding strand is also important for siRNA function. We examined cleavage of an anti-sense target RNA for the siRNA with a 5′ methoxy anti-sense strand and a standard sense strand (anti-sense, CH_3O-dT; sense, HO-rC). With respect to an anti-sense target RNA, this siRNA duplex is blocked for 5′ phosphorylation only on the nonguiding strand. As expected, a standard siRNA (anti-sense, HO-rU; sense, HO-rC) cleaved a 510 nt, anti-sense *Pp*-luc target RNA to yield a diagnostic 436 nt cleavage product (Figure 6D). Significantly less target cleavage was observed for the siRNA containing a 5′ blocked anti-sense strand (anti-sense CH_3O-dT; sense, HO-rC). Since it is the sense strand that guides anti-sense target cleavage, these data imply that recognition of the 5′ phosphates of both siRNA strands occurs during the RNAi pathway. In support of this idea, an siRNA in which the anti-sense strand is 5′ dT was also less efficient in anti-sense target cleavage than a siRNA duplex with a rU at this position (data not shown). For the siRNA sequence examined here, the 5′ phosphate of the nonguiding strand contributes to cleavage efficiency, whereas the 5′ phosphate of the target-complementary, guide strand is required for cleavage. The difference in effect of a 5′ phosphate on the guide versus the nonguiding strand suggests that two distinct 5′ phosphate-recognition steps occur in the RNAi reaction.

To test the idea that one of these 5′ phosphate recognition steps precedes assembly of a protein complex on the siRNA duplex, we repeated the experiments in Figure 4 using synthetic siRNA duplexes containing either 5′ hydroxyl or 5′ phosphate groups. siRNAs, radiolabeled on the 3′ end of the anti-sense strand, were incubated in a standard in vitro RNAi reaction in the presence or absence of ATP, then fractionated by gel filtration. siRNAs were detected by scintillation counting of the

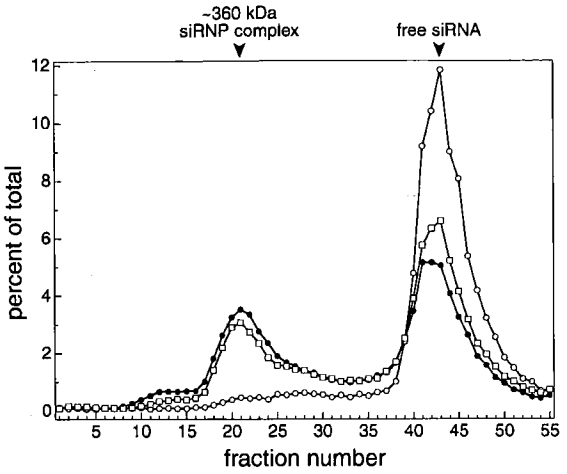

Figure 7. 5′ Phosphates Are Required for siRNP Formation

Complex formation was monitored by gel filtration on Superdex-200. Filled circles, siRNA duplex bearing 5′ hydroxyl groups incubated with *Drosophila* embryo lysate and ATP. Open circles, siRNA duplex bearing 5′ hydroxyl groups incubated in the absence of ATP. Open squares, siRNA duplex bearing 5′ phosphate groups incubated in the absence of ATP.

gel filtration fractions (Figure 7). As shown previously (Figure 4D), synthetic siRNA bearing 5′ hydroxyl groups are incorporated into a ~360 kDa complex upon incubation with *Drosophila* embryo lysate in the presence of ATP (Figure 7, filled circles). However, in the absence of ATP, no such complex is observed, and virtually all the siRNA remains unbound by protein (Figure 7, open circles). These results contrast with those of Figure 4C, in which purified native siRNAs, generated by cleavage of long dsRNA, readily assembled with proteins in the absence of ATP to yield a ~360 kDa complex. Unlike the synthetic siRNA duplexes used in Figure 7, native siRNAs contain 5′ phosphate groups. Thus, one explanation for our results is that 5′ phosphates are required for incorporation of siRNA duplexes into the ~360 kDa complex. In support of this idea, 5′-phosphorylated, synthetic siRNA duplexes form the ~360 kDa complex upon incubation in lysate in the absence of ATP (Figure 7, open squares). These results suggest that the ~360 kDa siRNA-protein complex, although inactive for target cleavage, is a bona fide intermediate in the assembly of the RISC*, the active siRNA complex. Furthermore, they argue that 5′ phosphate recognition occurs early in the RNAi pathway, since we detected no stable siRNA-protein complexes for siRNAs lacking a 5′ phosphate. Interestingly, normal levels of ~360 kDa complex were formed with an siRNA containing a 5′ blocked (CH_3O, dT) anti-sense strand paired with a 5′ hydroxyl sense strand (HO, rC), suggesting that a 5′ phosphate on one of the two siRNA strands is sufficient for siRNP formation (data not shown) and consistent with our finding that a 5′ PO_4, dT anti-sense siRNA strand paired with a 5′ HO, dC sense strand mediates efficient sense target cleavage (see above).

A Model for the RNAi Pathway

Our data suggest that ATP plays at least three distinct roles in the RNAi pathway. In Figure 8, we propose a

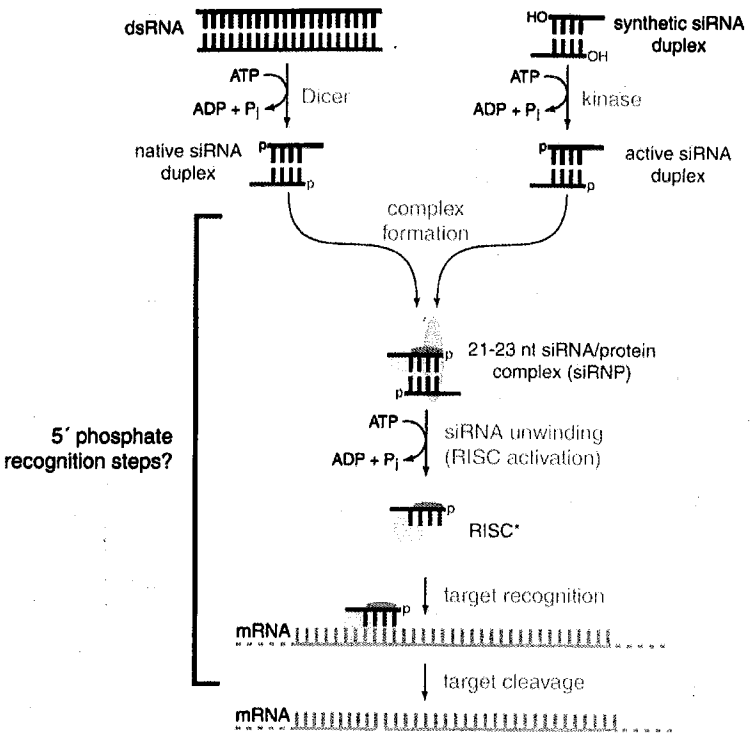

Figure 8. A Model for the RNAi Pathway

We do not yet know if only one or both siRNA strands are present in the same RISC* complex.

model for RNAi that incorporates these three ATP-dependent steps. First, as previously reported, ATP is essential for the cleavage of long dsRNA into native siRNAs. These siRNAs are fully competent to direct RNAi, since when purified, they reenter the RNAi pathway so long as their double-stranded character is maintained. siRNAs are then proposed to bind specific proteins that commit them to the RNAi pathway. In *Drosophila* embryo lysate, the majority of siRNAs are incorporated into a ~360 kDa complex. Although this complex is not competent to direct target cleavage, it seems likely that it is an intermediate in the RNAi pathway, since it is not formed with siRNAs that do not mediate RNAi because they lack 5′ phosphates. Conversion of the inactive ~360 kDa complex into an active complex, RISC*, is proposed to occur in a second ATP-dependent step: the unwinding of the siRNA duplex by an RNA helicase. We do not yet know if the two unwound, single strands are retained in the same complex, or if a single RISC* contains only one of the two strands of the original siRNA duplex. siRNA unwinding is likely to be a stable rather than a transient change in siRNA conformation, because siRNA duplexes preincubated with lysate and ATP are competent to recognize and cleave a corresponding target RNA after extensive dialysis to remove ATP and other cofactors.

5′ phosphorylation of siRNAs corresponds to a third ATP-dependent step in the pathway. Our experiments with synthetic siRNAs reveal the requirement for a 5′ phosphate on the siRNA strand complementary to the target RNA, and a partial requirement for 5′ phosphorylation of the siRNA strand sharing sequence with the target RNA. Tuschl and coworkers have proposed that the site of cleavage of the target RNA is measured from the 5′ end of the complementary siRNA strand. They find that additional nucleotides at the 3′ end of the siRNA do not alter the site of cleavage of the target RNA, but additional nucleotides at the 5′ end move the target cleavage site correspondingly (Elbashir et al., 2001c). The 5′ phosphate of the siRNA may therefore serve as a molecular reference point from which the cleavage site is measured. 5′ phosphorylation of synthetic siRNA duplexes in the *Drosophila* embryo lysate is catalyzed by a kinase that can discriminate between 5′ ribo and 5′ deoxy siRNAs. Might the kinase that phosphorylates synthetic 5′ hydroxyl-containing siRNAs also act on the native siRNAs generated by processing of long dsRNA? While we have not yet devised methods to follow a single phosphate from long dsRNA into an individual siRNA sequence, we note that in the lysate, the half-life of a 5′ ^{32}P on a synthetic siRNA is short, yet virtually all of these siRNAs are 5′ phosphorylated throughout the reaction. The 5′ phosphate of siRNAs generated by the cleavage of long dsRNA may also be exchanging rapidly, with an siRNA-specific kinase serving to regenerate functional siRNA duplexes. We propose that this kinase acts in vivo to maintain the 5′ phosphates of siRNAs, thereby allowing them to participate in multiple rounds of target cleavage.

Why should the RNAi machinery examine the phosphorylation status of an siRNA? Three features—a 21–23 nt length, a double-stranded structure with 2 nt 3′ overhangs, and 5′ phosphates—distinguish siRNAs in flies from other small RNAs, and therefore allow the cell to discriminate between authentic siRNAs and imposters. In this view, the 5′ phosphate is one feature that licenses an siRNA for RNAi. An siRNA-specific kinase would maintain 5′ phosphates on bona fide siRNAs that have

entered the RNAi pathway but have subsequently lost their 5′ phosphate, but would not add 5′ phosphates to other small RNAs, ensuring that only authentic siRNAs target mRNAs for cleavage.

Experimental Procedures

General Methods

Drosophila embryo lysate preparation, in vitro RNAi reactions, dsRNA processing reactions, 501 bp *Rr*-luc and 505 bp *Pp*-luc dsRNAs, full-length *Rr*-luc and *Pp*-luc target mRNAs, and cap-radiolabeling of target RNAs with guanylyl transferase were as described (Tuschl et al., 1999; Zamore et al., 2000). In the experiment shown in Figure 4D, the control RNA was a 441 nt fragment of the *Drosophila pumilio* cDNA transcribed with T7 RNA polymerase from a PCR template prepared with the following primers: 5′ primer, GCG TAA TAC GAC TCA CTA TAG GCG CCC ACA ATT GCC ATA TC; 3′ primer, AAG GTT GAG CCT ACG GCT C. The 510 bp *Rr*-luc target RNA was transcribed with T7 RNA polymerase from a PCR template prepared with the following primers: 5′ primer, GCG TAA TAC GAC TCA CTA TAG GAA AAA CAT GCA GAA AAT GC; 3′ primer, GAA GAA TGG TTC AAG ATA TGC TG. The 510 bp *Pp*-luc sense target RNA was transcribed from a PCR template prepared with the following primers: 5′ primers, GCG TAA TAC GAC TCA CTA TAG GAG ATA CGC CCT GGT TCC TG; 3′ primer, GAA GAG AGG AGT TCA TGA TCA GTG. For transcription templates for the 510 nt *Pp*-luc anti-sense target RNA, the PCR primers were GCG TAA TAC GAC TCA CTA TAG GAG AGG AGT TCA TGA TCA GTG (5′ primer) and GAA GAG ATA CGC CCT GGT TCC TG (3′ primer). Gels were dried and exposed to image plates (Fuji or Kodak), which were scanned using a Bio-Rad Personal FX imager and analyzed with QuantityOne 4.0 (Bio-Rad). Images for figures were prepared with QuantityOne 4.0 and PhotoShop 5.5 (Adobe). Graphs were prepared and rates determined using Microsoft Excel and IgorPro 3.1 (Wavemetrics).

Synthetic siRNAs

The siRNA duplexes in Figures 4B, 5D, 6, and 7 were prepared from synthetic 21 nt RNAs (Dharmacon Research). Sense siRNA sequences were 5′-HO-CGU ACG CGG AAU ACU UCG AUU-3′ (HO-rC) and 5′-HO-dCGU ACG CGG AAU ACU UCG AUU-3′ (HO-dC). Anti-sense siRNAs used were 5′-HO-UCG AAG UAU UCC GCG UAC GUG-3′ (HO-rU); 5′-CH_3O-dTCG AAG UAU UCC GCG UAC GUG-3′ (5′ blocked; CH_3O-dT); and 5′-HO-dTCG AAG UAU UCC GCG UAC GUG-3′ (HO-dT). siRNAs were deprotected according to the manufacturer's instructions, dried in vacuo, resuspended in 400 μl water, dried in vacuo again, resuspended in water, and annealed to form duplex siRNAs as described (Elbashir et al., 2001a). siRNA duplexes were used at 50 nM final concentration. siRNA strands were phosphorylated with PNK (New England Biolabs) and 1 mM ATP according to the manufacturer's directions. siRNAs were 3′ end-labeled with α-^{32}P-cordycepin 5′ triphosphate (5000 Ci/mmol; New England Nuclear) and Poly(A) polymerase (Life Technologies) according to the manufacturer's instructions. Radiolabeled siRNA strands were purified from 15% denaturing acrylamide gels. 5′ phosphorylation status was monitored by electrophoresis of siRNAs on a 15% sequencing gel.

Gel Filtration of Native siRNAs and siRNP Complexes

Preparative scale dsRNA processing reactions (1 ml) were deproteinized at room temperature by the addition of 1 ml 2× PK buffer (200 mM Tris-HCl [pH 7.4], 25 mM EDTA, 300 mM NaCl, 2% w/v sodium dodecyl sulfate) and Proteinase K (E.M. Merck; 20 μg/μl dissolved in water) to a final concentration of 1 μg/μl. After incubation at room temperature for 1 hr, the reaction was extracted with an equal volume of phenol/chloroform/isoamyl alcohol (25:24:1) and the RNA recovered by precipitation with 3 volumes absolute ethanol. The precipitate was redissolved in 250 μl lysis buffer (30 mM HEPES-KOH [pH 7.5], 100 mM potassium acetate, 2 mM magnesium acetate) and chromatographed at room temperature on a Superdex-200 HR 10/30 column (Pharmacia) at 0.75 ml/min in lysis buffer using a BioCad Sprint (PerSeptive Biosystems). After 7.5 ml had passed through the column, sixty 200 μl fractions were collected using a cooled stage to maintain the fractions at 4°C. To compensate for dilution of the original reaction on the gel filtration column, each fraction was concentrated by precipitation with ethanol and redissolved in 30 μl lysis buffer.

For siRNP analysis, a 200 μl RNAi reaction was assembled using the purified native siRNAs (fractions 44 and 45) or synthetic siRNA duplexes, incubated for 1 hr at 25°C, and fractionated on Superdex-200 HR 10/30 at 0.75 ml/min in lysis buffer containing 1 mM DTT, 0.1 mM EDTA, and 10% (v/v) glycerol. Fractions were collected as described above. To analyze RNAi activity, 6 μl of each fraction was analyzed in a 10 μl standard RNAi reaction.

ATP Depletion

ATP depletion by hexokinase treatment was as described (Zamore et al., 2000), except that 20 mM glucose was used. In Figure 4B, NEM was freshly prepared from powder as a 1 M stock in absolute ethanol, added to an RNAi reaction at 4°C to a final concentration of 10 mM, incubated 10 min, and quenched with 10 mM DTT added from a 1 M stock dissolved in water. In Figure 4D, an RNAi reaction was adjusted to 10% saturation by addition of a 100% saturated solution of ammonium sulfate dissolved in lysis buffer containing 0.1 mM EDTA. After 30 min at 4°C, the reaction was centrifuged at 16,060× g for 20 min at 4°C, and the supernatant adjusted to 45% saturation. After an additional 30 min at 4°C, the 10%–45% ammonium sulfate precipitate was collected by centrifugation. The precipitate was redissolved in lysis buffer containing 2 mM DTT and dialyzed in a microdialysis chamber (Pierce; 10,000 MW cutoff) for 16 hr against two changes of a >5,000-fold excess of lysis buffer containing 2 mM DTT and 20% w/v glycerol. ATP concentration was measured with a Bioluminescent ATP Assay Kit (Sigma) according to the manufacturer's directions. Luminescence was measured in a Mediators PhL luminometer.

siRNA Unwinding Assay

RNAi reactions (10 μl) were quenched with 90 μl of stop mix containing 1.11× PK buffer, 1.11 ug/ul Proteinase K, 20 μg glycogen (Roche), and a 25-fold molar excess (12.5 pmol) of either unlabeled 21 nt RNA identical to the radiolabeled siRNA strand or a 510 nt *Pp*-luc RNA which contains the sequence of the first 19 nt of the radiolabeled siRNA strand, incubated at 25°C for 15 min, and immediately precipitated with 3 volumes absolute ethanol, chilled for at least 1 hr at −20°C, collected by centrifugation, redissolved in 10 μl 3% w/v Ficoll-400, 0.04% w/v Bromophenol Blue, and 2 mM Tris-HCl (pH 7.4), and immediately analyzed by electrophoresis at 10 W at 4°C through a 15% native polyacrylamide gel (19:1, acrylamide:bis-acrylamide) cast in 1× and run in 0.5× Tris-Borate-EDTA buffer.

Acknowledgments

The authors acknowledge Craig Mello and Tom Tuschl for sharing data prior to publication and for numerous helpful conversations, Dave Bartel, Phil Sharp, Reid Gilmore, and Kendall Knight for continuing advice and encouragement, Stephen Scaringe for advice on siRNA design and synthesis, and members of the Zamore laboratory for comments on the manuscript and many helpful discussions. Guanylyl transferase was the kind gift of Jeff Wilusz. P.D.Z. is a Pew Scholar in the Biomedical Sciences. This work was supported by a Cutler Award from the Worcester Foundation for Biomedical Research and by a grant from the National Institutes of Health (GM62862-01) to P.D.Z.

Received August 21, 2001; revised October 3, 2001.

References

Aravin, A.A., Naumova, N.M., Tulin, A.V., Vagin, V.V., Rozovsky, Y.M., and Gvozdev, V.A. (2001). Double-stranded RNA-mediated silencing of genomic tandem repeats and transposable elements in the *D. melanogaster* germline. Curr. Biol. *11*, 1017–1027.

Baulcombe, D.C. (1999). RNA makes RNA makes no protein. Curr. Biol. *9*, R599–R601.

Bernstein, E., Caudy, A.A., Hammond, S.M., and Hannon, G.J. (2001). Role for a bidentate ribonuclease in the initiation step of RNA interference. Nature *409*, 363–366.

Caplen, N.J., Parrish, S., Imani, F., Fire, A., and Morgan, R.A. (2001). Specific inhibition of gene expression by small double-stranded RNAs in invertebrate and vertebrate systems. Proc. Natl. Acad. Sci. USA *98*, 9742–9747.

Catalanotto, C., Azzalin, G., Macino, G., and Cogoni, C. (2000). Transcription: Gene silencing in worms and fungi. Nature *404*, 245.

Cerutti, L., Mian, N., and Bateman, A. (2000). Domains in gene silencing and cell differentiation proteins: the novel PAZ domain and redefinition of the Piwi domain. Trends Biochem. Sci. *10*, 481–482.

Cogoni, C., Romano, N., and Macino, G. (1994). Suppression of gene expression by homologous transgenes. Antonie Van Leeuwenhoek *65*, 205–209.

Cogoni, C., Irelan, J.T., Schumacher, M., Schmidhauser, T.J., Selker, E.U., and Macino, G. (1996). Transgene silencing of the al-1 gene in vegetative cells of Neurospora is mediated by a cytoplasmic effector and does not depend on DNA-DNA interactions or DNA methylation. EMBO J. *15*, 3153–3163.

Cogoni, C., and Macino, G. (1997). Isolation of quelling-defective (qde) mutants impaired in posttranscriptional transgene-induced gene silencing in Neurospora crassa. Proc. Natl. Acad. Sci. USA *94*, 10233–10238.

Cogoni, C., and Macino, G. (1999). Posttranscriptional gene silencing in Neurospora by a RecQ DNA helicase. Science *286*, 2342–2344.

Dalmay, T., Hamilton, A., Rudd, S., Angell, S., and Baulcombe, D.C. (2000). An RNA-dependent RNA polymerase gene in Arabidopsis is required for posttranscriptional gene silencing mediated by a transgene but not by a virus. Cell *101*, 543–553.

Dalmay, T., Horsefield, R., Braunstein, T.H., and Baulcombe, D.C. (2001). SDE3 encodes an RNA helicase required for post-transcriptional gene silencing in Arabidopsis. EMBO J. *20*, 2069–2078.

Dernburg, A.F., Zalevsky, J., Colaiácovo, M.P., and Villeneuve, A.M. (2000). Transgene-mediated cosuppression in the C. elegans germ line. Genes Dev. *14*, 1578–1583.

Djikeng, A., Shi, H., Tschudi, C., and Ullu, E. (2001). RNA interference in *Trypanosoma brucei*: cloning of small interfering RNAs provides evidence for retroposon-derived 24–26 nt RNAs. RNA *7*, 1–9.

Elbashir, S.M., Lendeckel, W., and Tuschl, T. (2001a). RNA interference is mediated by 21- and 22-nucleotide RNAs. Genes Dev. *15*, 188–200.

Elbashir, S.M., Harborth, J., Lendeckel, W., Yalcin, A., Weber, K., and Tuschl, T. (2001b). Duplexes of 21-nucleotide RNAs mediate RNA interference in mammalian cell culture. Nature *411*, 494–498.

Elbashir, S.M., Martinez, J., Patkaniowska, A., Lendeckel, W., and Tuschl, T. (2001c). Functional anatomy of siRNAs for mediating efficient RNAi in *Drosophila melanogaster* embryo lysate. EMBO J., in press.

Elmayan, T., Balzergue, S., Beon, F., Bourdon, V., Daubremet, J., Guenet, Y., Mourrain, P., Palauqui, J.C., Vernhettes, S., Vialle, T., et al. (1998). Arabidopsis mutants impaired in cosuppression. Plant Cell *10*, 1747–1758.

Fagard, M., Boutet, S., Morel, J.-B., Bellini, C., and Vaucheret, H. (2000). AGO1, QDE-2, and RDE-1 are related proteins required for post-transcriptional gene silencing in plants, quelling in fungi, and RNA interference in animals. Proc. Natl. Acad. Sci. USA. *97*, 11650–11654.

Fire, A. (1999). RNA-triggered gene silencing. Trends Genet. *15*, 358–363.

Fire, A., Xu, S., Montgomery, M.K., Kostas, S.A., Driver, S.E., and Mello, C.C. (1998). Potent and specific genetic interference by double-stranded RNA in *Caenorhabditis elegans*. Nature *391*, 806–811.

Grant, S.R. (1999). Dissecting the mechanisms of posttranscriptional gene silencing: divide and conquer. Cell *96*, 303–306.

Grishok, A., Tabara, H., and Mello, C. (2000). Genetic requirements for inheritance of RNAi in *C. elegans*. Science *287*, 2494–2497.

Grishok, A., Pasquinelli, A.E., Conte, D., Li, N., Parrish, S., Ha, I., Baillie, D.L., Fire, A., Ruvkun, G., and Mello, C.C. (2001). Genes and mechanisms related to RNA interference regulate expression of the small temporal RNAs that control C. elegans developmental timing. Cell *106*, 23–34.

Hamilton, A.J., and Baulcombe, D.C. (1999). A species of small antisense RNA in posttranscriptional gene silencing in plants. Science *286*, 950–952.

Hammond, S.M., Bernstein, E., Beach, D., and Hannon, G.J. (2000). An RNA-directed nuclease mediates post-transcriptional gene silencing in Drosophila cells. Nature *404*, 293–296.

Hammond, S., Boettcher, S., Caudy, A., Kobayashi, R., and Hannon, G.J. (2001a). Argonaute2, a link between genetic and biochemical analyses of RNAi. Science *293*, 1146–1150.

Hammond, S.M., Caudy, A.A., and Hannon, G.J. (2001b). Post-transcriptional gene silencing by double-stranded RNA. Nat. Rev. Genet. *2*, 110–119.

Hunter, C.P. (1999). A touch of elegance with RNAi. Curr. Biol. *9*, R440–442.

Hutvágner, G., Mlynarova, L., and Nap, J.P. (2000). Detailed characterization of the posttranscriptional gene-silencing-related small RNA in a GUS gene-silenced tobacco. RNA *6*, 1445–1454.

Hutvágner, G., McLachlan, J., Pasquinelli, A.E., Bálint, É., Tuschl, T., and Zamore, P.D. (2001). A cellular function for the RNA-interference enzyme Dicer in the maturation of the let-7 small temporal RNA. Science *293*, 834–838.

Jacobsen, S.E., Running, M.P., and Meyerowitz, E.M. (1999). Disruption of an RNA helicase/RNase III gene in Arabidopsis causes unregulated cell division in floral meristems. Development *126*, 5231–5243.

Jensen, S., Gassama, M.P., and Heidmann, T. (1999). Cosuppression of I transposon activity in Drosophila by I-containing sense and antisense transgenes. Genetics *153*, 1767–1774.

Ketting, R.F., and Plasterk, R.H. (2000). A genetic link between cosuppression and RNA interference in C. elegans. Nature *404*, 296–298.

Ketting, R.F., Haverkamp, T.H., van Luenen, H.G., and Plasterk, R.H. (1999). Mut-7 of C. elegans, required for transposon silencing and RNA interference, is a homolog of Werner syndrome helicase and RNaseD. Cell *99*, 133–141.

Knight, S.W., and Bass, B.L. (2001). A Role for the RNase III Enzyme DCR-1 in RNA Interference and Germ Line Development in C. elegans. Science *293*, 2269–2271.

Li, W.X., and Ding, S.W. (2001). Viral suppressors of RNA silencing. Curr. Opin. Biotechnol. *12*, 150–154.

Malinsky, S., Bucheton, A., and Busseau, I. (2000). New insights on homology-dependent silencing of I factor activity by transgenes containing ORF1 in *Drosophila melanogaster*. Genetics *156*, 1147–1155.

Matsuda, S., Ichigotani, Y., Okuda, T., Irimura, T., Nakatsugawa, S., and Hamaguchi, M. (2000). Molecular cloning and characterization of a novel human gene (HERNA) which encodes a putative RNA-helicase. Biochim. Biophys. Acta *1490*, 163–169.

Montgomery, M.K., and Fire, A. (1998). Double-stranded RNA as a mediator in sequence-specific genetic silencing and co-suppression. Trends Genet. *14*, 255–258.

Montgomery, M.K., Xu, S., and Fire, A. (1998). RNA as a target of double-stranded RNA-mediated genetic interference in *Caenorhabditis elegans*. Proc. Natl. Acad. Sci. USA *95*, 15502–15507.

Mourrain, P., Béclin, C., Elmayan, T., Feuerbach, F., Godon, C., Morel, J.-B., Jouette, D., Lacombe, A.-M., Nikic, S., Picault, N., et al. (2000). Arabidopsis SGS2 and SGS3 genes are required for post-transcriptional gene silencing and natural virus resistance. Cell *101*, 533–542.

Parrish, S., Fleenor, J., Xu, S., Mello, C., and Fire, A. (2000). Functional anatomy of a dsRNA trigger. Differential requirement for the two trigger strands in RNA interference. Mol. Cell *6*, 1077–1087.

Ratcliff, F.G., MacFarlane, S.A., and Baulcombe, D.C. (1999). Gene silencing without DNA. RNA-mediated cross-protection between viruses. Plant Cell *11*, 1207–1216.

Sharp, P.A. (2001). RNA interference-2001. Genes Dev. *15*, 485–490.

Smardon, A., Spoerke, J., Stacey, S., Klein, M., Mackin, N., and Maine, E. (2000). EGO-1 is related to RNA-directed RNA polymerase

and functions in germ-line development and RNA interference in C. *elegans*. Curr. Biol. *10*, 169–178.

Tabara, H., Sarkissian, M., Kelly, W.G., Fleenor, J., Grishok, A., Timmons, L., Fire, A., and Mello, C.C. (1999). The rde-1 gene, RNA interference, and transposon silencing in C. elegans. Cell *99*, 123–132.

Tuschl, T., Zamore, P.D., Lehmann, R., Bartel, D.P., and Sharp, P.A. (1999). Targeted mRNA degradation by double-stranded RNA in vitro. Genes Dev. *13*, 3191–3197.

Worthington, C.C. ed. (1988). Worthington Enzyme Manual (Freehold, NJ, Worthington Biochemical Corp.).

Wu-Scharf, D., Jeong, B., Zhang, C., and Cerutti, H. (2000). Transgene and transposon silencing in chlamydomonas reinhardtii by a DEAH-Box RNA helicase. Science *290*, 1159–1163.

Yang, D., Lu, H., and Erickson, J.W. (2000). Evidence that processed small dsRNAs may mediate sequence-specific mRNA degradation during RNAi in Drosophila embryos. Curr. Biol. *10*, 1191–1200.

Zamore, P., Tuschl, T., Sharp, P., and Bartel, D. (2000). RNAi: double-stranded RNA directs the ATP-dependent cleavage of mRNA at 21 to 23 nucleotide intervals. Cell *101*, 25–33.

Molecular Cell, Vol. 10, 537–548, September, 2002, Copyright ©2002 by Cell Press

Evidence that siRNAs Function as Guides, Not Primers, in the *Drosophila* and Human RNAi Pathways

Dianne S. Schwarz,[2] György Hutvágner,[2] Benjamin Haley, and Phillip D. Zamore[1]
Department of Biochemistry
and Molecular Pharmacology
University of Massachusetts Medical School
Lazare Research Building, Room 825
364 Plantation Street
Worcester, Massachusetts 01605

Summary

In *Drosophila*, two features of small interfering RNA (siRNA) structure—5′ phosphates and 3′ hydroxyls—are reported to be essential for RNA interference (RNAi). Here, we show that as in *Drosophila*, a 5′ phosphate is required for siRNA function in human HeLa cells. In contrast, we find no evidence in flies or humans for a role in RNAi for the siRNA 3′ hydroxyl group. Our in vitro data suggest that in both flies and mammals, each siRNA guides endonucleolytic cleavage of the target RNA at a single site. We conclude that the underlying mechanism of RNAi is conserved between flies and mammals and that RNA-dependent RNA polymerases are not required for RNAi in these organisms.

Introduction

In diverse eukaryotes, double-stranded RNA (dsRNA) triggers the destruction of mRNA sharing sequence with the double strand (Hutvágner and Zamore, 2002b; Hannon, 2002). In animals and basal eukaryotes, this process is called RNA interference (RNAi) (Fire et al., 1998). There is now wide agreement that RNAi is initiated by the conversion of dsRNA into 21–23 nt fragments by the multidomain RNase III enzyme, Dicer (Billy et al., 2001; Bernstein et al., 2001; Grishok et al., 2001; Ketting et al., 2001; Knight and Bass, 2001; Martens et al., 2002). These short RNAs are known as small interfering RNAs (siRNAs), and they direct the degradation of target RNAs complementary to the siRNA sequence (Zamore et al., 2000; Elbashir et al., 2001c, 2001b, 2001a; Nykänen et al., 2001; Elbashir et al., 2002). In addition to its role in initiating RNAi, Dicer also cleaves ~70 nt precursor RNA stem-loop structures into single-stranded 21–23 nt RNAs known as microRNAs (miRNAs; Hutvágner et al., 2001; Grishok et al., 2001; Ketting et al., 2001; Reinhart et al., 2002). Like siRNAs, miRNAs bear 5′ monophosphate and 3′ hydroxyl groups, the signatures of RNase III cleavage products (Hutvágner et al., 2001; Elbashir et al., 2001b). miRNAs are hypothesized to function in animals as translational repressors (Lee et al., 1993; Wightman et al., 1993; Ha et al., 1996; Moss et al., 1997; Olsen and Ambros, 1999; Reinhart et al., 2000; Zeng et al., 2002; Seggerson et al., 2002). The conversion of dsRNA into siRNAs requires additional protein cofactors that may recruit the dsRNA to Dicer or stabilize the siRNA products (Tabara et al., 1999; Hammond et al., 2001; Grishok et al., 2001; Tabara et al., 2002). How siRNAs direct target cleavage and whether a single mechanism explains the function of siRNAs in posttranscriptional gene silencing in plants, quelling in fungi, and RNAi in animals remain unknown. Furthermore, how siRNAs are permitted to enter the RNAi pathway while other 21–23 nt RNAs seem to be excluded cannot yet be fully explained.

Three models have been proposed for RNAi in *Drosophila*. Each model seeks to explain the mechanism by which siRNAs direct target RNA destruction. In one model (Figure 1), target destruction requires an RNA-dependent RNA polymerase (RdRP) to convert the target mRNA into dsRNA (Lipardi et al., 2001). The RdRP is hypothesized to use single-stranded siRNAs as primers for the target RNA-templated synthesis of complementary RNA (cRNA). The resulting cRNA/target RNA hybrid is proposed to then be cleaved by Dicer, destroying the mRNA and generating new siRNAs in the process. Key features of this model are that the ATP-dependent, dsRNA-specific endonuclease Dicer acts twice in the RNAi pathway, that target destruction should require nucleotide triphosphates to support the production of cRNA, and that a 3′ hydroxyl group is essential for siRNA function, since siRNAs are proposed to serve as primers for new RNA synthesis.

A second model proposes that single-stranded siRNAs do not act as primers for an RdRP, but instead assemble along the length of the target RNA and are then ligated together by an RNA ligase to generate cRNA (Lipardi et al., 2001; Nishikura, 2001). The cRNA/target RNA hybrid would then be destroyed by Dicer. This model predicts that target recognition and destruction should require ATP (or perhaps an NAD-derived high-energy cofactor) to catalyze ligation, as well as to support Dicer cleavage. Like the first model, the ligation hypothesis predicts that an siRNA 3′ hydroxyl group should be required for RNAi. Furthermore, a 5′ phosphate should be required for siRNA ligation, but ribonucleotide triphosphates other than ATP should not be required for target destruction.

A third model (Figure 1) hypothesizes that two distinct enzymes or enzyme complexes act in the RNAi pathway (Hammond et al., 2000; Zamore et al., 2000; Nykänen et al., 2001). As in the first model, Dicer is proposed to generate siRNAs from dsRNA. These siRNAs are then incorporated into a second enzyme complex, the RNA-induced silencing complex (RISC), in an ATP-dependent step or series of steps during which the siRNA duplex is unwound into single strands. The resulting single-stranded siRNA is proposed to guide the RISC to recognize and cleave the target RNA in a step or series of steps requiring no nucleotide cofactors whatsoever. The absence of a nucleotide triphosphate requirement for target recognition and cleavage is a key feature of this model.

We have previously demonstrated by two different experimental protocols that both recognition and endonucleolytic cleavage of a target RNA proceeds efficiently in the presence of less than 50 nM ATP, a concentration

[1]Correspondence: phillip.zamore@umassmed.edu
[2]These authors contributed equally to this work.

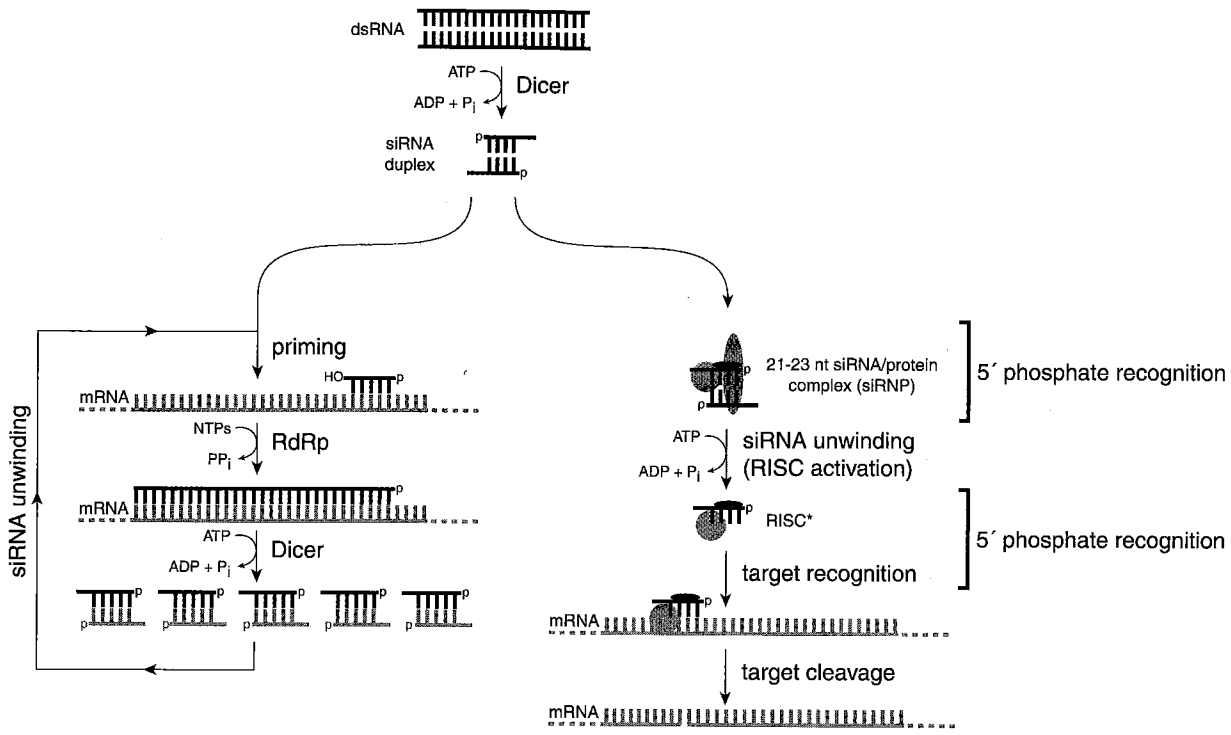

Figure 1. Two Models Proposed for the RNAi Pathway in *Drosophila*

Both models postulate that dsRNA is converted to siRNA by the ATP-dependent endoribonuclease Dicer, but the models differ as to the subsequent function of siRNAs. In the "random degradative PCR" model (at left), siRNAs are postulated to function as primers for the target RNA-templated synthesis of cRNA by an RdRP. The resulting dsRNA is then proposed to be cleaved by Dicer into a new crop of siRNAs, which can prime the conversion of additional target RNAs into dsRNA. In the endonucleolytic cleavage model for RNAi (at right), siRNAs are proposed to be incorporated into an endonuclease complex distinct from Dicer, the RISC. Assembly of the RISC is proposed to be ATP dependent, whereas endonucleolytic cleavage of the target RNA is postulated to require no high-energy cofactors.

likely to be insufficient to support either the synthesis of new RNA or the ligation of multiple siRNAs into cRNA (Nykänen et al., 2001). However, our data also revealed an absolute requirement for a 5′ phosphate for siRNAs to direct target RNA cleavage in *Drosophila* embryo lysates, a finding we interpreted as reflecting an authentication step in the assembly of the RNAi-enzyme complex, the RISC. We envisioned that the 5′ phosphate was involved in obligatory noncovalent interactions with one or more protein components of the RNAi pathway. Nonetheless, the 5′ phosphate requirement might formally reflect a requirement for the phosphate group in covalent interactions, such as the ligation of multiple siRNAs to generate cRNA (Nishikura, 2001).

Here, we more fully define the mechanism of RNAi in flies and mammals by examining the requirement for a 5′ phosphate and a 3′ hydroxyl group on the antisense strand of the siRNA duplex. First, we analyze the role of these functional groups in siRNA function in vitro, using both *Drosophila* and human cell-free systems that recapitulate siRNA-directed target RNA destruction. Then, we validate our findings in vivo in human HeLa cells. Our data support a model for the RNAi pathway in which siRNAs function as guides for an endonuclease complex that mediates target RNA destruction. We find that the requirement for a 5′ phosphate is conserved between *Drosophila* and human cells and that an siRNA 3′ hydroxyl is dispensable in both systems. Our data argue against an obligatory role for an RdRP in *Drosophila* or human RNAi, despite the clear requirement for such enzymes in PTGS in plants, quelling in *Neurospora crassa*, and RNAi in *C. elegans* and *Dictyostelium discoideum* (Cogoni and Macino, 1999; Smardon et al., 2000; Dalmay et al., 2000; Mourrain et al., 2000; Sijen et al., 2001; Martens et al., 2002). In this respect, the mechanism of RNAi in flies and mammals appears to be distinct from that of PTGS, quelling, and RNAi in worms and *Dictyostelium*, suggesting that the pathway in flies and mammals may be more restricted in the range of triggers that can elicit an RNAi response.

Results and Discussion

Requirement for the siRNA 5′ Phosphate in Human RNAi

Synthetic siRNAs bearing a 5′ hydroxyl can efficiently mediate RNAi both in vitro in *Drosophila* embryo lysates and in vivo in cultured human cells (Elbashir et al., 2001b, 2001a; Nykänen et al., 2001). However, in the *Drosophila* in vitro system, an endogenous kinase rapidly converts the 5′ hydroxyl group to a phosphate (Nykänen et al., 2001). Blocking siRNA phosphorylation by substituting the 5′ hydroxyl with a methoxy moiety completely blocks RNAi in *Drosophila* embryo lysates (Nykänen et al., 2001). Furthermore, 5′ phosphorylated siRNAs more efficiently trigger RNAi in vivo in *Drosophila* embryos than

do 5′ hydroxyl-containing siRNAs (Boutla et al., 2001). 5′ hydroxyl-containing, synthetic siRNAs that trigger RNAi in cultured mammalian cells (Elbashir et al., 2001a, 2002), in mice (McCaffrey et al., 2002; Lewis et al., 2002), and perhaps even in plants (Klahre et al., 2002) may likewise be phosphorylated by a cellular kinase prior to entering the RNAi pathway.

To determine if a 5′ phosphate is required for RNAi in mammals, we first analyzed mammalian RNAi in vitro, using HeLa cell S100 extract. These reactions accurately recapitulate the known features of siRNA-directed RNAi in mammalian cell culture: exquisite sequence specificity (Elbashir et al., 2001a) and target RNA cleavage (Holen et al., 2002). RNAi reactions were performed in HeLa S100 extracts using siRNA duplexes in which the antisense strand, which we refer to as the guide strand, contained either a 5′ hydroxyl or a 5′ methoxy group (Figure 2A) and a chimeric target RNA in which nucleotides 62 to 81 were complementary to the siRNA (Figure 2B). When the guide strand of the siRNA duplex contained a 5′ hydroxyl group, and could, therefore, be phosphorylated, it directed cleavage of the target RNA within the sequence complementary to the siRNA (Figure 3). Target cleavage directed by this siRNA occurred at the same site in the HeLa S100 as in *Drosophila* embryo lysate. These data suggest that endonucleolytic cleavage of the target RNA is a common feature of RNAi in flies and mammals. siRNAs with a 5′ methoxy group cannot be phosphorylated by nucleic acid kinases and cannot direct RNAi in lysates of *Drosophila* embryos (Nykänen et al., 2001). Such siRNAs were likewise unable to direct cleavage of the target RNA in the HeLa S100 reaction (Figure 3A). Although the exogenous, methoxy-blocked siRNA did not trigger sequence-specific target cleavage, an endogenous HeLa RISC complex that contains the miRNA *let-7* (Hutvágner and Zamore, 2002a) cleaved the chimeric target RNA within the *let-7* complementary sequence near its 3′ end (Figure 2B) in all of the human in vitro RNAi reactions. This diagnostic 5′ cleavage product (indicated by an asterisk) serves as an internal control for these and subsequent in vitro HeLa S100 reactions. Our data suggest that mammalian RNAi, like RNAi in *Drosophila* (Nykänen et al., 2001; Boutla et al., 2001), requires the siRNA 5′ phosphate for target cleavage and suggest that 5′ hydroxyl-containing siRNA duplexes must be phosphorylated by a cellular kinase before they become competent to mediate RNAi in human cells. Consistent with this idea, 5′ hydroxyl-containing siRNAs are rapidly 5′ phosphorylated after only 5 min incubation in the HeLa S100 (Figure 3B). Thus, like *Drosophila*, human cells contain a nucleic acid kinase that can add a 5′ phosphate to a synthetic siRNA.

Role of the siRNA 3′ Hydroxyl Group in Flies and Mammals

Both siRNAs produced by enzymatic cleavage of dsRNA and those prepared by chemical synthesis contain 3′ hydroxyl termini (Elbashir et al., 2001b). Experiments using nuclease-treated siRNAs suggested that a 3′ phosphate blocks RNAi in *Drosophila* embryo lysates (Lipardi et al., 2001), a finding consistent with authentication of siRNA 3′ structure by the RNAi machinery, with siRNAs acting as primers for cRNA synthesis, or with RNA-templated ligation of multiple siRNAs into cRNA. To determine if the siRNA 3′ hydroxyl group plays an essential role in RNAi, we synthesized two siRNAs in which the 3′ hydroxyl group of the guide strand was blocked (Figure 2). In one siRNA, the 3′ hydroxyl was replaced by a 2′,3′ dideoxy terminus. In the other, the 3′ position contained 3-amino-propyl phosphoester (3′ "amino modifier"). Each of the blocked siRNA guide strands was analyzed by electrospray mass spectrometry to confirm its identity and purity. The two modified siRNA guide strands, as well as a 3′ hydroxyl-containing control strand, were annealed to a standard 21 nt siRNA sense strand. The three resulting siRNA duplexes were tested for their ability to direct cleavage of a complementary target RNA in an in vitro RNAi reaction containing *Drosophila* embryo lysate. Figure 4A shows that the two 3′-blocked siRNAs produced the same degree of target cleavage as the 3′ hydroxyl-containing siRNA control.

Next, we repeated the experiment in HeLa S100 extract to determine if an siRNA 3′ hydroxyl group is required for RNAi in mammalian cells. 3′ modification of an siRNA has been reported to be permitted for RNAi in mammalian cells (Holen et al., 2002), but it was not shown in those experiments that all of the siRNA was 3′ modified. In contrast to the 5′ methoxy modification, which completely blocked target RNA cleavage in the HeLa S100 reaction, 3′ modification had no effect on the efficiency or specificity of RNAi (Figure 4B). The identity and purity of these siRNAs was confirmed by electrospray mass spectrometry. However, we could envision that a fraction of the siRNA guide strand was cleaved within the single-stranded, two nucleotide, 3′ overhang by a nuclease in the HeLa S100, regenerating the 3′ hydroxyl. If this occurred, the cleaved siRNAs could then act as primers. To exclude this possibility, we performed RNAi reactions using progressively shorter guide siRNAs blocked at the 3′ end by either a 2′,3′ dideoxy or a 3′ amino modifier group. The 20 or 19 nt guide strands were annealed to the same 21 nt sense siRNA strand. Figure 4B shows that target RNA cleavage occurred in all cases, although the efficiency of cleavage decreased as the siRNA guide strand was shortened, even when it contained a 3′ hydroxyl terminus. If the 3′ blocked 21 nt siRNA was active because it had been shortened to a 20-mer, it could not have attained the activity of the 3′ hydroxyl 21 nt siRNA. Similarly, if nucleolytic removal of the 3′ block accounted for the activity of the 20 nt guide siRNA, it should have only been as active as the 19 nt, 3′ hydroxyl-containing siRNA. These results suggest that the 3′ hydroxyl group of the siRNA guide strand does not play an obligatory role in siRNA-directed RNAi in flies or mammals.

Single-Stranded siRNAs

All current models for RNAi—including those that propose siRNA to function as guides for an endonuclease and models that propose siRNAs to act as primers for target-RNA templated RNA synthesis—predict that siRNAs ultimately function as single strands. In fact, in *Drosophila* embryos, single-stranded antisense siRNAs corresponding to the *Notch* mRNA elicited *Notch* phenotypes in 12% of injected embryos, although the expres-

A

guide strand length (nt)	guide strand 5′ end	guide strand 3′ end	siRNA sequence
21	OH	OH	5′-UCGAAGUAUUCCGCGUACGUG-3′ 3′-UUAGCUUCAUAAGGCGCAUGC-5′
21	CH_3O	OH	5′-CH_3O-dTCGAAGUAUUCCGCGUACGUG-3′ 3′-UUAGCUUCAUAAGGCGCAUGC-5′
21	OH	2′,3′ ddC	5′-UCGAAGUAUUCCGCGUACGUddC-3′ 3′-UUAGCUUCAUAAGGCGCAUGC-5′
21	OH	AM	5′-UCGAAGUAUUCCGCGUACGUG-AM-3′ 3′-UUAGCUUCAUAAGGCGCAUGC-5′
20	OH	OH	5′-UCGAAGUAUUCCGCGUACGU-3′ 3′-UUAGCUUCAUAAGGCGCAUGC-5′
20	OH	2′,3′ ddC	5′-UCGAAGUAUUCCGCGUACGddC-3′ 3′-UUAGCUUCAUAAGGCGCAUGC-5′
20	OH	AM	5′-UCGAAGUAUUCCGCGUACGU-AM-3′ 3′-UUAGCUUCAUAAGGCGCAUGC-5′
20	OH	OH	5′-UCGAAGUAUUCCGCGUACGC-3′ 3′-UUAGCUUCAUAAGGCGCAUGC-5′
19	OH	OH	5′-UCGAAGUAUUCCGCGUACG-3′ 3′-UUAGCUUCAUAAGGCGCAUGC-5′
19	OH	AM	5′-UCGAAGUAUUCCGCGUACG-AM-3′ 3′-UUAGCUUCAUAAGGCGCAUGC-5′
21	OH	OH	5′-UGAGGUAGUAGGUUGUAUAGU-3′ 3′-UUACUCCAUCAUCCAACAUAU-5′
21	OH, 2′dT	AM	5′-dTGAGGUAGUAGGUUGUAUAGU-AM-3′ 3′-UUACUCCAUCAUCCAACAUAU-5′

B

Figure 2. RNAs Used in This Study

(A) Photinus pyralis (firefly) luciferase (blue) and *let-7* (red) siRNAs used in this study. The guide strand (antisense strand) is shown 5′-to-3′ as the upper strand of each siRNA. Single-stranded siRNAs used in Figures 4, 5, and 6 correspond to the indicated guide strands. ddC, dideoxy Cytosine; AM, amino modifier. siRNAs corresponding to firefly luciferase sequence are blue; those corresponding to *let-7* sequence are red.

(B) A schematic representation of the chimeric target RNA, indicating the relative positions of firefly luciferase sequences and sequences complementary to the *let-7* miRNA found naturally in HeLa cells.

sivity was quite low (Boutla et al., 2001). Furthermore, single-stranded RNAs of various lengths trigger RNAi in *C. elegans*, but only when they contain a 3′ hydroxyl group, suggesting that single-stranded siRNA functions in that organism as a primer for an RdRP (Tijsterman et al., 2002). Consistent with single-stranded siRNAs acting in nematodes as primers that direct the production of new dsRNA, they fail to trigger RNAi in the absence of Dicer (Dcr-1) (Tijsterman et al., 2002).

We examined if the guide siRNA strand alone could trigger target cleavage in an in vitro RNAi reaction containing either *Drosophila* embryo lysate or human HeLa cell S100. We first examined if single-stranded siRNA could direct target RNA cleavage in *Drosophila* embryo lysates (Figure 5A). For this experiment, we used siRNA with the sequence of the miRNA *let-7* (Figure 2A). Cleavage of the target RNA (Figure 2B) by a *let-7*-containing siRNA duplex produces a diagnostic 522 nt 5′ product (Hutvágner and Zamore, 2002a). When the synthetic siRNA was used as a single strand, the target RNA was not cleaved (Figure 5A). Similarly, a single-stranded siRNA of the same sequence but bearing a 2′ deoxy thymidine (dT) instead of uracil as its first nucleotide, was also a poor trigger of target cleavage. However,

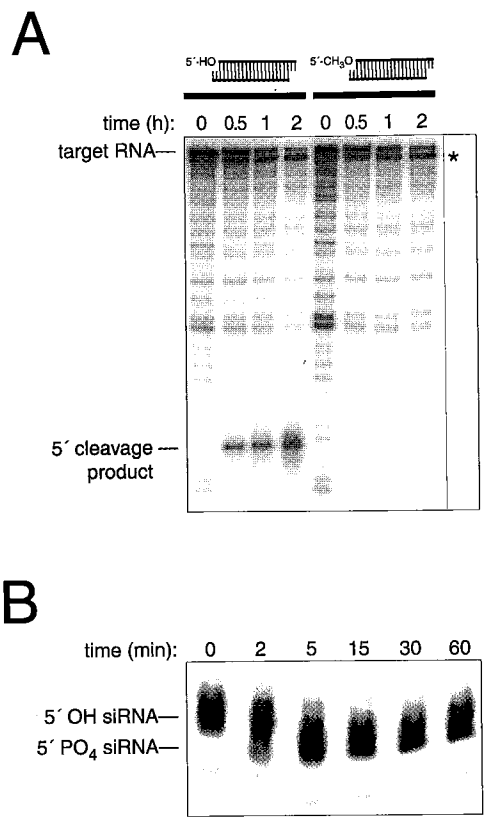

Figure 3. The siRNA 5′ Phosphate Group Is Required for siRNA-Directed Target Cleavage in HeLa S100 Extracts

(A) RNAi in vitro in human HeLa cell S100 extract. At left, a time course of in vitro RNAi for a standard siRNA; at right, for an siRNA duplex bearing a 5′ methoxy guide strand. The asterisk indicates the position of a 5′ cleavage product catalyzed by an endogenous, human *let-7*-programmed RISC complex, which cleaves this target RNA within a *let-7* complementary sequence located near the 3′ end of the RNA (Hutvágner and Zamore, 2002a). This cleavage product serves as an internal control.

(B) Phosphorylation status of the guide strand of an siRNA duplex upon incubation in HeLa S100. An siRNA duplex containing a guide strand 3′-end-labeled with α-^{32}P cordycepin (3′ deoxyadenosine triphosphate) was incubated in a standard HeLa S100 RNAi reaction, then analyzed on a 15% sequencing gel. Phosphorylation accelerates the gel mobility of the labeled siRNA strand, because it adds two additional negative charges. The radiolabeled RNA is 3′ deoxy; therefore, we infer that the added phosphate is on the 5′ end.

both these siRNAs contain a 5′ hydroxyl, and a 5′ phosphate is required for siRNA duplexes to trigger target RNA cleavage in *Drosophila* embryo lysates (Nykänen et al., 2001). Therefore, we considered that the defect with the single-stranded siRNAs might be that they lacked a 5′ phosphate and cannot obtain one because they are not substrates for the *Drosophila* kinase. In support of this hypothesis, when the single-stranded siRNA starting with dT was prephosphorylated with polynucleotide kinase, it directed target cleavage.

To confirm these findings, we examined the activity of a second single-stranded siRNA, complementary to the luciferase portion of the target RNA. When prephosphorylated, this single-stranded siRNA again directed target cleavage in *Drosophila* embryo lysate, albeit less efficiently than the same molar concentration of an siRNA duplex (Figure 5B). Cleavage occurred at precisely the same site in the target RNA for both single-stranded and double-stranded siRNAs, suggesting that the single-stranded siRNA entered the RNAi pathway, rather than triggered RNA destruction by a different route. The same single-stranded siRNA sequence bearing a 5′ methoxy group did not direct target RNA cleavage (Figure 5B). Together, the experiments in Figure 5 demonstrate that single-stranded siRNAs—like the guide strands of siRNA duplexes—do not function in the RNAi pathway unless they bear a 5′ phosphate.

To determine if single-stranded siRNAs trigger target destruction in *Drosophila* embryo lysates by acting as primers, we modified the 3′ end of the siRNA to 2′,3′ dideoxy. As with double-stranded siRNAs, blocking the 3′ end of the single-stranded siRNA had no effect on the efficiency or specificity with which the target was cleaved (Figure 5B). We note that the efficiency of target cleavage by single-stranded siRNAs is significantly less than that of siRNA duplexes. The lower efficiency might simply reflect the remarkably short lifespan of single-stranded siRNA in the *Drosophila* embryo lysate: the vast majority is destroyed within the first 2 min of incubation (Figure 5C). One explanation for the requirement for a 5′ phosphate might be that, without it, the single-stranded siRNA is destroyed even faster. This explanation is unlikely, because the rate of single-stranded RNA destruction is only 1.4-fold faster for 5′ hydroxy siRNAs (Figure 5C). More likely is that the 5′ phosphate of the single-stranded siRNA is required for its entry into the RISC and that because a small fraction of 5′ phosphorylated, single-stranded siRNA enters the RISC, it is protected from degradation, enhancing its stability in the lysate.

Next, we examined if single-stranded siRNAs could function to trigger RNAi in HeLa S100 extracts. Again, single-stranded siRNAs directed target cleavage at the same site as the corresponding siRNA duplex (Figure 6A). Prephosphorylation of single-stranded siRNA was not required for it to function in target cleavage in HeLa S100, but blocking the 5′ end with a methoxy group completely eliminated RNAi (Figure 6B). These results suggest that a 5′ phosphate is required for mammalian RNAi, but that the nucleic acid kinase(s) responsible for phosphorylating siRNAs in HeLa S100 acts on single-stranded siRNA, unlike its *Drosophila* counterpart. Blocking the 3′ end of the single-stranded siRNA had no effect on the ability of the single-stranded siRNA to cleave the target RNA in HeLa S100 (Figure 6A). Thus, the structural requirements for single-stranded siRNA function in target cleavage are conserved between flies and mammals: a 5′ phosphate is required, but a 3′ hydroxyl is not.

Together, these data support the view that siRNAs do not direct target RNA destruction by priming the synthesis of new RNA, nor are siRNAs ligated together to generate cRNA. Both processes should require a 3′ hydroxyl group, which is dispensable for target cleavage in either *Drosophila* or human cell extracts. Instead, our data suggest that siRNAs act as guides to direct a protein endoribonuclease to cleave the target RNA. The finding that single-stranded siRNAs can function as guides in the RNAi pathway suggests that each individual RISC contains only one siRNA strand. Consistent

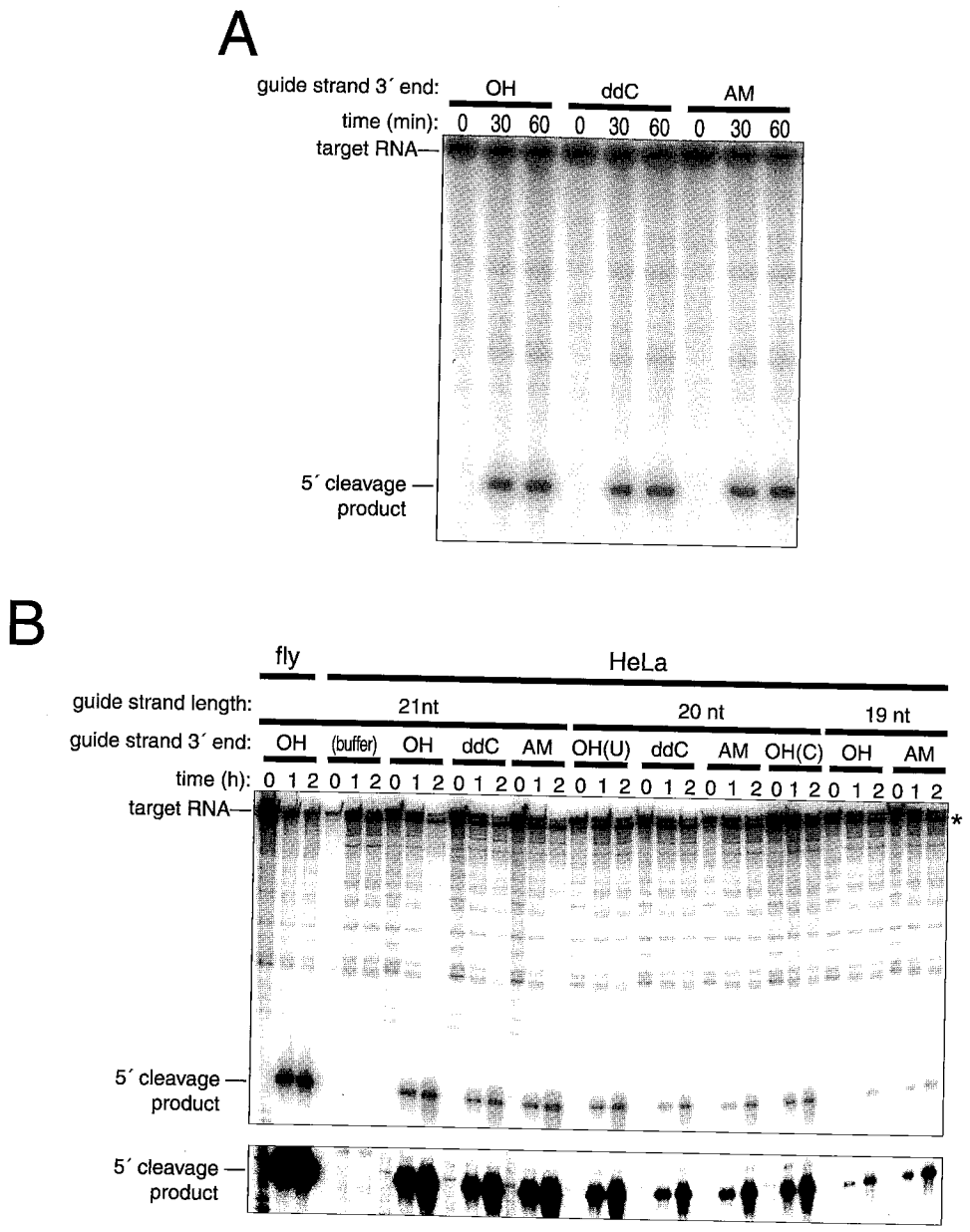

Figure 4. The siRNA 3′ Hydroxyl Is Dispensable for siRNA-Directed Target Cleavage in *Drosophila* and Human Cell Extracts

(A) 3′-blocked siRNAs trigger RNAi in *Drosophila* embryo lysates with the same efficiency as 3′-hydroxyl-containing siRNAs. ddC, 2′,3′ dideoxy C; AM, amino modifier.

(B) 3′-blocked siRNAs trigger RNAi in HeLa S100 extracts with the same efficiency as standard, 3′-hydroxyl-containing siRNAs. An overexposure of the region of the gel containing the 5′ cleavage product is shown in the lower panel. The asterisk marks the internal control 5′ cleavage product described in Figure 3.

with this view, in HeLa cell S100 extracts, the single stranded miRNA, *let-7*, is in an endogenous RISC that catalyzes multiple rounds of cleavage of a perfectly complementary target RNA (Hutvágner and Zamore, 2002a).

Previously, it was proposed that the siRNA 5′ phosphate was recognized twice during the assembly of the siRNA-containing endoribonuclease complex (Nykänen et al., 2001) (Figure 1). That study placed one 5′ phosphate recognition event before siRNA duplex unwinding but could not distinguish whether the 5′ phosphate is required subsequently at the unwinding step itself or after unwinding is complete. The absence of target cleavage by single-stranded siRNAs lacking a 5′ phosphate suggests that the second phosphate recognition step occurs after the siRNA duplex is unwound. In both *Drosophila* embryo lysates and human HeLa S100, cleavage directed by single-stranded siRNA was less efficient than RNAi triggered by siRNA duplexes. This inefficiency correlated with the general instability of short RNA in the in vitro extracts, as determined by

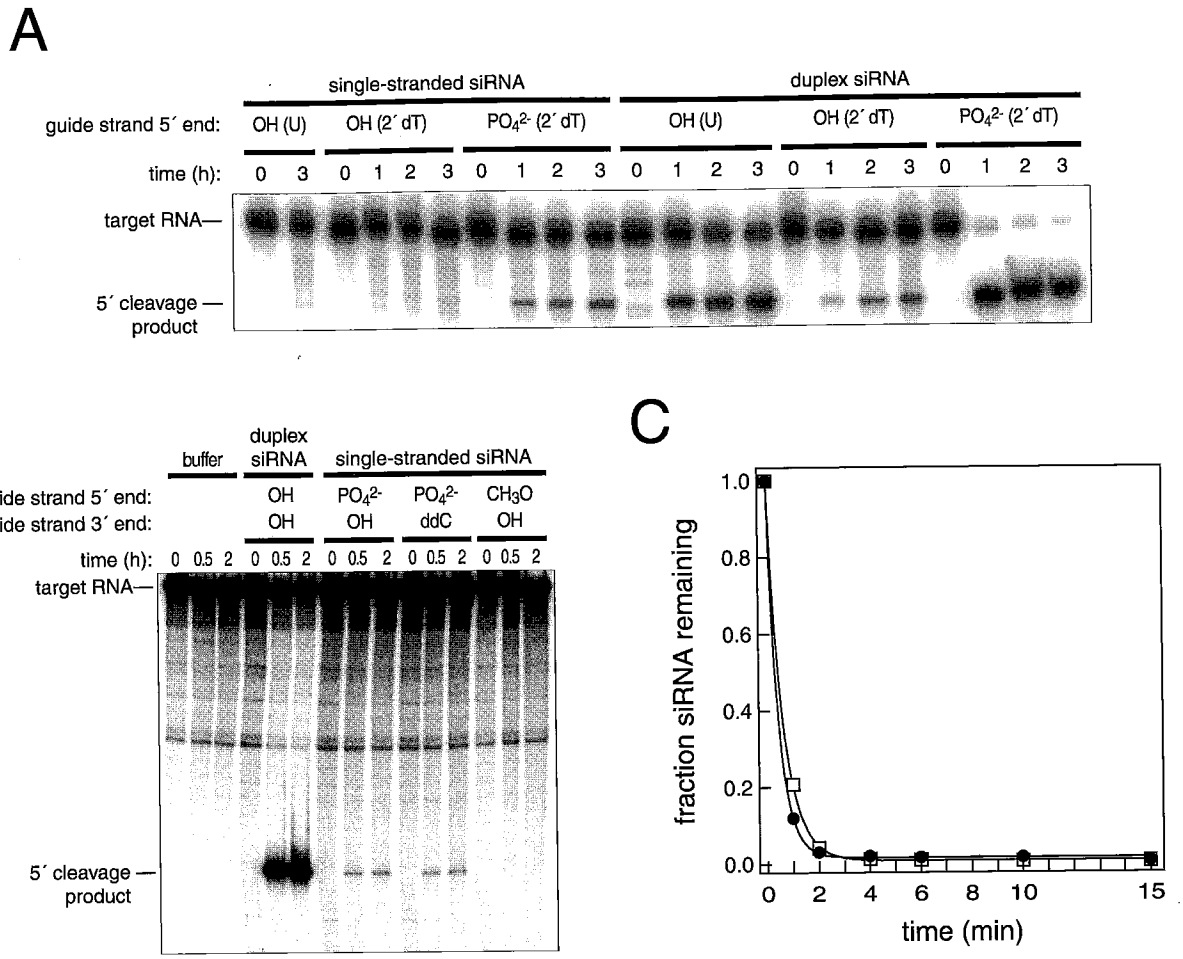

Figure 5. Single-Stranded siRNA Guides Target Cleavage in *Drosophila* Embryo Lysates

(A) Single-stranded siRNAs with the sequence of the miRNA *let-7* triggered target cleavage in *Drosophila* embryo lysate, but only if the 5′ end was prephosphorylated.

(B) Single-stranded siRNAs complementary to firefly luciferase sequence triggered target cleavage in *Drosophila* embryo lysate, even if the 3′ end was blocked (2′,3′ddC). No target cleavage was observed using an siRNA with a 5′ methoxy group.

(C) Rate of degradation of single-stranded siRNA in the *Drosophila* embryo lysate. siRNA single strands were 3′ end-labeled with α-^{32}P cordycepin and their stability measured with (filled circles) or without (open squares) a 5′ phosphate. The curves represent the best-fit to a single exponential, consistent with pseudo first-order kinetics for single-stranded siRNA decay. The difference in rates is 1.4-fold (with versus without a 5′ phosphate).

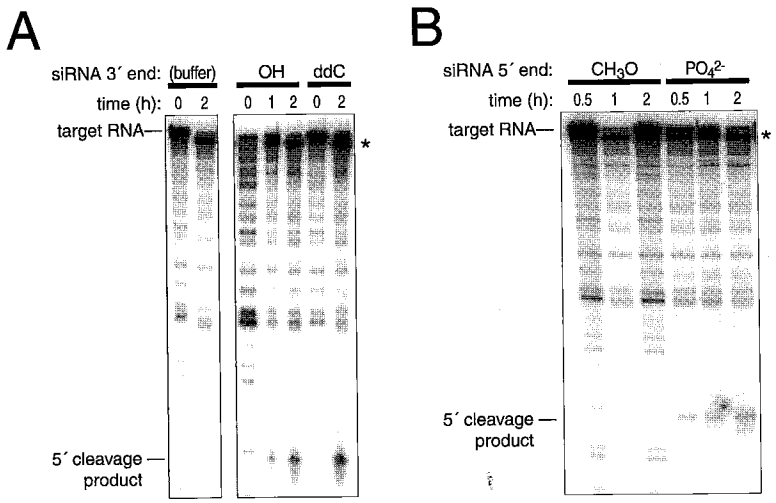

Figure 6. A 5′ Phosphate but Not a 3′ Hydroxyl Is Required for Single-Stranded Antisense siRNAs to Trigger RNAi in HeLa S100 Extract

(A) Single-stranded siRNA triggered target cleavage in HeLa S100, even if the 3′ end of the siRNA was blocked (2′,3′ dideoxy).

(B) Blocking the 5′ end of the siRNA with a methoxy group eliminated the ability of the single-stranded RNA to trigger RNAi. The asterisk marks the control 5′ cleavage product described in Figure 3.

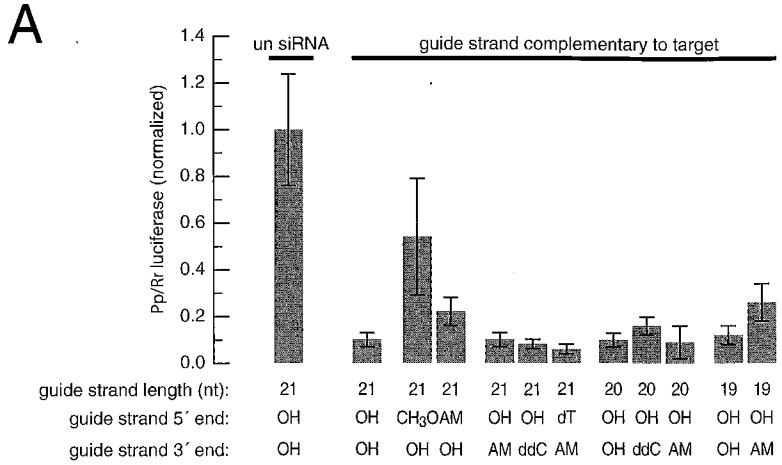

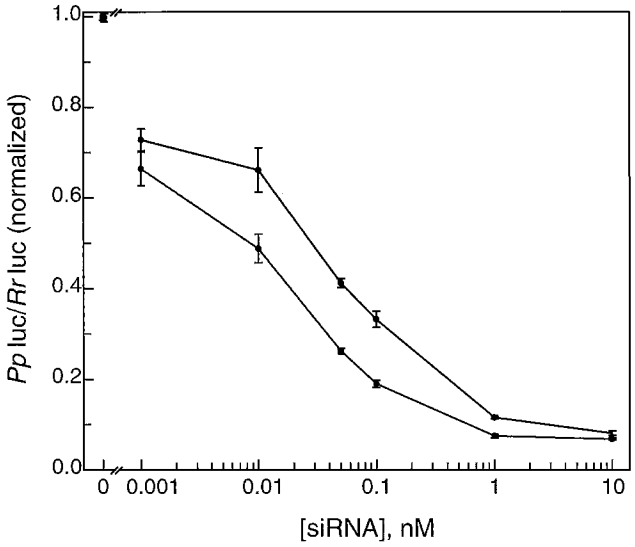

Figure 7. A 5′ Phosphate but Not a 3′ Hydroxyl Is Required for siRNA Duplexes to Trigger RNAi In Vivo in Cultured Human HeLa Cells

(A) siRNA duplexes were examined for their ability to silence the *Photinus pyralis* (Pp; firefly) luciferase target reporter, relative to the *Renilla reniformis* (Rr) luciferase control reporter. ddC, 2′,3′ dideoxy C; AM, amino modifier.

(B) Relative efficacy at limiting siRNA concentrations for siRNA duplexes with guide strands bearing either hydroxy (black symbols) or ddC (red symbols) 3′ termini. Data are the average ± standard deviation for three trials.

measuring single-stranded siRNA half-life using 3′ radiolabeled siRNAs (Figure 5C) and by Northern hybridization (data not shown).

siRNAs Need Not Function as Primers to Trigger RNAi in HeLa Cells

To assess if our in vitro results accurately predict the RNAi mechanism in vivo, cultured human cells were used to assess the structural requirements for siRNA function. Synthetic siRNAs were cotransfected into HeLa cells with plasmids expressing target (*Photinus pyralis, Pp*) and control (*Renilla reniformis, Rr*) luciferase mRNAs. Luciferase expression was measured, and target (firefly) luciferase levels were normalized to the *Renilla* control. The results of these experiments are shown in Figure 7.

First, the requirement for a 5′ phosphate observed in *Drosophila* and HeLa extracts was conserved in vivo (Figure 7A). A 5′ hydroxyl-containing siRNA duplex triggered efficient gene silencing in vivo, reducing expression of the target luciferase >90%. In contrast, a 5′ methoxy-modified siRNA reduced firefly luciferase levels by only 2-fold. This small reduction may reflect inhibition of translation, perhaps by an antisense mechanism. Alternatively, some of the methoxy-blocked siRNA may inefficiently enter the RNAi pathway in vivo. An siRNA in which the guide strand contained a 5′ amino modifier group—6-amino-hexyl phosphoester—was significantly more effective in suppressing target mRNA expression than the siRNA with the 5′ methoxy group (Figure 7A). This finding is consistent with the idea that a 5′ phosphate group is required for siRNA function, but that the 5′ phosphate participates in noncovalent interactions only, since the modified 5′ phosphate should be less able to act as an electron acceptor. The in vivo studies agree with the in vitro results: a 5′ phosphate is essential for efficient siRNA function in flies and mammals. However, in flies only duplex siRNAs can be 5′ phosphorylated by cellular kinases, whereas in mammals, both single-stranded and double-stranded siRNAs are phosphorylated.

Consistent with the view that the core function of siRNA in human cells is as guides, not primers, blocking the 3′ end of the siRNA guide strand had no effect on

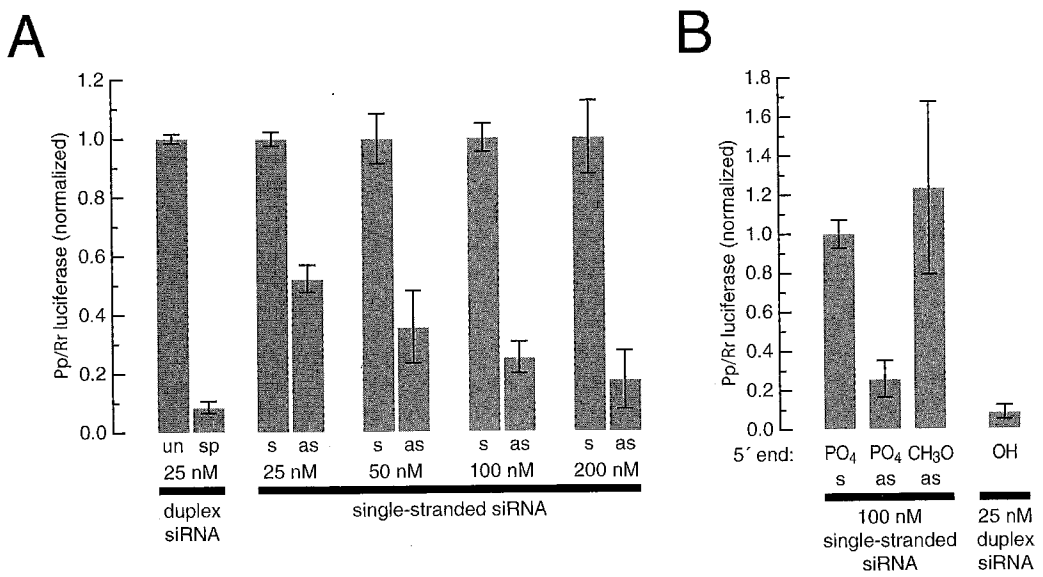

Figure 8. Single-Stranded siRNA Triggers Gene Silencing in HeLa Cells

(A) Single-stranded siRNA silencing as a function of siRNA concentration.

(B) Blocking the 5′ end of single-stranded siRNAs prevented their triggering target gene silencing. Gray bars indicate the average ± standard deviation for three trials. Un, siRNA unrelated in sequence to the target RNA; sp, specific siRNA corresponding to the target RNA; s, sense strand; as, antisense strand.

RNAi in vivo. siRNA duplexes in which the guide strand contained a 3′ hydroxyl, a 2′,3′ dideoxy, or a 3′ amino modifier were all equally effective in triggering RNAi in vivo (Figure 7A). The silencing activity in vivo of a 21 nt, 3′-blocked siRNA guide strand was greater than that of a 20 nt, 3′ hydroxy siRNA guide strand, indicating that the 3′ block was not removed in vivo. We believe that these data exclude an obligatory role for the siRNA 3′ hydroxyl group in RNAi in mammalian cells and argue that siRNAs do not normally trigger target destruction in human cells by functioning as primers.

These experiments were conducted at siRNA concentrations where the siRNA is not limiting for RNA silencing. An siRNA function in priming the synthesis of dsRNA might be used when siRNAs are limiting. We tested the relative ability of siRNA duplexes in which the guide strand either contained a 3′ hydroxyl or a 2′,3′ dideoxy group at low siRNA concentrations (Figure 7B). We find that the efficacy of the two types of siRNAs did differ when siRNA was rate limiting for target mRNA silencing, but never by more than 1.8-fold. The observed difference in efficacy between the two types of siRNAs does not seem sufficiently great to support the view that the 3′ hydroxyl group of the siRNA is used to prime the synthesis of dsRNA from the target mRNA. If the siRNA were used to prime dsRNA synthesis, the production of new dsRNA by an RdRP using the siRNA as a primer should have amplified the silencing activity of the 3′ hydroxy but not the 2′,3′ dideoxy siRNA at limiting concentrations. For example, if the 3′ hydroxy guide strand had primed synthesis of one molecule of dsRNA (~130 bp long based on the site of siRNA/target complementarity) for each target mRNA molecule, and this new dsRNA was then Diced into just two of the possible six new siRNAs, at least a 2-fold difference between the two siRNAs should have been observed. This analysis fails to take into account the new crop of siRNAs acting in a subsequent cycle of priming, which would further amplify the difference between 3′ deoxy and 3′ hydroxy siRNA at limiting concentrations. The simplest interpretation of our finding that 3′ hydroxy siRNAs trigger no significant amplification of RNA silencing relative to 3′ blocked siRNAs is that an siRNA-primed, RdRP-dependent cycle of siRNA amplification plays no productive role in RNAi in cultured HeLa cells, even at low siRNA concentrations. The small difference in efficacy between 3′ OH and 2′,3′ dideoxy siRNAs likely indicates that the blocked siRNAs have a subtle defect such as a lower affinity for components of the RNAi machinery, slightly reduced intracellular half-life, or a minor reduction in phosphorylation rate. This defect may result from the 2′ deoxy modification of the terminal nucleotide, rather than the 3′ block, since siRNAs with 2′ deoxythymidine tails have been reported to be less efficient than those containing uracil in HeLa cells (Hohjoh, 2002).

Our in vitro studies suggest that single-stranded siRNAs can enter the RNAi pathway, albeit inefficiently. To test if single-stranded siRNAs could trigger mRNA silencing in vivo, we substituted various concentrations of single-stranded, sense or antisense siRNA for siRNA duplexes in our HeLa cell cotransfections (Figure 8A). As the concentration of antisense single strand was increased, the expression of the firefly luciferase decreased relative to the Renilla internal control. Note that single-stranded siRNAs are less efficient than siRNA duplexes: it takes nearly eight times more single-stranded siRNA to approach the potency of the corresponding duplex. This inefficiency may simply reflect rapid degradation of the majority of the transfected single-stranded siRNA before it can enter the RISC com-

plex. Cells may possess a mechanism that stabilizes siRNA duplexes and shuttles them to the RISC as single strands without exposing them to degradatory enzymes. Thus, if endogenous siRNAs are double-stranded in vivo, they may be double-stranded so as to facilitate their entry into the RNAi pathway and to exclude them from a competing pathway that degrades small, single-stranded RNA. Alternatively, single-stranded siRNAs may bypass a key step in RISC assembly, making them less efficient than duplexes in triggering RNAi. The dramatic instability of single-stranded siRNAs in vitro may simply reflect their inefficiency in assembling into a RISC, which could protect them from degradation.

Gene silencing by single-stranded siRNA was sequence specific, and single-stranded sense siRNA did not alter the expression of the target RNA (Figure 8B). Thus, it is unlikely that siRNAs themselves are copied by an RdRP in mammalian cells, since copying the sense siRNA should generate the antisense siRNA strand. However, copying sense siRNA into a duplex would not generate the characteristic 3′ overhanging ends of siRNAs. Such 3′ overhangs might be required for siRNA unwinding and/or efficient RISC assembly. Prephosphorylation of single-stranded siRNA did not enhance its potency in HeLa cells, consistent with our observations in HeLa S100 extracts, but blocking phosphorylation with a 5′ methoxy group abolished silencing, pointing to the importance of 5′ phosphorylation for single-stranded siRNA function in vivo (Figure 8B). Our findings are not entirely unexpected, since endogenous, single-stranded miRNAs enter the RNAi pathway in HeLa cells (Hutvágner and Zamore, 2002a). Superficially, the finding that single-stranded siRNAs can elicit RNA silencing blurs the distinction between RNAi and antisense effects. We have presented here evidence that single-stranded siRNAs trigger the same pathway as siRNA duplexes: both guide endonucleolytic cleavage of target RNAs at the same site, and both require 5′ phosphates but not 3′ hydroxyl groups to function.

Our in vitro experiments with *Drosophila* embryo lysates and HeLa S100 extracts and our in vivo experiments in HeLa cells argue against siRNAs functioning as primers in the RNAi pathway. These findings are consistent with the absence of any genes encoding canonical RdRPs in the currently available release of either the *Drosophila* or human genome. A hallmark of the involvement of RdRPs in posttranscriptional silencing is the spread of silencing beyond the confines of an initial trigger dsRNA or siRNA into regions of the target RNA 5′ to the silencing trigger. In *C. elegans*, this spreading ("transitive RNAi") is manifest in the production of new siRNAs corresponding to target sequences not contained in the exogenous trigger dsRNA (Sijen et al., 2001). Furthermore, small RNAs as long as 40 nt can initiate silencing in worms, but only if they contain 3′ hydroxyls, suggesting that they act as primers for the synthesis of cRNA (Tijsterman et al., 2002). In contrast, 5′ spreading is not detected in *Drosophila*, either in vitro (Zamore et al., 2000), in cultured *Drosophila* S2 cells (Celotto and Graveley, 2002), or in vivo in flies (J.-Y. Roignant and C. Antoniewski, personal communication). Our data support the view that, in both flies and mammals, siRNAs trigger target RNA destruction not by acting as primers but rather by guiding a protein endoribonuclease to a site on the target RNA that is complementary to one strand of the siRNA. The observation that the target cleavage site is across from the center of the complementary siRNA (Elbashir et al., 2001c, 2001b) is consistent with an enzyme other than Dicer acting in target RNA destruction and not with models that propose that Dicer destroys target RNAs. Furthermore, mammalian extracts depleted of Dicer still catalyze siRNA-directed target cleavage (Martinez et al., 2002).

Will it be possible to design siRNAs to degrade just one of several mRNA isoforms that differ at only a single nucleotide? If siRNAs do not act as RdRP primers in flies and mammals, then there is no fear that the silencing signal will spread 5′ to a region of sequence common to the entire family of mRNAs. Despite earlier concerns that such siRNAs would not be possible (Nishikura, 2001), our data suggest that isoform- and polymorphism-specific siRNAs will be used in mammals in the future to dissect the function of individual gene isoforms and perhaps even to treat inherited autosomal dominant human diseases.

Experimental Procedures

General Methods

Drosophila embryo lysate preparation, in vitro RNAi reactions, and cap-labeling of target RNAs using Guanylyl transferase were carried out as previously described (Zamore et al., 2000). Human S100 extracts were prepared as described (Dignam et al., 1983). HeLa S100 was substituted for *Drosophila* embryo lysate in an otherwise standard RNAi reaction, except that incubation was at 37° instead of 25°C. Cleavage products of RNAi reactions were analyzed by electrophoresis on 8% denaturing acrylamide gels. 3′ end labeling with α-^{32}P cordycepin and determination of 5′ phosphorylation status were according to Nykänen et al. (2001). Gels were dried and exposed to image plates (Fuji), which were scanned with a Fuji FLA-5000 phosphorimager. Images were analyzed using Image Reader FLA-5000 version 1.0 (Fuji) and Image Gauge version 3.45 (Fuji).

siRNA Preparation

Synthetic RNAs (Dharmacon) were deprotected according to the manufacturer's protocol and processed as previously described (Nykänen et al., 2001). siRNA strands were annealed (Elbashir et al., 2001a) and used at 100 nM final concentration unless otherwise noted. siRNA single strands were phosphorylated with polynucleotide kinase (New England Biolabs) and 1 mM ATP according to the manufacturer's directions.

Tissue Culture

siRNA transfections were as described (Elbashir et al., 2001a). In brief, cultured HeLa cells were propagated in Dulbecco's modified Eagle's medium (DMEM) supplemented with 10% fetal bovine serum (FBS) and 1% penicillin/streptomycin (Life Technologies). Cells were trypsinized and seeded at 1×10^5 cells/ml in 24-well plates (5×10^4 cells/well) in DMEM supplemented with 10% FBS. Twenty-four hours after seeding, 1 μg pGL2 control firefly luciferase (*Pp*-luc GL2; Promega) and 0.1 μg pRL-TK Renilla luciferase (*Rr*-luc; Promega) plasmids and the luciferase siRNA (25 nM) were cotransfected with LipofectAMINE 2000 reagent (Invitrogen) in DMEM (Life Technologies) lacking serum and antibiotics according to manufacturer's instructions. Media was replaced 4 hr after transfection with DMEM containing 10% fetal bovine serum (Life Technologies); 1 day after transfection, the cells were lysed in 1x Passive Lysis Buffer (Promega) according to the manufacturer's instructions. Luciferase expression was determined by the Dual luciferase assay kit (Promega) using a Mediators PhL luminometer. Data analysis was performed using Excel (Microsoft) and IgorPro 5.0 (Wavemetrics). Experiments were performed in triplicate, and error was propagated through all calculations.

Acknowledgments

We thank David Bartel, Andrew Fire, Craig Mello, Tariq Rana, and Stephen Scaringe for discussions; Jean-Yves Roignant and Tom Tuschl for sharing data prior to publication; Melissa Moore and members of the Moore lab for a generous gift of HeLa S100 extract and for assistance in the preparation of HeLa S100 extracts; and members of the Zamore lab for helpful discussions and comments on the manuscript. G.H. is a Charles A. King Trust fellow of the Medical Foundation. P.D.Z. is a Pew Scholar in the Biomedical Sciences and a W.M. Keck Foundation Young Scholar in Medical Research. Supported in part by a grant to P.D.Z. from the National Institutes of Health (GM62862-01).

Received: July 16, 2002
Revised: August 30, 2002

References

Bernstein, E., Caudy, A.A., Hammond, S.M., and Hannon, G.J. (2001). Role for a bidentate ribonuclease in the initiation step of RNA interference. Nature *409*, 363–366.

Billy, E., Brondani, V., Zhang, H., Muller, U., and Filipowicz, W. (2001). Specific interference with gene expression induced by long, double-stranded RNA in mouse embryonal teratocarcinoma cell lines. Proc. Natl. Acad. Sci. USA *98*, 14428–14433.

Boutla, A., Delidakis, C., Livadaras, I., Tsagris, M., and Tabler, M. (2001). Short 5′-phosphorylated double-stranded RNAs induce RNA interference in *Drosophila*. Curr. Biol. *11*, 1776–1780.

Celotto, A.M., and Graveley, B.R. (2002). Exon-specific RNAi: a tool for dissecting the functional relevance of alternative splicing. RNA *8*, 718–724.

Cogoni, C., and Macino, G. (1999). Gene silencing in *Neurospora crassa* requires a protein homologous to RNA-dependent RNA polymerase. Nature *399*, 166–169.

Dalmay, T., Hamilton, A., Rudd, S., Angell, S., and Baulcombe, D.C. (2000). An RNA-dependent RNA polymerase gene in *Arabidopsis* is required for posttranscriptional gene silencing mediated by a transgene but not by a virus. Cell *101*, 543–553.

Dignam, J.D., Lebovitz, R.M., and Roeder, R.G. (1983). Accurate transcription initiation by RNA polymerase II in a soluble extract from isolated mammalian nuclei. Nucleic Acids Res. *11*, 1475–1489.

Elbashir, S.M., Harborth, J., Lendeckel, W., Yalcin, A., Weber, K., and Tuschl, T. (2001a). Duplexes of 21-nucleotide RNAs mediate RNA interference in mammalian cell culture. Nature *411*, 494–498.

Elbashir, S.M., Lendeckel, W., and Tuschl, T. (2001b). RNA interference is mediated by 21- and 22-nucleotide RNAs. Genes Dev. *15*, 188–200.

Elbashir, S.M., Martinez, J., Patkaniowska, A., Lendeckel, W., and Tuschl, T. (2001c). Functional anatomy of siRNAs for mediating efficient RNAi in *Drosophila melanogaster* embryo lysate. EMBO J. *20*, 6877–6888.

Elbashir, S., Harborth, J., Weber, K., and Tuschl, T. (2002). Analysis of gene function in somatic mammalian cells using small interfering RNAs. Methods Finds. Exp. Clin. Pharmacol. *26*, 199–213.

Fire, A., Xu, S., Montgomery, M.K., Kostas, S.A., Driver, S.E., and Mello, C.C. (1998). Potent and specific genetic interference by double-stranded RNA in *Caenorhabditis elegans*. Nature *391*, 806–811.

Grishok, A., Pasquinelli, A.E., Conte, D., Li, N., Parrish, S., Ha, I., Baillie, D.L., Fire, A., Ruvkun, G., and Mello, C.C. (2001). Genes and mechanisms related to RNA interference regulate expression of the small temporal RNAs that control *C. elegans* developmental timing. Cell *106*, 23–34.

Ha, I., Wightman, B., and Ruvkun, G. (1996). A bulged *lin-4/lin-14* RNA duplex is sufficient for *Caenorhabditis elegans lin-14* temporal gradient formation. Genes Dev. *10*, 3041–3050.

Hammond, S.M., Bernstein, E., Beach, D., and Hannon, G.J. (2000). An RNA-directed nuclease mediates post-transcriptional gene silencing in *Drosophila* cells. Nature *404*, 293–296.

Hammond, S.M., Boettcher, S., Caudy, A.A., Kobayashi, R., and Hannon, G.J. (2001). Argonaute2, a link between genetic and biochemical analyses of RNAi. Science *293*, 1146–1150.

Hannon, G.J. (2002). RNA interference. Nature *418*, 244–251.

Hohjoh, H. (2002). RNA interference (RNAi) induction with various types of synthetic oligonucleotide duplexes in cultured human cells. FEBS Lett. *521*, 195–199.

Holen, T., Amarzguioui, M., Wiiger, M.T., Babaie, E., and Prydz, H. (2002). Positional effects of short interfering RNAs targeting the human coagulation trigger Tissue Factor. Nucleic Acids Res. *30*, 1757–1766.

Hutvágner, G., McLachlan, J., Pasquinelli, A.E., Balint, É., Tuschl, T., and Zamore, P.D. (2001). A cellular function for the RNA-interference enzyme Dicer in the maturation of the *let-7* small temporal RNA. Science *293*, 834–838.

Hutvágner, G., and Zamore, P.D. (2002a). A microRNA in a multiple-turnover RNAi enzyme complex. Science, in press. Published online August 1, 2002. 10.1126/science.1073827

Hutvágner, G., and Zamore, P.D. (2002b). RNAi: nature abhors a double-strand. Curr. Opin. Genet. Dev. *12*, 225–232.

Ketting, R.F., Fischer, S.E., Bernstein, E., Sijen, T., Hannon, G.J., and Plasterk, R.H. (2001). Dicer functions in RNA interference and in synthesis of small RNA involved in developmental timing in *C. elegans*. Genes Dev. *15*, 2654–2659.

Klahre, U., Crete, P., Leuenberger, S.A., Iglesias, V.A., and Meins, F., Jr. (2002). High molecular weight RNAs and small interfering RNAs induce systemic posttranscriptional gene silencing in plants. Proc. Natl. Acad. Sci. USA *99*, 11981–11986.

Knight, S.W., and Bass, B.L. (2001). A role for the RNase III enzyme DCR-1 in RNA interference and germ line development in *Caenorhabditis elegans*. Science *293*, 2269–2271.

Lee, R.C., Feinbaum, R.L., and Ambros, V. (1993). The *C. elegans* heterochronic gene *lin-4* encodes small RNAs with antisense complementarity to *lin-14*. Cell *75*, 843–854.

Lewis, D.L., Hagstrom, J.E., Loomis, A.G., Wolff, J.A., and Herweijer, H. (2002). Efficient delivery of siRNA for inhibition of gene expression in postnatal mice. Nat. Genet. *33*, 107–108.

Lipardi, C., Wei, Q., and Paterson, B.M. (2001). RNAi as random degradative PCR. siRNA primers convert mRNA into dsRNAs that are degraded to generate new siRNAs. Cell *107*, 297–307.

Martens, H., Novotny, J., Oberstrass, J., Steck, T.L., Postlethwait, P., and Nellen, W. (2002). RNAi in Dictyostelium: the role of RNA-directed RNA polymerases and double-stranded RNase. Mol. Biol. Cell *13*, 445–453.

Martinez, J., Patkaniowska, A., Urlaub, H., Lührmann, R., and Tuschl, T. (2002). Single-stranded antisense siRNAs guide target RNA cleavage in RNAi. Cell *110*, 563–574.

McCaffrey, A.P., Meuse, L., Pham, T.T., Conklin, D.S., Hannon, G.J., and Kay, M.A. (2002). Gene expression: RNA interference in adult mice. Nature *418*, 38–39.

Moss, E.G., Lee, R.C., and Ambros, V. (1997). The cold shock domain protein LIN-28 controls developmental timing in *C. elegans* and is regulated by the *lin-4* RNA. Cell *88*, 637–646.

Mourrain, P., Beclin, C., Elmayan, T., Feuerbach, F., Godon, C., Morel, J.B., Jouette, D., Lacombe, A.M., Nikic, S., Picault, N., et al. (2000). Arabidopsis SGS2 and SGS3 genes are required for posttranscriptional gene silencing and natural virus resistance. Cell *101*, 533–542.

Nishikura, K. (2001). A short primer on RNAi: RNA-directed RNA polymerase acts as a key catalyst. Cell *107*, 415–418.

Nykänen, A., Haley, B., and Zamore, P.D. (2001). ATP requirements and small interfering RNA structure in the RNA interference pathway. Cell *107*, 309–321.

Olsen, P.H., and Ambros, V. (1999). The *lin-4* regulatory RNA controls developmental timing in *Caenorhabditis elegans* by blocking LIN-14 protein synthesis after the initiation of translation. Dev. Biol. *216*, 671–680.

Reinhart, B.J., Slack, F.J., Basson, M., Pasquinelli, A.E., Bettinger, J.C., Rougvie, A.E., Horvitz, H.R., and Ruvkun, G. (2000). The 21-

nucleotide *let-7* RNA regulates developmental timing in *Caenorhabditis elegans*. Nature *403*, 901–906.

Reinhart, B.J., Weinstein, E.G., Rhoades, M.W., Bartel, B., and Bartel, D.P. (2002). microRNAs in plants. Genes Dev. *16*, 1616–1626.

Seggerson, K., Tang, L., and Moss, E.G. (2002). Two genetic circuits repress the *Caenorhabditis elegans* heterochronic gene *lin-28* after translation initiation. Dev. Biol. *243*, 215–225.

Sijen, T., Fleenor, J., Simmer, F., Thijssen, K.L., Parrish, S., Timmons, L., Plasterk, R.H., and Fire, A. (2001). On the role of RNA amplification in dsRNA-triggered gene silencing. Cell *107*, 465–476.

Smardon, A., Spoerke, J., Stacey, S., Klein, M., Mackin, N., and Maine, E. (2000). EGO-1 is related to RNA-directed RNA polymerase and functions in germ-line development and RNA interference in *C. elegans*. Curr. Biol. *10*, 169–178.

Tabara, H., Sarkissian, M., Kelly, W.G., Fleenor, J., Grishok, A., Timmons, L., Fire, A., and Mello, C.C. (1999). The *rde-1* gene, RNA interference, and transposon silencing in *C. elegans*. Cell *99*, 123–132.

Tabara, H., Yigit, E., Siomi, H., and Mello, C.C. (2002). The dsRNA binding protein RDE-4 interacts with RDE-1, DCR-1, and a DexH-Box helicase to direct RNAi in *C. elegans*. Cell *109*, 861–871.

Tijsterman, M., Ketting, R.F., Okihara, K.L., Sijen, T., and Plasterk, R.H. (2002). RNA helicase MUT-14-dependent gene silencing triggered in *C. elegans* by short antisense RNAs. Science *295*, 694–697.

Wightman, B., Ha, I., and Ruvkun, G. (1993). Posttranscriptional regulation of the heterochronic gene *lin-14* by *lin-4* mediates temporal pattern formation in *C. elegans*. Cell *75*, 855–862.

Zamore, P., Tuschl, T., Sharp, P., and Bartel, D. (2000). RNAi: double-stranded RNA directs the ATP-dependent cleavage of mRNA at 21 to 23 nucleotide intervals. Cell *101*, 25–33.

Zeng, Y., Wagner, E.J., and Cullen, B.R. (2002). Technique: both natural and designed microRNAs can inhibit the expression of cognate mRNAs when expressed in human cells. Mol. Cell *9*, 1327–1333.

ACADEMIC PRESS

Available online at www.sciencedirect.com

SCIENCE DIRECT®

Methods 30 (2003) 330–336

METHODS

www.elsevier.com/locate/ymeth

In vitro analysis of RNA interference in *Drosophila melanogaster*

Benjamin Haley, Guiliang Tang, and Phillip D. Zamore*

Department of Biochemistry and Molecular Pharmacology, University of Massachusetts Medical School, Lazare Research Building, Room 825, 364 Plantation Street, Worcester, MA 01605, USA

Accepted 7 February 2003

Abstract

Double-stranded RNA (dsRNA) triggers the destruction of mRNA sharing sequence with the dsRNA, a phenomenon termed RNA interference (RNAi). The dsRNA is converted by endonucleolytic cleavage into 21- to 23-nt small interfering RNAs (siRNAs), which direct a multiprotein complex, the RNA-induced silencing complex to cleave RNA complementary to the siRNA. RNAi can be recapitulated in vitro in lysates of syncytial blastoderm Drosophila embryos. These lysates reproduce all of the known steps in the RNAi pathway in flies and mammals. Here we explain how to prepare and use *Drosophila* embryo lysates to dissect the mechanism of RNAi.

Keywords: RNA interference; RNAi; Double-stranded RNA; Small interfering RNA; siRNA; RNA degradation; Posttranscriptional gene silencing; PTGS

1. Introduction

In animals, double-stranded RNA (dsRNA) induces potent and specific gene silencing by a phenomenon known as RNA interference (RNAi). When the complete sequence of an animal's genome is known, RNAi can be used to induce a loss-of-function phenotype for any gene, without recourse to labor-intensive, traditional genetic methods. RNAi can also be used to verify or complement existing genetic mutations. The rapid adoption of RNAi as a surrogate genetics tool stems from both its potency and its specificity [1–5]. Despite apparent differences in mechanism, the RNAi pathway is widely conserved, and RNAi has been demonstrated in such widely diverged eukaryotes as *Neurospora*, trypanosomes, and mammals [1,3,6–15]. However, while many researchers routinely use RNAi as a tool, the actual mechanism by which it works remains incompletely understood.

RNAi is triggered by the introduction of dsRNA, typically longer than 200 bp [4]. The dsRNA is converted into 21- to 23-nt RNA duplexes, termed small interfering RNAs (siRNAs), by ATP-dependent endonucleolytic cleavage [16,17]. siRNAs are the specificity determinants of the RNAi pathway [17–19]. The RNase III enzyme, Dicer, mediates this initial cleavage event [20], yielding double-stranded siRNAs with 2-nucleotide 3′ overhangs, 5′-terminal phosphates, and 3′ hydroxyls [17,21]. The initial processing of dsRNA can be bypassed by synthetic oligonucleotides bearing the same structure as Dicer-produced siRNAs [3,17,18]. In *Drosophila* these siRNAs are ultimately incorporated into in an ~550-kDa ribonucleoprotein complex (RNP) that mediates target cleavage [22,23], although a smaller complex with target-cleaving activity has also been identified [21]. This smaller complex likely corresponds to a minimal active RNA-induced silencing complex and contains single-stranded siRNA [21]. In addition, in vitro experiments have identified an ~360-kDa RNP that contains double-stranded siRNA but is not yet competent for mediating target cleavage [21]. Although the 360-kDa complex is inactive, its formation seems to be a prerequisite for downstream events in the RNAi pathway.

2. Preparation of translationally active *Drosophila* embryo lysates that recapitulate RNAi in vitro

A cell-free system for studying RNAi in vitro was first described by Tuschl and co-workers in 1999 [24]. This

* Corresponding author.
E-mail address: phillip.zamore@umassmed.edu (P.D. Zamore).

1046-2023/03/$ - see front matter © 2003 Elsevier Science (USA). All rights reserved.
doi:10.1016/S1046-2023(03)00052-5

lysate, which is prepared from early *Drosophila melanogaster* syncytial blastoderm embryos, efficiently translates ^{7m}G-capped exogenous mRNAs and recapitulates in vitro RNAi triggered by both long dsRNA and synthetic or native siRNAs. The use of syncytial blastoderm embryos allows the identification of 5′ cleavage products during the RNAi reaction, because ^{7m}G-capped mRNA lacking a poly(A) tail is stable in *Drosophila* embryos prior to the midblastula transition, which occurs at 25 °C about 2 h after egg-laying.

Rearing large populations of fruit flies and the preparation of yeast paste and apple juice agar have been described elsewhere [25]. Zero- to 2-h-old fly embryos are collected on yeasted apple juice agar from population cages maintained at 25 °C and 70–80% relative humidity. Embryos are harvested using a wet, $1\frac{1}{2}$-in. (~3.75-cm), synthetic-bristle paint brush and washed into a set of stacked nylon-mesh sieves. The sieve is designed so that flies, larvae, and debris are retained on the upper sieve (500-μm nylon mesh; McMaster–Carr) and embryos are captured by the lower (70-μm nylon mesh; McMaster–Carr). The upper sieve is removed, and the embryos in the lower sieve are dechorionated by immersion in 50% (v/v) bleach, prepared immediately before use, for 4–5 min, washed extensively with cold water to remove all traces of bleach, blotted dry with paper tissues (Kimwipes; Kimberly–Clark) from beneath the sieve, and transferred to a chilled, tared Potter–Elvehjem tissue grinder (Kontes). Embryos are lysed in 1 ml lysis buffer (see Appendix A) containing 5 mM DTT and 1 mg/ml complete "mini" protease inhibitor tablets (Roche) per gram of damp embryos. The lysate is then clarified by centrifugation at 14,000×g for 25 min at 4 °C. The supernatant is aliquoted into chilled microcentrifuge tubes, flash frozen in liquid nitrogen and stored at −80 °C. Lysate typically retains activity for at least 6 months.

3. Preparation of double-stranded RNA

3.1. PCR strategy for producing transcription templates

We typically use PCR to generate DNA templates for the transcription of RNA. The 5′ PCR primer is designed to include at its 5′ end a T7 promoter sequence, although T3 or SP6 could, in principle, be used instead. The T7 promoter is followed by 15–20 bases of sequence from the desired transcript RNA. In addition to the final transcribed G of the T7 promoter, one or two additional guanosines should be included immediately after the promoter sequence to ensure efficient transcription. A 20-nt, 3′ PCR primer is designed to be complementary to the target sequence 200–1000 bases downstream of the 5′ sequences. Two separate primer pairs are used to generate templates for the transcription of sense and antisense RNA strands. We typically pool 5 to 10 100-μl PCR reaction for each DNA template. The PCR products are precipitated directly from the reaction by the addition of 2.5 volumes of absolute ethanol and 1/10 volume of 3 M sodium acetate. The precipitate is recovered by centrifugation, washed in 70% ethanol, dried under vacuum, and redissolved in 1× T7 transcription buffer to give a stock of DNA template 10-fold more concentrated than the original PCR reaction.

3.2. In vitro transcription with T7 RNA polymerase

To generate uniformly ^{32}P-radiolabeled RNA, we typically assemble a 50-μl reaction containing 5-μl 10× T7 buffer (see Appendix A), 0.5 μl 1 M DTT, 2.5 μl 10 mM ATP, 2.5 μl 100 mM UTP, 2.5 μl 100 mM CTP, 4 μl 100 mM GTP, 25 μl [α-^{32}P]ATP (40 mCi/ml, 3000 Ci/mmol, available from ICN as a custom order), 2.5 μl PCR template (as described above), 1 μl RNasin (Promega), 2.5 μl H_2O, and 2 μl recombinant, histidine-tagged T7 polymerase. For the production of nonradioactive RNA, we typically prepare a 100-μl reaction containing 10 μl 10× T7 transcription buffer, 3 μl PCR template (described above), 0.5 μl 1 M DTT, 5 μl 100 mM ATP, 5 μl 100 mM CTP, 5 μl 100 mM UTP, 8 μl 100 mM GTP, 61.5 μl H_2O, and 2 μl T7 polymerase.

3.3. Gel purification of in vitro-transcribed RNA

Gel purification is an essential step to eliminate the DNA template and ensure full-length RNA. After incubation at 37 °C for 2 h, reactions are stopped by adding an equal volume of 8 M urea stop mix (see Appendix A), heated at 95 °C for 2 min, and then purified by electrophoresis on a preparative denaturing acrylamide gel. RNA is detected by UV shadowing or phosphorimagery. The RNA-containing portion of the gel is excised and transcripts are recovered by soaking the gel slice in 1–2 ml of 2× PK buffer (see Appendix A) tumbling overnight at room temperature. The eluate is then phenol extracted and the RNA precipitated with 2.5 volumes of absolute ethanol. The RNA precipitate is resuspended in pure, sterile H_2O. Diethyl pyrocarbonate (DEPC)-treated water should not be used as it is impossible to get rid of all the DEPC, which can inhibit RNAi and translation.

After purification, the concentration of each transcript is determined. We typically measure the absorbance at 260 nm of 2 μl RNA stock diluted into 198 μl H_2O. Concentration is calculated by the equation

$$C = (A_{260} \times \text{dilution factor}) / (10,313 \times \text{number of nucleotides}),$$

where C is in molar and the dilution factor in this instance is 100.

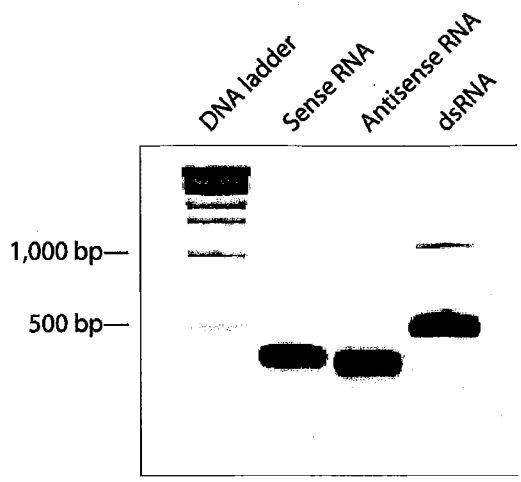

Fig. 1. Native gel analysis of dsRNA. 1 μM stocks of in vitro-transcribed sense and antisense RNAs (501 nt each) were annealed in 1× lysis buffer. dsRNA formation was confirmed by electrophoresis through a 2% native agarose gel. The markers are a 1 kb DNA ladder (Gibco BRL). The gel was stained with ethidium bromide.

3.4. Annealing the in vitro-transcribed dsRNA

Equal volumes of 1 μM stocks of each sense and antisense RNA strands are annealed by mixing them with an equal volume of 2× lysis buffer. The mixture is heated for 5 min at 95 °C and then annealed overnight at 37 °C. To confirm double-strand formation, we typically analyze a small portion of the dsRNA on a native agarose gel run in 1× TBE buffer. ssRNA for both sense and antisense strands of the dsRNA should be run adjacent to the dsRNA product. dsRNA, unlike single-stranded RNA, typically runs with the same mobility as dsDNA, so we use dsDNA markers as size standards on the gel. The RNA is visualized by staining the gel with ethidium bromide or, for [^{32}P]RNAs, by drying the gel under vacuum onto a positively charged nylon membrane and detecting the RNA by phosphorimagery (Fig. 1).

4. Analysis of Dicer activity

A typical Dicer activity assay is performed as follows: for a 10-μl reaction, add 5 μl *Drosophila* lysate, 3 μl 40× reaction mixture (see Appendix A), 1 μl water, and 1 μl 50 nM uniformly ^{32}P-labeled dsRNA (5 nM final concentration). The reaction is incubated for 1–3 h at 25 °C. After an appropriate time, an aliquot of the reaction mixture should be quenched in 100 μl 2× PK buffer. Reactions are deproteinized by adding 10 μl 20 μg/μl proteinase K and 1 μl 20 μg/μl glycogen carrier (Roche) to each aliquot. After 10–60 min at 65 °C, the sample is phenol extracted and the RNA precipitated with 3 vol absolute ethanol. The precipitate is washed with 80% ethanol and the pellet redissolved in 20 μl formamide loading dye (see Appendix A). Dicer products are resolved by electrophoresis on a 15% denaturing polyacrylamide sequencing gel. 5′-^{32}P-radiolabeled synthetic RNA oligonucleotides are used as size markers. We typically include 14-, 19-, 21-, 25-, and 34-nt RNA markers (Fig. 2).

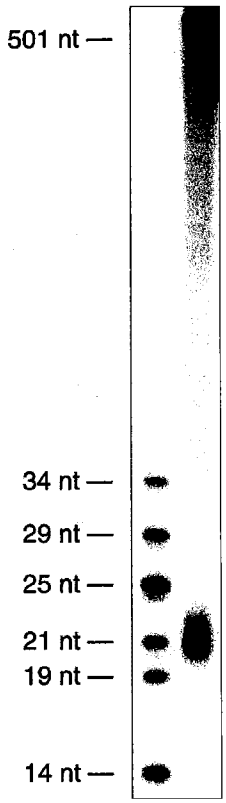

Fig. 2. A Dicer activity assay. Radiolabeled 501-nt dsRNA was incubated with *Drosophila* embryo lysate in a standard reaction. The reaction products were resolved by electrophoresis through a 15% sequencing gel. The markers are 5′-radiolabeled synthetic RNAs.

5. Design and preparation of synthetic siRNAs

Native siRNAs contain 5′-terminal phosphates and 2-nt 3′ overhangs [17]. Because native siRNAs are generated from much longer dsRNA, they form a pool of siRNA sequences spanning the length of the dsRNA. Therefore, they induce target RNA cleavage at a diverse array of sites. In contrast, synthetic siRNAs correspond to a single 21-nt sequence and trigger target cleavage at a corresponding single site [17,18,21]. How to design synthetic siRNAs, as well as where to purchase them, has been described elsewhere [26,27]. Synthetic siRNAs typically bear a 5′ hydroxyl, but are rapidly phosphorylated in the *Drosophila* embryo lysate by an endogenous kinase [21].

6. ^{32}P radiolabeling and purification of synthetic siRNAs

6.1. 5′ Radiolabeling of siRNA

A typical 10-μl siRNA 5′-end-labeling reaction contains 100 pmol (in 1 μl of water) of a single siRNA strand, 5 μl of [γ-^{32}P]ATP (6000 Ci/mmol, ⩾10 mCi/ml; NEN or ICN), 1 μl of T4 polynucleotide kinase (PNK; New England Biolabs (NEB)), 2 μl of PNK reaction buffer (NEB), and 1 μl of H_2O. The reaction is incubated at 37 °C for 1 h and then adjusted to 100 μl with water and run through a G-25 spin column (Roche) to remove unincorporated [^{32}P]ATP. The column flowthrough is precipitated with 3 vol of absolute ethanol, 1/10 vol of 3 M sodium acetate, and 1 μl of 20 mg/ml glycogen carrier. The precipitate is washed with 80% ethanol and then redissolved in 10 μl of formamide loading dye. The sample is then heated to 95 °C for 2 min and purified by electrophoresis on a 15% denaturing polyacrylamide gel. The radiolabeled siRNA is then visualized by phosphorimagery, excised from the gel, and eluted by tumbling overnight in 1 ml of 2× PK buffer. The eluate is phenol extracted, precipitated with 3 vol of absolute ethanol and then washed with 80% ethanol. Finally, the resulting precipitate is dissolved in 10 μl of H_2O. Typically, our yield is about 40% of the input siRNA.

6.2. 3′ Radiolabeling of siRNA

To label the 3′ end of an siRNA strand, we use radioactive cordycepin (3′ deoxyadenosine triphosphate) and poly(A) polymerase. Our typical reaction mixture contains 100 pmol (in 1 μl of water) of single-stranded siRNA, 2 μl of 5× reaction buffer (United States Biochemical), 5 μl of [^{32}P]cordycepin (5000 Ci/mmol, 10 mCi/ml; NEN), 1 μl of poly(A) polymerase, and 1 μl of H_2O. The reaction is incubated at 30 °C for 20 min. The ^{32}P-radiolabeled siRNA is purified as described above for 5′ siRNA radiolabeling.

6.3. Annealing the siRNA strands

To anneal the two complementary, 21-nt RNA strands, add equimolar concentrations of the antisense and sense siRNAs to an equal volume of 2× lysis buffer. Heat the mixture to 90 °C for 1 min, and cool at 37 °C for 1 h. At this point, the siRNA can be stored at −20 °C until needed.

A small portion of the duplexed siRNA should be resuspended in native loading dye (see Appendix A), resolved by electrophoresis on a 15% native polyacrylamide gel, and visualized by phosphorimagery. To ensure the siRNA does not denature during electrophoresis, the temperature of the gel should not exceed 25 °C. We clamp to the front glass plate a heat-dissipating aluminum plate bearing an inexpensive, self-stick, LCD thermometer (McMaster–Carr) on its face to ensure the gel does not exceed 25 °C. The ^{32}P-radiolabeled single-stranded siRNA used in the annealing reaction should be run in adjacent lanes of the gel as markers (Fig. 3).

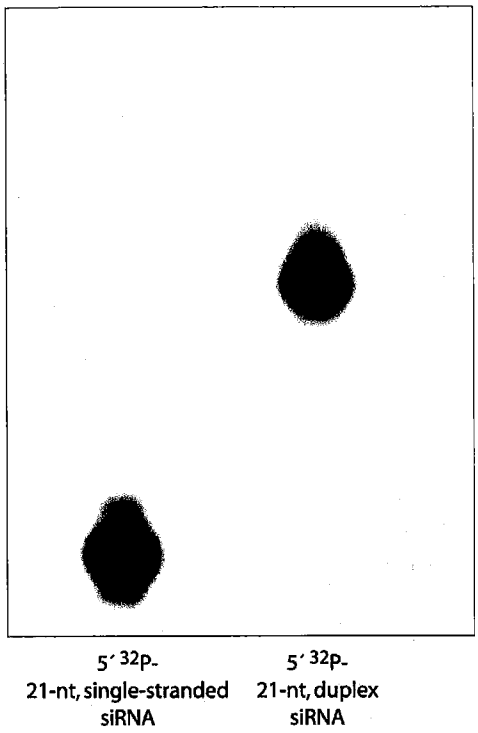

Fig. 3. Analysis of siRNA duplex formation. 5′-^{32}P-radiolabeled single-stranded or annealed siRNAs were electrophoresed in adjacent lanes of a 15% native polyacrylamide gel.

7. Analysis of RNAi in vitro using a translation-based assay

The usefulness of RNAi lies in its ability rapidly and specifically to destroy a target mRNA. RNAi can be monitored either by directly following the fate of the target mRNA or by using a dual luciferase-based translation assay [24]. The dual luciferase strategy provides less information about the mechanism of the RNAi pathway, but has the virtues of including an internal control and of high throughput. This assay relies on two evolutionarily distinct luciferase reporter genes from the firefly *Pyralis photinus* (*Pp*-luc) and the sea pansy *Renilla reniformis* (*Rr*-luc). In this system, dsRNA or siRNA can be used to target either of the two mRNAs, effectively knocking down expression of that target. Expression of the other, nonhomologous target is left unaltered and functions as an internal specificity control. Results are usually expressed by normalizing the expression of the targeted luciferase to the control

luciferase (e.g., *Pp*-luc/*Rr*-luc). A commercial kit for analyzing the dual luciferase expression is available from Promega (DLR Assay System) and single-tube and plate-reading luminometers are widely available. The assay is usually performed in triplicate, and errors are propagated by standard methods.

7.1. Design and preparation of capped mRNA

Because translation in the *Drosophila* embryo lysate is cap-dependent [24], mRNAs for *Pp*-luc or *Rr*-luc are transcribed in the presence of ^{7m}G(5′)ppp(5′)G cap analog. Although PCR templates can be used, we typically use plasmid transcription templates linearized with an appropriate restriction enzyme immediately after a 25- to 30-nt poly(A) stretch. We use 3 μl of a 2 μg/μl stock of linearized plasmid transcription template for a 100-μl reaction. From 100 mM stock solutions, add 5 μl each of ATP, CTP, and UTP, plus 1 μl of GTP. To this, add 10 μl of 10× T7 reaction buffer, 0.5 μl of 1 M DTT, 26.5 μl of water, 1 μl of RNasin (40 U/ml; Promega), 40 μl of 10 mM cap analog (^{7m}G(5′)ppp(5′)G; New England Biolabs), and 2 μl of the appropriate recombinant bacteriophage RNA polymerase (e.g., SP6 or T7). Incubate for 2 h at 37 °C. Stop the reaction by adding 7 μl of 500 mM EDTA to redissolve the insoluble Mg^{2+} · inorganic pyrophosphate precipitate. Precipitate the RNA transcripts with 2.5 M LiCl for 1 h on ice, centrifuge at 13,000×g for 10 min, wash with 80% ethanol, and resuspend pellet in 75 μl of H_2O. Examine 5 μl on a denaturing 2% agarose gel and visualize with ethidium bromide. To the remaining 70 μl add 10 μl of RQ1 DNase buffer (Promega), 5 μl of RQ1 DNase (Promega) and incubate for 30 min at 37 °C. Proteinase K digest (see above), phenol extract, and precipitate with 2.5 vol of absolute ethanol. Resuspend purified transcripts in H_2O, and determine concentrations by absorbance at 260 nm.

7.2. Translation-based dual-luciferase RNAi assay

For each reaction, place 5 μl *Drosophila* embryo lysate, 3 μl 40× reaction mix, 0.01–5 nM (final concentration) each capped luciferase transcript (as a mix in 1 μl water), and 100 nM siRNA or 5 nM long dsRNA corresponding to one of the two luciferase mRNA transcripts. As a translation efficiency control, a separate reaction should be made, in which lysis buffer is substituted for siRNA or dsRNA trigger. Incubate reactions at 25 °C for up to 3 h. At each appropriate time point, place a small aliquot into Passive Lysis Buffer (Promega) to quench the reaction. The DLR Assay System kit from Promega provides all the reagents necessary to generate a separate luminescent signal from either reporter gene. This assay effectively provides a quick and quantitative method for examining the effectiveness and specificity of RNAi. It works best with a dual-dispensing, plate-reading luminometer.

8. Analysis of RNAi in vitro using an mRNA cleavage assay

An alternative method for analyzing RNAi efficiency and specificity in vitro has been described [17,18,21]. This assay relies on the accumulation of the stable, 5′-capped cleavage products formed during RNAi. It is important to note that the accumulation of these 5′ cleavage products is proportional to the decrease in target mRNA only during the early, linear phase of the RNAi reaction. This phenomenon may likewise be true in vivo [28]. Each synthetic siRNA directs mRNA cleavage at a single site 10–11 nt from the siRNA 5′ end, across from the center of the siRNA. By using cap-radiolabeled mRNA, the 5′ cleavage product can be readily detected. The presence of an appropriately sized 5′ cleavage product is diagnostic of RNAi, providing a positive result that bolsters confidence that the disappearance of the target mRNA

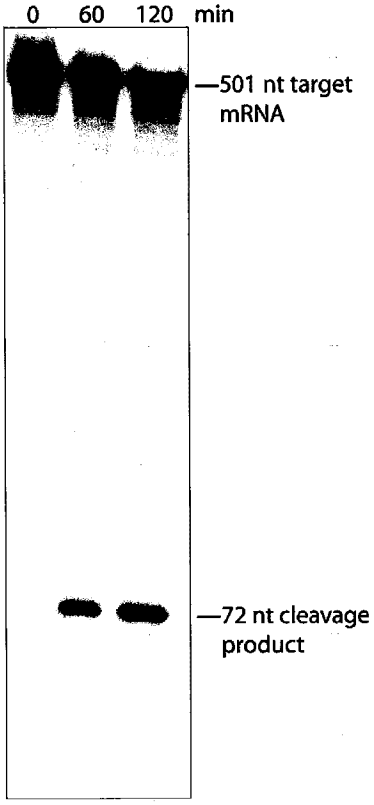

Fig. 4. In vitro RNAi reaction. A standard RNAi reaction was performed using a 501-nt, ^{32}P-cap-radiolabeled target RNA and 50 nM siRNA duplex corresponding to nucleotides 62–81 of the target. Reaction products were resolved by electrophoresis through an 8% denaturing polyacrylamide sequencing gel. The 72-nt 5′ cleavage product is diagnostic of siRNA-directed RNAi.

reflects RNAi rather than other nonsequence-specific RNA-degrading processes.

8.1. Design and preparation of cap-radiolabeled mRNA

Design and preparation of the target mRNA sequence should be performed as described under 'In vitro transcription with T7 RNA polymerase,' above. Following gel purification, 10 pmol of the uncapped mRNA target (in 1.75 μl of H_2O) is added to 5 μl of [α-^{32}P]GTP (3000 Ci/mmol, 40 mCi/ml, custom order; ICN), 1 μl of 10× guanylyl transferase buffer (see Appendix A), 0.5 μl of 0.1 mM DTT, 0.25 μl of 20 U/μl RNasin (Promega), 1 μl of 10 mM *S*-adenosyl methionine (SAM; Sigma) in SAM dilution buffer, and 0.5 μl of recombinant, heterodimeric vaccinia virus guanylyl transferase (e.g., Ambion). Incubate for 2 h at 37 °C, adjust the reaction to 100 μl with H_2O, and pass through a G-50 spin column (Roche). Gel purification of the radiolabeled target is performed by electrophoresis as described.

8.2. In vitro RNAi reaction using cap-radiolabeled mRNA

A standard RNAi reaction containing the 5′-^{32}P-cap-radiolabeled target mRNA is performed essentially as described for the translation-based assay. A 10-μl reaction is set up as follows: 5 μl *Drosophila* embryo lysate is added to 3 μl 40× reaction mix, 1 μl target mRNA (stock concentration 10–50 nM), and 1 μl synthetic siRNA (stock concentration 250–1000 nM) or dsRNA (stock concentration 50–100 nM). A control reaction substituting 1 μl 1× lysis buffer for the siRNA or dsRNA trigger serves as a control for nonspecific mRNA degradation. Incubate for up to 3 h at 25 °C and quench at each time point with 100 μl 2× PK buffer. Deproteinize as described above, add 1 μl 20 mg/ml glycogen carrier, and phenol extract. Precipitate with 3 vol absolute ethanol, wash with 80% ethanol, and redissolve in 20 μl formamide loading dye. Analyze by electrophoresis on a denaturing polyacrylamide sequencing gel, and visualize the 5′ cleavage products by phosphorimagery (Fig. 4). Radiolabeled markers are readily prepared by cap-radiolabeling commercially available 100 nt RNA ladder marker mixes with guanylyl transferase and [α-^{32}P]GTP as described above.

Appendix A

1. *1× lysis buffer*
   100 mM potassium acetate
   30 mM Hepes–KOH, pH 7.4
   2 mM magnesium acetate

2. *10× T7 transcription buffer*
   400 mM Tris–Cl, pH 7.9
   25 mM spermidine
   260 mM $MgCl_2$
   0.1% w/v Triton X-100

3. *10× PCR buffer*
   100 mM Tris–Cl, pH 8.3
   500 mM KCl
   15 mM $MgCl_2$
   0.1% w/v gelatin

4. *2× proteinase K buffer*
   200 mM Tris–Cl, pH 7.5
   25 mM EDTA, pH 8.0
   300 mM NaCl
   2% w/v sodium dodecyl sulfate

5. *2× urea stop mix/loading dye*
   8 M urea
   25 mM EDTA, pH 8.0
   0.025% w/v xylene cyanol FF
   0.025% w/v bromophenol blue

6. *Formamide loading dye*
   98% w/v deionized formamide
   10 mM EDTA, pH 8.0
   0.025% w/v xylene cyanol
   0.025% w/v bromophenol blue

7. *Native loading dye*
   3% w/v Ficoll-400
   0.04% w/v bromophenol blue
   2 mM Tris–Cl, pH 7.4

8. *10× Guanylyl transferase buffer*
   500 mM Tris–Cl, pH 8.0
   60 mM KCl
   12 mM $MgCl_2$
   25 mM DTT

9. *SAM dilution buffer*
   (To make 50 ml, add 6.96 μl 36 M H_2SO_4 and 5 ml absolute ethanol to 45 ml deionized water.)

10. *40× reaction mix*
    50 μl water
    20 μl 500 mM creatine monophosphate (Fluka; prepared fresh from powder)
    20 μl amino acid stock (Sigma; 1 mM each amino acid)
    2 μl 1 M DTT
    2 μl 20 U/μl RNasin (Promega)
    4 μl 100 mM ATP
    1 μl 100 mM GTP
    6 μl 2 U/μl creatine phosphokinase (Cal-Biochem), prepared by diluting 2 μl of a 20 U/μl stock in 18 μl 1 × lysis buffer containing 2 mM DTT
    16 μl 1 M potassium acetate

References

[1] J.R. Kennerdell, R.W. Carthew, Cell 95 (1998) 1017–1026.

[2] A. Grishok, H. Tabara, C. Mello, Science 287 (2000) 2494–2497.
[3] S.M. Elbashir, J. Harborth, W. Lendeckel, A. Yalcin, K. Weber, T. Tuschl, Nature 411 (2001) 494–498.
[4] A. Fire, S. Xu, M.K. Montgomery, S.A. Kostas, S.E. Driver, C.C. Mello, Nature 391 (1998) 806–811.
[5] L. Timmons, A. Fire, Nature 395 (1998) 854.
[6] K. Ui-Tei, S. Zenno, Y. Miyata, K. Saigo, FEBS Lett. 479 (2000) 79–82.
[7] L. Misquitta, B.M. Paterson, Proc. Natl. Acad. Sci. USA 96 (1999) 1451–1456.
[8] H. Ngo, C. Tschudi, K. Gull, E. Ullu, Proc. Natl. Acad. Sci. USA 95 (1998) 14687–14692.
[9] J.U. Lohmann, I. Endl, T.C. Bosch, Dev. Biol. 214 (1999) 211–214.
[10] A. Sánchez-Alvarado, P.A. Newmark, Proc. Natl. Acad. Sci. USA 96 (1999) 5049–5054.
[11] N.J. Caplen, S. Parrish, F. Imani, A. Fire, R.A. Morgan, Proc. Natl. Acad. Sci. USA 98 (2001) 9742–9747.
[12] J.C. Clemens, C.A. Worby, N. Simonson-Leff, M. Muda, T. Maehama, B.A. Hemmings, J.E. Dixon, Proc. Natl. Acad. Sci. USA 97 (2000) 6499–6503.
[13] N.J. Caplen, J. Fleenor, A. Fire, R.A. Morgan, Gene 252 (2000) 95–105.
[14] E. Billy, V. Brondani, H. Zhang, U. Muller, W. Filipowicz, Proc. Natl. Acad. Sci. USA 98 (2001) 14428–14433.
[15] S. Yang, S. Tutton, E. Pierce, K. Yoon, Mol. Cell. Biol. 21 (2001) 7807–7816.
[16] P. Zamore, T. Tuschl, P. Sharp, D. Bartel, Cell 101 (2000) 25–33.
[17] S.M. Elbashir, W. Lendeckel, T. Tuschl, Genes Dev. 15 (2001) 188–200.
[18] S.M. Elbashir, J. Martinez, A. Patkaniowska, W. Lendeckel, T. Tuschl, EMBO J. 20 (2001) 6877–6888.
[19] A.J. Hamilton, D.C. Baulcombe, Science 286 (1999) 950–952.
[20] E. Bernstein, A.A. Caudy, S.M. Hammond, G.J. Hannon, Nature 409 (2001) 363–366.
[21] A. Nykänen, B. Haley, P.D. Zamore, Cell 107 (2001) 309–321.
[22] S.M. Hammond, E. Bernstein, D. Beach, G.J. Hannon, Nature 404 (2000) 293–296.
[23] S.M. Hammond, S. Boettcher, A.A. Caudy, R. Kobayashi, G.J. Hannon, Science 293 (2001) 1146–1150.
[24] T. Tuschl, P.D. Zamore, R. Lehmann, D.P. Bartel, P.A. Sharp, Genes Dev. 13 (1999) 3191–3197.
[25] J.C. Sisson, in: W. Sullivan, M. Ashburner, R.S. Hawley (Eds.), Drosophila melanogaster, Cold Spring Harbor Laboratory Press, Cold Spring Harbor, NY, 2000, pp. 541–555.
[26] **http://www.mpibpc.gwdg.de/abteilungen/100/105/sirna.html**.
[27] S. Elbashir, J. Harborth, K. Weber, T. Tuschl, Methods Findings Exp. Clin. Pharmacol. 26 (2002) 199–213.
[28] T. Holen, M. Amarzguioui, M.T. Wiiger, E. Babaie, H. Prydz, Nucleic Acids Res. 30 (2002) 1757–1766.

Cell, Vol. 116, 831–841, March 19, 2004, Copyright ©2004 by Cell Press

RISC Assembly Defects in the *Drosophila* RNAi Mutant *armitage*

Yukihide Tomari,[1,3] Tingting Du,[1,3]
Benjamin Haley,[1,3] Dianne S. Schwarz,[1]
Ryan Bennett,[1] Heather A. Cook,[2]
Birgit S. Koppetsch,[2] William E. Theurkauf,[2,*]
and Phillip D. Zamore[1,*]
[1]Department of Biochemistry and Molecular Pharmacology
University of Massachusetts Medical School
Worcester, Massachusetts 01605
[2]Program in Molecular Medicine
University of Massachusetts Medical School
Worcester, Massachusetts 01605

Summary

The putative RNA helicase, Armitage (Armi), is required to repress *oskar* translation in *Drosophila* oocytes; *armi* mutant females are sterile and *armi* mutations disrupt anteroposterior and dorsoventral patterning. Here, we show that *armi* is required for RNAi. *armi* mutant male germ cells fail to silence *Stellate*, a gene regulated endogenously by RNAi, and lysates from *armi* mutant ovaries are defective for RNAi in vitro. Native gel analysis of protein-siRNA complexes in wild-type and *armi* mutant ovary lysates suggests that *armi* mutants support early steps in the RNAi pathway but are defective in the production of active RNA-induced silencing complex (RISC), which mediates target RNA destruction in RNAi. Our results suggest that *armi* is required for RISC maturation.

Introduction

In eukaryotes, long double-stranded RNA (dsRNA) silences genes homologous in sequence, a process termed RNA interference (RNAi; Fire et al., 1998). RNAi and other examples of RNA silencing have been observed in animals, plants, protozoa, and fungi (Cogoni and Macino, 1997; Kennerdell and Carthew, 1998; Ngo et al., 1998; Waterhouse et al., 1998; Lohmann et al., 1999; Sánchez-Alvarado and Newmark, 1999; Wianny and Zernicka-Goetz, 2000; Caplen et al., 2001; Elbashir et al., 2001a; Volpe et al., 2002; Schramke and Allshire, 2003). In plants, green algae, and invertebrates, RNAi defends the genome against mobile genetic elements, such as transposons and viruses, whose expression and activity increase in RNAi-defective mutants (Ketting et al., 1999; Ratcliff et al., 1999; Tabara et al., 1999; Dalmay et al., 2000; Mourrain et al., 2000; Wu-Scharf et al., 2000; Aravin et al., 2001; Sijen and Plasterk, 2003). The RNAi pathway also regulates endogenous gene expression for at least one *Drosophila* gene, *Stellate* (*Ste*), which is targeted for destruction by dsRNA transcribed from the *Suppressor-of-Stellate* (*Su(Ste)*) locus (Aravin et al., 2001).

*Correspondence: phillip.zamore@umassmed.edu (P.D.Z.) or william.theurkauf@umassmed.edu (W.E.T.)
[3]These authors contributed equally to this work.

Long dsRNA is converted by Dicer, a multidomain ribonuclease III enzyme, into small interfering RNAs (siRNAs) (Zamore et al., 2000; Bernstein et al., 2001; Billy et al., 2001), which serve as the specificity determinants of the RNAi pathway (Hamilton and Baulcombe, 1999; Hammond et al., 2000; Zamore et al., 2000; Elbashir et al., 2001b). siRNAs direct mRNA cleavage as part of a protein-siRNA complex called the RNA-induced silencing complex (RISC; Hammond et al., 2000, 2001). Members of the Argonaute family of proteins are core components of RISC or RISC-like complexes in flies (Hammond et al., 2001), worms (Tabara et al., 2002; Hutvágner et al., 2004), and humans (Caudy et al., 2002; Hutvágner and Zamore, 2002; Martinez et al., 2002; Mourelatos et al., 2002) and are required genetically for RNA silencing in every organism where their function has been studied (Tabara et al., 1999; Fagard et al., 2000; Grishok et al., 2000; Catalanotto et al., 2002; Caudy et al., 2002; Morel et al., 2002; Pal-Bhadra et al., 2002; Williams and Rubin, 2002; Doi et al., 2003).

Genetic studies also reveal the importance of helicase-domain proteins in the RNAi pathway. Putative DEA(H/D)-box helicases are required for posttranscriptional gene silencing (PTGS) in the green alga *Chlamydomonas reinhardtii* (Wu-Scharf et al., 2000) and RNAi in *C. elegans* (Tabara et al., 2002; Tijsterman et al., 2002). In *Drosophila*, mutations in *spindle-E* (*spn-E*), a gene encoding a putative DEAD-box helicase, abrogate endogenous RNAi-based repression of the *Ste* locus and trigger expression of retrotransposon mRNA in the germline (Aravin et al., 2001; Stapleton et al., 2001). In cultured *Drosophila* S2 cells, the putative helicase Dmp68 is a component of affinity-purified RISC (Ishizuka et al., 2002). Similarly, a putative DEAD-box RNA helicase, Gemin3, is a component of human RISC (Hutvágner and Zamore, 2002). Dicer, too, contains a putative ATP-dependent RNA helicase domain (Bernstein et al., 2001). Except for Dicer, no specific biochemical function in RNAi has been ascribed to any of these helicase proteins.

armitage (*armi*) was identified in a screen for maternal effect mutants that disrupt axis specification in *Drosophila* (Cook et al., 2004 [this issue of *Cell*]). Armitage protein (Armi) is a member of a family of putative ATP-dependent helicases distinct from the DEA(H/D) box proteins (Koonin, 1992). Armi is homologous across its putative helicase domain to SDE3 (Cook et al., 2004), which is required for PTGS in *Arabidopsis* (Dalmay et al., 2001). Because PTGS in plants is mechanistically related to RNAi in animals, Armi may play a role in RNAi in flies. Here, we show that *armi* is required for RNAi. *armi* mutant male germ cells fail to silence *Stellate*, a gene regulated endogenously by RNAi (Schmidt et al., 1999; Aravin et al., 2001; Stapleton et al., 2001), and lysates from *armi* mutant ovaries are defective for RNAi in vitro. Native gel analysis of protein-siRNA complexes in wild-type and *armi* mutant ovary lysates suggests that *armi* mutants support early steps in the RNAi pathway but are defective in the production of the RISC. Our

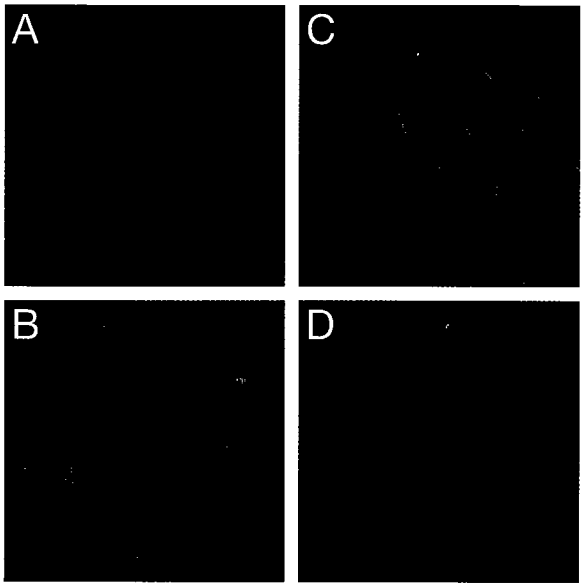

Figure 1. Armi Is Required for *Ste* Silencing in Fly Testes

The testes from wild-type (A), *armi*^{1} (B), *armi*$^{72.1}$ (C), and *armi*$^{rev39.2}$ flies (D) were stained for DNA (red) and Ste protein (green).

results suggest that *armi* is required for the assembly of siRNA into functional RISC.

Results

Armi Is Required for *Ste* Silencing

Silencing of the X-linked *Ste* gene by the highly homologous Y-linked *Su(Ste)* locus is an example of endogenous RNAi (Aravin et al., 2001; Gvozdev et al., 2003). In *Drosophila* testes, symmetrical transcription of *Su(Ste)* produces dsRNA, which is processed into siRNAs (Gvozdev et al., 2003). *Su(Ste)* siRNAs direct the degradation of *Ste* mRNA (Aravin et al., 2001). Inappropriate expression of Ste protein in testes is diagnostic of disruption of the RNAi pathway. Both the Argonaute protein, *aub*, and the putative DEAD-box helicase, *spn-E,* are required for RNAi in *Drosophila* oocytes (Kennerdell et al., 2002). Both mutants fail to silence *Ste*, as evidenced by the accumulation of Ste protein crystals in the testes of *aub* and *spn-E* mutants (Schmidt et al., 1999; Stapleton et al., 2001). No Ste protein is detected in wild-type testes (Figure 1A). Strikingly, Ste protein accumulates in testes of two different *armi* alleles, *armi*^{1} and *armi*$^{72.1}$ (Figures 1B and 1C). Neither allele is expected to be a true null because *armi*^{1} is caused by a P element insertion 5′ to the open reading frame, whereas *armi*$^{72.1}$, which was created by an imprecise excision of the *armi*^{1} P element, corresponds to a deletion of sequences in the 5′ untranslated region (C. Klattenhoff and W.E.T., unpublished observations). Ste silencing is re-established in males homozygous for the revertant chromosome, *armi*$^{rev\ 39.2}$ (henceforth, *armi*^{rev}; Cook et al., 2004), which was generated by excision of the *armi*^{1} P element (Figure 1D). These data suggest a role for Armi in *Drosophila* RNAi.

Immunofluorescent detection of Ste protein in testes implicates both *armi* alleles in endogenous RNAi, but provides only a qualitative measure of allele strength. Since Ste protein in males reduces their fertility (Belloni et al., 2002), the percent of embryos that hatch when mutant males are mated to wild-type (Oregon R) females provides a more quantitative measure of *Ste* dysregulation. We measured hatch rates for the offspring of wild-type, *armi*^{1}, *armi*$^{72.1}$, and *spn-E*^{1} homozygous males mated to Oregon R females. For *spn-E*^{1} males, 82% of the progeny hatched (n = 652). Seventy-five percent of the progeny of *armi*^{1} males hatched (n = 571), but only 45% for *armi*$^{72.1}$ (n = 710). In contrast, 97% of the offspring of wild-type males hatched (n = 688). Thus, *armi*$^{72.1}$ is a stronger allele than *armi*^{1}, at least with respect to the requirement for *armi* in testes.

Ovary Lysate Recapitulates RNAi In Vitro

Drosophila syncitial blastoderm embryo lysate has been used widely to study the RNAi pathway (Tuschl et al., 1999). However, *armi* flies lay few eggs, making it difficult to collect enough embryos to make lysate. To surmount this problem, we prepared lysates from ovaries manually dissected from wild-type or mutant females. Approximately 10 μl of lysate can be prepared from ~50 ovaries.

We used the well-characterized siRNA-directed mRNA cleavage assay (Elbashir et al., 2001b, 2001c) to evaluate the capacity of ovary lysate to support RNAi in vitro. Incubation in ovary lysate of a 5′ ^{32}P-cap-radiolabeled firefly luciferase mRNA target with a complementary siRNA duplex yielded the 5′ cleavage product diagnostic of RNAi (Figure 2A). siRNAs containing 5′ hydroxyl groups are rapidly phosphorylated in vitro and in vivo, but modifications that block phosphorylation eliminate siRNA activity (Nykänen et al., 2001; Chiu and Rana, 2002; Martinez et al., 2002; Schwarz et al., 2002; Saxena et al., 2003). Replacing the 5′ hydroxyl of the antisense siRNA strand with a 5′ methoxy group completely blocked RNAi in the ovary lysate (Figure 2A). In *Drosophila*, siRNAs bearing a single 2′-deoxy nucleotide at the 5′ end are poor substrates for the kinase that phosphorylates 5′ hydroxy siRNAs (Nykänen et al., 2001). A comparison of initial cleavage rates shows that in ovary lysate, target cleavage was slower for siRNAs with a 2′-deoxy nucleotide at the 5′ end of the antisense strand than for standard siRNAs (Figure 2B). Furthermore, the rate of target cleavage was fastest when the siRNA was phosphorylated before its addition to the reaction (Figure 2B). A similar enhancement from pre-phosphorylation was reported for siRNA injected into *Drosophila* embryos (Boutla et al., 2001). We conclude that lysates from *Drosophila* ovaries faithfully recapitulate RNAi directed by siRNA duplexes.

armi Ovary Lysates Are Defective in RNAi

In contrast to wild-type, lysates prepared from *armi*$^{72.1}$ ovaries do not support siRNA-directed target cleavage in vitro: no cleavage product was observed in the *armi*$^{72.1}$ lysate after 2 hr (Figure 3A). This result was observed for more than ten independently prepared lysates. To determine if the RNAi defect was allele specific, we tested ovaries from *armi*^{1}. Phenotypically, this allele is weaker than *armi*$^{72.1}$ in its effects on both male fertility (above) and oogenesis. For *armi*$^{72.1}$ females, 92% of the eggs lacked dorsal appendages, compared to 67% for *armi*^{1} eggs, and some *armi*^{1} eggs had wild-type or par-

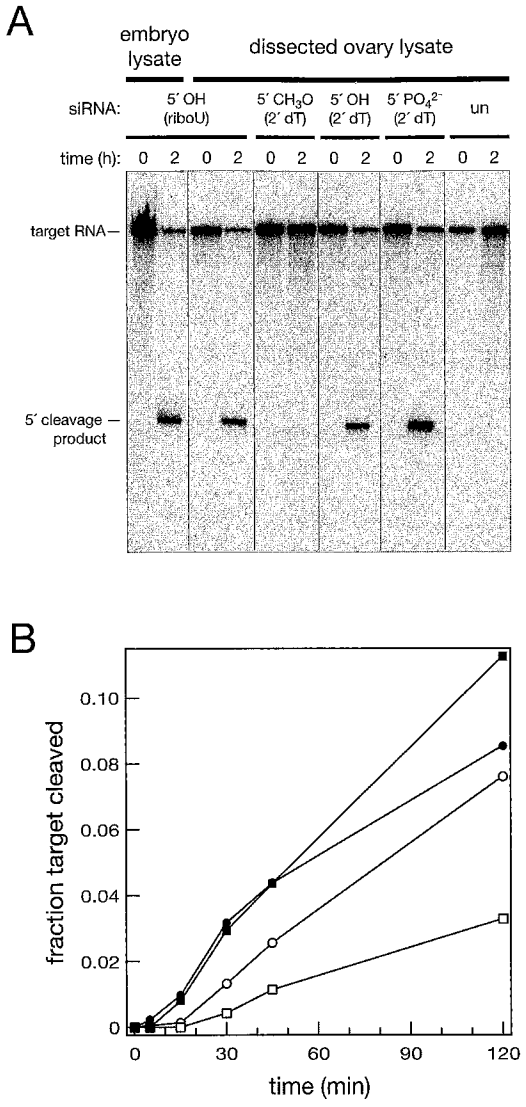

Figure 2. *Drosophila* Ovary Lysate Can Recapitulate RNAi In Vitro

(A) RNAi reactions in embryo and ovary lysates using complementary siRNA duplexes (with 5′ modifications) or an unrelated siRNA (un).

(B) mRNA cleavage rate in ovary lysate using 5′ modified siRNA. Filled squares, 5′ PO_4^{2-} (2′ dT); filled circles, 5′ PO_4^{2-} (2′ riboU); open squares, 5′ OH (2′ dT); open circles, 5′ OH (2′ riboU).

tially fused dorsal appendages (Figure 3B). Consistent with its weaker phenotype, the *armi*^{1} allele showed a small amount of RNAi activity in vitro (Figure 3C). The two alleles were analyzed together at least four times using independently prepared lysates. In all assays, total protein concentration was adjusted to be equal. Lysate from the revertant allele, *armi*^{rev}, which has wild-type dorsal appendages, showed robust RNAi, demonstrating that the RNAi defect in the mutants is caused by mutation of *armi*, not an unlinked gene.

armi Ovary Lysates Are Impaired in RISC Assembly

The rate of target cleavage was much slower for *armi*^{1} than for wild-type (Figure 3D). Since the rate of target cleavage in this assay usually reflects the concentration of RISC (Schwarz et al., 2003), we hypothesized that *armi* mutants are defective in RISC assembly. To test this hypothesis, we developed a method to measure RISC that requires less lysate than previously described techniques (Figure 4A). Double-stranded siRNA was incubated with ovary lysate in a standard RNAi reaction. To detect RISC, we added a 5′ ^{32}P-radiolabled, 2′-*O*-methyl oligonucleotide complementary to the antisense strand of the siRNA. Like target RNAs, 2′-*O*-methyl oligonucleotides can bind to RISC containing a complementary siRNA, but unlike RNA targets, they cannot be cleaved and binding is essentially irreversible (Hutvágner et al., 2004). RISC/2′-*O*-methyl oligonucleotide complexes were then resolved by electrophoresis through an agarose gel.

To validate the method, we examined RISC formation in embryo lysate. Four distinct complexes (C1, C2, C3, C4) were formed when siRNA was added to the reaction (Supplemental Figure S1A at http://www.cell.com/cgi/content/full/116/6/831/DC1). Formation of these complexes required ATP and was disrupted by pre-treatment of the lysate with the alkylating agent *N*-ethylmaleimide (NEM), but it was refractory to NEM treatment after RISC assembly; these are all properties of RNAi itself (Nykänen et al., 2001). No complex was observed with an siRNA unrelated to the 2′-*O*-methyl oligonucleotide (Supplemental Figure S1A on the *Cell* website, "un"). The amount of complex formed by different siRNA sequences correlated well with their capacity to mediate cleavage (data not shown). The four complexes were also detected in wild-type ovary lysate (Supplemental Figure S1B online), suggesting that the same RNAi machinery is used during oogenesis and early embryogenesis. The lower amount of RISC formed in ovary compared to embryo lysates can be explained by the lower overall protein concentration of ovary lysates.

We used the 2′-*O*-methyl oligonucleotide/native gel assay to analyze RISC assembly in *armi* mutant ovary lysates. *armi* mutants were deficient in RISC assembly. Representative data are shown in Figure 4B and quantitative results from four independent assays in Figure 4C. The extent of the deficit correlated with allele strength: less C3/C4 complex formed in lysate from the strong *armi*$^{72.1}$ allele than from *armi*^{1} (Figures 4B and 4C). Compared to the phenotypically wild-type *armi*^{rev}, >10-fold less RISC was produced in *armi*$^{72.1}$.

The defect in RISC assembly in *armi* mutants is similar to that observed in lysates from *aub*^{HN2} ovaries (Figures 4B and 4C). *aub* mutants do not support RNAi following egg activation and fail to silence the *Ste* locus in testes (Schmidt et al., 1999; Kennerdell et al., 2002), and lysates from *aub*^{HN2} ovaries do not support RNAi in vitro (data not shown). Aub is one of five *Drosophila* Argonaute proteins, core constituents of RISC. It is therefore not surprising that Aub is required for RISC assembly. Since RISC assembly in vitro was not detectable in *aub*^{HN2} lysates, our data suggest that Aub is the primary Argonaute protein recruited to exogenous siRNA in *Drosophila* ovaries. In contrast, ovaries from *nanos*^{BN}, a maternal effect mutant not implicated in RNAi, were fully competent for both RISC assembly (Figure 4C) and siRNA-directed target RNA cleavage (data not shown).

Identification of Intermediates in RISC Assembly

These data suggest that both *armi* and *aub* are required genetically for RISC assembly, but they provide no in-

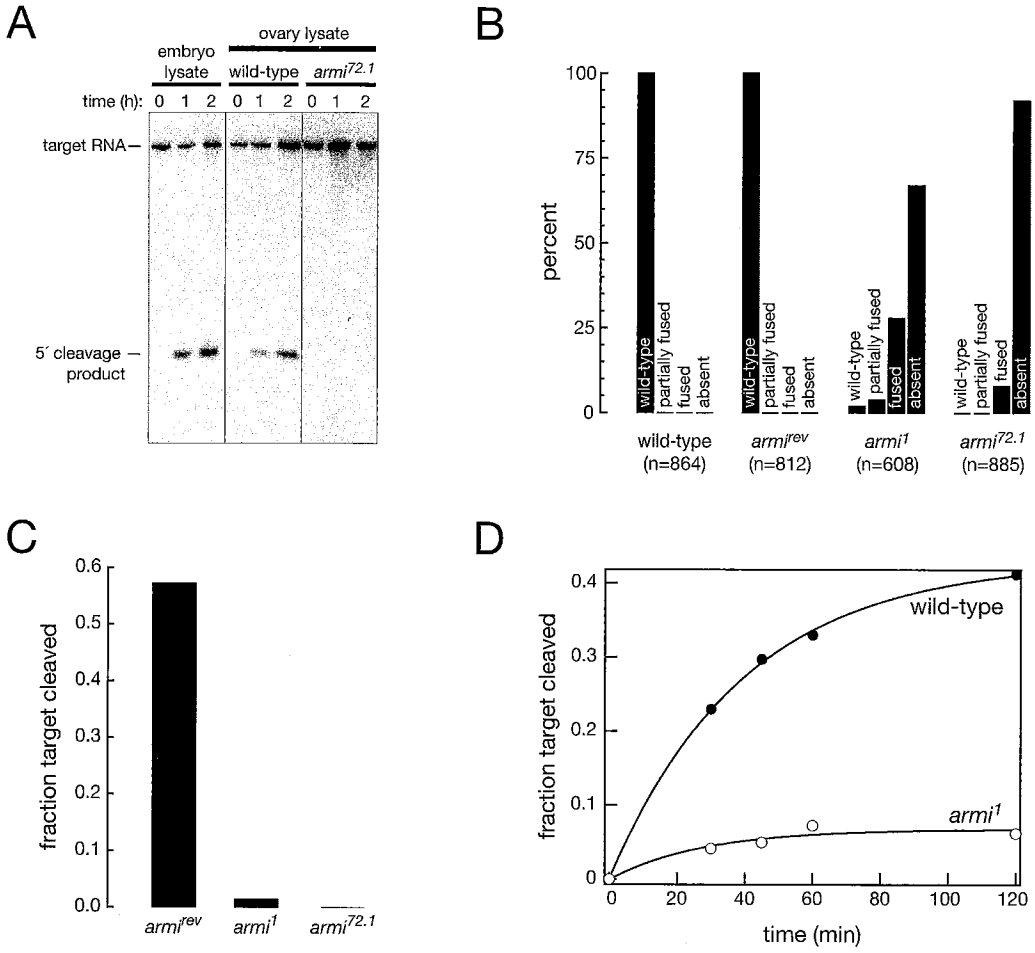

Figure 3. *armi* Ovary Lysates Are Defective in RNAi

(A) RNAi reactions in lysates from 0–2 hr embryos, wild-type or $armi^{72.1}$ mutant ovaries.

(B) Dorsal appendage phenotype was assessed for alleles of *armi*.

(C) The fraction of target mRNA cleaved after 2 hr in an RNAi reaction using ovary lysates from *armi* alleles.

(D) mRNA cleavage rate in wild-type and $armi^{1}$ ovary lysates programmed with siRNA.

sight into the molecular basis of their RISC assembly defect(s). At what step(s) in RISC assembly are *armi* and *aub* blocked? In order to answer this question, we identified protein-siRNA intermediates in the RISC assembly pathway. Our 2′-O-methyl oligonucleotide/native gel method detects only complexes competent to bind target RNA (mature RISC). Therefore, we used a native gel assay designed to detect intermediates in the assembly of RISC. We radiolabeled the siRNA, allowing detection of complexes containing either single-stranded or double-stranded siRNA and used functionally asymmetric siRNAs (Schwarz et al., 2003) to distinguish between complexes containing single- and double-stranded siRNA.

RISC contains only a single siRNA strand (Martinez et al., 2002; Schwarz et al., 2002, 2003). Functionally asymmetric siRNAs load only one of the two strands of an siRNA duplex into RISC and degrade the other strand (Schwarz et al., 2003); the relative stability of the 5′ ends of the two strands determines which is loaded into RISC (Aza-Blanc et al., 2003; Khvorova et al., 2003; Schwarz et al., 2003). siRNA 1 (Figure 5A) loads its antisense strand into RISC, whereas siRNA 2 loads the sense strand (Schwarz et al., 2003). The two siRNA duplexes are identical, except that siRNA 2 contains a C-to-U substitution at position 1, which inverts the asymmetry (Schwarz et al., 2003). For both siRNAs, the antisense strand was 3′ ^{32}P-radiolabeled and will always be present in complexes that contain double-stranded siRNA. However, RISC will contain the ^{32}P-radiolabeled antisense strand only for siRNA 1. siRNA 2 will also make RISC, but it will contain the nonradioactive sense strand.

When either siRNA 1 or siRNA 2 was used to assemble RISC in embryo lysate, two complexes (B and A, Figure 5B) were detected in the native gel assay; a third complex was detected only with siRNA 1 (Figure 5B). This third complex therefore contains single-stranded siRNA and corresponds to RISC. Complexes B and A are good candidates for RISC assembly intermediates. Formation of all three complexes was dramatically reduced when the antisense siRNA strand contained a 5′ methoxy group (siRNA 3, Figure 5B), a modification which blocks RNAi (Nykänen et al., 2001). When the antisense strand of the siRNA contained a single 5′-deoxy nucleotide,

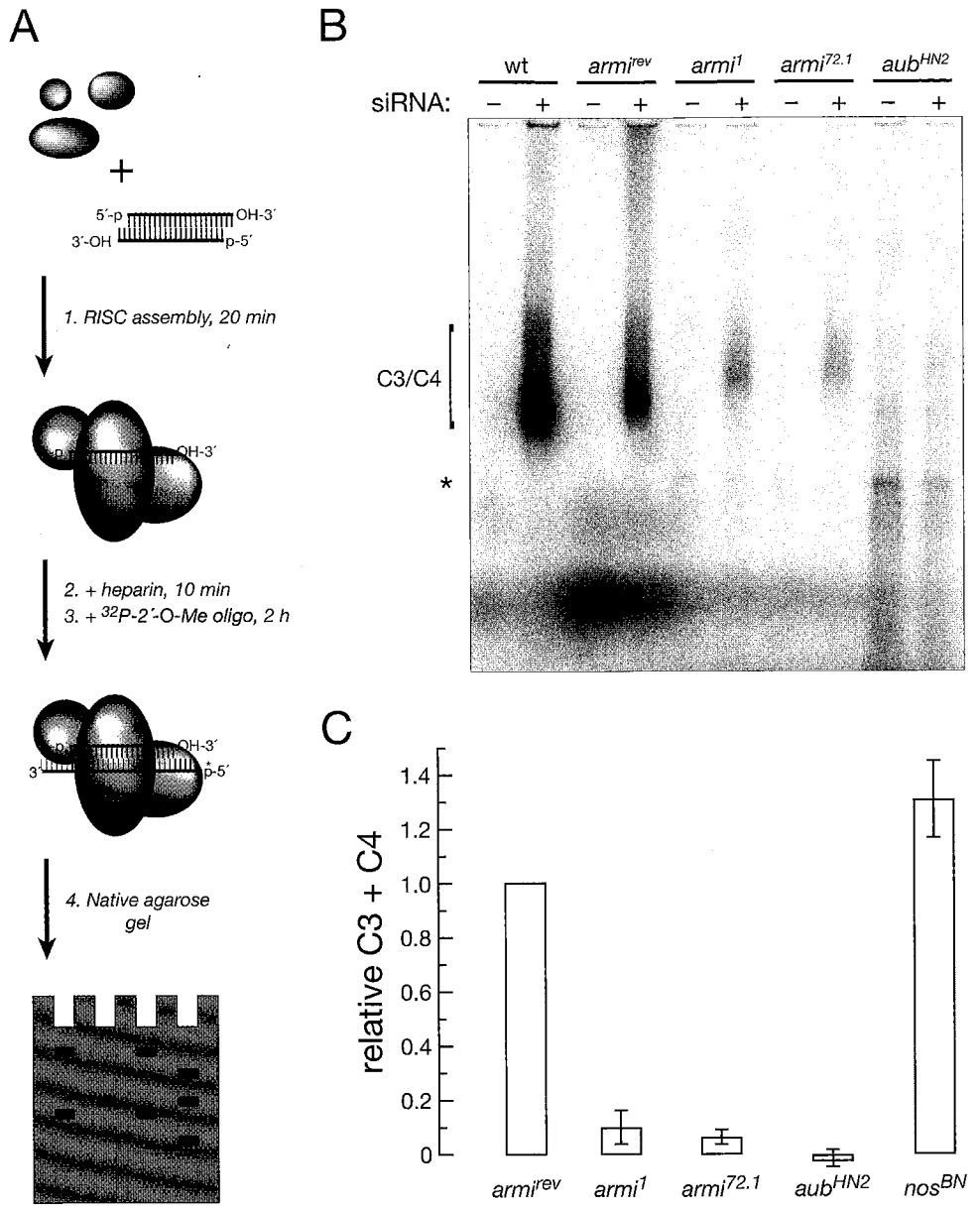

Figure 4. Armi and Aub Are Required for RISC Assembly

(A) RISC assembly assay.

(B) A representative RISC assembly assay using wild-type and mutant *Drosophila* ovary lysates. A complex formed irrespective of siRNA addition is marked with an asterisk.

(C) Amount of RISC complexes C3/C4 formed in wild-type and mutant ovary lysates. The data are the average of four independent trials; error bars indicate standard deviation. For each trial, the data were normalized to the amount of complex observed in *armi*^{rev} lysate, and the background observed in the absence of siRNA was subtracted from the amount of complex formed when siRNA was included in the corresponding reaction. 5′-phosphorylated, 2′ dT siRNA was used to maximize RISC assembly. All reactions contained equal amounts of total protein.

making it a poor substrate for phosphorylation in the lysate (Nykänen et al., 2001), assembly of all three complexes was reduced (siRNA 4, Figure 5B). Phosphorylating the 5′ deoxy-substituted siRNA before the reaction restored complex assembly (siRNA 5, Figure 5B). Formation of complex A and of RISC required ATP. In contrast, complex B assembled efficiently in the absence of ATP, but only if the siRNA was phosphorylated prior to the reaction (compare −ATP, siRNA 4 versus siRNA 5, Figure 5B).

Complexes B, A, and RISC also formed in ovary lysate (Figure 5C). As for embryo lysate, complexes B and A contained double-stranded siRNA, whereas RISC contained single-stranded (compare siRNA 1 and 2, Figure 5C). No complexes formed in ovary lysate when siRNA 5′ phosphorylation was blocked (siRNA 3, Figure 5C) and complex assembly was reduced when siRNA phosphorylation was slow (siRNA 4, Figure 5C).

To determine the relationship of complexes B, A, and RISC, we monitored the kinetics of complex formation

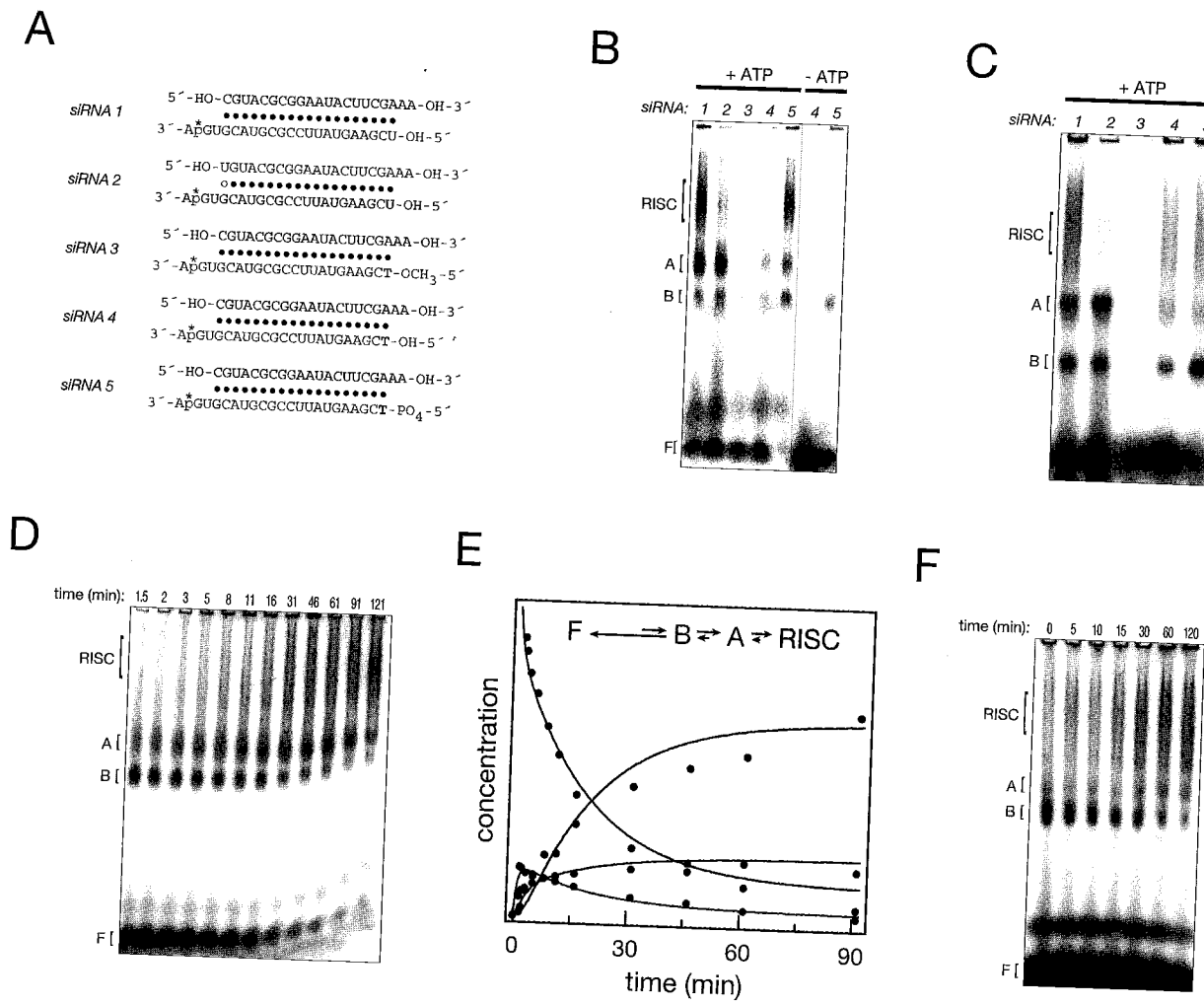

Figure 5. Identification of Intermediates in RISC Assembly

(A) siRNA duplexes used for native gel analysis. The strand that enters the RISC is indicated in blue, deoxynucleotides are in green, and the ^{32}P-radiolabeled phosphates are red, marked with an asterisk.

(B) Native gel analysis of the protein-siRNA complexes formed in embryo lysate using the 3′ ^{32}P-radiolabeled siRNAs in (A). F, free siRNA.

(C) Native gel analysis of the protein-siRNA complexes formed in wild-type ovary lysate using the 3′ ^{32}P-radiolabeled siRNAs in (A). Free siRNA is not shown on this gel.

(D) Timecourse of the assembly of 5′ ^{32}P-radiolabeled siRNA into protein complexes.

(E) Kinetic modeling of the data in (D). Blue circles, free siRNA; red, complex B; green, complex A; black, RISC. Solid lines show the corresponding modeled timecourses. The length of the arrows indicates the relative forward and reverse rate constants that best describe the data.

(F) Complex B can be "chased" into RISC. 5′ ^{32}P-radiolabeled siRNA was preincubated with embryo lysate for 5 min to assemble complex B, then a 20-fold excess of unlabeled siRNA was added (time = 0) and the disappearance of complex B and the production of complexes A and RISC monitored by native gel electrophoresis.

(Figure 5D) and analyzed the data by kinetic modeling (Figure 5E). Of all possible models relating free siRNA, B, A, and RISC, only the simple linear pathway siRNA → B → A → RISC fit well to our data (see Experimental Procedures). The modeled rate constants for the pathway are consistent with the observation that formation of complex B is ATP independent, but RISC is ATP dependent.

We also performed a "chase" experiment to confirm our prediction that complex B is a precursor to RISC (via A). Complex B was assembled by incubating ^{32}P-radiolabeled siRNA in embryo lysate for 5 min, then a 20-fold excess of unlabeled siRNA added to prevent further incorporation of ^{32}P-siRNA into complex. Then we continued the incubation and monitored the formation of complexes. Complex B disappeared with time, A increased with time then peaked at ~60 min, and RISC accumulated throughout the experiment (Figure 5F). The amount of radiolabeled free siRNA was essentially unchanged throughout the experiment, demonstrating that the unlabeled siRNA effectively blocked incorporation of ^{32}P-free siRNA into complex. Thus, B was chased into RISC, likely via A. Together, our kinetic modeling and chase experiment provide support for a RISC assembly pathway in which the siRNA passes through two successive, double-stranded siRNA-containing complexes, B and A, in order to be transformed into the single-stranded siRNA-containing RISC.

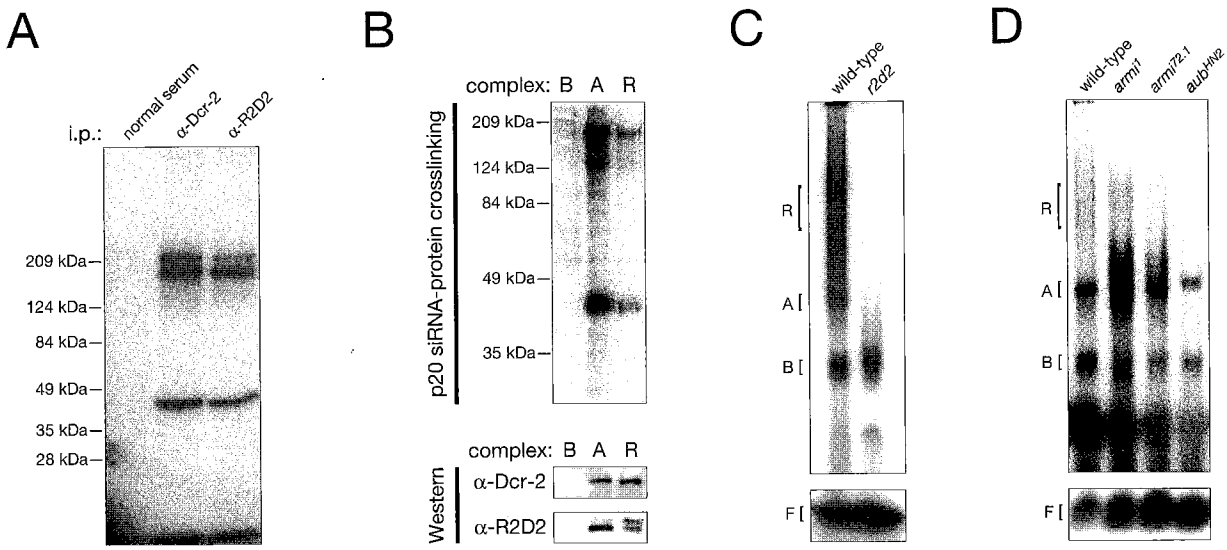

Figure 6. A Dcr-2/R2D2-Containing Complex Is Formed in *armi* and *aub*, but Not *r2d2* Mutant Ovary Lysate

(A) Dcr-2 and R2D2 are efficiently crosslinked by 302 nm light to an siRNA containing 5-iodouracil at position 20. The siRNA was incubated with embryo lysate, crosslinked with UV light, immunoprecipitated with the antiserum indicated above each lane, then analyzed by 4%–20% gradient SDS-PAGE.

(B) Upper panel: the 5-iodouracil siRNA was incubated with embryo lysate crosslinked, then resolved on a native gel. Complexes B, A, and R (RISC) were excised from the gel and the protein-siRNA crosslinks present in complexes B, A, and R (RISC) analyzed by 10% SDS-PAGE. Lower panel: complexes B, A, and R (RISC) were isolated from a native gel, then analyzed by Western blotting with α-Dcr-2 or α-R2D2 antisera.

(C) Native gel analysis of the complexes formed in *r2d2* and (D) $armi^{1}$, $armi^{72.1}$, and aub^{HN2} homozygous mutant ovary lysates. Minor variations in the abundance of B and A did not correlate with *armi* allele strength, suggesting that neither Armi nor Aub are required for their production. In (C) and (D), the portion of the gel corresponding to free siRNA, F, is shown below. Equal amounts of total protein were used in each reaction. The siRNA was 5′ ^{32}P-radiolabeled in (A)–(C) and 3′ ^{32}P-radiolabeled in (D). Less RISC was detected for wild-type lysate in this experiment compared to (C) because the lysate was diluted 3-fold to equalize its protein concentration to that of the *aub* mutant lysate.

Complex A Contains the R2D2/Dicer-2 Heterodimer

Liu and colleagues have previously proposed that a heterodimeric complex, comprising Dicer-2 (Dcr-2) and the dsRNA binding protein R2D2, loads siRNA into RISC (Liu et al., 2003). Complex A contains the Dcr-2/R2D2 heterodimer. R2D2 and Dcr-2 are readily crosslinked to ^{32}P-radiolabeled siRNA with UV light (Liu et al., 2003). We synthesized an siRNA containing a single photocrosslinkable nucleoside base (5-iodouracil) at position 20 (Supplemental Figure S2A online). The ^{32}P-5-iodouracil siRNA was incubated with embryo lysate to assemble complexes, then irradiated with 302 nm light, which initiates protein-RNA crosslinking only at the 5-iodo-substituted nucleoside. Proteins covalently linked to the ^{32}P-radiolabeled siRNA were resolved by SDS-PAGE. Two proteins—~200 kDa and ~40 kDa—efficiently crosslinked to the siRNA (Supplemental Figure S2D online). Both crosslinked proteins were coimmunoprecipitated with either α-Dcr-2 or α-R2D2 serum, but not normal rabbit serum (Figure 6A). Neither crosslink was observed in ovary lysates prepared from *r2d2* homozygous mutant females (data not shown), a result expected because Dcr-2 is unstable in the absence of R2D2 (Liu et al., 2003). Additional experiments validating the UV crosslinking assay are provided in Supplemental Methods, Supplemental Figure S2, and Supplemental Table S1.

The crosslinking was repeated, and the reaction analyzed by native gel electrophoresis to resolve complexes B, A, and RISC. Each complex was eluted from the gel and analyzed by SDS-PAGE. Figure 6B shows that the R2D2 and Dcr-2 crosslinks were present in complexes A and RISC, but not B. In a parallel experiment, complexes B, A, and RISC were isolated (without crosslinking) and analyzed by Western blotting with either α-Dcr-2 or α-R2D2 antibodies. Again, complexes A and RISC, but not B, contained both Dcr-2 and R2D2 (Figure 6B). Finally, we tested complex assembly in ovary lysates prepared from *r2d2* homozygous mutant females. Only complex B formed in these lysates (Figure 6C). We conclude that complex A contains the previously identified Dcr-2/R2D2 heterodimer (Liu et al., 2003), and that both Dcr-2 and R2D2 remain associated with at least a subpopulation of RISC, consistent with earlier reports that Dcr-2 in flies and both DCR-1 and the nematode homolog of R2D2, RDE-4, coimmunoprecipitate with Argonaute proteins (Hammond et al., 2001; Tabara et al., 2002).

armi Mutants Are Defective for the Conversion of Complex A to RISC

RISC does not form in ovary lysates from *armi* or *aub* mutants (Figures 4B and 4C). However, both complexes B and A were readily detected in *armi* and *aub* mutants (Figure 6D). Thus, *armi* and *aub* mutants are impaired in a step in RISC assembly after binding of the siRNA to the Dcr-2/R2D2 heterodimer.

Armi might act after the formation of complex A to unwind siRNA duplexes prior to their assembly into RISC. To test this hypothesis, we tested if single-stranded siRNA circumvented the requirement for *armi*. In vitro and in vivo, single-stranded siRNA triggers RNAi, albeit inefficiently (Martinez et al., 2002; Schwarz et al.,

2002). *armi* ovary lysates failed to support RNAi when the reactions were programmed with 5′-phosphorylated, single-stranded siRNA (Supplemental Figure S3A online). The defect with single-stranded siRNA correlated with allele strength: some activity was seen in lysates from the weak allele, $armi^{1}$, but none for the strong allele, $armi^{72.1}$. The requirement for a putative ATPase—Armi—in RNAi triggered by single-stranded siRNA suggested to us the presence of an additional ATP-dependent step in the RISC assembly, after siRNA unwinding.

To test if loading of single-stranded siRNA into RISC requires ATP, we added 5′-phosphorylated, single-stranded siRNA to embryo lysates depleted of ATP. After incubation for 2 hr, no cleavage product was detected, suggesting that there is at least one ATP-dependent step downstream of siRNA unwinding (Supplemental Figure S3B). The stability of single-stranded siRNA was not reduced by ATP depletion. In fact, single-stranded siRNA was slightly more stable in the absence of ATP (Supplemental Figure S3C online). Thus differential stability cannot account for the requirement for ATP in RNAi triggered by single-stranded siRNA. In the RNAi pathway, there are at least three steps after siRNA unwinding: RISC assembly, target recognition, and target cleavage. To assess if either target recognition or cleavage was ATP dependent, we incubated single-stranded siRNA in a standard RNAi reaction with ATP to assemble RISC. Next, NEM was added to inactivate the ATP-regenerating enzyme, creatine kinase, and to block further RISC assembly. NEM was quenched with dithiothreitol (DTT), and hexokinase and glucose added to deplete ATP. Finally, mRNA target was added and the reaction incubated for 2 hr. Using this protocol, high ATP levels were maintained during RISC assembly, but less than 100 nM ATP was present during the encounter of RISC with the target RNA. Target recognition and cleavage did not require ATP when RISC was programmed with either double- or single-stranded siRNA, provided that ATP was supplied during RISC assembly (Supplemental Figure S3D).

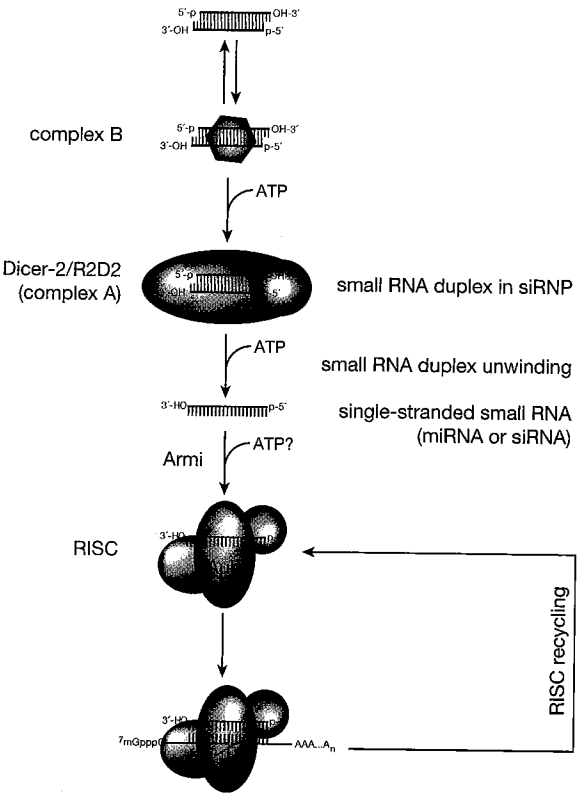

Figure 7. A Model for RNA Silencing in *Drosophila*

Armi is envisioned to facilitate the ATP-dependent incorporation of siRNA into RISC, whereas Aub is drawn as a RISC component.

Discussion

In *Drosophila*, mutations affecting the RNAi pathway are often lethal or female sterile, making the molecular characterization of these mutants difficult. Our finding that lysates that support RNAi in vitro can be prepared from manually dissected ovaries has allowed us to analyze the molecular function of *armi*, a maternal effect gene required for RNAi. Our methods should find broad application in the molecular characterization of other maternal genes required for the RNAi pathway.

We detected four distinct RISC-like complexes common to embryo and ovary lysates (C1-4 in Supplemental Figure S1 and Figure 4). In ovaries, formation of these complexes is reduced >10-fold in *armi* mutants and is undetectable in *aub* mutants, which were shown previously to be RNAi defective (Kennerdell et al., 2002). The requirement for Aub, an Argonaute protein, suggests that the complexes correspond to distinct RISC isoforms built on a common core of Aub and siRNA. These isoforms may play distinct regulatory roles (e.g., translational repression versus cleavage). Alternatively, the smallest, most abundant complexes may contain only the most stably associated protein constituents, whereas the larger, less abundant complexes may correspond to "holo-RISC" that retain more weakly bound proteins. Clearly, a major challenge for the future is to define the protein constituents of each complex, their functional capacity, and their biological role. The development of a native gel assay that resolves distinct RISC complexes represents a step toward that goal.

We have also identified two intermediates in RISC assembly. Complex B forms rapidly upon incubation of siRNA in lysate, in the absence of ATP. The siRNA is then transferred to complex A, which contains the previously identified R2D2/Dcr-2 heterodimer. The siRNA is double stranded in both B and A. RISC is formed from complex A by a process that requires both siRNA unwinding and ATP. Both *aub* and *armi* are required genetically for the production of RISC from complex A. The involvement of Armi, a putative RNA helicase protein, in the production of RISC from complex A and our finding that incorporation of single-stranded siRNA into RISC requires ATP suggest that Armi functions to incorporate single-stranded siRNA into RISC (Figure 7). However, our data cannot distinguish between direct and indirect roles for Armi in RISC assembly.

The *Arabidopsis* homolog of Armi, SDE3, together with the RNA-dependent RNA polymerase (RdRP) SDE1/SGS2, is required for PTGS triggered by transgenes that express single-stranded sense mRNA, but not silencing

triggered by some RNA viruses (Dalmay et al., 2001). SDE3 has been proposed to facilitate the conversion of dsRNA into siRNA or the conversion of mRNA into complementary RNA by SDE1/SGS2 (Dalmay et al., 2001; Jorgensen, 2003). Recent studies show that SDE3 is not required for the production of siRNAs derived directly from a long dsRNA hairpin (Himber et al., 2003). Instead, SDE3 seems to play a role in the production of siRNAs generated by an RdRP-dependent amplification mechanism. Our data are not consistent with either of these functions for Armi. First, *Drosophila* genomic, biochemical, and genetic data exclude a role for an RdRP in RNAi (Celotto and Graveley, 2002; Schwarz et al., 2002; Roignant et al., 2003; Tang et al., 2003). Second, Armi is required for RISC assembly in *Drosophila* ovary lysates when RISC is programmed with siRNA, suggesting a role for Armi downstream of the conversion of dsRNA into siRNA, but upstream of target recognition by RISC. The apparently divergent functions of SDE3 and Armi could be reconciled if RISC is required for RdRP-mediated amplification of silencing. Alternatively, SDE3 and Armi may not have homologous functions.

armi mRNA is abundant in oocytes and syncitial blastoderm embryos, but a low level can be detected throughout development, including in somatic tissues (Cook et al., 2004). While the requirement for *armi* in spermatogenesis and oogenesis makes Armi a good candidate for a component of the RNAi machinery in germ cells and early embryos, somatic functions for Armi are also possible. In this respect, *armi* is reminiscent of the maternally expressed Argonaute protein, *piwi*, which is also required during oogenesis. Although *piwi* mutants display no obvious somatic phenotype (Cox et al., 1998), Piwi is required in the soma both for posttranscriptional transgene silencing and for some types of transcriptional silencing (Pal-Bhadra et al., 2002). Whether Armi is likewise required for somatic transgene silencing remains to be tested.

Experimental Procedures

General Methods

Target RNA cleavage assay was performed as described (Haley et al., 2003). ATP depletion and NEM quenching were as published (Nykänen et al., 2001).

Stellate Immunofluorescence

Testes were dissected in testes fixation buffer (1 mM EDTA, 183 mM KCl, 47 mM NaCl, 10 mM Tris, pH 6.8) and fixed with formaldehyde as described (Theurkauf, 1994). Ste protein was labeled with anti-Ste IgG at 1:100. Images were analyzed by confocal microscopy using a Leica TCS-SP inverted laser scanning microscope. DNA was stained with TOTO-3 (Molecular Probes).

Ovary Lysate Preparation

Wild-type or mutant fly ovaries were dissected with forceps (World Precision Instruments 500232) and collected in 1 × PBS buffer in 0.5 ml microcentrifuge tubes. Ovaries were centrifuged at 11,000 × g for 5 min at 4°C. The PBS was removed from the ovary pellet, then ovaries were homogenized in 1 ml ice-cold lysis buffer (100 mM potassium acetate, 30 mM HEPES-KOH at pH 7.4, 2 mM magnesium acetate) containing 5 mM DTT and 1 mg/ml complete "mini" EDTA-free protease inhibitor tablets (Roche) per gram of ovaries using a plastic "pellet pestle" (Kontes). Lysate was clarified by centrifugation at 14,000 × g for 25 min at 4°C. The supernatant was aliquoted into chilled microcentrifuge tubes, flash frozen in liquid nitrogen, and stored at −80°C. RNAi reactions were assembled using equal amounts of total protein for all genotypes within an experiment.

Synthetic siRNA

The siRNAs were prepared from synthetic 21 nt RNAs (Dharmacon Research). Sense siRNA sequences used were 5′-HO-CGU ACG CGG AAU ACU UCG AAA-3′ (5′ OH [riboU], 5′ CH_3O [2′ dT], 5′ OH [2′ dT]) and 5′-HO-UGA GGU AGU AGG UUG UAU AGU-3′ (un). Antisense siRNA sequences used were 5′-HO-UCG AAG UAU UCC GCG UAC GUG-3′ (5′ OH [riboU]); 5′-CH_3O-dTCG AAG UAU UCC GCG UAC GUG-3′ (5′ CH_3O [2′ dT]); 5′-HO-dTCG AAG UAU UCC GCG UAC GUG-3′ (5′ OH [2′ dT]); and 5′-HO-UAU ACA ACC UAC UAC CUC AUU-3′ (un). Appropriate pairs of siRNA strands were annealed to form siRNA duplexes as described (Elbashir et al., 2001b) and used at a final concentration of ≤20 nM (Figures 2, 5H, and 5I) or ≤50 nM (Figure 3). siRNA single strands were phosphorylated with polynucleotide kinase according to the manufacturer's protocol (PNK; New England Biolabs) and used at 200 nM (final concentration).

RISC Assembly

RISC assembly was as described (Zamore et al., 2000), except that the reaction contained 40% (v/v) embryo or ovary lysate and 50 nM siRNA duplex. Lysates were adjusted with lysis buffer to contain equal amounts of protein. Following incubation at 25°C for 20 min, 1 mg/ml heparin was added and incubated for 10 min. Heparin served to reduce nonspecific binding of proteins to the 2′-*O*-methyl oligonucleotide and to quench RISC assembly. (Mature RISC is refractory to heparin: 1 mg/ml [final concentration] heparin added at the start of the reaction blocked RNAi in the cleavage assay, but had no effect when added together with target RNA.) Then the 5′ ^{32}P-radiolabled 2′-O-methyl oligonucleotide (5′-CAU CAC GUA CGC GGA AUA CUU CGA AAU GUC C-3′) was added at 2 nM final concentration and incubated for 2 hr. After the addition of 3.0% (w/v) Ficoll-400, complexes were resolved by native gel electrophoresis at 4 W for 2 hr at room temperature. Native gels were 1 mm thick, 1.5% (w/v) agarose (GTG grade), 0.5 × TBE with 1.5 mM $MgCl_2$, cast vertically between a standard glass plate and a ground glass plate (National Glass Works, Worcester, Massachusetts). To detect intermediates in RISC assembly, ^{32}P-radiolabeled siRNA was incubated with lysate for 1 hr, unless otherwise noted. No heparin was added to these reactions. After incubation, the samples were adjusted to 3.0% (w/v) Ficoll-400 and resolved by vertical native gel electrophoresis as above. Gels were dried under vacuum onto Hybond-N+ nylon membrane (Amersham).

Kinetic Modeling

Data from native gel analysis of siRNA-containing complexes were initially fit using Berkeley Madonna 8.0.1 software to the global model:

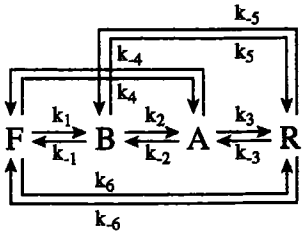

Rates for k_4, k_{-4}, k_5, k_{-5}, k_6, and k_{-6} ranged from 5-fold (k_5) to 10^8-fold (k_{-4}) slower than the slowest forward rate for the linear pathway F → B → A → RISC. The data were therefore modeled neglecting rates k_4, k_{-4}, k_5, k_{-5}, k_6, and k_{-6} to generate Figure 5E.

Crosslinking

5′ ^{32}P-radiolabeled siRNA duplex was used at 4 million counts per minute in a standard RNAi reaction, incubated 45–60 min at 25°C, then transferred to a 96-well round bottom plate on ice. Samples were irradiated for 10–15 min with 302 nm light using an Ultraviolet Products model TM-36 transilluminator inverted directly onto the polystyrene lid of the 96-well plate. Samples were then adjusted to 1 × SDS-SB (62.5 mM Tris-HCl, pH 6.8, 10% glycerol, 2% SDS,

0.02% (w/v) Bromophenol Blue, 100 mM DTT), heated to 95°C for 5 min, and resolved by SDS-polyacrylamide gel electrophoresis.

Immunoprecipitation and Western Blotting

Normal rabbit, α-Dcr-2, and α-R2D2 antisera were first bound to protein A agarose beads for 2 hr at 4°C in lysis buffer. After washing with RIPA buffer (150 mM NaCl, 1% [v/v] NP40, 0.5% [w/v] sodium deoxycholate, 0.1% SDS, 25 mM Tris-HCl, pH 7.6), the beads (25 μl) were incubated with 15 μl of crosslinked lysate for 2 hr at 4°C. After washing in RIPA buffer, the beads were boiled in 1 × SDS-SB and the eluted proteins resolved by SDS-PAGE. For Western blotting, the complexes were excised from the native gel, boiled in 1 × SDS-SB at 95°C for 10 min, and resolved by SDS-PAGE. Western blotting was performed with 1:1000 dilution for α-Dcr-2 antisera and 1:5000 for α-R2D2.

Acknowledgments

We thank John Leszyk for mass spectrometry; Juanita McLachlan for maintaining our fly colony; and members of the Zamore lab for encouragement and helpful discussions. α-Dcr-2 and α-R2D2 antibodies were the kind gifts of Qinghua Liu and Xiaodong Wang; α-Ste antibody was the kind gift of Maria Pia Bozzetti; normal rabbit serum was the kind gift of Alonzo Ross. r2d2 mutant flies were kindly provided by Dean P. Smith. H.A.C. was supported by a postdoctoral training from the NIH and a Research Scholar Grant from the American Cancer Society. P.D.Z. is a Pew Scholar in the Biomedical Sciences and a W.M. Keck Foundation Young Scholar in Medical Research. This work was supported in part by grants from the National Institutes of Health to P.D.Z. (GM62862-01 and GM65236-01) and a grant from the Human Frontiers Science Program to W.E.T. (RG0356/1997-M).

Received: October 3, 2003
Revised: December 31, 2003
Accepted: February 9, 2004
Published: March 18, 2004

References

Aravin, A.A., Naumova, N.M., Tulin, A.V., Vagin, V.V., Rozovsky, Y.M., and Gvozdev, V.A. (2001). Double-stranded RNA-mediated silencing of genomic tandem repeats and transposable elements in the *D. melanogaster* germline. Curr. Biol. *11*, 1017–1027.

Aza-Blanc, P., Cooper, C.L., Wagner, K., Batalov, S., Deveraux, Q.L., and Cooke, M.P. (2003). Identification of modulators of TRAIL-induced apoptosis via RNAi-based phenotypic screening. Mol. Cell *12*, 627–637.

Belloni, M., Tritto, P., Bozzetti, M.P., Palumbo, G., and Robbins, L.G. (2002). Does Stellate cause meiotic drive in Drosophila melanogaster? Genetics *161*, 1551–1559.

Bernstein, E., Caudy, A.A., Hammond, S.M., and Hannon, G.J. (2001). Role for a bidentate ribonuclease in the initiation step of RNA interference. Nature *409*, 363–366.

Billy, E., Brondani, V., Zhang, H., Muller, U., and Filipowicz, W. (2001). Specific interference with gene expression induced by long, double-stranded RNA in mouse embryonal teratocarcinoma cell lines. Proc. Natl. Acad. Sci. USA *98*, 14428–14433.

Boutla, A., Delidakis, C., Livadaras, I., Tsagris, M., and Tabler, M. (2001). Short 5′-phosphorylated double-stranded RNAs induce RNA interference in Drosophila. Curr. Biol. *11*, 1776–1780.

Caplen, N.J., Parrish, S., Imani, F., Fire, A., and Morgan, R.A. (2001). Specific inhibition of gene expression by small double-stranded RNAs in invertebrate and vertebrate systems. Proc. Natl. Acad. Sci. USA *98*, 9742–9747.

Catalanotto, C., Azzalin, G., Macino, G., and Cogoni, C. (2002). Involvement of small RNAs and role of the qde genes in the gene silencing pathway in Neurospora. Genes Dev. *16*, 790–795.

Caudy, A.A., Myers, M., Hannon, G.J., and Hammond, S.M. (2002). Fragile X-related protein and VIG associate with the RNA interference machinery. Genes Dev. *16*, 2491–2496.

Celotto, A.M., and Graveley, B.R. (2002). Exon-specific RNAi: A tool for dissecting the functional relevance of alternative splicing. RNA *8*, 8–24.

Chiu, Y.-L., and Rana, T.M. (2002). RNAi in human cells: Basic structural and functional features of small interfering RNA. Mol. Cell *10*, 549–561.

Cogoni, C., and Macino, G. (1997). Isolation of quelling-defective (qde) mutants impaired in posttranscriptional transgene-induced gene silencing in Neurospora crassa. Proc. Natl. Acad. Sci. USA *94*, 10233–10238.

Cox, D.N., Chao, A., Baker, J., Chang, L., Qiao, D., and Lin, H. (1998). A novel class of evolutionarily conserved genes defined by piwi are essential for stem cell self-renewal. Genes Dev. *12*, 3715–3727.

Dalmay, T., Hamilton, A., Rudd, S., Angell, S., and Baulcombe, D.C. (2000). An RNA-dependent RNA polymerase gene in Arabidopsis is required for posttranscriptional gene silencing mediated by a transgene but not by a virus. Cell *101*, 543–553.

Dalmay, T., Horsefield, R., Braunstein, T.H., and Baulcombe, D.C. (2001). SDE3 encodes an RNA helicase required for post-transcriptional gene silencing in Arabidopsis. EMBO J. *20*, 2069–2078.

Doi, N., Zenno, S., Ueda, R., Ohki-Hamazaki, H., Ui-Tei, K., and Saigo, K. (2003). Short-interfering-RNA-mediated gene silencing in mammalian cells requires Dicer and eIF2C translation initiation factors. Curr. Biol. *13*, 41–46.

Elbashir, S.M., Harborth, J., Lendeckel, W., Yalcin, A., Weber, K., and Tuschl, T. (2001a). Duplexes of 21-nucleotide RNAs mediate RNA interference in cultured mammalian cells. Nature *411*, 494–498.

Elbashir, S.M., Lendeckel, W., and Tuschl, T. (2001b). RNA interference is mediated by 21- and 22-nucleotide RNAs. Genes Dev. *15*, 188–200.

Elbashir, S.M., Martinez, J., Patkaniowska, A., Lendeckel, W., and Tuschl, T. (2001c). Functional anatomy of siRNAs for mediating efficient RNAi in Drosophila melanogaster embryo lysate. EMBO J. *20*, 6877–6888.

Fagard, M., Boutet, S., Morel, J.-B., Bellini, C., and Vaucheret, H. (2000). AGO1, QDE-2, and RDE-1 are related proteins required for post-transcriptional gene silencing in plants, quelling in fungi, and RNA interference in animals. Proc. Natl. Acad. Sci. USA *97*, 11650–11654.

Fire, A., Xu, S., Montgomery, M.K., Kostas, S.A., Driver, S.E., and Mello, C.C. (1998). Potent and specific genetic interference by double-stranded RNA in Caenorhabditis elegans. Nature *391*, 806–811.

Grishok, A., Tabara, H., and Mello, C. (2000). Genetic requirements for inheritance of RNAi in *C. elegans*. Science *287*, 2494–2497.

Gvozdev, V.A., Aravin, A.A., Abramov, Y.A., Klenov, M.S., Kogan, G.L., Lavrov, S.A., Naumova, N.M., Olenkina, O.M., Tulin, A.V., and Vagin, V.V. (2003). Stellate repeats: targets of silencing and modules causing cis-inactivation and trans-activation. Genetica *117*, 239–245.

Haley, B., Tang, G., and Zamore, P.D. (2003). In vitro analysis of RNA interference in Drosophila melanogaster. Methods *30*, 330–336.

Hamilton, A.J., and Baulcombe, D.C. (1999). A species of small antisense RNA in posttranscriptional gene silencing in plants. Science *286*, 950–952.

Hammond, S.M., Bernstein, E., Beach, D., and Hannon, G.J. (2000). An RNA-directed nuclease mediates post-transcriptional gene silencing in Drosophila cells. Nature *404*, 293–296.

Hammond, S.M., Boettcher, S., Caudy, A.A., Kobayashi, R., and Hannon, G.J. (2001). Argonaute2, a link between genetic and biochemical analyses of RNAi. Science *293*, 1146–1150.

Himber, C., Dunoyer, P., Moissiard, G., Ritzenthaler, C., and Voinnet, O. (2003). Transitivity-dependent and -independent cell-to-cell movement of RNA silencing. EMBO J. *22*, 4523–4533.

Hutvágner, G., and Zamore, P.D. (2002). A microRNA in a multiple-turnover RNAi enzyme complex. Science *297*, 2056–2060.

Hutvágner, G., Simard, M.J., Mello, C.C., and Zamore, P.D. (2004). Sequence-specific inhibition of small RNA function. PLoS Biol. *2*, e98. DOI:10.1371/journal.pbio.0020098.

Ishizuka, A., Siomi, M.C., and Siomi, H. (2002). A Drosophila fragile

X protein interacts with components of RNAi and ribosomal proteins. Genes Dev. *16*, 2497–2508.

Jorgensen, R.A. (2003). Sense cosuppression in plants: Past, present, and future. In RNAi: A Guide To Gene Silencing, G.J. Hannon, ed. (Cold Spring Harbor, NY: Cold Spring Harbor Laboratory Press), pp. 5–22.

Kennerdell, J.R., and Carthew, R.W. (1998). Use of dsRNA-mediated genetic interference to demonstrate that *frizzled* and *frizzled 2* act in the wingless pathway. Cell *95*, 1017–1026.

Kennerdell, J.R., Yamaguchi, S., and Carthew, R.W. (2002). RNAi is activated during Drosophila oocyte maturation in a manner dependent on aubergine and spindle-E. Genes Dev. *16*, 1884–1889.

Ketting, R.F., Haverkamp, T.H., van Luenen, H.G., and Plasterk, R.H. (1999). Mut-7 of C. elegans, required for transposon silencing and RNA interference, is a homolog of Werner syndrome helicase and RNaseD. Cell *99*, 133–141.

Khvorova, A., Reynolds, A., and Jayasena, S.D. (2003). Functional siRNAs and miRNAs exhibit strand bias. Cell *115*, 209–216.

Koonin, E.V. (1992). A new group of putative RNA helicases. Trends Biochem. Sci. *17*, 495–497.

Liu, Q., Rand, T.A., Kalidas, S., Du, F., Kim, H.E., Smith, D.P., and Wang, X. (2003). R2D2, a bridge between the initiation and effector steps of the Drosophila RNAi pathway. Science *301*, 1921–1925.

Lohmann, J.U., Endl, I., and Bosch, T.C. (1999). Silencing of developmental genes in hydra. Dev. Biol. *214*, 211–214.

Martinez, J., Patkaniowska, A., Urlaub, H., Lührmann, R., and Tuschl, T. (2002). Single stranded antisense siRNA guide target RNA cleavage in RNAi. Cell *110*, 563–574.

Morel, J.B., Godon, C., Mourrain, P., Beclin, C., Boutet, S., Feuerbach, F., Proux, F., and Vaucheret, H. (2002). Fertile hypomorphic ARGONAUTE (ago1) mutants impaired in post-transcriptional gene silencing and virus resistance. Plant Cell *14*, 629–639.

Mourelatos, Z., Dostie, J., Paushkin, S., Sharma, A.K., Charroux, B., Abel, L., Rappsilber, J., Mann, M., and Dreyfuss, G. (2002). miRNPs: a novel class of Ribonucleoproteins containing numerous microRNAs. Genes Dev. *16*, 720–728.

Mourrain, P., Beclin, C., Elmayan, T., Feuerbach, F., Godon, C., Morel, J.B., Jouette, D., Lacombe, A.M., Nikic, S., Picault, N., et al. (2000). Arabidopsis SGS2 and SGS3 genes are required for posttranscriptional gene silencing and natural virus resistance. Cell *101*, 533–542.

Ngo, H., Tschudi, C., Gull, K., and Ullu, E. (1998). Double-stranded RNA induces mRNA degradation in *Trypanosoma brucei*. Proc. Natl. Acad. Sci. USA *95*, 14687–14692.

Nykänen, A., Haley, B., and Zamore, P.D. (2001). ATP requirements and small interfering RNA structure in the RNA interference pathway. Cell *107*, 309–321.

Pal-Bhadra, M., Bhadra, U., and Birchler, J.A. (2002). RNAi related mechanisms affect both transcriptional and posttranscriptional transgene silencing in *Drosophila*. Mol. Cell *9*, 315–327.

Ratcliff, F.G., MacFarlane, S.A., and Baulcombe, D.C. (1999). Gene silencing without DNA. RNA-mediated cross-protection between viruses. Plant Cell *11*, 1207–1216.

Roignant, J.Y., Carre, C., Mugat, B., Szymczak, D., Lepesant, J.A., and Antoniewski, C. (2003). Absence of transitive and systemic pathways allows cell-specific and isoform-specific RNAi in Drosophila. RNA *9*, 299–308.

Sánchez-Alvarado, A., and Newmark, P.A. (1999). Double-stranded RNA specifically disrupts gene expression during planarian regeneration. Proc. Natl. Acad. Sci. USA *96*, 5049–5054.

Saxena, S., Jonsson, Z.O., and Dutta, A. (2003). Small RNAs with imperfect match to endogenous mRNA repress translation: implications for off-target activity of siRNA in mammalian cells. J. Biol. Chem. *278*, 44312–44319. Published online September 2, 2003. 10.1074/jbc.M307089200.

Schmidt, A., Palumbo, G., Bozzetti, M.P., Tritto, P., Pimpinelli, S., and Schafer, U. (1999). Genetic and molecular characterization of sting, a gene involved in crystal formation and meiotic drive in the male germ line of Drosophila melanogaster. Genetics *151*, 749–760.

Schramke, V., and Allshire, R. (2003). Hairpin RNAs and retrotransposon LTRs effect RNAi and chromatin-based gene silencing. Science *301*, 1069–1074.

Schwarz, D.S., Hutvágner, G., Haley, B., and Zamore, P.D. (2002). Evidence that siRNAs function as guides, not primers, in the *Drosophila* and human RNAi pathways. Mol. Cell *10*, 537–548.

Schwarz, D.S., Hutvágner, G., Du, T., Xu, Z., Aronin, N., and Zamore, P.D. (2003). Asymmetry in the assembly of the RNAi enzyme complex. Cell *115*, 199–208.

Sijen, T., and Plasterk, R.H. (2003). Transposon silencing in the Caenorhabditis elegans germ line by natural RNAi. Nature *426*, 310–314.

Stapleton, W., Das, S., and McKee, B.D. (2001). A role of the Drosophila homeless gene in repression of Stellate in male meiosis. Chromosoma *110*, 228–240.

Tabara, H., Sarkissian, M., Kelly, W.G., Fleenor, J., Grishok, A., Timmons, L., Fire, A., and Mello, C.C. (1999). The rde-1 gene, RNA interference, and transposon silencing in *C. elegans*. Cell *99*, 123–132.

Tabara, H., Yigit, E., Siomi, H., and Mello, C.C. (2002). The dsRNA binding protein RDE-4 interacts with RDE-1, DCR-1, and a DexH-box helicase to direct RNAi in *C. elegans*. Cell *109*, 861–871.

Tang, G., Reinhart, B.J., Bartel, D.P., and Zamore, P.D. (2003). A biochemical framework for RNA silencing in plants. Genes Dev. *17*, 49–63.

Theurkauf, W.E. (1994). Immunofluorescence analysis of the cytoskeleton during oogenesis and early embryogenesis. Methods Cell Biol. *44*, 489–505.

Tijsterman, M., Ketting, R.F., Okihara, K.L., Sijen, T., and Plasterk, R.H. (2002). RNA helicase MUT-14-dependent gene silencing triggered in C. elegans by short antisense RNAs. Science *295*, 694–697.

Tuschl, T., Zamore, P.D., Lehmann, R., Bartel, D.P., and Sharp, P.A. (1999). Targeted mRNA degradation by double-stranded RNA in vitro. Genes Dev. *13*, 3191–3197.

Volpe, T.A., Kidner, C., Hall, I.M., Teng, G., Grewal, S.I.S., and Martienssen, R.A. (2002). Regulation of heterchromatic silencing and histone H3 lysine-9 methylation by RNAi. Science *297*, 1833–1837.

Waterhouse, P.M., Graham, M.W., and Wang, M.B. (1998). Virus resistance and gene silencing in plants can be induced by simultaneous expression of sense and antisense RNA. Proc. Natl. Acad. Sci. USA *95*, 13959–13964.

Wianny, F., and Zernicka-Goetz, M. (2000). Specific interference with gene function by double-stranded RNA in early mouse development. Nat. Cell Biol. *2*, 70–75.

Williams, R.W., and Rubin, G.M. (2002). ARGONAUTE1 is required for efficient RNA interference in Drosophila embryos. Proc. Natl. Acad. Sci. USA *99*, 6889–6894.

Wu-Scharf, D., Jeong, B., Zhang, C., and Cerutti, H. (2000). Transgene and transposon silencing in chlamydomonas reinhardtii by a DEAH-Box RNA helicase. Science *290*, 1159–1163.

Zamore, P.D., Tuschl, T., Sharp, P.A., and Bartel, D.P. (2000). RNAi: double-stranded RNA directs the ATP-dependent cleavage of mRNA at 21 to 23 nucleotide intervals. Cell *101*, 25–33.

nature
structural &
molecular biology

Kinetic analysis of the RNAi enzyme complex

Benjamin Haley & Phillip D Zamore

The siRNA-directed ribonucleoprotein complex, RISC, catalyzes target RNA cleavage in the RNA interference pathway. Here, we show that siRNA-programmed RISC is a classical Michaelis-Menten enzyme in the presence of ATP. In the absence of ATP, the rate of multiple rounds of catalysis is limited by release of the cleaved products from the enzyme. Kinetic analysis suggests that different regions of the siRNA play distinct roles in the cycle of target recognition, cleavage, and product release. Bases near the siRNA 5′ end disproportionately contribute to target RNA-binding energy, whereas base pairs formed by the central and 3′ regions of the siRNA provide a helical geometry required for catalysis. Finally, the position of the scissile phosphate on the target RNA seems to be determined during RISC assembly, before the siRNA encounters its RNA target.

In the RNA interference (RNAi) pathway[1,2], 21-nucleotide (nt), double-stranded siRNAs guide the RISC[3–5] (RNA-induced silencing complex) to destroy its RNA target[6]. siRNA-directed RNAi has become an essential laboratory tool for reducing the expression of specific genes in mammalian cells[7], but the limits of siRNA specificity remain to be determined[8–11]. Some siRNAs can discriminate between mRNAs that differ by only a single nucleotide[7,9,12,13], but genome-wide assessments of siRNA specificity suggest that mRNAs with only partial complementarity to an siRNA can also be targeted for destruction[14]. Why some mismatches are tolerated, whereas others are not, remains poorly understood. One hypothesis is that the 5′ region of siRNAs and the related microRNAs (miRNAs) play a special role in target recognition, nucleating binding of RISC to the RNA target[15–17]. Alternatively, mismatched siRNA might recruit RISC to targets lacking complementarity to the 5′ region of the siRNA, but the geometry of such siRNA-target pairing is incompatible with target silencing.

To understand how the 5′, central and 3′ sequences of the siRNA guide strand function to direct target cleavage, we undertook a detailed *in vitro* kinetic analysis of a single siRNA sequence. Here, we show that RISC can cleave RNA targets with up to five contiguous mismatches at the siRNA 5′ end and nine mismatches at the siRNA 3′ end. Our data show that 5′ bases contribute disproportionately to target RNA binding, but do not play a role in determining the catalytic rate, k_{cat}. This finding resembles the earlier observations by Doench and Sharp that 5′ complementarity is essential for translational repression by siRNAs designed to act like animal miRNAs, which typically repress translation[18]. For siRNAs directing target cleavage, we find that the 3′ bases of the siRNA contribute much less than 5′ bases to the overall strength of binding, but instead help to establish the helical geometry required for RISC-mediated target cleavage, consistent with the view that catalysis by RISC requires a central A-form helix[19]. Finally, we show that when an siRNA fails to pair with the first three, four or five nucleotides of the target RNA, the phosphodiester bond severed in the target RNA is unchanged; for perfectly matched siRNA, RISC measures the site of cleavage from the siRNA 5′ end[2,9]. We conclude that the identity of the scissile phosphate is determined before the encounter of the RISC with its target RNA, perhaps because the RISC endonuclease is positioned with respect to the siRNA 5′ end during RISC assembly.

RESULTS

The siRNA-programmed RISC is an enzyme

RISC programmed with small RNA *in vivo* catalyzes the destruction of target RNA *in vitro* without consuming its small RNA guide[11,20]. To begin a kinetic analysis of RISC, we first confirmed that RISC programmed *in vitro* with siRNA is likewise a multiple-turnover enzyme. To engineer an RNAi reaction that contained a high substrate concentration relative to RISC, we used an siRNA in which the guide strand is identical to the *let-7* miRNA, but unlike the miRNA, the *let-7* siRNA is paired to an RNA strand that is antisense to *let-7*[20]. The *let-7* strand of this siRNA has a high intrinsic cleaving activity, but a reduced efficiency of incorporation into RISC (**Supplementary Fig. 1** online).

After incubating the *let-7* siRNA with *Drosophila melanogaster* embryo lysate in the presence of ATP, RISC assembly was inactivated by treatment with *N*-ethyl maleimide (NEM), and the amount of RISC generated was measured using the previously described tethered 2′-*O*-methyl oligonucleotide assay[21,22] (**Supplementary Fig. 1** online). The amount of *let-7*-programmed RISC increased with increasing siRNA concentration, until the assembly reaction began to saturate at ~50 nM, reaching an asymptote between 3 and 4 nM RISC. Using 0.6 nM RISC, we observed >50 cycles of target recognition and cleavage per enzyme complex (data not shown), confirming that siRNA-programmed RISC is a multiple-turnover enzyme.

Multiple turnover is limited by product release

Next, we evaluated the kinetics of siRNA-directed target cleavage in the presence and absence of ATP (–ATP; **Fig. 1**). RISC was assembled

Department of Biochemistry and Molecular Pharmacology, University of Massachusetts Medical School, Worcester, Massachusetts 01605, USA. Correspondence should be addressed to P.Z. (phillip.zamore@umassmed.edu).

Published online 30 May 2004; doi:10.1038/nsmb780

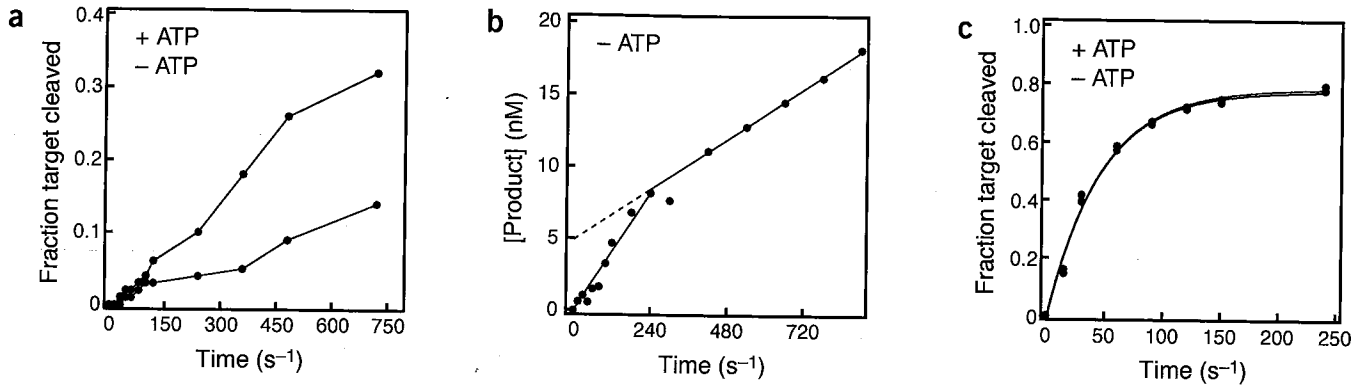

Figure 1 Product release limits the rate of catalysis by RISC. (**a**) ATP stimulates multiple rounds of RISC cleavage of the RNA target. siRNA was incubated with ATP in *D. melanogaster* embryo lysate, and then NEM was added to quench RISC assembly and to disable the ATP-regenerating system. The energy-regenerating system was either restored by adding additional creatine kinase (+ATP) or the reaction was ATP-depleted by adding hexokinase and glucose (–ATP). The target RNA concentration was 49 nM and the concentration of RISC was ~4 nM. The siRNA sequence is given in **Supplementary Figure 3** online. (**b**) In the absence of ATP, cleavage by RISC produces a pre-steady-state burst equal, within error, to the concentration of active RISC. The target concentration was 110 nM and the RISC concentration was ~4 nM. (**c**) Catalysis by RISC is not enhanced by ATP under single-turnover conditions. RISC was present in about eight-fold excess over target. Each data point represents the average of two trials.

in the presence of ATP (+ATP), and then the energy-regenerating enzyme creatine kinase was inactivated with NEM, and ATP was depleted by the addition of hexokinase and glucose (–ATP conditions). For +ATP measurements, we added back creatine kinase to the reaction after NEM treatment, and omitted the hexokinase treatment. We observed a faster rate of cleavage in the presence of ATP than in its absence. This difference was only apparent late in the reaction time course, suggesting that the ATP-dependent rate of cleavage was faster than the ATP-independent rate only at steady state (**Fig. 1a**). We therefore repeated the analysis in more detail (**Fig. 1b**). In the absence of ATP, we observed a burst of cleaved product early in the reaction, followed by an approximately four-fold slower rate of target cleavage. No burst was observed in the presence of ATP (**Fig. 1a**). If the burst corresponds to a single turnover of enzyme, then extrapolation of the slower steady-state rate back to the *y*-axis should give the amount of active enzyme in the reaction. The *y*-intercept at the start of the reaction for the steady-state rate was 4.9 nM, in good agreement with the amount of RISC estimated using the tethered 2′-*O*-methyl oligonucleotide assay (~4 nM; **Fig. 1b**).

In principle, ATP could enhance target recognition by RISC, promote a rearrangement of the RISC–target complex to an active form, facilitate cleavage itself, promote the release of the cleavage products from the siRNA guide strand, or help restore RISC to a catalytically competent state after product release. All of these steps, except product release and restoration to catalytic competence, should affect the rate of both multiple- and single-turnover reactions. Therefore, we next analyzed the rate of reaction in the presence and in the absence of ATP under conditions in which RISC was in excess over the RNA target. At early times under these conditions, the reaction rate should reflect only single-turnover cleavage events, in which events after cleavage do not determine the rate of reaction. Using single-turnover reaction conditions, we observed identical rates of RISC-mediated cleavage in the presence and absence of ATP (**Fig. 1c**). Thus, ATP must enhance a step that occurs only when each RISC catalyzes multiple cycles of target cleavage.

If product release is rate-determining for multiple-turnover catalysis by RISC in the absence, but not the presence, of ATP, then modifications that weaken the strength of pairing to the target RNA might enhance product release, but would not be expected to accelerate the return of the RISC to a catalytically competent state. We incorporated mismatches between the siRNA and its RNA target at the 3′ end of the siRNA guide strand and designed the siRNAs to be functionally asymmetric, ensuring efficient and predictable incorporation of the *let-7* strand into RISC (**Fig. 2a**)[22]. We compared the reaction velocity under conditions of substrate excess in the presence and absence of ATP for siRNAs with zero to four mismatches between the guide strand 3′ end and the RNA target. Cleavage was measured from 100 to 540 s, when >90% of the target remained uncleaved, ensuring that the multiple-turnover reaction was at steady state. Even a single 3′ mismatch between the siRNA and its target increased the –ATP rate, relative to the +ATP rate, and siRNAs with two or more mismatches showed no substantial difference in rate between the presence and absence of ATP (**Fig. 2b**). We conclude that in the absence of ATP, product release is the rate-determining step for siRNAs fully matched to their RNA targets.

siRNA-target complementarity and RISC function

Mismatches between the siRNA and its target facilitate product release, but not without cost: the rate of reaction, irrespective of ATP concentration, decreases with each additional 3′ mismatch. When the concentration of RISC was ~16–80-fold greater than the target RNA concentration, each additional mismatch between the 3′ end of the siRNA guide strand and the RNA target further slowed the reaction (**Fig. 2c,d**). Under conditions of substrate excess, the effect of mismatches between the 3′ end of the siRNA guide strand and its RNA target was more marked (**Fig. 3a**): the rate of cleavage slowed ~20% for each additional mismatch. To test the limits of the tolerance of RISC for 3′ mismatches, we analyzed cleavage under modest (8-fold, **Fig. 3b**) and vast (~80-fold, **Figs. 3c** and **Fig. 4**) enzyme excess over target RNA. Notably, cleavage was detected for siRNAs with as many as nine 3′ mismatches to the RNA target (**Figs. 3c** and **4c**), but only after 24 h incubation. No cleavage was detected for an siRNA with ten 3′ mismatches to the RNA target (**Fig. 3c**).

Linsley and colleagues have proposed siRNA-directed downregulation of an mRNA with as few as 11 contiguous bases complementary to the siRNA guide strand[14]. In that study, the mRNA target paired with positions 2–5 and 7–17 of the siRNA guide strand, but was mismatched at positions 1 and 6 of the siRNA. We find that up to five mismatched bases are tolerated between the 5′ end of the siRNA and its

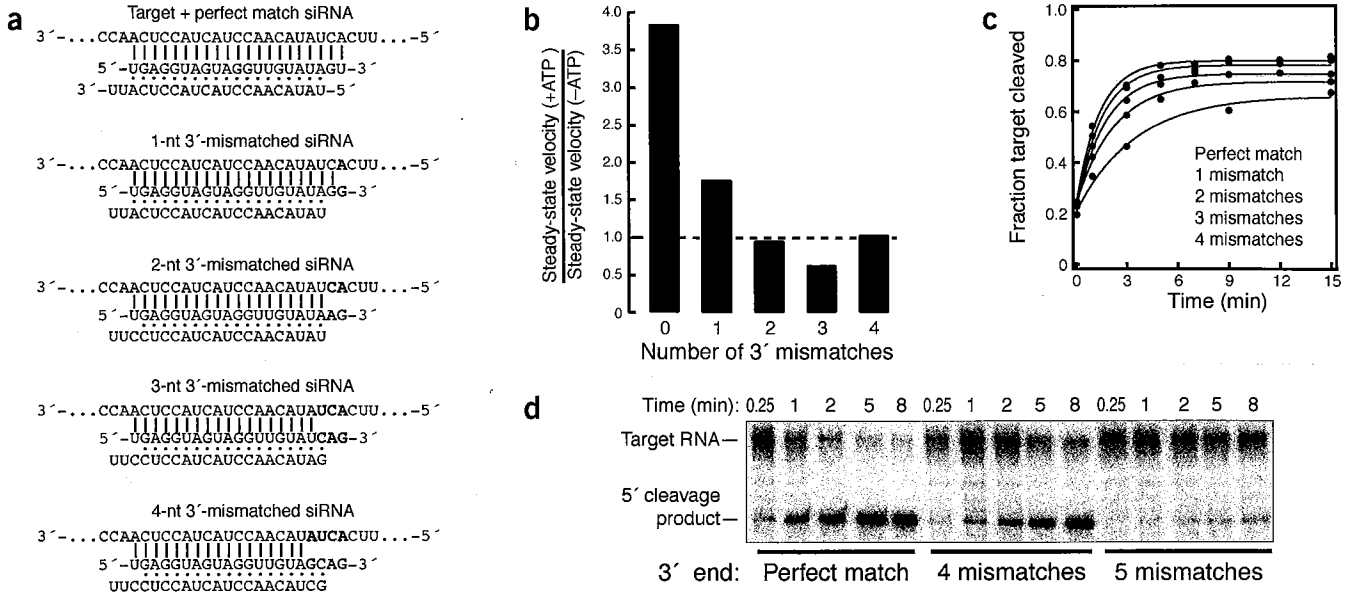

Figure 2 In the absence of ATP, mismatches between the 3′ end of the siRNA guide strand and the target RNA facilitate product release, but reduce the rate of target cleavage. (**a**) Representative siRNA sequences aligned with the target sequence. The siRNA guide strand is colored (5′→3′) and the mismatch with the target site is highlighted yellow. A complete list of siRNA sequences appears in **Supplementary Figure 3** online. (**b**) The steady-state rate of cleavage in the presence and absence of ATP was determined for siRNAs with zero to four 3′ mismatches with the target site. The target RNA concentration was 49 nM and the concentration of RISC was either ~4 nM (no mismatches) or ~6 nM (1–4 mismatches). The steady-state velocity with ATP, relative to the velocity without ATP, is shown for each siRNA. (**c**) Time course of cleavage for perfectly matched (~16-fold excess of RISC relative to target) and mismatched (~80-fold excess of RISC) siRNA. (**d**) Data representative of those used in the analysis in **c** for target cleavage directed by siRNAs with zero, four and five 3′ mismatches.

RNA target (Fig. 4a,b). No cleavage was detected for siRNAs with six, seven or eight 5′ mismatches to the target, even after 24 h incubation. The siRNA bearing eight mismatches between its 5′ end and the *let-7* complementary target was fully active when eight compensatory mutations were introduced into the *let-7*-binding site (Figs. 3c and 4b), demonstrating that mutation of the siRNA was not the cause of its inactivity against the mismatched target. Similarly, when eight mismatches with the 3′ or 5′ end of the siRNA were created by changing the sequence of the RNA target, we detected target RNA cleavage when the target contained eight mismatches with the siRNA 3′ end, but not with the 5′ end (Fig. 4b,c).

To begin to estimate the minimal number of base pairs between the siRNA and its target that permit detectable cleavage by RISC at 24 h incubation, we combined seven, eight or nine 3′ mismatches with increasing numbers of 5′ mismatches (Fig. 4c). Cleavage was detected for as many as nine 3′ mismatches. But no detectable cleavage occurred when seven, eight or nine 3′ mismatches were combined with two or more 5′ mismatches. In contrast, a single 5′ mismatch (p1) enhanced target cleavage directed by all three 3′ mismatched siRNAs. Only 6% of the target RNA was cleaved after 24 h when the siRNA contained nine contiguous 3′ mismatches with the target RNA, but 10% was cleaved when the siRNA contained both nine 3′ mismatches and a single (p1)

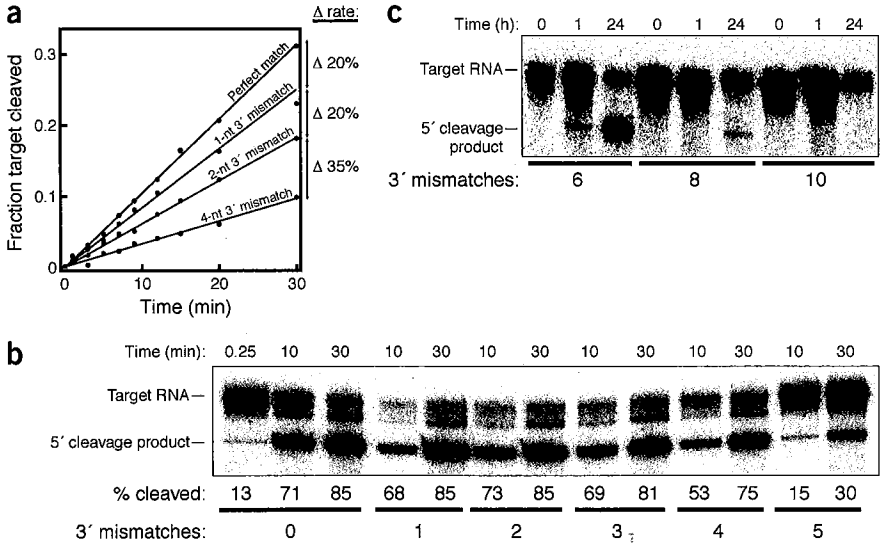

Figure 3 Tolerance of RISC for 3′ mismatches. (**a**) Each additional 3′ mismatch further reduced the rate of cleavage by RISC. The steady-state rates of cleavage were determined for siRNA with zero, one, two and four mismatches under multiple-turnover conditions (~49 nM target mRNA and ~4–6 nM RISC). (**b**) Analysis of siRNAs bearing zero to five 3′ mismatches with the target RNA under conditions of slight enzyme excess (about two-fold more RISC than target). siRNA sequences used in **a** and **b** are shown in **Figure 2a** and **Supplementary Figure 3** online. (**c**) Extended endpoint analysis of RISC cleavage under conditions of ~80-fold enzyme excess reveals that cleavage can occur for siRNAs with as many as eight mismatches to the target RNA. Note the different time scales in **c** versus **b**. All reactions were under standard *in vitro* RNAi (+ATP) conditions.

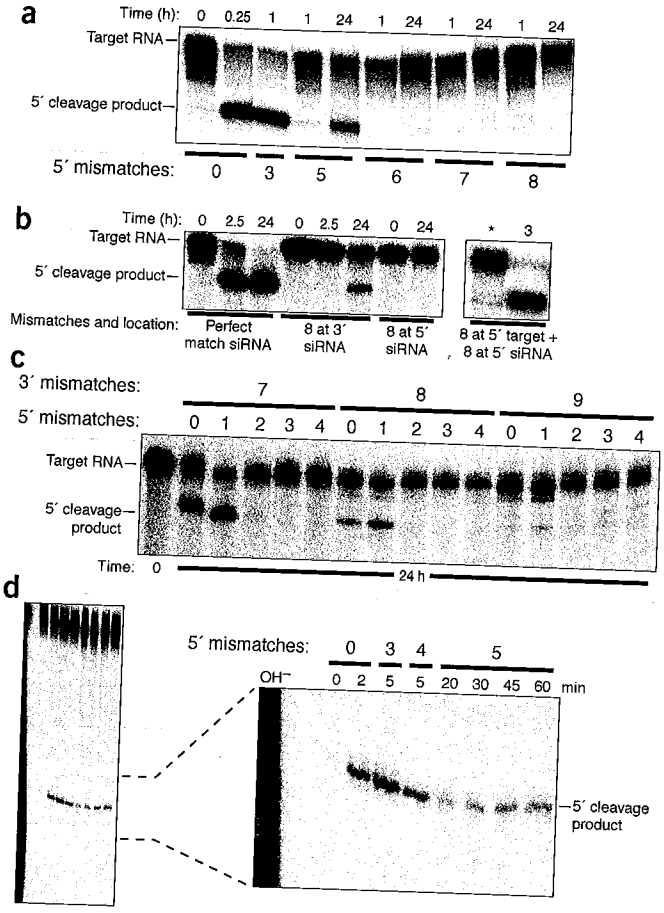

Figure 4 Limited tolerance of RISC for 5′ mismatches. (**a**) RISC cleavage was analyzed as in **Figure 3c** using 5′-mismatched siRNAs whose sequences are given in **Supplementary Figure 3** online. The target RNA was the same for all siRNAs. (**b**) RISC cleavage was analyzed using a single siRNA sequence. Mismatches were created by altering the sequence of the target RNA. For the target containing compensatory mutations, the target concentration was 0.25 nM and the siRNA concentration was ~20 nM; RISC concentration was not determined. Asterisk, 15-s time point. (**c**) RISC cleavage was analyzed by incubating 50 nM siRNA with 0.5 nM target RNA. 3′ mismatches were created by modifying the target sequence, and 5′ mismatches by changing the siRNA. Target and siRNA sequences are given in **Supplementary Figure 3** online. (**d**) Perfectly base-paired and 5′-mismatched siRNAs direct cleavage at the same phosphodiester bond. Cleavage reactions were carried out with ~20 nM RISC generated from 50 nM siRNA and 0.5 nM target RNA and analyzed on 8% (w/v) denaturing PAGE. The lengths of the target mRNA and 5′ cleavage product were 182 nt and 148 nt, respectively. After RISC was assembled, the extract was treated with NEM to inactivate nucleases[43]. After NEM treatment, the ATP-regenerating system was restored by adding additional creatine kinase, target RNA was added and the incubation was continued for the indicated time. OH^- denotes a base hydrolysis ladder.

5′ mismatch. Cleavage was similarly enhanced by the addition of a p1 mismatch to seven 3′ mismatches (49% cleavage versus 75% cleavage at 24 h) or to eight 3′ mismatches (21% versus 42% cleavage at 24 h). The finding that unpairing of the first base of the siRNA guide strand potentiated cleavage under single-turnover conditions suggests that a conformational change occurs in RISC during which the paired p1 base becomes unpaired before cleavage. Notably, p1 is often predicted to be unpaired for miRNAs bound to their targets[23–25].

For siRNAs that pair fully with their RNA targets, the scissile phosphate always lies between the target nucleotides that pair with siRNA bases 10 and 11 (refs. 2,9). Analysis at single-nucleotide resolution of the 5′ cleavage products generated by siRNAs with three, four or five 5′ mismatches (**Fig. 4d**) or six 3′ terminal mismatches (data not shown) revealed that the scissile phosphate on the target RNA remained the same, even when five 5′ nucleotides of the siRNA guide strand were mismatched with the target RNA (**Fig. 4d**). As discussed below, this result suggests that the identity of the scissile phosphate is a consequence of the structure of RISC, rather than being measured from the 5′ end of the helix formed between the siRNA and its RNA target.

Kinetic analysis of RISC catalysis

What role do nucleotides in the terminal regions of the siRNA guide strand play in directing RISC activity? Reduced pairing between an siRNA and its target might disrupt the binding of RISC to its target alternatively, mismatches might disrupt the structure, but not the affinity, of the siRNA-target interaction. Fully matched siRNAs are thought to form a 21-base pair, A-form helix with the target RNA[19,26], but do all parts of this helix contribute equally to target binding or do some regions provide only a catalytically permissive geometry? To distinguish between these possibilities, we analyzed the Michaelis-Menten kinetics of siRNA-directed target-RNA cleavage for a perfectly matched siRNA and for three siRNAs mismatched at their termini. siRNAs were assembled into RISC, diluted with reaction buffer to the desired RISC concentration and mixed with target RNA. For each siRNA, the initial velocity of reaction was determined at multiple substrate concentrations (**Supplementary Fig. 3** online), and K_m and k_{cat} were determined from a nonlinear least squares fit of substrate concentration versus initial velocity (**Fig. 5a**). By this assay, we estimate that the K_m of the *let-7* siRNA with complete complementarity to its target is ~8.4 nM (**Table 1**). We could not detect a difference in K_m, within error, between the fully paired siRNA and siRNA variants bearing three to five mismatches at their 3′ end or three mismatches at their 5′ end (**Fig. 5a** and **Table 1**). We note that for the mismatched siRNAs we used a higher than optimal enzyme concentration to detect cleavage. Therefore, our K_m measurements for the mismatched siRNAs represent an upper bound for the actual K_m values.

Although the K_m was unaltered for the *let-7* siRNA containing several terminal mismatches, the turnover number, k_{cat}, was decreased by terminal mismatches (**Table 1**). Three mismatches at the 5′ end of the siRNA halved the k_{cat}, whereas three 3′ mismatches decreased k_{cat} more than six-fold. The introduction of five 3′ mismatches did not increase the K_m, yet decreased k_{cat} >25-fold.

K_m reflects the binding strength of RISC

To estimate the contribution of binding to K_m, we used a competition assay that measures the ability of 2′-*O*-methyl oligonucleotides to inhibit target cleavage by RISC (**Fig. 5b**). Such a strategy has been used previously to analyze the mechanism of target destruction by antisense oligonucleotides that recruit RNase H[27]. We anticipated that 2′-*O*-methyl oligonucleotides would act as competitive inhibitors of RISC, because they bind to RISC containing complementary siRNA but not to RISC containing unrelated siRNA[21,28]. We designed 31-nt, 2′-*O*-methyl oligonucleotides as described[21], taking care to exclude sequences predicted to form stable internal structures. We chose 2′-*O*-methyl oligonucleotides because of their marked stability in *D. melanogaster* lysate and because they can be added to the reaction at high micromolar concentration.

Competition by 2′-*O*-methyl oligonucleotides and authentic RNA targets was quantitatively similar. We analyzed the reaction

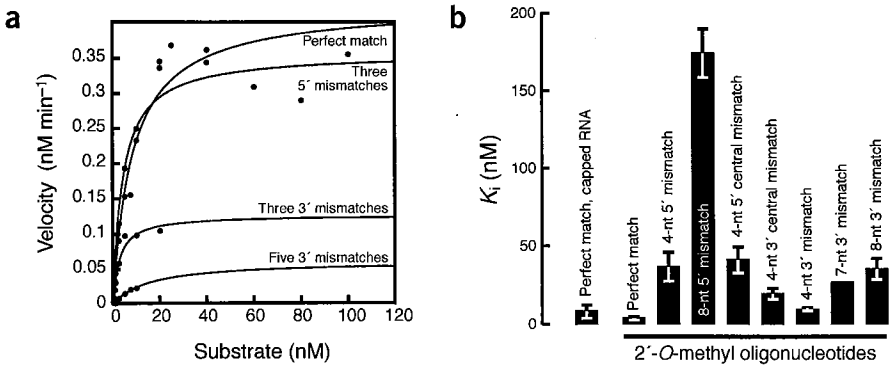

Figure 5 Michaelis-Menten and K_i analysis for matched and mismatched siRNAs reveal distinct contributions to binding and catalysis for the 5′, central and 3′ regions of the siRNA. (**a**) siRNA was assembled into RISC under standard *in vitro* RNAi conditions, and then diluted to achieve the desired RISC concentration. The initial rates of cleavage were determined for increasing concentrations of 5′ ^{32}P-cap-radiolabled target mRNA. Plot of initial velocity versus substrate concentration. K_m and V_{max} were determined by fitting the data to the Michaelis-Menten equation. See **Table 1** for analysis. Representative initial rate determinations appear in **Supplementary Figure 2** online. (**b**) K_i values were determined in competition assays using 2′-*O*-methyl oligonucleotides bearing 5′, central and 3′ mismatches to the siRNA guide strand. Representative data are presented in **Supplementary Figure 2** online, and a complete list of the 2′-*O*-methyl oligonucleotides used appears in **Supplementary Figure 3** online.

velocities of siRNA-directed cleavage of a ^{32}P-radiolabled target in the presence of increasing concentrations of unlabeled capped RNA target or a 31-nt 2′-*O*-methyl oligonucleotide corresponding to the region of the target containing the siRNA-binding site (**Fig. 5b**). Lineweaver-Burk analysis of the data confirms that 2′-*O*-methyl oligonucleotides act as competitive inhibitors of RISC (data not shown). These data were used to calculate K_i values for the perfectly matched RNA and 2′-*O*-methyl competitors. For the capped RNA competitor, the K_i was ~7.7 ± 4 nM (**Fig. 5b**), nearly identical to the K_m for this siRNA, 8.4 nM (**Table 1**). The K_i for the perfectly matched 2′-*O*-methyl competitor oligonucleotide was 3.2 ± 1 nM (**Fig. 5b**), essentially the same, within error, as that of the all-RNA competitor. We conclude that 2′-*O*-methyl oligonucleotides are good models for 5′-capped RNA targets and that the K_m for target cleavage by RISC is largely determined by the affinity (K_d) of RISC for its target RNA.

Although targets with more than five contiguous mismatches to either end of the siRNA are poor substrates for cleavage, they might nonetheless bind RISC and compete with the ^{32}P-radiolabeled target RNA. We used the 2′-*O*-methyl oligonucleotide competition assay to determine the K_i values for oligonucleotides containing as many as eight mismatches to the siRNA guide strand (**Fig. 5b**). 2′-*O*-methyl oligonucleotides with 3′ terminal mismatches to the siRNA were good competitors: a 4-nt mismatch with the 3′ end of the siRNA increased the K_i by only about three-fold (9.0 ± 0.9 nM) and an 8-nt mismatch with the 3′ end of the siRNA increased the K_i by about ten-fold (34.8 ± 7 nM). In contrast, mismatches with the 5′ end of the siRNA had a marked effect on binding. A 4-nt mismatch to the 5′ end of the siRNA increased the K_i ~12-fold (36.4 ± 9.2 nM) and an 8-nt mismatch to the 5′ end of the siRNA increased the K_i 53-fold (173 ± 16 nM). The differential effect on binding between 5′ and 3′ mismatches was maintained even at the center of the siRNA: a 2′-*O*-methyl oligonucleotide bearing four mismatches with siRNA nucleotides 11, 12, 13 and 14 (4-nt 3′ central mismatch, **Fig. 5b**) bound more tightly to RISC (that is, had a lower K_i) than an oligonucleotide with four mismatches to siRNA positions 7, 8, 9 and 10 (4-nt 5′ central mismatch, **Fig. 5b**).

DISCUSSION

RISC programmed with exogenous siRNA is an enzyme capable of multiple rounds of target cleavage. Our previous work has shown that cleavage of a target RNA by RISC does not require ATP[3,29]. The more detailed kinetic analysis presented here suggests that there are no ATP-assisted steps in either target recognition or cleavage by *D. melanogaster* RISC; we detect no difference in rate in the presence or absence of ATP for RNAi reactions analyzed under conditions of substrate excess at early time points (pre-steady state) or under conditions of enzyme excess where the reaction was essentially single-turnover. In contrast, the steady-state rate of cleavage under multiple-turnover conditions was enhanced four-fold by ATP. Our data suggest that release of the products of the RISC endonuclease is rate-determining under these conditions in the absence of ATP, but not in the presence of ATP. The most straightforward explanation for this finding is that an ATP-dependent RNA helicase facilitates the dissociation of the products of target cleavage from the RISC-bound

Table 1 Kinetic analysis of RISC

Mismatches and position	K_m (nM)	V_{max} (nM s^{-1})	[RISC] (nM)	k_{cat} (s^{-1})	k_{cat} K_m^{-1} (nM^{-1} s^{-1})	Fold change (k_{cat} K_m^{-1})
None	8.4 ± 1.6	0.0071	1	7.1×10^{-3}	8.4×10^{-4}	1.00
3-nt 3′	2.7 ± 0.6	0.0022	2	1.1×10^{-3}	3.8×10^{-4}	0.46
5-nt 3′	6.0 ± 1.8	0.0054	2	2.7×10^{-4}	4.5×10^{-5}	0.05
3-nt 5′	4.7 ± 1.3	0.0063	2	3.2×10^{-3}	6.7×10^{-4}	0.80
Reference enzymes	**K_m (nM)**			**k_{cat} (s^{-1})**	**k_{cat} K_m^{-1} (nM^{-1} s^{-1})**	**k_{cat} K_m^{-1} relative to RISC**
Urease	2.5×10^7			1×10^4	4.0×10^{-4}	0.47
Fumarase	5.0×10^3			8×10^2	1.6×10^{-1}	190
Catalase	2.5×10^7			1×10^7	4.0×10^{-1}	8,940
RNase H1	3.8×10^1			5×10^2	1.3×10^{-3}	0.03

Summary of kinetic data from the analysis in **Figure 5a**. For comparison, the K_m and k_{cat} values of four well-studied protein enzymes, urease[44], fumarase[44], catalase[44] and RNase H1 (ref. 45), are provided. K_m ± error of fit is reported.

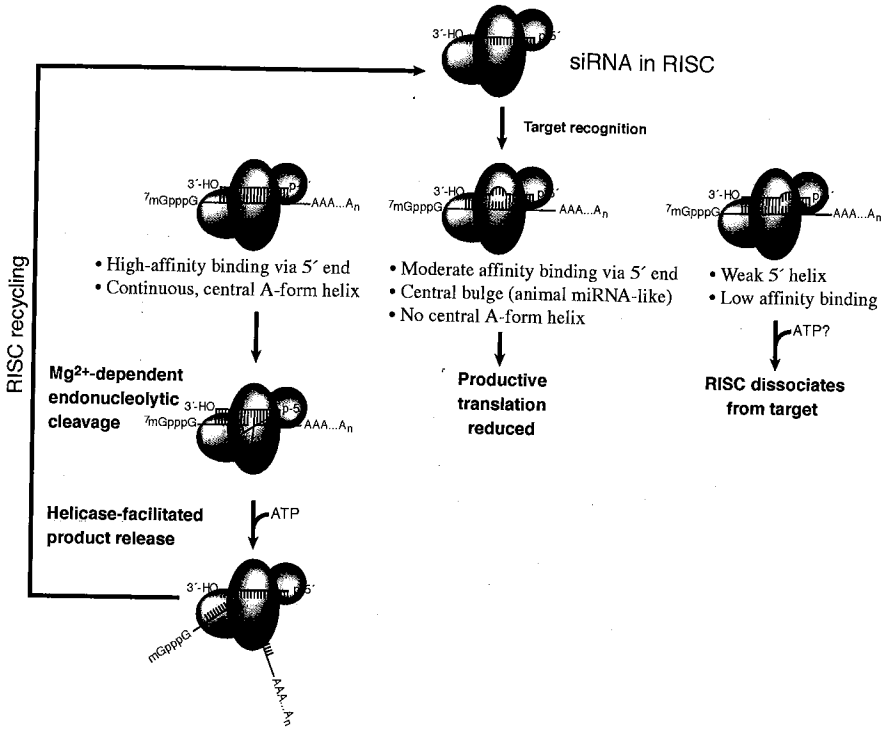

Figure 6 A model for the cycle of RISC assembly, target recognition, catalysis and recycling.

siRNA. The involvement of such an ATP-dependent helicase in RNAi *in vivo* may explain why siRNAs can be active within a broad range of GC content[30].

In the presence of ATP, siRNA-programmed *D. melanogaster* RISC is a classical Michaelis-Menten enzyme. The guide strand of the siRNA studied here has the sequence of *let-7*, an endogenous miRNA. *In vivo*, *let-7* is not thought to direct mRNA cleavage, but rather is believed to repress productive translation of its mRNA targets. Nonetheless, the *let-7* siRNA is among the most potent of the siRNAs we have studied *in vitro* and provides a good model for effective siRNA in general. With a k_{cat} of ~7×10^{-3} s^{-1}, the *let-7* siRNA-programmed RISC was slow compared with enzymes with small molecule substrates (Table 1). The K_m for this RISC was ~8 nM. Enzymes typically have K_m values between 1- and 100-fold greater than the physiological concentrations of their substrates[31]. Our data suggest that RISC is no exception: individual abundant mRNA species are present in eukaryotic cells at high picomolar or low nanomolar concentration. The K_m of RISC is probably determined primarily by the strength of its interaction with the target RNA, because the K_m is nearly identical to the K_i of a noncleavable 2′-*O*-methyl oligonucleotide inhibitor.

Recently, Tuschl and colleagues have measured the kinetic parameters of target RNA cleavage by human RISC[32]. In that study, the minimal active human RISC was highly purified; in this study, *D. melanogaster* RISC activity was measured for the unpurified, intact holo-RISC, believed to be an 80S multiprotein complex[33]. Different siRNAs were used in the two studies. Nonetheless, the K_m and k_{cat} values reported here and for the minimal human RISC are markedly similar: the K_m was 2.7–8.4 nM and the k_{cat} was 7.1×10^{-3} s^{-1} for the *let-7* siRNA-programmed *D. melanogaster* holo-RISC versus a K_m of 1.1–2.3 nM and a k_{cat} of 1.7×10^{-2} s^{-1} for a different siRNA in minimal human RISC. As in this study, Tuschl and colleagues also observed a pre-steady-state burst in the absence of ATP, consistent with the idea that product release is ATP-assisted *in vivo*.

The ratio of k_{cat} to K_m is a classical measure of enzyme efficiency and corresponds to the second-order rate constant for the reaction when the concentration of substrate is much less than the K_m. For the *let-7* programmed RISC, k_{cat} K_m^{-1} equals ~8.4×10^5 M^{-1} s^{-1} (~8.4×10^{-4} nM^{-1} s^{-1}), a value far slower than the expected rate of collision of RISC with mRNA, ≥10^7 M^{-1} s^{-1}. What then limits the rate of catalysis by RISC? Perhaps cleavage by RISC is constrained by the rate of conformational changes required for formation of the enzyme–substrate complex or by subsequent conformational rearrangements required for catalysis. Future studies will be needed to determine if siRNAs can be designed that substantially improve either the k_{cat} or K_m of RISC without compromising specificity.

Although siRNAs are typically envisioned to bind their target RNAs through 19–21 complementary base pairs, we find that the 5′, central and 3′ regions of the siRNA make distinct contributions to binding and catalysis (Fig. 6). Measurements of K_m and K_i suggest that the 5′ nucleotides of the siRNA contribute more to target binding than do the 3′ nucleotides. At least for the siRNA examined here, the first three and the last five nucleotides of a 21-nt siRNA contribute little to binding. If the K_d of RISC bound to its target RNA is essentially its K_m, ~8 nM, then the free energy ($\Delta G^\circ = -RT \ln K_d$) of the *let-7*-programmed RISC-target interaction is about −11 kcal mol^{-1}, considerably less than the −35 kcal mol^{-1} (K_d ~10^{-29}) predicted (http://ozone2.chem.wayne.edu/Hyther/hytherm1main.html) for the *let-7* RNA bound to a fully complementary RNA in 100 mM K^+ and 1.2 mM Mg^{2+} at 25 °C. Why does RISC seem to discard so much potential binding energy? Perhaps by binding less tightly to its target, an siRNA in RISC gains the ability to discriminate between well matched and poorly matched targets, but only for bases in the 5′ region of the siRNA guide strand.

Mismatches between the central and 3′ regions of an siRNA and its target RNA reduce k_{cat} far more than mismatches at the 5′ end of the siRNA. These results fit well with recent findings by Doench and Sharp that translational repression by siRNA, designed to act like animal miRNA, is markedly disrupted by mismatches with the 5′ end of the siRNA, but not with similar mismatches at the 3′ end[18]. These authors propose that miRNA binding is mediated primarily by nucleotides at the 5′ end of the small RNA. In fact, complementarity between the 5′ end of miRNAs and their targets has been required by all computational approaches for predicting animal miRNA targets[16,23,25,34]. Our finding that central and 3′ siRNA sequences must pair with the target sequence for effective target cleavage but not for target binding reinforces this view; both central and 3′ miRNA sequences are usually mismatched with their binding sites in their natural targets[35–41].

Formation of a contiguous A-form helix surrounding the scissile phosphate of the target mRNA has been proposed to be a quality control step for RISC-mediated target cleavage[19]. We find that RISC can direct cleavage when the siRNA is paired with the target RNA only at positions 2–12 of the guide strand, corresponding to one complete turn of an RNA-RNA helix. This region of the siRNA includes

nucleotides 2–8, which seem to be critical for miRNA recognition of mRNAs targeted for translational repression, plus two nucleotides flanking either side of the scissile phosphate. Our finding that unpairing the first nucleotide of the guide strand enhances the activity of siRNAs with seven, eight or nine 3′ mismatches to the RNA target is notable, as many miRNAs do not pair with their targets at this position. Furthermore, such pairing resembles that reported by Linsley and colleagues for siRNA-directed off-target effects in cultured mammalian cells[14].

The requirement for a full turn of a helix may reflect a mechanism of 'quality control' by RISC. Because RISC can apparently assemble on any siRNA sequence, it must use the structure of the siRNA paired to its target to determine whether or not to cleave. Despite the apparent surveillance of the structure of the siRNA-target pair, the identity of the scissile phosphate is unaltered by extensive mismatch between the 5′ end of the siRNA and its target. Yet the scissile phosphate is determined by its distance from the 5′ end of the siRNA guide strand[2,9]. The simplest explanation for our findings is that the scissile phosphate is identified by a protein loaded onto the siRNA during RISC assembly, that is, before the encounter of the RISC with its target RNA.

The remarkable tolerance of RISC for mismatches between the siRNA and its targets—up to nine contiguous 3′ nucleotides—implies that a large number of off-target genes should be expected for many siRNA sequences when RISC is present in excess over its RNA targets. However, RISC with extensive mismatches between the siRNA and target is quite slow to cleave, so off-target effects may be minimized by keeping the amount of RISC as low as possible. As our understanding of the molecular basis of siRNA-directed gene silencing grows, we anticipate that siRNA will be able to be designed to balance the competing demands of siRNA efficacy and specificity.

METHODS

General methods. *D. melanogaster* embryo lysate, siRNA labeling with polynucleotide kinase (New England Biolabs), target RNA preparation and labeling with guanylyl transferase were carried out as described[20,42], and the forward primer sequence for 379-nt target mRNA was 5′-CGC TAA TAC GAC TCA CTA TAG CAG TTG GCG CCG CGA ACG A-3′, and 5′-GCG TAA TAC GAC TCA CTA TAG TCA CAT CTC ATC TAC CTC C-3′ for the 182-nt target. Reverse primers used to generate fully matched and mismatched target RNAs were: 5′-CCC ATT TAG GTG ACA CTA TAG ATT TAC ATC GCG TTG AGT GTA GAA CGG TTG TAT AAA AGG TTG AGG TAG TAG GTT GTA TAG TGA AGA GAG GAG TTC ATG ATC AGT G-3′ (perfect match to let-7); 5′-CCC ATT TAG GTG ACA CTA TAG ATT TAC ATC GCG TTG AGT GTA GAA CGG TTG TAT AAA AGG TTG AGG TAG TAG GTT CAT GCA GGA AGA GAG GAG TTC ATG ATC AGT G-3′ (7-nt 3′ mismatch); 5′-CCC ATT TAG GTG ACA CTA TAG ATT TAC ATC GCG TTG AGT GTA GAA CGG TTG TAT AAA AGG TTG AGG TAG TAG GTA CAU GCA GGA AGA GAG GAG TTC ATG ATC AGT G-3′ (8-nt 3′ mismatch); 5′-CCC ATT TAG GTG ACA CTA TAG ATT TAC ATC GCG TTG AGT GTA GAA CGG TTG TAT AAA AGG TTG AGG TAG TAG GAA CAT GCA GGA AGA GAG GAG TTC ATG ATC AGT G-3′ (9-nt 3′ mismatch); 5′-CCC ATT TAG GTG ACA CTA TAG ATT TAC ATC GCG TTG AGT GTA GAA CGG TTG TAT AAA AGG TAC TCC ATC TAG GTT GTA TAG TGA AGA GAG GAG TTC ATG ATC AGT G-3′ (8-nt 5′ mismatch); 5′-CCC ATT TAG GTG ACA CTA TAG ATT TAC ATC GCG TTG AGT GTA GAA CGG TTG TAT AAA AGG TAC TCG TAG TAG GTT GTA TAG TGA AGA GAG GAG TTC ATG ATC AGT G-3′ (4-nt 5′ mismatch). The lengths of the target sequences were 613 nt (**Figs. 1–3** and **5a** and **Supplementary Figures 1** and **2** online); 379 nt (**Figs. 4a–c** and **5b** and **Supplementary Figure 2** online); and 182 nt (**Fig. 4d**). All siRNAs were deprotected according to the manufacturer's protocol (Dharmacon), 5′-radiolabeled where appropriate, and then gel-purified on 15% (w/v) denaturing PAGE. 2′-*O*-methyl oligonucleotides were from Dharmacon. siRNA strands were annealed at high concentrations and serially diluted into lysis buffer (30 nM HEPES, pH 7.4, 100 mM KOAc, and 2 mM $MgCl_2$). Gels were dried and imaged as described[22]. Images were analyzed using Image Gauge 4.1 (Fuji). Initial rates were determined by linear regression using Excel X (Microsoft) or IgorPro 5.01 (Wavemetrics). Kaleidagraph 3.6.2 (Synergy Software) was used to determine K_m and K_i by global fitting to the equations: $V = (V_{max} \times S)\ (K_m + S)^{-1}$ and $V = (V_{max} \times K_{i(app)})\ (K_{i(app)} + I)^{-1}$, where V is velocity, S is target RNA concentration, and I is the concentration of 2′-*O*-methyl oligonucleotide competitor. K_i was calculated by correcting $K_{i(app)}$ by the K_m and substrate concentration, $K_i = K_{i(app)}\ (1 + (S\,K_m^{-1}))^{-1}$.

ATP depletion and NEM inhibition. RNAi reactions using *D. melanogaster* embryo lysate were done as described[42]. To compare –ATP and +ATP conditions, samples were treated with 10 mM NEM (Pierce) for 10 min at 4 °C, and then the NEM was quenched with 11 mM DTT. For ATP depletion (–ATP), 1 unit of hexokinase and 20 mM (final concentration) glucose were added and the incubation continued for 30 min at 25 °C. For +ATP reactions, 0.05 mg ml^{-1} (final concentration) creatine kinase and one-tenth volume H_2O were substituted for hexokinase and glucose, respectively. The addition of fresh creatine kinase after NEM treatment did not rescue the defect in RISC assembly, but did restore ATP to high levels[3]. ATP levels were measured using an ATP assay kit (Sigma) and a PhL luminometer (Mediators Diagnostika).

Note: Supplementary information is available on the Nature Structural & Molecular Biology website.

ACKNOWLEDGMENTS

We thank J. McLachlan for maintaining our fly colony, and members of the Zamore lab, S. Blacklow, T. Carruthers and D. Turner for encouragement, helpful discussions and comments on the manuscript. P.D.Z. is a Pew scholar in the biomedical sciences and a W.M. Keck Foundation young scholar in medical research. This work was supported in part by grants from the US National Institutes of Health to P.D.Z. (GM62862-01 and GM65236-01).

COMPETING INTERESTS STATEMENT

The authors declare competing financial interests (see *Nature Structural & Molecular Biology* website for details).

Received 31 March; accepted 12 May 2004
Published online at http://www.nature.com/nsmb/

1. Fire, A. *et al.* Potent and specific genetic interference by double-stranded RNA in Caenorhabditis elegans. *Nature* **391**, 806–811 (1998).
2. Elbashir, S.M., Lendeckel, W. & Tuschl, T. RNA interference is mediated by 21- and 22-nucleotide RNAs. *Genes Dev.* **15**, 188–200 (2001).
3. Nykänen, A., Haley, B. & Zamore, P.D. ATP requirements and small interfering RNA structure in the RNA interference pathway. *Cell* **107**, 309–321 (2001).
4. Martinez, J., Patkaniowska, A., Urlaub, H., Lührmann, R. & Tuschl, T. Single-stranded antisense siRNA guide target RNA cleavage in RNAi. *Cell* **110**, 563–574 (2002).
5. Hammond, S.M., Bernstein, E., Beach, D. & Hannon, G.J. An RNA-directed nuclease mediates post-transcriptional gene silencing in *Drosophila* cells. *Nature* **404**, 293–296 (2000).
6. Hannon, G.J. & Zamore, P.D. Small RNAs, big biology and biochemical studies of RNA interference. In *RNAi: A Guide To Gene Silencing* (ed. Hannon, G.J.) 87–108 (Cold Spring Harbor Laboratory Press, Cold Spring Harbor, NY, 2003).
7. Elbashir, S.M. *et al.* Duplexes of 21-nucleotide RNAs mediate RNA interference in cultured mammalian cells. *Nature* **411**, 494–498 (2001).
8. Amarzguioui, M., Holen, T., Babaie, E. & Prydz, H. Tolerance for mutations and chemical modifications in a siRNA. *Nucleic Acids Res.* **31**, 589–595 (2003).
9. Elbashir, S.M., Martinez, J., Patkaniowska, A., Lendeckel, W. & Tuschl, T. Functional anatomy of siRNAs for mediating efficient RNAi in *Drosophila melanogaster* embryo lysate. *EMBO J.* **20**, 6877–6888 (2001).
10. Holen, T., Amarzguioui, M., Babaie, E. & Prydz, H. Similar behaviour of single-strand and double-strand siRNAs suggests they act through a common RNAi pathway. *Nucleic Acids Res.* **31**, 2401–2407 (2003).
11. Tang, G., Reinhart, B.J., Bartel, D.P. & Zamore, P.D. A biochemical framework for RNA silencing in plants. *Genes Dev.* **17**, 49–63 (2003).
12. Phipps, K.M., Martinez, A., Lu, J., Heinz, B.A. & Zhao, G. Small interfering RNA molecules as potential anti-human rhinovirus agents: *in vitro* potency, specificity, and mechanism. *Antiviral Res.* **61**, 49–55 (2004).
13. Ding, H. *et al.* Selective silencing by RNAi of a dominant allele that causes amyotrophic lateral sclerosis. *Aging Cell* **2**, 209–217 (2003).
14. Jackson, A.L. *et al.* Expression profiling reveals off-target gene regulation by RNAi. *Nat. Biotechnol.* **21**, 635–637 (2003).
15. Bartel, D.P. MicroRNAs: genomics, biogenesis, mechanism, and function. *Cell* **116**, 281–297 (2004).
16. Rajewsky, N. & Socci, N.D. Computational identification of microRNA targets. *Dev. Biol.* **267**, 529–535 (2004).

17. Lai, E.C. Micro RNAs are complementary to 3′ UTR sequence motifs that mediate negative post-transcriptional regulation. *Nat. Genet.* **30**, 363–364 (2002).
18. Doench, J.G. & Sharp, P.A. Specificity of microRNA target selection in translational repression. *Genes Dev.* **18**, 504–511 (2004).
19. Chiu, Y.L. & Rana, T.M. siRNA function in RNAi: a chemical modification analysis. *RNA* **9**, 1034–1048 (2003).
20. Hutvágner, G. & Zamore, P.D. A microRNA in a multiple-turnover RNAi enzyme complex. *Science* **297**, 2056–2060 (2002).
21. Hutvágner, G., Simard, M.J., Mello, C.C. & Zamore, P.D. Sequence-specific inhibition of small RNA function. *PLoS Biol.* **2**, 1–11 (2004).
22. Schwarz, D.S. *et al.* Asymmetry in the assembly of the RNAi enzyme complex. *Cell* **115**, 199–208 (2003).
23. Lewis, B., Shih, I., Jones-Rhoades, M., Bartel, D. & Burge, C. Prediction of mammalian microRNA targets. *Cell* **115**, 787–798 (2003).
24. Rhoades, M.W. *et al.* Prediction of plant microRNA targets. *Cell* **110**, 513–520 (2002).
25. Stark, A., Brennecke, J., Russel, R. & Cohen, S. Identification of *Drosophila* microRNA targets. *PLoS Biol.* **1**, 1–13 (2003).
26. Chiu, Y.-L. & Rana, T.M. RNAi in human cells: basic structural and functional features of small interfering RNA. *Molecular Cell* **10**, 549–561 (2002).
27. Lima, W.F. & Crooke, S.T. Binding affinity and specificity of *Escherichia coli* RNase H1: impact on the kinetics of catalysis of antisense oligonucleotide-RNA hybrids. *Biochemistry* **36**, 390–398 (1997).
28. Meister, G., Landthaler, M., Dorsett, Y. & Tuschl, T. Sequence-specific inhibition of microRNA- and siRNA-induced RNA silencing. *RNA* **10**, 544–550 (2004).
29. Tomari, Y. *et al.* RISC assembly defects in the *Drosophila* RNAi mutant armitage. *Cell* **116**, 831–841 (2004).
30. Reynolds, A. *et al.* Rational siRNA design for RNA interference. *Nat. Biotechnol.* **22**, 326–330 (2004).
31. Stryer, L. *Biochemistry.* (W. H. Freeman and Company, San Francisco; 1981).
32. Martinez, J. & Tuschl, T. RISC is a 5′ phosphomonoester-producing RNA endonuclease. *Genes Dev.* **18**, 975–980 (2004).
33. Pham, J.W., Pellino, J.L., Lee, Y.S., Carthew, R.W. & Sontheimer, E.J. A Dicer-2-dependent 80S complex cleaves targeted mRNAs during RNAi in *Drosophila. Cell* **117**, 83-94 (2004).
34. Enright, A. *et al.* MicroRNA targets in *Drosophila. Genome Biol.* **5**, R1 (2003).
35. Lee, R.C., Feinbaum, R.L. & Ambros, V. The *C. elegans* heterochronic gene *lin-4* encodes small RNAs with antisense complementarity to *lin-14. Cell* **75**, 843–854. (1993).
36. Reinhart, B.J. *et al.* The 21-nucleotide *let-7* RNA regulates developmental timing in *Caenorhabditis elegans. Nature* **403**, 901–906. (2000).
37. Brennecke, J., Hipfner, D.R., Stark, A., Russell, R.B. & Cohen, S.M. *bantam* encodes a developmentally regulated microRNA that controls cell proliferation and regulates the proapoptotic gene *hid* in *Drosophila. Cell* **113**, 25–36 (2003).
38. Abrahante, J.E. *et al.* The *Caenorhabditis elegans hunchback*-like gene *lin-57/hbl-1* controls developmental timing and is regulated by microRNAs. *Dev. Cell* **4**, 625–637 (2003).
39. Vella, M., Choi, E., Lin, S., Reinert, K. & Slack, F. The *C. elegans* microRNA *let-7* binds to imperfect *let-7* complementary sites from the *lin-41* 3′UTR. *Genes Dev.* **18**, 132–137 (2004).
40. Xu, P., Vernooy, S.Y., Guo, M. & Hay, B.A. The *Drosophila* microRNA miR-14 suppresses cell death and is required for normal fat metabolism. *Curr. Biol.* **13**, 790–795 (2003).
41. Johnston, R.J. & Hobert, O. A microRNA controlling left/right neuronal asymmetry in *Caenorhabditis elegans. Nature* **426**, 845–849 (2003).
42. Haley, B., Tang, G. & Zamore, P.D. *In vitro* analysis of RNA interference in *Drosophila melanogaster. Methods* **30**, 330–336 (2003).
43. Schwarz, D.S., Tomari, Y. & Zamore, P.D. The RNA-induced silencing complex is a Mg^{2+}-dependent endonuclease. *Curr. Biol.* **14**, 787–791 (2004).
44. Voet, D. & Voet, J.G. *Biochemistry.* (John Wiley & Sons, Hoboken, NJ; 2004).
45. Wu, H., Lima, W.F. & Crooke, S.T. Investigating the structure of human RNase H1 by site-directed mutagenesis. *J. Biol. Chem.* **276**, 23547–23553. (2001).

The siRNA-infected cells were assessed for changes in Ca^{2+} oscillation patterns. Average Ca^{2+} signals from Jurkat cells infected with TRPM4 siRNA (n = 64 cells, 5 experiments) and control siRNA (n = 33 cells, 4 experiments) were determined (Fig. 4G). Jurkat cells infected with TRPM4 siRNA exhibited a more prolonged sustained Ca^{2+} influx as compared to cells infected with the siRNA control, which exhibit oscillatory changes typical of wt-Jurkat cells (compare Fig. 4, E and F). PHA stimulation of these cells resulted in a twofold increase in the amount of IL-2 secreted by the TRPM4 siRNA–infected cells as compared with the amount of IL-2 secreted by the control cells (Fig. 4H).

In summary, our results establish that TRPM4 is a previously unrecognized ion channel in Jurkat T cells with a profound influence on Ca^{2+} signaling. Molecular suppression of TRPM4 converts oscillatory changes of $[Ca^{2+}]_i$ into long-lasting sustained elevations in Ca^{2+} and leads to augmented IL-2 production. It is conceivable that this effect occurs physiologically in cells that express the short splice variant TRPM4a, which is of a similar length to ΔN-TRPM4 and could therefore act as a native dominant negative subunit. In electrically nonexcitable cells, TRPM4 would tend to reduce Ca^{2+} influx by depolarizing the membrane potential and reducing the driving force for Ca^{2+} entry through store-operated CRAC (Ca^{2+} release–activated Ca^{2+}) channels.

The molecular and electrophysiological identification of TRPM4 in Jurkat T cells may call for a reinterpretation of the interplay of ionic currents that shape intracellular Ca^{2+} signals (*4*, *16*, *19*). We propose that TRPM4 acts in concert with CRAC, Kv1.3, and K_{Ca} channels to control $[Ca^{2+}]_i$ oscillations in lymphocytes through oscillatory changes in membrane potential according to the following model.

At rest, the lymphocyte membrane potential is around –60 mV, owing to the basal activity of K^+ channels (*20*). Engagement of T cell receptors induces phospholipase C–mediated production of $InsP_3$ (inositol 1,4, 5-trisphosphate), which causes Ca^{2+} release and activation of store-operated CRAC channels. Current models of Ca^{2+} oscillations in lymphocytes (*19*) propose that the I_{CRAC}-mediated Ca^{2+} influx triggers the activation of Ca^{2+}-activated K^+ channels, which provides the driving force for Ca^{2+} entry by hyperpolarizing the membrane potential until $[Ca^{2+}]_i$ reaches a high-enough level to inhibit I_{CRAC}. As Ca^{2+} entry through I_{CRAC} is reduced, $[Ca^{2+}]_i$ falls until it reaches a level that removes the negative feedback on I_{CRAC}, and the cycle resumes by increasing Ca^{2+} entry through I_{CRAC}. This model lacks a strong depolarizing conductance that would be required to recruit voltage-dependent Kv1.3 channels present in T cells and could account for the observed oscillations in membrane potential (*20*, *21*). The $[Ca^{2+}]_i$-dependent activation of TRPM4 channels may provide this mechanism by becoming activated at around the peak of an oscillatory Ca^{2+} transient, causing the membrane potential to depolarize and thereby substantially reducing the driving force for Ca^{2+} influx. The depolarization would then recruit voltage-dependent K^+ currents (Kv1.3), which would tend to repolarize the membrane potential and also aid in the closure of TRPM4 channels, because the open probability of TRPM4 channels is reduced at negative membrane voltages (*5*, *6*, *8*). The repolarization would reestablish the driving force for Ca^{2+} influx through I_{CRAC} so that the next oscillation in $[Ca^{2+}]_i$ can take place.

References and Notes

1. G. R. Crabtree, *J. Biol. Chem.* **276**, 2313 (2001).
2. R. E. Dolmetsch, K. Xu, R. S. Lewis, *Nature* **392**, 933 (1998).
3. W. Li, J. Llopis, M. Whitney, G. Zlokarnik, R. Y. Tsien, *Nature* **392**, 936 (1998).
4. R. S. Lewis, *Annu. Rev. Immunol.* **19**, 497 (2001).
5. P. Launay *et al.*, *Cell* **109**, 397 (2002).
6. T. Hofmann, V. Chubanov, T. Gudermann, C. Montell, *Curr. Biol.* **13**, 1153 (2003).
7. M. Murakami *et al.*, *Biochem. Biophys. Res. Commun.* **307**, 522 (2003).
8. B. Nilius *et al.*, *J. Biol. Chem.* **278**, 30813 (2003).
9. X. Z. Xu, F. Moebius, D. L. Gill, C. Montell, *Proc. Natl. Acad. Sci. U.S.A.* **98**, 10692 (2001).
10. O. H. Petersen, *Curr. Biol.* **12**, R520 (2002).
11. B. Nilius, G. Droogmans, R. Wondergem, *Endothelium* **10**, 5 (2003).
12. Materials and methods are available as supporting material on *Science* Online.
13. A. T. Harootunian, J. P. Kao, B. K. Eckert, R. Y. Tsien, *J. Biol. Chem.* **264**, 19458 (1989).
14. A. Minta, R. Y. Tsien, *J. Biol. Chem.* **264**, 19449 (1989).
15. P. Launay *et al.*, data not shown.
16. M. D. Cahalan, H. Wulff, K. G. Chandy, *J. Clin. Immunol.* **21**, 235 (2001).
17. R. T. Abraham, A. Weiss, *Nat. Rev. Immunol.* **4**, 301 (2004).
18. T. R. Brummelkamp, R. Bernards, R. Agami, *Science* **296**, 550 (2002).
19. R. E. Dolmetsch, R. S. Lewis, *J. Gen. Physiol.* **103**, 365 (1994).
20. J. A. Verheugen, H. P. Vijverberg, *Cell Calcium* **17**, 287 (1995).
21. C. M. Fanger *et al.*, *J. Biol. Chem.* **276**, 12249 (2001).

22. We thank M. K. Monteilh-Zoller and C. E. Oki for technical assistance, L. Glimcher's laboratory for providing the murine T cell clone D10.G4, and S. Kraft for insightful advice on the RNAi method. This work was supported in part by NIH grants R01-AI46734 (J.-P.K.); R01-NS40927, R01-AI50200, and R01-GM63954 (R.P.); and R01-GM65360 (A.F.). P.L. was supported by a fellowship from the Human Frontier Science Program Organization.

Supporting Online Material

www.sciencemag.org/cgi/content/full/306/5700/1374/DC1

Materials and Methods

6 April 2004; accepted 14 September 2004

A Protein Sensor for siRNA Asymmetry

Yukihide Tomari, Christian Matranga, Benjamin Haley, Natalia Martinez, Phillip D. Zamore*

To act as guides in the RNA interference (RNAi) pathway, small interfering RNAs (siRNAs) must be unwound into their component strands, then assembled with proteins to form the RNA-induced silencing complex (RISC), which catalyzes target messenger RNA cleavage. Thermodynamic differences in the base-pairing stabilities of the 5′ ends of the two ~21-nucleotide siRNA strands determine which siRNA strand is assembled into the RISC. We show that in *Drosophila*, the orientation of the Dicer-2/R2D2 protein heterodimer on the siRNA duplex determines which siRNA strand associates with the core RISC protein Argonaute 2. R2D2 binds the siRNA end with the greatest double-stranded character, thereby orienting the heterodimer on the siRNA duplex. Strong R2D2 binding requires a 5′-phosphate on the siRNA strand that is excluded from the RISC. Thus, R2D2 is both a protein sensor for siRNA thermodynamic asymmetry and a licensing factor for entry of authentic siRNAs into the RNAi pathway.

In *Drosophila* lysates, siRNAs are loaded into the RISC by an ordered pathway in which one of the two siRNA strands, the guide strand, is assembled into the RISC, whereas the other strand, the passenger strand, is excluded and destroyed (*1*–*14*). A central step in RISC assembly is formation of the RISC-loading complex [RLC, previously designated complex A (*13*)], which contains double-stranded siRNA, the double-stranded RNA binding protein R2D2, and Dicer-2 (Dcr-2), as well as additional unidentified proteins. The function of Dicer in loading siRNA into the RISC is distinct from its role in generating siRNA from long double-stranded RNA (dsRNA) (*10*, *15*). Both R2D2 and Dcr-2 are

Department of Biochemistry and Molecular Pharmacology, University of Massachusetts Medical School, Worcester, MA 01605, USA.

*To whom correspondence should be addressed. E-mail: phillip.zamore@umassmed.edu

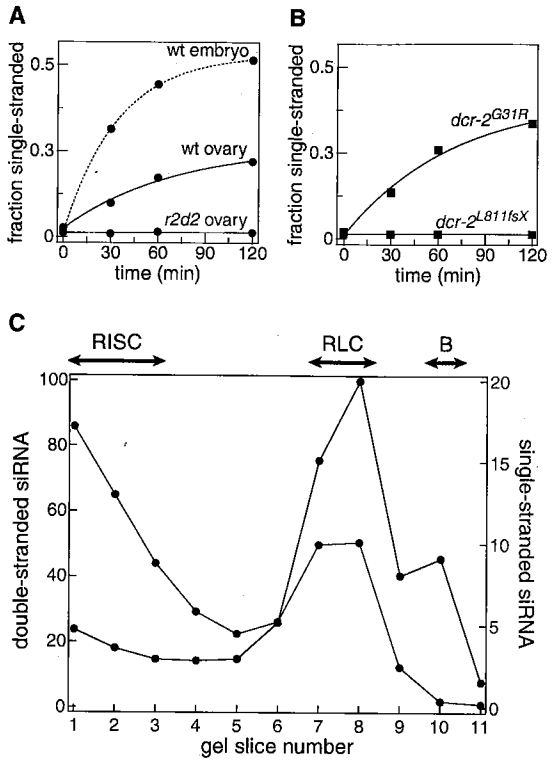

Fig. 1. The RISC-loading complex (RLC) initiates siRNA unwinding. (**A**) *r2d2* mutant ovary lysates, which cannot assemble RLC, do not unwind siRNA (wt, wild type). (**B**) siRNA unwinding was defective in ovary lysate from a mutation that disrupts all known Dcr-2 functions (L811fsX), including RLC assembly (*10, 12, 18*), but was normal for a point mutation in *dcr-2* ($Gly^{31} \rightarrow Arg$, G31R) that disrupts its function in dicing long dsRNA into siRNA, but not RISC assembly (*10, 12*). (**C**) The RLC, which is composed largely of double-stranded siRNA, also contains single-stranded siRNA. Note the different scales for the relative amounts of single- and double-stranded siRNA.

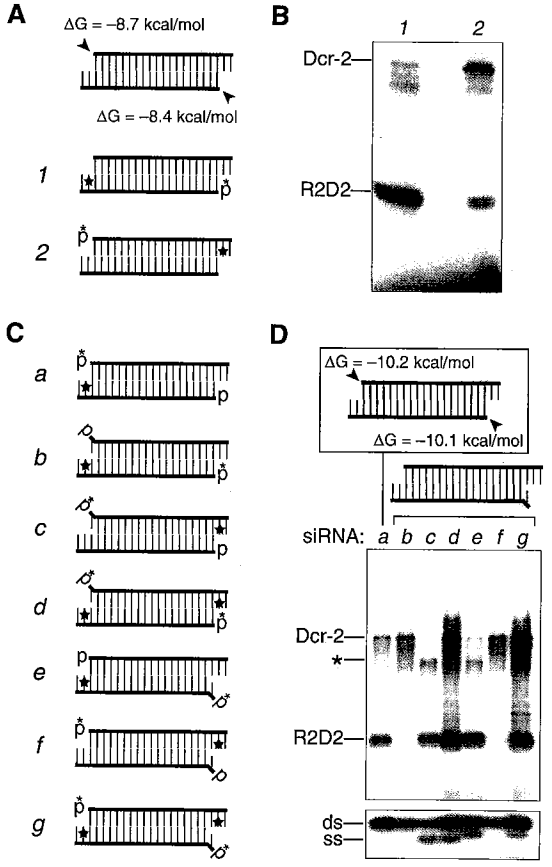

Fig. 2. Asymmetric binding of the Dcr-2/R2D2 heterodimer to siRNA duplexes in *Drosophila* embryo lysate. (**A**) Structure of the fully base-paired but asymmetric luciferase siRNA duplex used in (B) for protein-siRNA photocrosslinking. The local thermodynamic stability of the yellow highlighted base pairs is indicated here and in (D). Stars denote 5-iodouracil; an asterisk denotes a 5′-[^{32}P]phosphate. (**B**) The blue strand generates about 5 times as much RISC as the red; more Dcr-2 photocrosslinks to the 5-iodouracil nearest the less thermodynamically stable end, whereas more R2D2 photocrosslinks to the 5-iodouracil nearest the more thermodynamically stable end. (**C**) The series of 5-iodouracil substituted siRNAs used in (D). siRNA *a* is thermodynamically symmetric. siRNAs *b* to *g* contain a single unpaired nucleotide at the 5′ end of one strand, making them highly asymmetric (*7*). For siRNAs *b* to *d*, the red strand serves as the guide strand, whereas the blue strand serves as the guide for siRNAs *e* to *g*. (**D**) For the functionally asymmetric siRNAs, Dcr-2 binding was detected nearest the 5′ end of the guide strand, whereas R2D2 was detected near the 5′ end of the passenger strand, the more thermodynamically stable end. The lower panel shows the ^{32}P-radiolabeled siRNA strands at the bottom of the same gel. Single-stranded siRNA was detected only when the labeled strand served as a guide strand and entered the RISC. The asterisk indicates a photocrosslink to Ago2.

required to form RLC (*13*) and to unwind siRNA (Fig. 1, A and B), but recombinant Dcr-2/R2D2 heterodimer or Dcr-2 alone cannot catalyze siRNA unwinding (fig. S1). Thus, the Dcr-2/R2D2 heterodimer is necessary but not sufficient to unwind siRNA.

If siRNA unwinding is initiated in the RLC, then the RLC should contain some single-stranded siRNA. To test this idea, we briefly incubated siRNA duplex in lysate, resolved the complexes formed by native gel electrophoresis, divided the gel into 11 parts, and analyzed the structure of the siRNA in each gel slice (fig. S2A). Consistent with our previous findings, a peak of double-stranded siRNA comigrated with both the RLC and complex B, which is thought to be a precursor to RLC (*13*) (Fig. 1C). A small peak of single-stranded siRNA also comigrated with the RLC, but not with complex B (Fig. 1C), which suggests that the RLC initiates siRNA unwinding. Similar peaks of single-stranded siRNA comigrated with the RLC for the passenger strand of this siRNA and for the guide and passenger strands of a second siRNA (fig. S2B). We conclude that the RLC initiates siRNA unwinding.

The RLC also senses siRNA thermodynamic asymmetry, thereby determining which strand enters the RISC. siRNA containing 5-iodouracil at the 20th nucleotide (p20) can be photocrosslinked to R2D2 and Dcr-2 (*13*). Photocrosslinking is position-specific: An siRNA containing 5-iodouracil at position 12 was not cross-linked to R2D2 or Dcr-2 (*13*). Photocrosslinking attaches the radiolabel of the siRNA to the protein, identifying proteins that lie near p20 of the substituted siRNA strand. We evaluated the relative efficiency of photocrosslinking to R2D2 and Dcr-2 for three types of siRNA (Fig. 2) (table S1): a luciferase-specific siRNA whose sequence makes the 5′ end of the antisense strand less thermodynamically stable than the 5′ end of the sense strand; a nearly symmetric siRNA targeting human *Zn, Cu superoxide dismutase 1* (*sod1*), in which the stabilities of the 5′ ends are essentially the same; and a series of highly asymmetric *sod1*-directed siRNAs in which the first nucleotide of the guide strand is mismatched to the passenger strand, causing the guide strand to be loaded into the RISC almost exclusively. When we used the partially asymmetric luciferase-specific siRNA, R2D2 was more efficiently photocrosslinked when the 5-iodouracil was on the strand more frequently incorporated into the RISC, whereas when the 5-iodouracil was on the strand less often incorporated into the RISC, Dcr-2 was more efficiently photocrosslinked (Fig. 2, A and B). Because a 5-iodouracil at p20 of one siRNA strand is near the 5′ end of the other strand, Dcr-2 must lie near the 5′ end of the strand entering the RISC (the guide strand), whereas

R2D2 binds near the 5′ end of the strand destined for destruction.

When we used the symmetric *sod1* siRNA (Fig. 2, C and D, siRNA *a*), Dcr-2 and R2D2 were photocrosslinked with nearly equal efficiency to the 5-iodouracil strand (Fig. 2D, siRNA *a*); this finding suggests that each protein binds about half the time to one or the other end of the siRNA. In contrast, when we used derivatives of this siRNA that contained single-nucleotide mismatches that made them highly asymmetric, the 5-iodouracil strand was photocrosslinked to either Dcr-2 or R2D2, but not to both (Fig. 2, C and D, siRNAs *b* and *c*). With the asymmetric siRNA sequence, the photocrosslinking data suggest that Dcr-2 is almost always near the 5′ end of the guide strand and R2D2 near the 5′ end of the passenger strand. As expected when both siRNA strands contained p20 5-iodouracil and 5′-[^{32}P]phosphate groups, both proteins were photocrosslinked (Fig. 2, C and D, siRNA *d*). When we used a reciprocal series of siRNAs in which the strands assembled into and excluded from the RISC were reversed (Fig. 2, C and D, siRNAs *e*, *f*, and *g*), Dcr-2 was again found near the 5′ end of the guide strand and R2D2 near the 5′ end of the passenger strand.

Purified, recombinant Dcr-2/R2D2 heterodimer alone can also sense the thermodynamic stabilities of the ends of an siRNA duplex. At physiologically relevant concentrations of the proteins (*16*), photocrosslinking reflected siRNA asymmetry (Fig. 3A). Like heterodimer binding to an siRNA (*17*), differential photocrosslinking of recombinant Dcr-2/R2D2 heterodimer to an siRNA (*18*) did not require adenosine triphosphate (ATP). In contrast, formation of the RLC requires ATP (*13*). The orientation of Dcr-2 and R2D2 on the siRNA duplex was less asymmetric for the recombinant heterodimer than for embryo lysate (compare Figs. 2D and 3A). We propose that siRNA asymmetry is initially sensed by the Dcr-2/R2D2 heterodimer in an ATP-independent manner but is later amplified by the ATP-dependent action of other proteins.

Photocrosslinking of R2D2, but not Dcr-2, to the two ends of an siRNA duplex was influenced by the presence of a 5′-phosphate group on the siRNA. We prepared a series of highly asymmetric siRNAs in which the strand containing the p20 5-iodouracil was radiolabeled with ^{32}P at the 5′ end and the other strand contained either a 5′-hydroxyl or 5′-phosphate group (Fig. 3B). In four trials, R2D2 photocrosslinking to the nearby p20 5-iodouracil of the guide strand was greater by a factor of 4.6 ± 0.4 (average ± SD) when the passenger strand contained a 5′-phosphate rather than a hydroxyl group (Fig. 3C, left, siRNAs *c* and *e*). R2D2 photocrosslinking in ATP-depleted embryo lysate likewise required a 5′-phosphate at the more thermodynamically stable siRNA end (Fig. 3C, right, siRNAs *c* and *e*). Thus, R2D2 can sense two aspects of siRNA structure: the stability of an siRNA 5′ end, and the presence of a 5′-phosphate group. In contrast, Dcr-2 photocrosslinking was unperturbed by a 5′-hydroxyl group on the guide strand, both for the purified protein and in ATP-depleted lysate (Fig. 3C, siRNAs *b* and *f*).

Active siRNAs contain 5′-phosphate groups on both strands (*3*, *11*, *19*–*21*). A 5′-phosphate on the guide strand is essential for siRNA function, but blocking 5′-phosphorylation of the passenger strand impairs rather than eliminates siRNA activity (*11*). Our results suggest a molecular explanation for this observation: A 5′-phosphate on the passenger strand enhances R2D2 binding, thereby facilitating efficient incorporation of an siRNA into the RLC and consequently into the RISC. Thus, R2D2 is a licensing factor that ensures that only authentic siRNAs enter the RNAi pathway in *Drosophila*.

Dcr-2 alone does not efficiently bind siRNA (*17*), nor can Dcr-2 alone be photocrosslinked to any of the siRNAs in this study (*18*). Taken together, these results and the data presented here suggest that orientation of the Dcr-2/R2D2 heterodimer is determined largely by R2D2 binding to the siRNA end with the most double-stranded character. This binding is presumably mediated by one or both of the R2D2 double-stranded RNA binding domains. A 5′ mismatch on an siRNA strand may therefore be an antideterminant for R2D2 binding, acting to direct the R2D2 protein to the 5′ end of the passenger

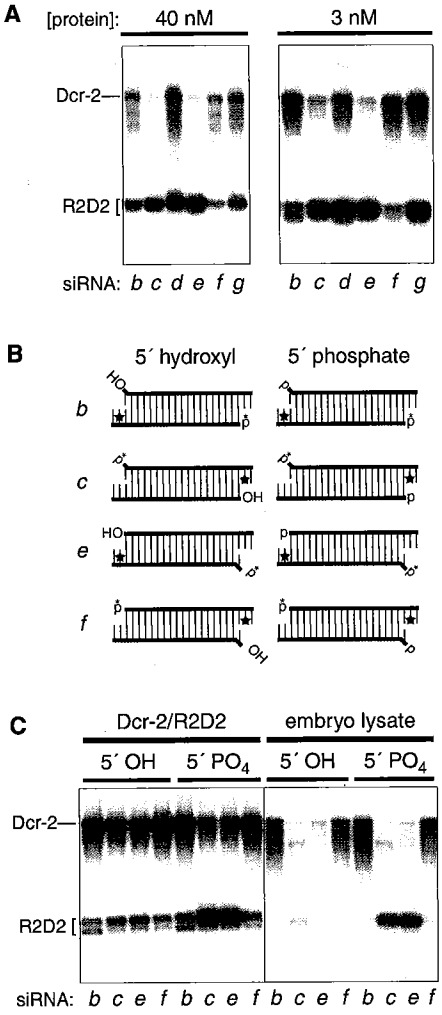

Fig. 3. The Dcr-2/R2D2 heterodimer alone can sense the asymmetry of an siRNA. (**A**) Photocrosslinking of recombinant Dcr-2/R2D2 heterodimer to the series of asymmetric siRNAs in Fig. 2C. (**B**) Structure of the siRNAs used in (C). The siRNAs all contained a single 5′-[^{32}P]phosphate on one strand and either a 5′-hydroxyl or 5′-phosphate group on the other. The siRNA sequences were as in Fig. 2C. (**C**) R2D2 senses the presence of a 5′-phosphate on the passenger strand. R2D2 photocrosslinking to the 5-iodouracil nearest the 5′ end of the passenger strand was reduced when the 5′ end of the passenger strand contained a 5′-hydroxyl rather than a 5′-phosphate group (siRNAs *c* and *e*); photocrosslinking of Dcr-2 was unaltered by the presence or absence of a 5′-phosphate on the guide strand (siRNAs *b* and *f*).

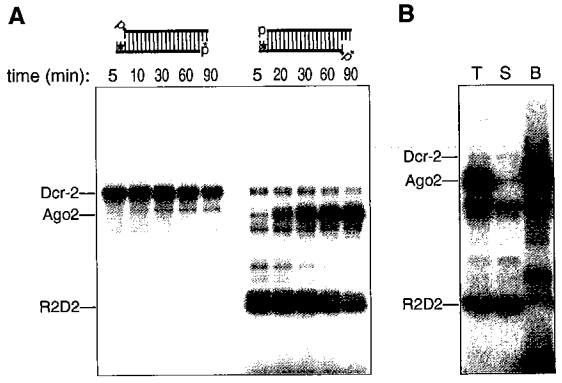

Fig. 4. Exchange of R2D2 for Ago2 at the 3′ end of the siRNA guide strand. (**A**) ^{32}P-radiolabeled siRNAs *b* and *e* (Fig. 2B) were incubated with embryo lysate in the presence of ATP for the times indicated, and binding of proteins near the 3′ end of the siRNA guide and passenger strands was monitored by photocrosslinking. Indicated times include the 4 min during which the sample was exposed to ultraviolet irradiation at room temperature. (**B**) ^{32}P-radiolabeled siRNA *c* was incubated with embryo lysate and photocrosslinked. The photocrosslinked proteins were then captured with a 2′-*O*-methyl oligonucleotide complementary to the siRNA guide strand. T, total reaction before incubation with the tethered oligonucleotide; S, supernatant after incubation; B, siRNA-photocrosslinked proteins bound to the tethered oligonucleotide.

strand and positioning Dcr-2 near the 5′ end of the strand to be loaded into the RISC. In this model, R2D2, as a component of the Dcr-2/R2D2 heterodimer, is the primary protein sensor of siRNA thermodynamic asymmetry.

How does the RLC, with the Dcr-2/R2D2 heterodimer positioned asymmetrically on the siRNA, progress to the RISC? Argonaute 2 (Ago2) is a ~130-kD protein that is a core component of the RISC (*22*) and is required for siRNA unwinding (*14*). We found that a ~130-kD protein was crosslinked to siRNA when the guide strand contained 5-iodouracil at p20 (asterisk in Fig. 2C, siRNAs *c*, *d*, *e*, and *g*). The ~130-kD protein was photocrosslinked only to the guide strand of the siRNA (Fig. 4), which suggests that this protein is a component of the RISC. The ~130-kD protein was immunoprecipitated with antibodies to Ago2 but not to Ago1 (fig. S3A) and was not observed in embryos lacking both maternal and zygotic Ago2 (*ago2*^{414}, fig. S3B). Thus, the ~130-kD protein is Ago2. When R2D2 and Ago2 were photocrosslinked to siRNAs *b* or *e* (which contain 5-iodouracil at p20 of the passenger or the guide strand), R2D2 was bound to the 3′ end of the guide strand and Dcr-2 to the 3′ end of the passenger strand at early times in the reaction (Fig. 4A). Later, binding of R2D2 and Dcr-2 decreased concurrently, accompanied by a corresponding increase in binding of Ago2 to the 3′ end of the guide strand. In *ago2*^{414} lysates, R2D2 binding to the 3′ end of the guide strand and Dcr-2 binding to the 3′ end of the passenger strand did not decrease with time (fig. S4A); this finding suggests that binding of Ago2 facilitates the release of the heterodimer from siRNA.

The siRNA bound by Ago2 is single-stranded, because Ago2, when photocrosslinked to siRNA, was captured by a tethered 2′-*O*-methyl oligonucleotide complementary to the siRNA guide strand (Fig. 4B) (*23*), as has been observed for the RISC (*7*, *23*–*25*). R2D2 was not captured by the 2′-*O*-methyl oligonucleotide, but was instead recovered in the supernatant, consistent with R2D2 binding of double-stranded siRNA.

Our data suggest a model for RISC assembly. First, R2D2 orients the Dcr-2/R2D2 heterodimer on the siRNA within the RLC. As siRNA unwinding proceeds, the heterodimer is exchanged for Ago2, the core component of the RISC. Indeed, we cannot detect single-stranded siRNA in the RLC assembled in *ago2*^{414} lysate (fig. S4, B and C). We hypothesize that unwinding occurs only when Ago2 is available, so that siRNA in the RLC is unwound only when the RISC can be assembled.

References and Notes

1. A. J. Hamilton, D. C. Baulcombe, *Science* **286**, 950 (1999).
2. S. M. Hammond, E. Bernstein, D. Beach, G. J. Hannon, *Nature* **404**, 293 (2000).
3. S. M. Elbashir, W. Lendeckel, T. Tuschl, *Genes Dev.* **15**, 188 (2001).
4. J. Martinez, T. Tuschl, *Genes Dev.* **18**, 975 (2004).
5. D. S. Schwarz, Y. Tomari, P. D. Zamore, *Curr. Biol.* **14**, 787 (2004).
6. P. D. Zamore, T. Tuschl, P. A. Sharp, D. P. Bartel, *Cell* **101**, 25 (2000).
7. D. S. Schwarz *et al.*, *Cell* **115**, 199 (2003).
8. A. Khvorova, A. Reynolds, S. D. Jayasena, *Cell* **115**, 209 (2003).
9. P. Aza-Blanc *et al.*, *Mol. Cell* **12**, 627 (2003).
10. Y. S. Lee *et al.*, *Cell* **117**, 69 (2004).
11. A. Nykänen, B. Haley, P. D. Zamore, *Cell* **107**, 309 (2001).
12. J. W. Pham, J. L. Pellino, Y. S. Lee, R. W. Carthew, E. J. Sontheimer, *Cell* **117**, 83 (2004).
13. Y. Tomari *et al.*, *Cell* **116**, 831 (2004).
14. K. Okamura, A. Ishizuka, H. Siomi, M. C. Siomi, *Genes Dev.* **18**, 1655 (2004).
15. N. Doi *et al.*, *Curr. Biol.* **13**, 41 (2003).
16. See supporting data on *Science* Online.
17. Q. Liu *et al.*, *Science* **301**, 1921 (2003).
18. Y. Tomari, C. Matranga, B. Haley, N. Martinez, P. D. Zamore, data not shown.
19. Y.-L. Chiu, T. M. Rana, *Mol. Cell* **10**, 549 (2002).
20. A. Boutla, C. Delidakis, I. Livadaras, M. Tsagris, M. Tabler, *Curr. Biol.* **11**, 1776 (2001).
21. D. S. Schwarz, G. Hutvágner, B. Haley, P. D. Zamore, *Mol. Cell* **10**, 537 (2002).
22. S. M. Hammond, S. Boettcher, A. A. Caudy, R. Kobayashi, G. J. Hannon, *Science* **293**, 1146 (2001).
23. G. Hutvágner, M. J. Simard, C. C. Mello, P. D. Zamore, *PLoS Biol.* **2**, 465 (2004).
24. G. Meister, M. Landthaler, Y. Dorsett, T. Tuschl, *RNA* **10**, 544 (2004).
25. B. Haley, P. D. Zamore, *Nature Struct. Mol. Biol.* **11**, 599 (2004).

26. We thank D. Turner, C. R. Matthews, Z. Gu, and members of the Zamore laboratory for advice and support, and Q. Liu, G. Hannon, T. Uemura, D. Smith, R. Carthew, M. Siomi, and H. Siomi for gifts of reagents. Y.T. is a recipient of a long-term fellowship from the Human Frontier Science Program. P.D.Z. is a Pew Scholar in the Biomedical Sciences and a W. M. Keck Foundation Young Scholar in Medical Research. Supported by NIH grants GM62862-01 and GM65236-01 (P.D.Z.).

Supporting Online Material

www.sciencemag.org/cgi/content/full/306/5700/1377/DC1
Materials and Methods
Table S1
Figs. S1 to S4
References

14 July 2004; accepted 20 September 2004

The Human Polyomavirus, JCV, Uses Serotonin Receptors to Infect Cells

Gwendolyn F. Elphick,[1] William Querbes,[1,2] Joslynn A. Jordan,[1,2] Gretchen V. Gee,[1,3] Sylvia Eash,[1,2] Kate Manley,[1,3] Aisling Dugan,[1,2] Megan Stanifer,[1,3] Anushree Bhatnagar,[4] Wesley K. Kroeze,[4] Bryan L. Roth,[4] Walter J. Atwood[1,2,3]*

The human polyomavirus, JCV, causes the fatal demyelinating disease progressive multifocal leukoencephalopathy in immunocompromised patients. We found that the serotonergic receptor $5HT_{2A}$R could act as the cellular receptor for JCV on human glial cells. The $5HT_{2A}$ receptor antagonists inhibited JCV infection, and monoclonal antibodies directed at $5HT_{2A}$ receptors blocked infection of glial cells by JCV, but not by SV40. Transfection of $5HT_{2A}$ receptor–negative HeLa cells with a $5HT_{2A}$ receptor rescued virus infection, and this infection was blocked by antibody to the $5HT_{2A}$ receptor. A tagged $5HT_{2A}$ receptor colocalized with labeled JCV in an endosomal compartment following internalization. Serotonin receptor antagonists may thus be useful in the treatment of progressive multifocal leukoencephalopathy.

The incidence of progressive multifocal leukoencephalopathy (PML) has increased 50-fold since 1979 and now affects nearly 1 in every 200,000 persons (*1*). The disease is due to infection of oligodendrocytes by the common human polyomavirus, JCV (*2*). Initial infection with JCV occurs early in childhood and eventually reaches a seroprevalence of between 70 and 80% in the adult population. The initial infection is subclinical, and the virus establishes a lifelong persistent infection. At any given time, ~5% of the population is actively excreting virus in the urine, and JCV is a frequent contaminant of untreated human sewage (*3*). PML occurs almost exclusively in severely immunosuppressed patients. The majority of cases occur in patients with AIDS, and to date there is no effective treatment (*4*). PML is initiated when JCV traffics from peripheral sites, such as the kidney and lymphoid organs, to the central nervous system (CNS) by unknown mechanisms. There is a strong association between JCV and human B lymphocytes, and the virus may traffic to the CNS in an

[1]Department of Molecular Microbiology and Immunology, [2]Graduate Program in Pathobiology, [3]Graduate Program in Molecular Biology, Cellular Biology, and Biochemistry, Brown University, Providence, RI 02912, USA. [4]Department of Biochemistry, Case Western Reserve University Medical School, Cleveland, Ohio 44106, USA.

*To whom correspondence should be addressed. E-mail: Walter_Atwood@Brown.edu

Ribo-gnome: The Big World of Small RNAs

Phillip D. Zamore* and Benjamin Haley

Small RNA guides—microRNAs, small interfering RNAs, and repeat-associated small interfering RNAs, 21 to 30 nucleotides in length—shape diverse cellular pathways, from chromosome architecture to stem cell maintenance. Fifteen years after the discovery of RNA silencing, we are only just beginning to understand the depth and complexity of how these RNAs regulate gene expression and to consider their role in shaping the evolutionary history of higher eukaryotes.

In 1969, Britten and Davidson proposed that RNAs specify which genes are turned on and which are turned off in eukaryotic cells (*1*). Their elegant idea was that the base-pairing rules of Watson and Crick could solve the problem of eukaryotic gene regulation. With the subsequent discovery of protein transcription factors—there are perhaps 1850 in humans—the idea that a diverse array of RNA guides sets the expression profile of each cell type in a plant or animal was abandoned.

In fact, RNAs—specifically, tiny RNAs known as "small RNAs"—do control plant and animal gene expression. Distinct classes of these small RNAs—microRNAs (miRNAs), small interfering RNAs (siRNAs), and repeat-associated small interfering RNAs (rasiRNAs)—are distinguished by their origins, not their functions [see the poster in this issue (*2*)]. One class alone, the miRNAs, is predicted to regulate at least one-third of all human genes (*3*). Small RNAs, 21 to 30 nucleotides (nt) in length, provide specificity to a remarkable range of biological pathways. Without these RNAs, transposons jump (wreaking havoc on the genome), stem cells are lost, brain and muscle fail to develop, plants succumb to viral infection, flowers take on shapes unlikely to please a bee, cells fail to divide for lack of functional centromeres, and insulin secretion is dysregulated. The production and function of small RNAs requires a common set of proteins: double-stranded RNA (dsRNA)–specific endonucleases such as Dicer (*4*), dsRNA-binding proteins, and small RNA–binding proteins called Argonaute proteins (*5*, *6*). Together, the small RNAs and their associated proteins act in distinct but related "RNA silencing" pathways that regulate transcription, chromatin structure, genome integrity, and, most commonly, mRNA stability. The RNAs may be small, but their production, maturation, and regulatory function require the action of a surprisingly large number of proteins.

Department of Biochemistry and Molecular Pharmacology, University of Massachusetts Medical School, Worcester, MA 01605, USA.

*To whom correspondence should be addressed. E-mail: phillip.zamore@umassmed.edu

A Brief History of Small RNA

In 1990, two groups overexpressed a pigment synthesis enzyme in order to produce deep purple petunia flowers, but instead generated predominantly white flowers (Fig. 1) (*7*, *8*). This phenomenon was dubbed "cosuppression" because the transgenic and endogenous genes were coordinately repressed, and its discovery quietly ushered in the study of RNA silencing. By the end of the decade, RNA silencing phenomena were discovered in a broad spectrum of eukaryotes, from fungi to fruit flies. RNA interference (RNAi) is perhaps the best known RNA silencing pathway, in part because its discovery makes it possible to block expression of nearly any gene in a wide range of eukaryotes, knowing only part of the gene's sequence (*9*, *10*). Human clinical trials testing RNAi-based drugs are currently under way.

Building on the unexpected finding that both sense and antisense RNA could silence gene expression in *Caenorhabditis elegans* (*11*), the key breakthrough in RNA silencing was the discovery that dsRNA is the actual trigger of specific mRNA destruction, with the sequence of the dsRNA determining which mRNA is destroyed (*9*). Later, the dsRNA was found to be converted into siRNAs—fragments of the original dsRNA, 21 to 25 nt in length, that guide protein complexes to complementary mRNA targets, whose expression is then silenced (*12*–*14*). Thus, the actual mechanism of RNAi is remarkably like an early model for plant cosuppression, which postulated that small RNAs derived from the overexpressed gene might guide inactivation of cosuppressed genes (*15*).

In contrast to siRNAs, which derive from dsRNA hundreds or thousands of base pairs long, miRNAs derive from long, largely unstructured transcripts (pri-miRNA) containing stem-loop or "hairpin" structures ~70 nt in length [reviewed in (*16*)]. The hairpins are cut out of the pri-miRNA by the dsRNA-specific endonuclease Drosha, acting with its dsRNA-binding protein partner DGCR8 in humans or Pasha in flies, to yield a pre-miRNA (Fig. 2) (*2*). Each mature miRNA resides in one of the two sides of the ~30–base pair stem of the pre-miRNA. The mature miRNA is excised from the pre-miRNA by another dsRNA-specific endonuclease, Dicer, again acting with a dsRNA-binding protein partner, the *tar*-binding protein (TRBP) in humans or Loquacious (Loqs) in flies. The April 2005 release of the miRNA Registry, an online database that coordinates miRNA annotation, records 1650 distinct miRNA genes, including 227 from humans and 21 from human viruses; 1648 of these were discovered in the 21st century. Whereas siRNAs are found in eukaryotes from the base to the crown of the phylogenetic tree, miRNAs have been discovered in plants and animals and their viruses only.

Ambros and co-workers discovered the first miRNA, *lin-4*, in 1993. They identified two RNA transcripts—one small and one smaller—derived from the *lin-4* locus of *C. elegans* (*17*). Earlier experiments showed that loss-of-function mutations in *lin-4* disrupted the developmental timing of worms, much as did gain-of-function mutations in the protein-coding gene *lin-14*. Noting that *lin-4* could form base pairs, albeit imperfectly, with sites in *lin-14*, Ambros and colleagues proposed that the 22-nt *lin-4* regulates the much longer *lin-14* mRNA by multiple RNA-RNA interactions between the miRNA and the 3′ untranslated region of its mRNA target. This remarkable paper predicted the contemporary miRNA pathway, suggesting that the longer 61-nt transcript corresponds to a precursor RNA that folds into a hairpin structure from which the 22-nt mature *lin-4* miRNA is excised. Eight years later, the prescient observation that "*lin-4* may represent a class of developmental regulatory genes that encode small antisense RNA products" (*17*) was amply validated by the discovery that miRNAs compose a large class of riboregulators (*18*–*23*).

The *lin-4* miRNA was discovered 3 years after the first reports of RNA silencing in plants (*7*, *8*) and 2 years before the first hint of RNAi in nematodes (*11*). However, no formal connection between miRNAs and siRNAs was made until 2001, when Dicer, the enzyme that converts long dsRNA into siRNAs (*4*, *24*), was shown to convert pre-miRNAs, such as the longer 61-nt transcript from *lin-4*, into mature miRNAs, like *lin-4* itself (*25*–*27*).

The human genome may contain ~1000 miRNAs, a few of which may not only be unique to humans, but may also contribute to making us uniquely human. Recent efforts to define the entirety of this small RNA class have uncovered 53 miRNAs unique to primates (*28*). Because miRNAs are small, they may evolve

rapidly, with new miRNA genes arising by duplication and mutation of the 21-nt miRNA sequence.

Small on Specificity

From the standpoint of binding specificity, small RNAs are truly diminutive. A mere six or seven of the 21 nucleotides within a miRNA or siRNA provide the bulk of binding specificity for the small RNA–protein complexes they guide. As first proposed by Lai (*29*), and subsequently confirmed computationally (*3*, *30*) and experimentally for miRNAs (*31*–*34*) and siRNAs (*35*, *36*), the 5′ end of a miRNA or an siRNA contributes disproportionately to target RNA binding. Kinetic and structural studies suggest that the first nucleotide of a small RNA guide is unpaired during small RNA function (*36*–*38*). The small region of the small RNA that mediates target binding has been called the "seed sequence," a term intended to suggest that the region nucleates binding between the small RNA guide and its target, and that the more 3′ regions of the small RNA subsequently zipper-up—if they can—with the 5′ regions of the binding site on the target RNA (*39*).

In truth, current experimental evidence cannot discern the order in which distinct regions of the small RNA interact with its binding site on the target RNA. Both computational and experimental approaches detect only the binding contributions of specific small RNA regions at equilibrium. But the finding that stable binding between the small RNA and its target derives from such a small region of an already puny RNA oligonucleotide implies that the manner in which the small RNA interacts with its target is very different from antisense oligonucleotide–target RNA pairing. This radical and unexpected mode of nucleic acid interaction is almost certainly a consequence of the way the small RNA—both alone and paired to its RNA target—is bound by a member of the Argonaute family of proteins. These multidomain proteins are specialized for binding the small RNAs that mediate RNA silencing; understanding the relationship of Argonaute protein structure to their functions in controlling gene expression is now the key to understanding the deeper physical meaning of the small RNA "seed sequence."

The small RNAs that act in RNA silencing pathways are like fancy restriction enzymes whose recognition sites occur at random once every ~4000 to ~65,000 nt of sequence. But unlike restriction enzymes, which cut DNA wherever they bind, small RNAs can act in two distinct ways, each of which dramatically extends their functional specificity (Fig. 3) (*2*). When a small RNA pairs extensively with its RNA target, it directs cleavage of a single phosphodiester bond in the target RNA, across from nucleotides 10 and 11 of the small RNA guide (*40*). Thus, small RNA–directed cleavage is much more specific than small RNA binding itself, as it occurs only when most of the 21 nt of the siRNA or miRNA can base pair to form at least one turn of an A-form helix with the RNA target (*36*, *41*, *42*). Even when the small RNA is fully complementary to its target RNA, cleavage only occurs when the RNA is bound to the right Argonaute protein (*43*, *44*). In humans, only one of the four Argonaute proteins examined in detail retains all the amino acids required to catalyze target RNA cleavage (*45*). Argonaute proteins contain two RNA-binding domains: the Piwi domain, which binds the small RNA guide at its 5′ end, and the PAZ domain, which binds the single-stranded 3′ end of small RNA. The endonuclease that cleaves target RNAs resides in the Piwi domain, and this domain is a structural homolog of the DNA-guided RNA endonuclease RNase H (*46*). Target RNA cleavage is commonly viewed as the siRNA or RNAi mode, but is actually the dominant mechanism by which plant miRNAs regulate their targets (*47*, *48*) and is found for at least a small number of animal (*49*, *50*) and viral miRNAs (*51*).

In *Drosophila* or human cell lysates, small RNA–programmed Argonaute2 (Ago2) acts as a multiple-turnover enzyme, with each small RNA directing the cleavage of hundreds of target molecules (*36*, *52*). Small RNA–directed mRNA cleavage cuts an mRNA into two pieces, and efficient release of these fragments requires adenosine triphosphate (ATP) (*36*). Proteins besides Ago2 may be required for release of the products of small RNA–directed target cleavage. In fact, Ago2 alone can direct a single round of target cleavage but cannot efficiently catalyze additional cycles, likely because the cleavage products remain bound to the small RNA within the enzyme (*45*). After the cleaved pieces of the target are released, the 3′ fragment is destroyed in the cytoplasm by the exonuclease Xrn1 while the 5′ fragment is degraded by the exosome, a collection of exonucleases dedicated to 3′-to-5′ RNA degradation (*53*). In plants and animals, when miRNAs direct mRNA cleavage, a short polyuridine [poly(U)] tail is subsequently added to the 3′ end of the 5′ cleavage fragment (*54*). Addition of poly(U) correlates with decapping and 5′-to-3′ destruction of the target RNA cleavage fragment, at least in plants, suggesting an alternative route to the exosome for degradation of the 5′ cleavage product.

When siRNAs or miRNAs pair only partially with their targets, they cannot direct mRNA cleavage. Instead, they block translation of the mRNA into protein (*55*, *56*). However, binding of a single miRNA alone is usually insufficient to measurably block translation; instead, several miRNAs bind to the same target—opening the door to combinatorial control of gene expression by sets of coordinately expressed miRNAs (*39*). Initially, miRNAs were proposed to repress translation at a step after ribosomes have bound the mRNA, i.e., after translational initiation (*55*). One idea was that they direct degradation of the nascent polypeptide as it emerges from the ribosome. Alternatively, they might "freeze" ribosomes in place on the mRNA, stalling elongation of the growing protein chain. Recent findings, however, call these ideas into question. For example, translational repression by miRNAs was thought to affect

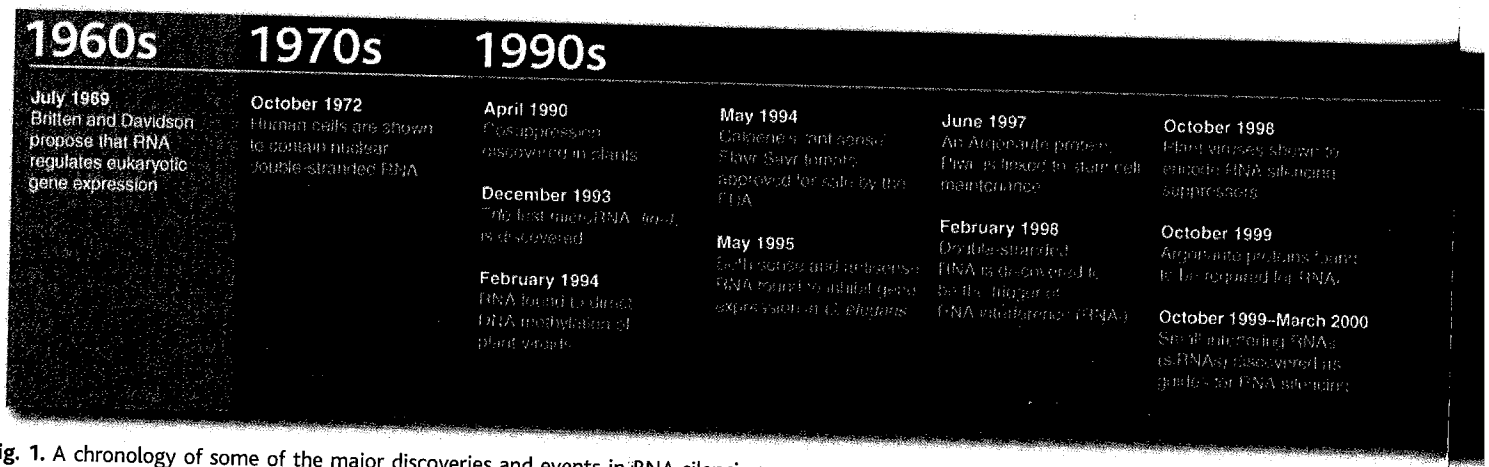

Fig. 1. A chronology of some of the major discoveries and events in RNA silencing.

only protein synthesis, not mRNA stability. Yet Lim and co-workers found that miRNAs can alter the stability of hundreds of mRNAs (*57*). And Pasquinelli and co-workers have now shown that even the founding miRNAs, worm *lin-4* and *let-7*, trigger destruction of their mRNA targets (*58*). These changes in steady-state mRNA levels are unlikely to reflect cleavage of the miRNA targets, because the complementarity between the miRNAs and their mRNA targets is restricted mainly to the seed sequence. How, then, could miRNAs make mRNA less stable? New studies offer a potential explanation.

Small RNAs, bound to Ago2, can move the mRNAs they bind from the cytosol to sites of mRNA destruction called "P-bodies" (*59*, *60*). Ago2 concentrates in P-bodies only when it binds small RNAs like miRNAs and siRNAs; Ago2 mutants that cannot bind small RNAs remain in the cytosol (*59*). Moreover, Ago2 associates with the enzymes that remove the 5′ 7-methylguanosine cap characteristic of mRNAs, a prerequisite for their destruction in the P-body (*59*, *60*). It is tempting to imagine that this new role for small RNAs, moving an mRNA to P-bodies, explains the mystery of small RNA–directed translational repression: By sequestering mRNA in the P-body, small RNAs would block translation. Subsequent destruction of the mRNA would then be a secondary consequence of relocating the mRNA from the cytosol to the P-body, which contains no ribosomal components (Fig. 4). Binding of a miRNA to the mRNA would not alter its inherent decay rate. The steady-state abundance of mRNAs that intrinsically turn over rapidly would therefore be reduced more than that of intrinsically more stable mRNAs when each is targeted by small RNA, but the translational rate of the two mRNAs would be reduced equally.

Is repression of mRNA translation by miRNAs just a consequence of the relocalization of the mRNA to the P-body? Filipowicz and colleagues argue in this issue of *Science* that translational repression comes first (*61*). They show that when bound to an mRNA target, human *let-7* miRNA blocks translational initiation. They propose that the consequence of miRNA-directed inhibition of translational initiation is relocalization of the mRNA target to the P-body. Once in the P-body, the mRNA may then be degraded, releasing the miRNA-programmed protein complex so it can return to the cytosol to begin a new round of target mRNA repression (Fig. 4). This pathway is presumed to be distinct from the small RNA–directed cleavage pathway, in which Ago2 in flies or mammals first cleaves a single phosphodiester bond in the mRNA target, and then the 5′ cleavage product is degraded by the exosome without obligate decapping.

Do all miRNAs repress gene expression? At least one human miRNA appears to act positively. Replication of hepatitis C virus (HCV) requires binding of human miR-122 to the 5′ noncoding region of the virus (*62*). Thus, for HCV, miR-122 acts as an enhancer of replication, and only cells expressing miR-122 support efficient HCV replication. Whether the positive effect of miR-122 on HCV is unique or represents an undiscovered mode of miRNA action remains unknown.

Aberrant, Unwanted

RNAi has been implicated in silencing parasitic DNA sequences, such as transposons and repetitive sequences. In many organisms, a specialized RNA silencing pathway senses the "aberrant RNA" transcribed from such sequences, and then initiates silencing posttranscriptionally and even transcriptionally. A candidate for an aberrant RNA sensor is a class of RNA silencing proteins that can copy single-stranded RNA into dsRNA. These RNA-dependent RNA polymerases (RdRPs) are found in nearly every eukaryote with a functioning RNA silencing pathway—except insects and mammals. In addition to initiating silencing responses from single-stranded trigger RNAs, RdRPs have been proposed to amplify and sustain silencing triggered by dsRNA. How RdRP enzymes distinguish between normal and aberrant transcription remains a key mystery of RNA silencing.

Meanwhile, Back in the Nucleus

RNA-directed transcriptional silencing was first identified in plants, where dsRNA corresponding to nontranscribed sequences can direct DNA methylation and transcriptional repression (*63*, *64*). Genetic studies in worms, plants, and *Schizosaccharomyces pombe* implicate small RNAs and the canonical components of the RNA silencing machinery—RdRP, Dicer, and Argonaute—in transcriptional silencing (*65*–*70*). Components of the RNAi machinery are also required for transcriptional silencing in flies (*71*, *72*). Transcriptional silencing directed by small RNAs is typically associated with the formation of heterochromatin, a transcriptionally repressed, compact form of chromatin in which the amino terminus of histone H3 is modified by methylation at lysine 9 ("H3K9"). In some organisms, such as plants and mammals, heterochromatic DNA is also hypermethylated. In *Tetrahymena*, small RNA–directed heterochromatin formation drives the deletion of specific regions of chromosomal DNA in the macronucleus (*73*, *74*).

A well-studied example of siRNA-directed assembly of heterochromatin is the outer regions of the centromere in *S. pombe*. Without this heterochromatin, *S. pombe* centromeres cannot reliably mediate chromosome segregation during cell division. Such a role for the RNA silencing machinery in assembling centromeric heterochromatin may be quite common, as chicken and mouse cells lacking Dicer also fail to assemble silent heterochromatin at their centromeres (*75*, *76*).

Repetitive, transposon-like sequences compose the outer regions of the *S. pombe* centromere. Mammalian centromeres likewise comprise repetitive sequences. Thus, how the RNA silencing machinery silences centromeric repeats may be just an example of the broader question of understanding the mechanism by which the RNA silencing machinery detects

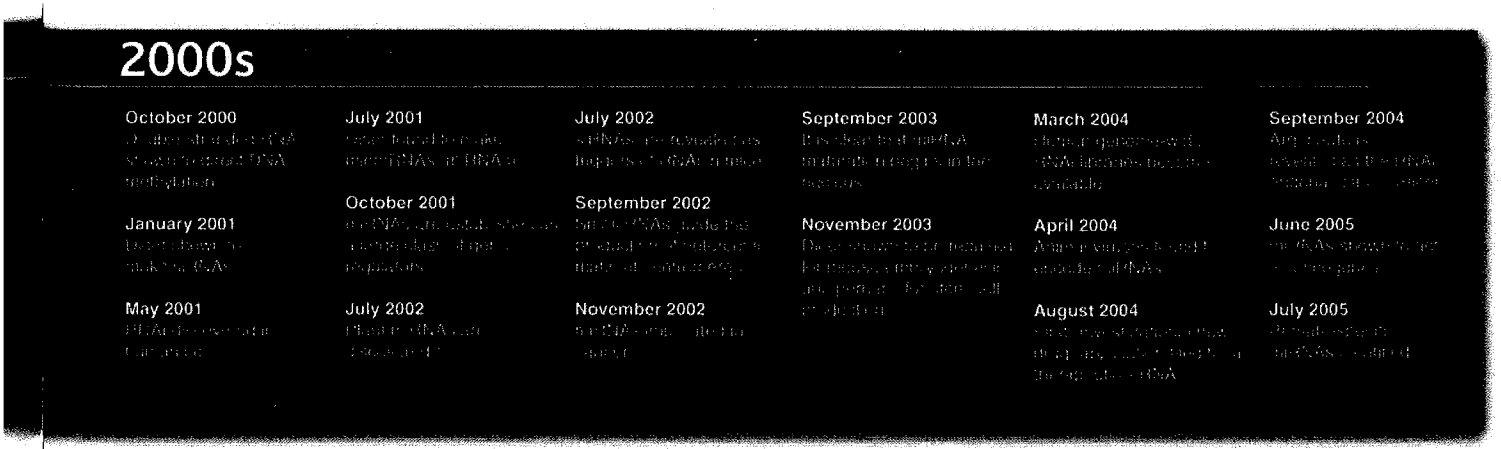

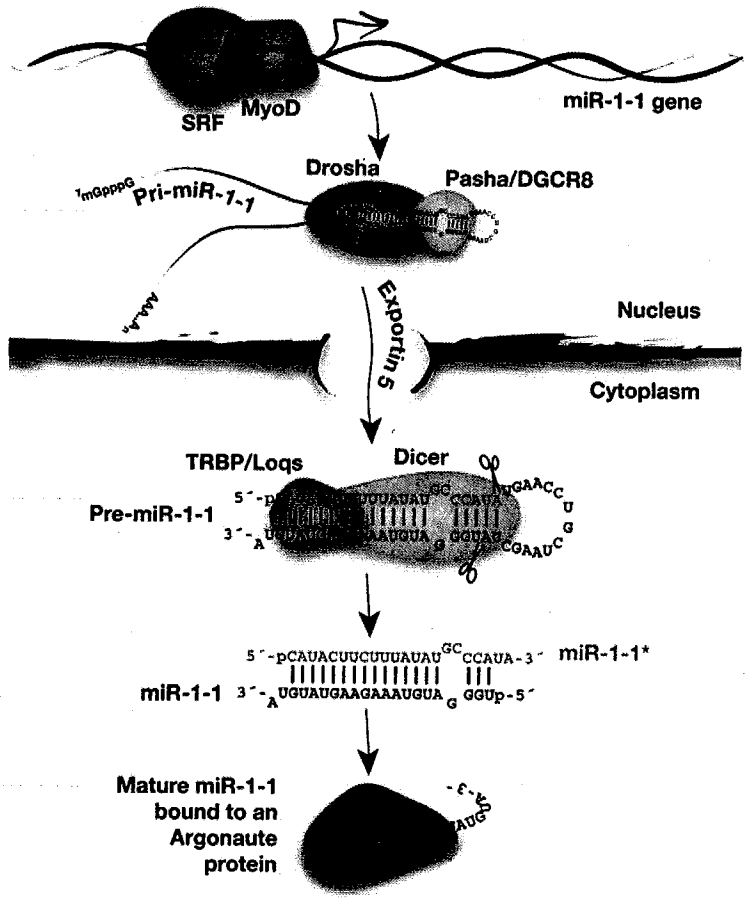

Fig. 2. A day in the life of the miRNA miR-1. In developing cardiac tissue, the transcription factors SRF (serum response factor) and MyoD promote RNA Pol II–directed transcription of pri-miR-1. In the nucleus, the RNase III endonuclease Drosha, together with its dsRNA-binding partner, Pasha/DGCR8, excises pre-miR-1 from pri-miR-1, breaking the RNA chain on both the 5′ and 3′ sides of the pre-miR-1 stem, leaving a ~2-nt, single-stranded 3′ overhang end. Exportin 5 recognizes this characteristic pre-miRNA end structure, transporting pre-miR-1 from the nucleus to the cytoplasm. In the cytoplasm, a second RNase III endonuclease, Dicer, together with its dsRNA-binding partner protein, Loqs/TRBP, makes a second pair of cuts, liberating miR-1 as a "miRNA/miRNA*" duplex. Mature, 21-nt long miR-1 is then loaded from the duplex into an Argonaute family member and miR-1* is destroyed. miR-1 guides the Argonaute protein to its target RNAs, such as the 3′ untranslated region of the *hand2* mRNA. Binding of the miR-1–programmed Argonaute protein represses production of Hand2 protein, halting cardiac cell proliferation.

and silences repetitive sequences. A coherent but speculative model of small RNA–directed transcriptional silencing emerges from recent studies in both *S. pombe* and plants. Transcripts from genomic regions to be targeted for silencing must first be converted to dsRNA. RdRPs have been assigned this role. Mutation of catalytically essential amino acids demonstrates that the polymerase activity of Rdp1, the sole *S. pombe* RdRP enzyme, is required for centromeric silencing (*77*), but what template RNA is copied by the RdRP has not been directly established in any organism. The dsRNA envisioned to be generated by the RdRP must next be converted to siRNAs, presumably by Dicer. In plants, distinct RdRP and Dicer paralogs are devoted to separate RNA silencing pathways, with RDR2, the RdRP, collaborating with DCL3, the Dicer, to generate siRNAs that target repetitive sequences for both cytosine and H3K9 methylation (*68*). Presumably the double-stranded siRNAs thus generated are unwound and the resulting single strands loaded into a member of the Argonaute family of proteins: Ago1 in *S. pombe* and AGO4, among others, in plants (*65–67*, *78*). The siRNAs, bound to the Argonaute protein within a larger complex of DNA and chromatin-modifying enzymes, guide the assembly of heterochromatin. How insects and mammals derive chromatin-silencing triggers in the absence of an RdRP is unknown.

What does it mean when we propose that siRNAs guide modifying enzymes to DNA, converting it to heterochromatin? Do we imagine that the siRNAs pair directly with single-stranded DNA, somehow separating the two strands of the chromosomal DNA, as proposed by Britten and Davidson (*1*)? Or rather, do the siRNAs bind RNA, as has been proposed for centromeric silencing in *S. pombe* (*79*)? This second model is comforting because it imagines that siRNAs interact with RNA in both

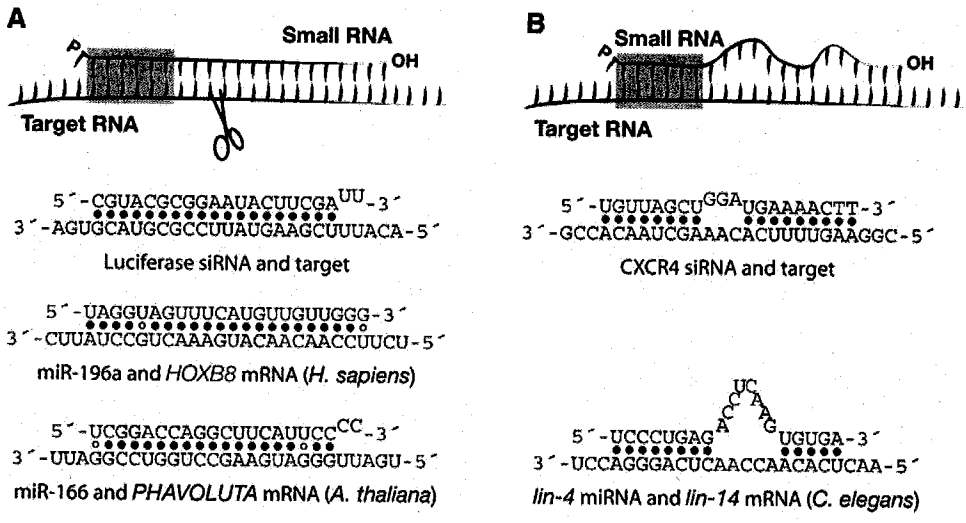

Fig. 3. Small RNA binding modes. (**A**) Extensive pairing of a small RNA to an mRNA allows the Piwi domain of a catalytically active Argonaute protein (e.g., Ago2 in humans or flies) to cut a single phosphodiester bond in the mRNA, triggering its destruction. Synthetic siRNAs typically exploit this mechanism, but some mammalian miRNAs (such as miR-196a) and most, if not all, plant miRNAs direct an Argonaute protein to cut their mRNA targets. (**B**) Partial pairing between the target RNA and the small RNA, especially through the "seed" sequence—roughly nucleotides 2 to 7 of the small RNA—tethers an Argonaute protein to its mRNA target. Binding of the miRNA and Argonaute protein prevents translation of the mRNA into protein. siRNAs can be designed to trigger such "translational repression" by including central mismatches with their target mRNAs; animal miRNAs such as *lin-4*, the first miRNA discovered, typically act by this mode because they are only partially complementary to their mRNA targets. The seed sequence of the small RNA guide is highlighted in blue.

transcriptional and post-transcriptional silencing, but it requires transcription across regions of DNA that were thought to lie untranscribed, such as promoters or intragenic regions. In plants, "transcriptionally silenced" DNA appears to be transcribed by a specialized type of DNA-dependent RNA polymerase, RNA polymerase IV (Pol IV) (*80–82*). RNA Pol IV may be specially adapted to transcribe silent heterochromatin, thereby providing a constant source of primary transcript to act as template for the RdRP and hence generating the dsRNA substrate required for Dicer to manufacture siRNAs (*80*). The model is appealing because it explains why siRNAs persist even after they have silenced the gene from which they arise.

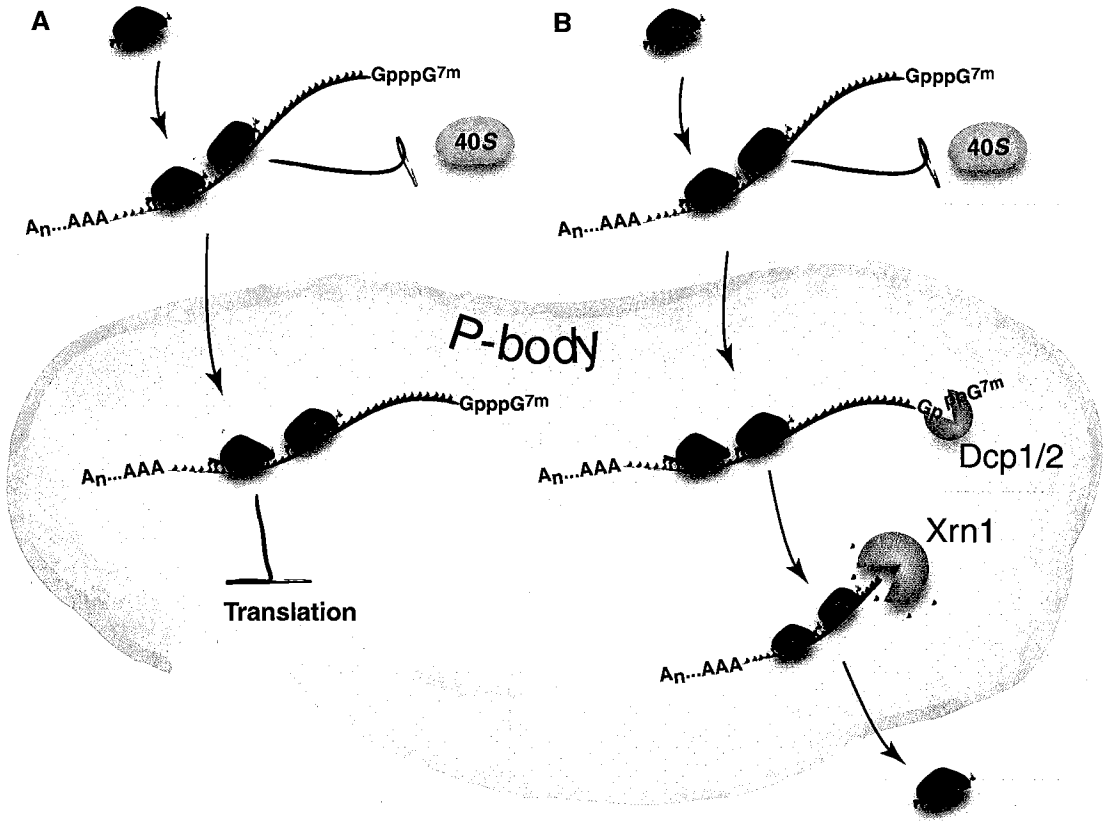

Fig. 4. A speculative model for translational repression by small RNAs: sequestration of a highly stable mRNA in the P-body. Binding of a small RNA–programmed Argonaute protein (red) to an mRNA blocks translational initiation, driving the mRNA into a P-body, the cytoplasmic site of mRNA decapping and degradation. Sequestering an mRNA in a P-body further excludes it from ribosomes, so it cannot be translated into protein. In (**A**), the mRNA is imagined to be degraded slowly in the P-body, so the miRNA appears only to repress translation. It is unknown whether mRNAs, once moved to the P-body by the binding of a small RNA, can ever return to the cytoplasm and resume translation. In (**B**), the mRNA is envisioned to be inherently prone to rapid degradation. Binding of an Argonaute-bound small RNA to an mRNA moves the mRNA to the P-body, where the decapping enzyme, Dcp1/2, is envisioned to remove its 7-methyl guanosine cap, triggering its destruction by the 5′-to-3′ exonuclease Xrn1. For the mRNA in (**A**), small RNAs appear to repress its translation without appreciably altering its steady-state abundance, whereas in (**B**), small RNAs appear to target the mRNA for exonucleolytic destruction, yet in both cases small RNAs change the cellular compartment in which the mRNA resides.

Pol IV might also supply the transcripts that provide a scaffold for siRNA-guided chromatin modification complexes to act on the adjacent DNA. Pol IV enzymes, however, occur only in plants; in *S. pombe*, formation of silent centromeric heterochromatin requires the classical RNA Pol II (*83*, *84*). This finding suggests that RNA Pol II may supply transcripts required for the production of the siRNAs themselves. For some *S. pombe* loci, perhaps even RNA Pol I provides these transcripts (*85*). Yet Pol II is required when the initial trigger of silencing is provided in trans—for example, by initiating silencing with a double-stranded hairpin—which suggests that Pol II transcription creates the target for the small RNAs as well as the trigger for small RNA production (*84*). Transcription per se is not sufficient; instead, a direct interaction between the carboxyl-terminal domain of Pol II and the RNA silencing machinery appears to help recruit the Argonaute protein, but only when loaded with siRNA, to the DNA (*84*).

These findings suggest that siRNAs interact directly with DNA and that siRNA-guided complexes can find their cognate DNA-binding sites only in the short interval during transcription of a sequence when the DNA is unpaired; when the DNA pairs again behind the polymerase, the site becomes inaccessible to the siRNA. However, most current data are also consistent with siRNAs binding nascent transcripts themselves, but in a manner that requires their being loaded on these sites by virtue of their association, through proteins, with RNA Pol II. Perhaps for genes transcribed by RNA Pol I (*85*), a similar protein-protein interaction allows the Argonaute-bound siRNA to follow closely behind the polymerase as it traverses the "silenced" gene.

Yet More RNA Polymerization, Just to Destroy RNA?

Template-dependent RNA polymerases are not the only RNA polymerases implicated in RNA silencing. Members of the polymerase β nucleotidyltransferase superfamily of proteins are required for RNA silencing in worms and fission yeast. This protein superfamily encompasses enzymes that either add polyadenosine to the 3′ end of RNA [poly(A) polymerases] or use ATP to make 2′-5′ polymers of adenosine monophosphate (2′-5′ oligoadenylate synthases). In worms, mutations in conserved residues in the nucleotidyltransferase domain of RDE-3 disrupt RNAi, suggesting that adenosine polymers may play a direct role in RNA silencing (*86*). In fission yeast, the putative nucleotidyl transferase Cid12 is required for heterochromatin assembly by the RNA silencing pathway (*79*). Cid12, a putative helicase protein, and Rdp1, the *S. pombe* RdRP, form a complex implicated in siRNA production. This complex also contains noncoding RNAs transcribed from centromeric DNA, the primary target of heterochromatin assembly in fission yeast, consistent with the idea that these noncoding transcripts act as templates for Rdp1, which may convert them into dsRNA, which in turn could be converted to siRNA by Dcr1, thereby triggering RNA silencing. But what do Cid12 and RDE-3 do? These enzymes may play a direct role in RNA silencing; a poly(A) tail synthesized by Cid12 may recruit enzymes that mediate heterochromatin-specific modifications to transcripts under surveillance by the RNA

silencing machinery (*79*). Alternatively, Cid12 and Rdp1 may be components of a common surveillance complex—and hence dependent on each other for their stability. This complex would contain components of two separate pathways that protect cells against "aberrant RNA"—transcripts that are misfolded, incorrectly spliced, or damaged such that they encode truncated proteins. Favoring this view, the budding yeast protein Trf4p, another polymerase β nucleotidyltransferase, adds poly(A) tails to misfolded tRNAs and to aberrant mRNAs, targeting them for destruction by the nuclear exosome, a complex of RNA-degrading enzymes (*87*–*89*). Use of a poly(A) tail as a degradation signal, rather than as a stabilizing feature that promotes mRNA translation, may be quite ancient, as bacteria use poly(A) tails to target RNA for destruction.

Stem Cells

Epigenetic marks play an important role in stem cells, which must divide to yield a daughter cell that differentiates and another that regenerates the original stem cell. RNA silencing has emerged as a vital regulatory mechanism for maintaining normal stem cell pools. Mice lacking Dicer die at embryonic day 7.5, devoid of Oct-4–expressing cells (*90*); in mammals, Oct-4 marks stem cell lineages. At least four genes in the RNA silencing pathway are required for germline stem cell function in *Drosophila melanogaster*. Piwi, an Argonaute protein, is required both to maintain female germline stem cells and to promote their proliferation (*91*). Dicer-1, which makes miRNAs and perhaps other types of small RNAs, and its dsRNA-binding protein partner, Loqs, are both required for normal germline stem cell function. In the fly ovary, germline stem cells lacking Dicer divide slowly, dramatically reducing the number of eggs generated (*92*). In contrast, in females mutant for Loqs in both the soma and the germ line, germline stem cells are lost, either because they die or because they differentiate into oocytes without replenishing the stem cell pool (*93*). It remains to be established whether these defects reflect loss of miRNAs (which require the coordinate action of Dicer-1 and Loqs for their maturation), loss of silent heterochromatin, or both.

Flies lacking Ago2 contain fewer pole cells, the germline stem cell progenitors, than do wild-type flies (*94*). The case of *ago2* mutants is particularly instructive, because loss of Ago2—like loss of the very first Argonaute protein implicated in RNA silencing, worm RDE-1 (*5*)—was originally reported to cause no cellular defects except loss of an RNAi response to exogenous dsRNA (*95*). Closer examination revealed that many aspects of early embryogenesis are defective, yet the flies somehow compensate and survive (*94*). In particular, *ago2* mutants show defects in chromosome condensation, nuclear division, spindle assembly, and nuclear timing, all perhaps caused by a loss of heterochromatin assembly normally guided by an RNA silencing pathway. It remains to be shown if Ago2 acts directly in the assembly of heterochromatin by the RNA silencing pathway, or if components common to the RNAi and transcriptional silencing pathways become unstable in the absence of Ago2 protein. But these results underscore the guiding principle of small RNA function: Small RNAs play a very big role in nearly every cellular process.

References and Notes

1. R. J. Britten, E. H. Davidson, *Science* **165**, 349 (1969).
2. G. Hutvágner, M. Simard, Eds., poster from the special issue on RNA, *Science* **309**, following p. 1518 (2 September 2005); published online 1 September 2005 (available at www.sciencemag.org/sciext/rna).
3. B. P. Lewis, C. B. Burge, D. P. Bartel, *Cell* **120**, 15 (2005).
4. E. Bernstein, A. A. Caudy, S. M. Hammond, G. J. Hannon, *Nature* **409**, 363 (2001).
5. H. Tabara *et al.*, *Cell* **99**, 123 (1999).
6. S. M. Hammond, S. Boettcher, A. A. Caudy, R. Kobayashi, G. J. Hannon, *Science* **293**, 1146 (2001).
7. C. Napoli, C. Lemieux, R. A. Jorgensen, *Plant Cell* **2**, 279 (1990).
8. A. R. van der Krol, L. A. Mur, M. Beld, J. N. M. Mol, A. R. Stuitji, *Plant Cell* **2**, 291 (1990).
9. A. Fire *et al.*, *Nature* **391**, 806 (1998).
10. S. Elbashir, J. Harborth, K. Weber, T. Tuschl, *Methods* **26**, 199 (2002).
11. S. Guo, K. J. Kemphues, *Cell* **81**, 611 (1995).
12. A. J. Hamilton, D. C. Baulcombe, *Science* **286**, 950 (1999).
13. S. M. Hammond, E. Bernstein, D. Beach, G. J. Hannon, *Nature* **404**, 293 (2000).
14. P. D. Zamore, T. Tuschl, P. A. Sharp, D. P. Bartel, *Cell* **101**, 25 (2000).
15. J. A. Lindbo, L. Silva-Rosales, W. M. Proebsting, W. G. Dougherty, *Plant Cell* **5**, 1749 (1993).
16. V. N. Kim, *Nat. Rev. Mol. Cell Biol.* **6**, 376 (2005).
17. R. C. Lee, R. L. Feinbaum, V. Ambros, *Cell* **75**, 843 (1993).
18. M. Lagos-Quintana, R. Rauhut, W. Lendeckel, T. Tuschl, *Science* **294**, 853 (2001).
19. N. C. Lau, L. P. Lim, E. G. Weinstein, D. P. Bartel, *Science* **294**, 858 (2001).
20. R. C. Lee, V. Ambros, *Science* **294**, 862 (2001).
21. C. Llave, K. D. Kasschau, M. A. Rector, J. C. Carrington, *Plant Cell* **14**, 1605 (2002).
22. W. Park, J. Li, R. Song, J. Messing, X. Chen, *Curr. Biol.* **12**, 1484 (2002).
23. B. J. Reinhart, E. G. Weinstein, M. W. Rhoades, B. Bartel, D. P. Bartel, *Genes Dev.* **16**, 1616 (2002).
24. S. W. Knight, B. L. Bass, *Science* **293**, 2269 (2001).
25. A. Grishok *et al.*, *Cell* **106**, 23 (2001).
26. G. Hutvágner *et al.*, *Science* **293**, 834 (2001).
27. R. F. Ketting *et al.*, *Genes Dev.* **15**, 2654 (2001).
28. I. Bentwich *et al.*, *Nat. Genet.* **37**, 766 (2005).
29. E. C. Lai, *Nat. Genet.* **30**, 363 (2002).
30. B. Lewis, I. Shih, M. Jones-Rhoades, D. Bartel, C. Burge, *Cell* **115**, 787 (2003).
31. J. G. Doench, P. A. Sharp, *Genes Dev.* **18**, 504 (2004).
32. A. Mallory *et al.*, *EMBO J.* **23**, 3356 (2004).
33. J. Brennecke, A. Stark, R. B. Russell, S. M. Cohen, *PLoS Biol.* **3**, e85 (2005).
34. E. C. Lai, B. Tam, G. M. Rubin, *Genes Dev.* **19**, 1067 (2005).
35. A. L. Jackson *et al.*, *Nat. Biotechnol.* **21**, 635 (2003).
36. B. Haley, P. D. Zamore, *Nat. Struct. Mol. Biol.* **11**, 599 (2004).
37. J. B. Ma *et al.*, *Nature* **434**, 666 (2005).
38. J. S. Parker, S. M. Roe, D. Barford, *Nature* **434**, 663 (2005).
39. D. P. Bartel, *Cell* **116**, 281 (2004).
40. S. M. Elbashir, W. Lendeckel, T. Tuschl, *Genes Dev.* **15**, 188 (2001).
41. Y.-L. Chiu, T. M. Rana, *Mol. Cell* **10**, 549 (2002).
42. J. Martinez, T. Tuschl, *Genes Dev.* **18**, 975 (2004).
43. J. Liu *et al.*, *Science* **305**, 1437 (2004).
44. G. Meister *et al.*, *Mol. Cell* **15**, 185 (2004).
45. F. V. Rivas *et al.*, *Nat. Struct. Mol. Biol.* **12**, 340 (2005).
46. J.-J. Song, S. K. Smith, G. J. Hannon, L. Joshua-Tor, *Science* **305**, 1434 (2004).
47. C. Llave, Z. Xie, K. D. Kasschau, J. C. Carrington, *Science* **297**, 2053 (2002).
48. G. Tang, B. J. Reinhart, D. P. Bartel, P. D. Zamore, *Genes Dev.* **17**, 49 (2003).
49. S. Yekta, I. Shih, D. P. Bartel, *Science* **304**, 594 (2004).
50. E. Davis *et al.*, *Curr. Biol.* **15**, 743 (2005).
51. S. Pfeffer *et al.*, *Science* **304**, 734 (2004).
52. G. Hutvágner, P. D. Zamore, *Science* **297**, 2056 (2002).
53. T. I. Orban, E. Izaurralde, *RNA* **11**, 459 (2005).
54. B. Shen, H. M. Goodman, *Science* **306**, 997 (2004).
55. P. H. Olsen, V. Ambros, *Dev. Biol.* **216**, 671 (1999).
56. J. G. Doench, C. P. Petersen, P. A. Sharp, *Genes Dev.* **17**, 438 (2003).
57. L. P. Lim *et al.*, *Nature* **433**, 769 (2005).
58. S. Bagga *et al.*, *Cell* **122**, 553 (2005).
59. J. Liu, M. A. Valencia-Sanchez, G. J. Hannon, R. Parker, *Nat. Cell Biol.* **7**, 719 (2005).
60. G. L. Sen, H. M. Blau, *Nat. Cell Biol.* **7**, 633 (2005).
61. R. S. Pillai *et al.*, *Science* **309**, 1573 (2005); published online 4 August 2005 (10.1126/science.1115079).
62. C. L. Jopling, M. Yi, A. M. Lancaster, S. M. Lemon, P. Sarnow, *Science* **309**, 1577 (2005).
63. M. Wassenegger, S. Heimes, L. Riedel, H. L. Sanger, *Cell* **76**, 567 (1994).
64. M. F. Mette, W. Aufsatz, J. van der Winden, M. A. Matzke, A. J. Matzke, *EMBO J.* **19**, 5194 (2000).
65. T. A. Volpe *et al.*, *Science* **297**, 1833 (2002).
66. D. Zilberman, X. Cao, S. E. Jacobsen, *Science* **299**, 716 (2003).
67. S. W. Chan *et al.*, *Science* **303**, 1336 (2004).
68. Z. Xie *et al.*, *PLoS Biol.* **2**, E104 (2004).
69. A. Grishok, J. L. Sinskey, P. A. Sharp, *Genes Dev.* **19**, 683 (2005).
70. V. J. Robert, T. Sijen, J. van Wolfswinkel, R. H. Plasterk, *Genes Dev.* **19**, 782 (2005).
71. M. Pal-Bhadra, U. Bhadra, J. A. Birchler, *Mol. Cell* **9**, 315 (2002).
72. M. Pal-Bhadra *et al.*, *Science* **303**, 669 (2004).
73. K. Mochizuki, N. A. Fine, T. Fujisawa, M. A. Gorovsky, *Cell* **110**, 689 (2002).
74. M. C. Yao, P. Fuller, X. Xi, *Science* **300**, 1581 (2003).
75. T. Fukagawa *et al.*, *Nat. Cell Biol.* **6**, 784 (2004).
76. C. Kanellopoulou *et al.*, *Genes Dev.* **19**, 489 (2005).
77. T. Sugiyama, H. Cam, A. Verdel, D. Moazed, S. I. Grewal, *Proc. Natl. Acad. Sci. U.S.A.* **102**, 152 (2005).
78. D. Zilberman *et al.*, *Curr. Biol.* **14**, 1214 (2004).
79. M. R. Motamedi *et al.*, *Cell* **119**, 789 (2004).
80. A. J. Herr, M. B. Jensen, T. Dalmay, D. C. Baulcombe, *Science* **308**, 118 (2005).
81. T. Kanno *et al.*, *Nat. Genet.* **37**, 761 (2005).
82. Y. Onodera *et al.*, *Cell* **120**, 613 (2005).
83. H. Kato *et al.*, *Science* **309**, 467 (2005).
84. V. Schramke *et al.*, *Nature* **435**, 1275 (2005).
85. H. P. Cam *et al.*, *Nat. Genet.* **37**, 809 (2005).
86. C. C. Chen *et al.*, *Curr. Biol.* **15**, 378 (2005).
87. S. Kadaba *et al.*, *Genes Dev.* **18**, 1227 (2004).
88. J. LaCava *et al.*, *Cell* **121**, 713 (2005).
89. S. Vanacova *et al.*, *PLoS Biol* **3**, e189 (2005).
90. E. Bernstein *et al.*, *Nat. Genet.* **35**, 215 (2003).
91. D. N. Cox, A. Chao, H. Lin, *Development* **127**, 503 (2000).
92. S. D. Hatfield *et al.*, *Nature* **435**, 974 (2005).
93. K. Forstemann *et al.*, *PLoS Biol.* **3**, e236 (2005).
94. G. Deshpande, G. Calhoun, P. Schedl, *Genes Dev.* **19**, 1680 (2005).
95. K. Okamura, A. Ishizuka, H. Siomi, M. C. Siomi, *Genes Dev.* **18**, 1655 (2004).

96. The authors acknowledge the support, advice, and critical comments of members of the Zamore laboratory. P.D.Z. is a W. M. Keck Foundation Young Scholar in Medical Research. Supported by NIH grants GM62862-01 and GM65236-01 (P.D.Z.). P.D.Z. is a founder of and member of the Scientific Advisory Board of Alnylam Pharmaceuticals, a biopharmaceutical company that develops therapeutic agents based on RNAi.

10.1126/science.1111444

7493-1